MORPHOLOGICAL, PHENOTYPIC AND MOLECULAR CHARACTERIZATION OF HUMAN ENDOCRINE AND NEUROENDOCRINE NEOPLASMS

Doctoral dissertation

Department of Oncology

PhD program in Biomedical Sciences and Oncology
Curriculum: Immunotherapy
Academic Field: MED/08

XXXIV Cycle

Candidate: Jasna Metovic

Tutor: Prof. Mauro Papotti

PhD program director: Prof. Emilio Hirsch
PhD program coordinator: Prof. Silvia Deaglio

September 2022

This thesis is dedicated to my mother Camila and her fearless battle with cancer.

Nothing in life is to be feared, it is only to be understood. Now is the time to understand more, so that we may fear less.

~ Marie Curie

SUMMARY

This thesis was conducted at the Department of Oncology, Pathology Unit, under the supervision of Professor Mauro Papotti representing the candidate's main research work during the course of PhD program (2018 – 2022). Candidate explored molecular and immunobiological aspects of endocrine and neuroendocrine tumors, that lead to carcinogenesis, tumor aggressiveness and could have an impact on patient's survival, based on tissue expression analyses correlated with clinico-pathological characteristics. The main research goal was to identify novel markers that could potentially help to tailor the best therapeutic approach for each individual patient or tumor type by depicting detailed molecular signatures associated with patients' prognosis and therapy-specific outcome.

Chapter 1 is dedicated to exploration of gene expression of principal transcriptional regulators of neuroendocrine differentiation, including *ASCL1, NEUROD1, DLL3, NOTCH1, INSM1, MYCL1, POU2F3* and *YAP1*, in pulmonary and extrapulmonary neuroendocrine neoplasms, by means of RT-PCR analyses.

Chapter 2 describes investigation of immune-related profile of poorly differentiated, follicular and hürtle cell thyroid carcinomas, based on the nCounter PanCancer Immune Profiling panel (NanoString Technologies, Seattle, WA, USA) and immunoexpression status of PD-L1. Moreover, a group of papillary aggressive and non-aggressive thyroid carcinomas, was analyzed employing nCounter PanCancer Pathways panel (NanoString Technologies, Seattle, WA, USA) that includes genes related to 13 canonical pathways.

Chapter 3 explores ALK expression in Merkel cell carcinoma cell lines and tumors and potential use of chimeric antigen receptor (CAR) T cells as an immune-targeted therapy. This portion of work was in part conducted at the Department of Pathology, Boston Children's Hospital, under the co-mentorship of Prof. Mauro Papotti and Prof. Roberto Chiarle.

Referees appointed by the University of Turin

Prof. Giuseppe Pelosi, University of Milan
Prof. Silvia Uccella, University of Insubria

Thesis Defense Committee Members

Prof. Mauro Papotti, University of Turin
Prof. Stefano La Rosa, University of Insubria
Prof. Ezio Fulcheri, University of Genova

Date of the oral defense: September 9th, 2022

Jasna Metovic
jasna.metovic@unito.it

University of Turin
Department of Oncology
Via Santena 7
10126 Torino
Italy

ABBREVIATIONS

Neuroendocrine – NE
Neuroendocrine differentiation – NED
Chromogranin A – CgA
Synapthophysin – SYN
Neuron-specific Enolase – NSE
Cytokeratin - CK
World Health Organization – WHO
International Agency for Research on Cancer – IARC
European Neuroendocrine Tumor Society – ENETS
Typical carcinoids – TC
Atypical carcinoids – AC
Neuroendocrine tumor – NET
Large cell neuroendocrine carcinoma - LCNEC
Small cell lung carcinoma – SCLC
Neuroendocrine carcinoma – NEC
Extrapulmonary neuroendocrine carcinoma – EPNEC
Mixed adenoneuroendocrine carcinoma - MANEC
Neuroendocrine neoplasm – NEN
Tumor mutational burden - TMB
Gastro-entero-pancreatic (tract) – GEP
Well differentiated thyroid cancer – WDTC
Papillary thyroid carcinoma – PTC
Follicular thyroid carcinoma – FTC
Medullary thyroid carcinoma – MTC
Poorly differentiated thyroid carcinoma – PDTC
Anaplastic thyroid carcinoma – ATC
Hürthle cell carcinoma – HCC
High-power field – HPF
Disease free interval – DFI
Overall survival – OS
Disease specific survival – DSS
Tumor microenvironment – TME
Tumor mutational burden - TMB
Sentinel lymph node biopsy – SLNB
Radiotherapy – RT
Merkel cell carcinoma – MCC
Merkel cell polyomavirus – MCPyV
Anaplastic lymphoma kinase – ALK
Chimeric antigen receptor T-cell – CAR-T cell
Human leukocyte antigen – HLA
Major histocompatibility complex – MHC

TABLE OF CONTENTS

CHAPTER 1: EXPLORATION OF NEUROENDOCRINE-LINEAGE TRANSCRIPTION FACTORS IN PULMONARY AND EXTRAPULMONARY MALIGNANCIES

This chapter is based on following papers:

1: **Metovic J**, La Salvia A, Rapa I, Napoli F, Birocco N, Pia Bizzi M, Garcia-Carbonero R, Ciuffreda L, Scagliotti G, Papotti M, Volante M. Molecular Subtypes of Extra-pulmonary Neuroendocrine Carcinomas Identified by the Expression of Neuroendocrine Lineage-Specific Transcription Factors. Endocr Pathol. 2022 May 24. doi: 10.1007/s12022-022-09722-4. PMID: 35608806.

2: **Metovic J**, Napoli F, Osella-Abate S, Bertero L, Tampieri C, Orlando G, Bianchi M, Carli D, Fagioli F, Volante M, Papotti M. Overexpression of a subset of neuroendocrine-lineage transcription factors is associated with adverse clinical outcome in pediatric neuroblastoma. (Accepted for publication - Virchows Archiv)

INTRODUCTION

Neuroendocrine differentiation in tumors.

Neuroendocrine (NE) cells are part of a large cell population, collectively known as the diffuse NE system, which is dispersed throughout the normal organism. The NE cells primarily exist within the organs that interface with the outside world, including gastrointestinal, respiratory, and genitourinary systems, as well as the skin (Merkel cells and melanocytes). Yet, they also can be found within endocrine glands or tissues, such as the hypothalamus, anterior pituitary, pineal gland, thyroid gland (calcitonin-secreting cells), thymus, breast, and the pancreatic islets of Langerhans (1–4). NE cells (formerly called APUD - Amine Precursor and Uptake Decarboxylation system) are chromaffin cells filled with secretory granules that produce biogenic amines, mainly catecholamines, but also hormones and other markers (5).

In the healthy organism, normal NE cells play complex local regulatory roles at the tissue level. For example, the NE cells of the gastrointestinal tract (also known as enteroendocrine cells) regulate secretion, motility, cell growth and differentiation in the gut. For this purpose, these cells employ endocrine, autocrine, paracrine, and neurocrine signaling mechanisms, and are, in turn, under neural control (6). The NE cells of the respiratory tract can control lung branching morphogenesis, cell growth and maturation during development, and it is believed that they provide a protective niche for a subset of lung stem cells. Similarly, to enteroendocrine cells, pulmonary NE cells are under control of a complex innervation (3).

Neuroendocrine differentiation (NED) represents a structural and functional feature of certain tumors, whereby a significant portion of malignant cells displays neuronal, endocrine, or mixed features. Of note, various studies have revealed that NED does influence patient prognosis. Bernick et al. (7) studied 38 colorectal cancer patients with NED and found that the prognosis of these patients was poor, as most patients have metastatic disease at the time of diagnosis. Moreover, some studies have indicated that colorectal cancer with NED was correlated with liver metastasis and advanced tumor stages (8). Similar findings were reported in a meta-analysis by Zeng et al. (9) that included 1,587 patients and revealed that patients with NED who underwent a radical operation had a lower 5-year survival rate (pooled OR 0.60, 95 % CI 0.37–0.97) compared with those without NED.

NE neoplasms are a group of rare diseases of the widespread NE system. These tumors represent a heterogeneous group of disease of varying degrees of differentiation and malignancy, characterized by well-defined histological and immunophenotypic features and clinico-biological characteristics.

In fact, NED is orchestrated by complex pathways (**Figure 1**, source ref. (10).

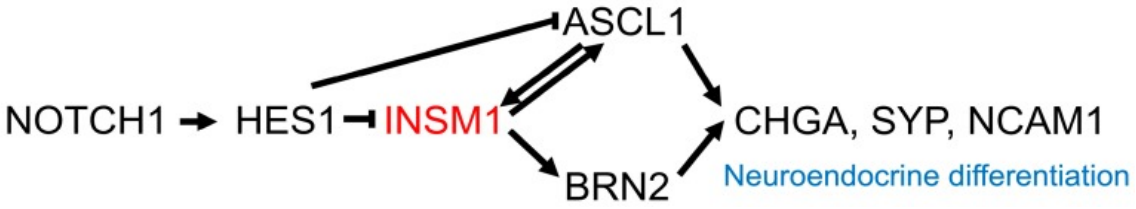

Figure 1. *Schematic of the complex pathways of neuroendocrine differentiation (blue) in lung tumors. INSM1 (red) is inactivated by HES1 and promotes the expression of the three neuroendocrine molecules (CHGA, SYP, and NCAM1) via activation of the transcription factors, ASCL1, and BRN2. INSM1 and ASCL1 activate each other* (10).

From an immunophenotypic point of view they are characterized by expressing specific markers of NE differentiation, namely Chromogranin A (CgA), Synaptophysin (SYN), Neuron-specific Enolase (NSE), CD56 (N-CAM / neural adhesion molecule), but also location-specific markers or transcription factors, for example TTF1 for the lung or CDX2 for the intestinal tract (11−14). CgA and SYN are well established NED markers (15,16), and together with CD56 are recommended markers to identify pulmonary tumors with NE differentiation (17) while on the other hand, NSE is considered generic NE markers of neurons and NE cells (18) with high sensitivity, and low specificity (19). More recently, a novel marker, namely INSM1 has been proposed a highly specific marker of neuroendocrine differentiation (**Figure 2**).

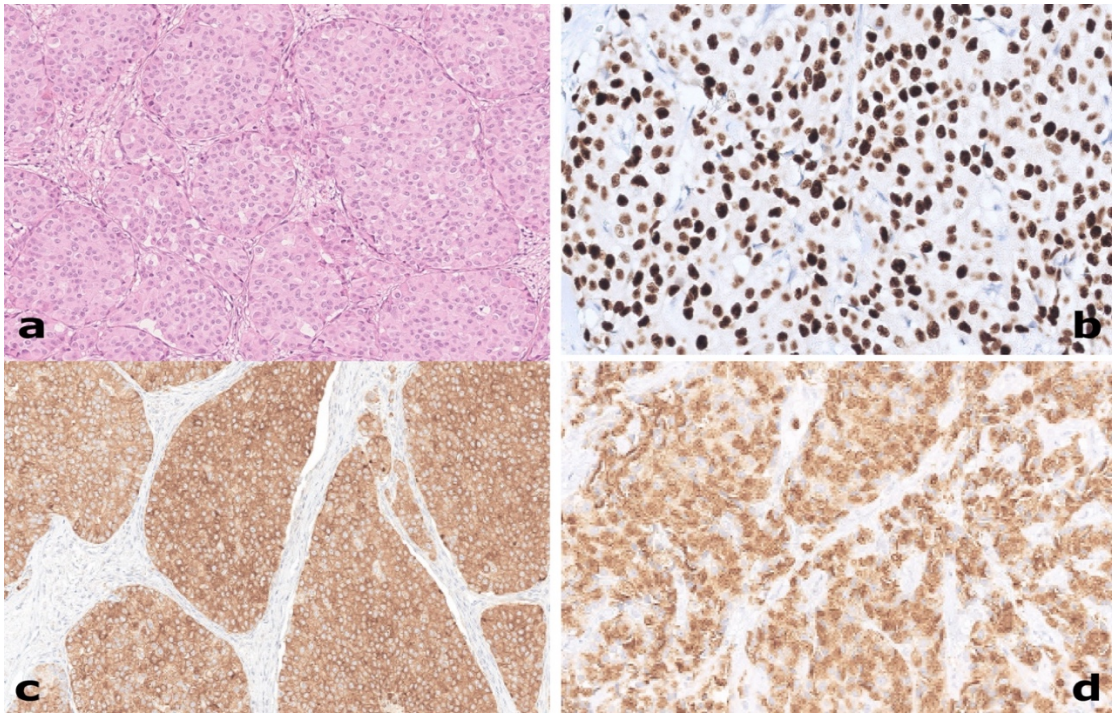

Figure 2. *A case of neuroendocrine tumor (G2) of breast origin (a, 100x), expressing INSM1 (b, 200x), Synaptophysin (c, 200x) and Chromogranin A (d, 200x).*

The WHO classification of neuroendocrine neoplasms.

The classification and nomenclature of NENs is complex and was often confusing in the past, due to the trend to focus on the organ of origin rather than the morphology and anatomo-pathological aspects. Recently, a common classification framework, developed by experts of the World Health Organization (WHO) and the International Agency for Research on Cancer (IARC), integrated with the European Neuroendocrine Tumor Society (ENETS) terminology for gastroenteropancreatic (GEP) NENs , is now applied in the latest 5th edition of WHO classification on lung NENs (20). The most important separation is between well differentiated neuroendocrine tumors of low (i.e., typical carcinoids - TC as G1) to intermediate (i.e., atypical carcinoids - AC as G2) grade (henceforth, NETs) and poorly differentiated NE carcinomas (henceforth, NECs), grouped together as high-grade neoplasms (G3) and consisting of small cell and/or large cell neuroendocrine carcinomas (LCNEC) (**Table 1,** source (21).

Table 1. *The WHO/IARC universal taxonomy for epithelial neuroendocrine neoplasia* (21).

Tumor category definition	Neuroendocrine neoplasia (NEN)	
Tumor family/class definition	Well-differentiated NEN	Poorly differentiated NEN
Tumor type definition	NET	NEC
Tumor subtype definition	Variable depending on site	Large cell NEC or small cell NEC
Tumor grade definition	G1, G2, G3	High grade (by definition)

This differentiation is of remarkable importance from a prognostic point of view, given that indolent forms tend to follow a prolonged course of disease, with low risk of metastatic spread (even in the absence of treatment), while malignant forms are associated with rapid progression and an adverse prognosis. The above categorization also has repercussions in the therapeutic field, where low-grade tumors are managed with simple resections surgical treatments or treatments based on somatostatin analogues and/or interferon-γ, while high-grade counterparts need platinum-based and etoposide-based chemotherapy drugs. The classification is reflected finally on the histological aspect of the lesions (in detail, below).

Furthermore, a third entity, namely mixed adeno-neuroendocrine tumors (MANEC), showing dual adenocarcinomatous and NE differentiation, in which each component represents at least 30% of the tumor, demonstrate by definition, high grade and poor prognosis (22,23). The latest WHO 2021 classification for lung neuroendocrine neoplasm (NENs) formally introduced the combined category (20).

Regarding the site of origin, NENs, more frequently emerge in the gastro-entero-pancreatic tract and lung. On the other hand, although rarely, NENs may arise in the upper respiratory tract, salivary glands, skin and the urogenital system. In most of these locations,

NECs are consistently more common than NETs (24). An additional site in which NENs may rarely occur is breast, where the last edition of the WHO classification has aligned the classification of the formerly called "carcinomas of the breast with neuroendocrine features" (25) to the classification framework proposed for all NENs (22,26,27). In fact, the classification of so-called breast NENs (Br-NENs) is still debated and a robust validation of Br-NENs as real entities with distinct molecular profiles is still lacking (28).
In order to render an accurate diagnosis, beside architectural and cellular features (especially small or large cells, but also organoid patterns and nuclear chromatin/nucleoli), it is also important to take into account the mitotic count, generally expressed for an area per mm^2, Ki-67 labeling index (henceforth, Ki-67) (29) and necrosis (generally described as absent, punctate, extensive) (22) (**Table 2**, source (21).

Table 2. *Neuroendocrine epithelial neoplasms: general features of well-differentiated neuroendocrine tumor (NET) versus poorly differentiated neuroendocrine carcinoma (NEC)* (21).

	Cytology	**Histology**	**IHC profile**
NET	• Clean smear • Cell monomorphism • Medium size, round shape • Abundant eosinophilic cytoplasm • Salt and pepper chromatin • No or very few mitotic figures	• Organoid structure (solid, trabecular, glandular, mixed) • No necrosis or only spotty • Delicate, highly vascularized stroma • Salt and pepper chromatin • Abundant cytoplasm • Cell monomorphism • Low nuclear/cytoplasm ratio • Round-oval shape • Rare or few mitoses	• CK + • CgA + • Syn + • INSM1 + • SSTR2/5 + • Hormones • Ki67 low • P53 wild-type staining • Rb retained
NEC	• Dirty smear—diffuse necrotic debris • Cell polymorphism • Absent or subtle rim of cytoplasm (SC type) • Evident/abundant cytoplasm (LC type) • Salt and pepper chromatin • Severe nuclear fragility • Frequent mitoses often atypical	• Solid/organoid structure • Abundant necrosis • Abundant fibrous stroma • Severe cell polymorphism • Round-irregular shape • High nuclear/cytoplasm ratio • Scant cytoplasm (SC type) • Abundant cytoplasm (LC type) • Severe nuclear molding • Salt and pepper chromatin • Frequent mitoses, often atypical	• CK + / − (dot-like) • CgA + / − • Syn + • INSM1+ • SSTR2/5 − / + • Hormones – • Ki67 high/very high (typically > 55%) • p53 global loss or diffuse positive • Rb global loss

*IHC, immunohistochemistry; NET, neuroendocrine tumor; NEC, neuroendocrine carcinoma; SC, small cell; LC, large cell; CK, cytokeratins; CgA, chromogranin A; Syn: synaptophysin; INSM1, insulinoma-associated protein 1; SSTR, somatostatin receptor; *: various, depending on anatomical site; p53, Tp53 gene product; Rb, retinoblastoma gene product*

Although NETs and NECs subtypes are part of the same family, they nevertheless have a different prognosis, response to therapies, different risk factors and hereditary predisposition (22).

Neuroendocrine neoplasms of the lung

Lung NENs comprise approximately 25% of all invasive lung cancers (30) and encompass four histologic subtypes whose terminology and defining criteria have been endorsed over the last three classifications by the WHO (20,31,32). Accordingly, lung NENs include TCs, ACs, LCNECs and small cell lung carcinoma (SCLC). There are major epidemiological, histological, clinical, genetic, and prognostic differences between the NETs (TC and AC) and high-grade NECs (both SCLC and LCNEC).
Around 90% of NENs are high-grade poorly differentiated tumours, including SCLC (approximately 75%) and LCNEC (approximately 15%), with carcinoids accounting for only a small proportion (2-10% TC and 0.2-1% AC) (20) (**Figure 3**, source (33).

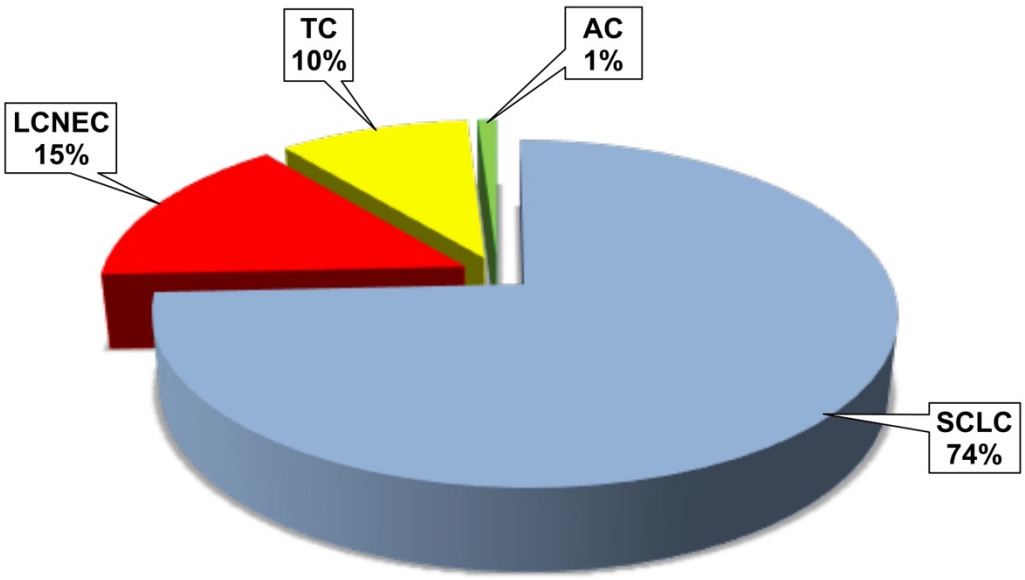

Figure 3. *Relative prevalence of lung neuroendocrine neoplasms. TC: typical carcinoid; AC: atypical carcinoid; LCNEC: large cell neuroendocrine carcinoma; SCLC: small cell carcinoma; LD: limited disease. SCLC and LCNEC account for the large majority of lung neuroendocrine neoplasms and TC are intermediately prevalent tumors, while AC make up truly uncommon lesions in population-wide tumor series* (33).

However, it should be underlined that around 25% of LCNEC or SCLC have histological components of adenocarcinoma or squamous carcinoma, identifying the subcategory of combined carcinomas (20,34). The distinction between NECs and NETs is currently based on morphologic characteristics, presence or absence of necrosis, and mitotic count (>10 per 2 mm^2 for NECs), and in particular for NECs, cytological characteristics of small or large cells, while immunohistochemical (IHC) markers are applied to reveal NE differentiation (35).
The assessment Ki67 has an important role to distinguish carcinoids from NEC, especially when studying scarce bioptic samples. Although there is no officially accepted cut-off proposed rates of Ki-67 ranged from 2.3–4.15% in TC (mean 2.60%), 9–17.8% in AC (mean 11.04%), 47.5–70.0% in LCNEC (mean 47.57%), and 64.5–77.5% in SCLC (mean 64.36%), in substantial agreement with the expected proliferation activity of these tumors (36). The upper limits of 5% and 30% for Ki-67 have been conceived to differentiate TC from AC and AC from NECs, respectively, with a better performance over mitotic count and/or necrosis in small-sized diagnostic material (37,38).

Several genomic studies have investigated the molecular profile of lung NENs for treatment purposes, however their underlying intrinsic mechanism is yet to be fully understood. The data regarding NETs indicate a low tumor mutational burden (TMB) and the presence of chromatin remodeling/histone modification gene mutations such as *MEN1* (10–25%), *ARID1A/B* (5–10%), *EIF1AX* (5–17%) and, more infrequently, members of the SWItch/Sucrose Non-Fermentable (*SWI/ SNF*) complex, such as *SMARCA4* (3–7%) (39–41). Rates of classical cancer driver involvement, such as *RB1* or *TP53* gene alterations, are negligible (42). These data are reported to be diametrically opposed to high grade NECs that consistently harbor *TP53* mutations, *RB1* alterations, and high TMB (42–45) (**Table 3**, source (33).

Moreover, in a series of 108 pulmonary NENs (52 LCNEC, 44 SCLC, 12 carcinoids) genomic alterations were found in 11% of the cases, including mutations of *PIK3CA* (4.6%), *EGFR* (2.8%), *KRAS* (1.9%), rearrangement of *ALK* (0.9%) and *RET* (0.9%), but no alterations of *ROS1, BRAF, NRAS* and *HER2*. Gene alterations occurred in 15.4% of LCNEC, 6.8% of SCLC and 8.3% of carcinoids (46). *JAK3, NRAS, RB1 a*nd *VHL1* gene alterations were exclusively identified in SCLC, whereas *FGFR2* mutation was detected in LCNEC, only (47) (**Table 3**, source (33).

Clinically, carcinoids (typical and atypical) occur more frequently in young patients, with no history of cigarette smoking and poorly responding to therapy with cisplatin/etoposide but therapy with inhibitors of the mTOR pathway, like *Everolimus*, gave promising results (48). On the other hand, NECs have different characteristics, appearing more frequently in elderly patients, smokers and have unfavorable prognosis. Typically, SCLC show an initial and complete response to therapy with cisplatin in combination with etoposide, as compared to carcinoids (49).

Table 3. *Main molecular alterations in neuroendocrine tumors and carcinomas (33).*

Tumor types → Gene alterations ↓	NET G1 – G2 TC and AC	NEC (G3) small cells SCLC	NEC (G3) large cells LCNEC
Mutation rate per million base pairs	<1	7–13	7–13
Genetic segregation	No	Yes	Yes
Cell cycle/differentiation abnormalities	-	TP53 and RB1 biallelic loss of function	More variable p53, RB1 inactivation
Main gene alterations	MEN1 (11-22%), EIF1AX, SWI/SNF complex (ARID1A, SMARCA2/4, SMARCB1)	mutations of KIAA1211,COLL22A1, RGS7, FPR1, CREBBP, EP300, MLL, FMN2, ASPM, ALMS1, PDE4DIP, XRN1 and Notch-family genes; copy number variations of FHIT, FGFR1, Sox, MYC, ROBO1; rearrangement of TP73; inactivation of NOTCH; molecular subtypes SCLC-ASCL1, SCLC-NeuroD1, SCLC-Yap1, SCLC-Pou2F3	10% LCNEC-carcinoid type (MEN1-, RB1+, SSTR+, p53-, EZH2+); 40% LCNEC-NSCC like (p53+, STK11, KEAP1, KRAS, NE+++, RAS/PIK3CA/AKT activation); 40% LCNEC-SCLC like (p53-, RB1+/, MYCL amplification, activation of NOTCH, REST, PIK3CA-AKT)
EZH2 expression	Negative to low	High	Low to High
Smoke association	Uncommon	Strong	Strong
G:C to T:A transversions	Uncommon	Common	Common

TC: typical carcinoid; AC: atypical carcinoid; LCNEC: large cell neuroendocrine carcinoma; SCLC: small cell carcinoma; G:C stands for guanine:cytosine; T:A stands for thymine:adenine

Typical and atypical pulmonary carcinoids (NETs)

Pulmonary NETs are rare and heterogeneous disease. The reported incidence of NETs is increasing, likely because of better diagnostic capabilities (50). Lung NETs demonstrate a variety of pathologic and clinical features and require varying treatment strategies.
Carcinoids, whether TC or AC, may show diverse architectural patterns and/or cellular variants, e.g., insular, lobular, trabecular, follicular, and solid) and/or cellular variants (polygonal, spindle, oncocytic, mucinous, melanin-laden, etc.) within the same tumors. Both TC and AC are characterized histologically by a uniform population of tumor cells growing in an organoid pattern and having moderate eosinophilic, finely granular cytoplasm with finely granular nuclear chromatin (20,51).

ACs are defined as carcinoid tumors showing mitoses between 2 and 10 per 2 mm^2 area of viable tumor (10 high power fields in certain microscopes) or the presence of necrosis. The presence of features such as pleomorphism, vascular invasion and increased cellularity is not as helpful in separating TC from AC. In TC, necrosis is absent and mitotic figures are rare (<2 per 2 mm^2). Necrosis in AC usually is manifest by punctate foci within tumor nests (20,51,52).

Although NETs are slow growing tumours, advanced disease is associated with poor survival. The primary tumour site has been shown to be a powerful predictor of survival duration, with the median survival of patients having metastatic lung nets being found to be 16 months. Although NETs are slow growing tumors, advanced disease leads to poor survival, and in patients with well-differentiated NETs with distant metastasis, 73% will die within 5 years (53,54).

Curiously, some carcinoids show genetic alterations very similar to LCNECs but with a different prevalence within the subtypes. The fact that the same genetic alterations found in LCNECs were also found in carcinoids (which are low/intermediate-grade) but with less prevalence suggests that there is progression of malignancy and the development of high-grade NE tumors from pre-existing carcinoids (40).
In fact, genomic studies show that atypical carcinoids show genetic and molecular characteristics somewhere between typical (low grade) and NECs (high grade) carcinoids.
By studying the link between the molecular alterations of LCNECs and atypical carcinoids it was possible to group these tumors into 3 clusters, respectively (C1-C3) based on the genetic alterations: the C3 group with predominantly atypical carcinoids and a small component of LCNEC, where the inactivation of MEN1 stands out; the C1 group with mainly LCNEC and a small proportion of carcinoids where there is mainly an inactivation of RB (type II, see ref. (55) and TP53 with no mutation in MEN1; and a mixed C2 group with intermediate characteristics between C1 and C3, with more frequent mutation in TP53, followed by mutation in MEN1 and RB in order of frequency (56).

All this leads us to an understanding that a progression of malignancy from low grade carcinoids to LCNEC is very likely. In particular, the C2 cluster shares intermediate alterations between the two tumor types, it can be further divided into two subtypes: C2a, very similar to

C1 with a Ki67 of approximately 60% and the presence of LCNEC with mutations in TP53 and alterations in RB; C2b, more similar to cluster C3 with a Ki67 of about 12% and predominantly MEN1 mutations. The C2a subgroup was recently labeled as "supracarcinoid" and identifies carcinoids that have histopathological characteristics as such but with molecular characteristics similar to LCNECs, which could strengthen the hypothesis that a carcinoid can evolve into an LCNEC with an accumulation of mutations. This is particularly true for that fraction of carcinoids with mutation in TP53 and no alterations in MEN1 (56). All this is also reflected at the prognostic level. For instance, cluster C1 shows a mean Ki67 of 66% with a median survival of 19 months, cluster C2 shows a mean Ki67 of 37% with a median survival of 47 months, However, patients pertinent to C3 cluster with a mean Ki67 of 21% did not reach the median survival during follow-up.

Moreover, performing integrative and comparative genomic analyses, Alcala and colleagues (57) revealed a separate very small subset of carcinoids (six instances), named “supra-carcinoids”, which suggested a molecular and behavioral link between atypical carcinoids and LCNEC. As a matter of fact, this subgroup displayed AC-like features (two to four mitoses per 2 mm2; no necrosis), but molecular and survival characteristics were analogous to fatal LCNEC rather than SCLC, along with higher expression levels of immune checkpoint genes (*i.e., PD-L1, CTLA4*) and higher expression of MHC class I and II genes (57). A relationship between these supra-carcinoids/LCNEC and the newly proposed categories of carcinoids with escalation of proliferation rates (58) and carcinoid-like LCNEC (43) is unlikely due to higher mutational load and different mutation profile of supra-carcinoids (57). These findings, however, support blurred boundary among tumors straddling AC and NECs (59,60).
The molecular intertwining between carcinoids and, at least, a few LCNECs is also reinforced by a recent next-generation sequencing study (43), where the authors revealed, in a minority of cases (10% of LCNEC), a carcinoid-like LCNEC profile enriched by *MEN1* mutations and with low TMB.

Large cell neuroendocrine carcinoma (LCNEC)

LCNEC tends to occur more commonly in males and in people aged > 65 years, and > 90% patients are heavy smokers (20). LCNECs exhibit NE morphology such as organoid growth, trabecular pattern, and peripheral rosette-like and palisading structures. Cancer cells are usually large with moderate to abundant cytoplasm. Nucleoli are frequent, often prominent, and their presence, in addition to cell size, facilitates the distinction from SCLC. This type of tumor is very often combined with adenocarcinoma or squamous carcinoma, and also some SCLCs have a component of LCNEC (55).

The genetic profile of some LCNECs is very similar to that of SCLC by highlighting the same transcriptional subgroups, in particular genes for cell cycle control and mitosis and DNA repairers, while it has been seen that the adenocarcinoma and squamous carcinoma mostly express genes for cellular differentiation, adhesion and for the immune response.

(42,61). Like SCLC, LCNEC exhibits an extremely high mutation rate (over 7.4 protein-changing mutations per million base pairs) compared to other types, possibly related to tobacco carcinogens. Inactivating mutations of *TP53* and *RB* are frequent, as are recurrent mutations of the *CREBBP*/*EP300* and MLL genes encoding histone modifiers, which are observed in 18% of SCLCs and are characteristic of a SCLC-like subset. In fact, the molecular spectrum of LCNEC is more heterogeneous, with two well-distinguished large groups of samples: type-I LCNEC, with frequent alterations in *TP53*, *STK11* and *KEAP1*, and type-II LCNEC, with alterations in both *TP53* and *RB1*(43,55).

In detail, type I (NSCLC-like LCNEC) besides the absence of *RB1/TP53* joint alterations, generally shows *KRAS* and/or *STK11* mutations, typical of adenocarcinomas, or *KEAP1*, typical of squamous cell carcinoma. Type II (SCLC-like LCNEC) is characterized by *RB1/ TP53* inactivation and *MYCL1* amplification along with the squamous carcinoma-related *KEAP1-NFE2L2* alterations (43,55,62,63). These molecular differences certainly influence histomorphology and proliferation rates of each tumor subset, with smaller cells and higher proliferative rates in the SCLC-like LCNEC subgroup as compared to the NSCLC-like one. The latter is dominated by larger cells and a more variable cell proliferation, despite some overlap exists between them. Moreover, NSCLC-like LCNEC exhibited low-level reactivity for napsin-A, whereas none of the SCLC-like tumors expressed this marker (64). On the other hand, a low-level expression of squamous differentiation marker, p40, likely related to *KEAP1–NFE2L2* alterations, was restricted to SCLC-like LCNEC (43), suggesting a link to NSCC ancestors (60). It has been suggested that patients with SCLC-like LCNEC had a shorter overall survival than those with NSCLC-like LCNEC, regardless of their higher response rate to chemotherapy (65). Furthermore, treatment with conventional SCLC chemotherapy (etoposide-platinum) was associated with superior response and longer survival in SCLC-like LCNEC as compared to pemetrexed-platinum and gemcitabine/taxane-platinum regimens, while treatment with gemcitabine/taxane-platinum suffered from shorter survival as compared to etoposide-platinum or pemetrexed-platinum in patients with NSCLC-like LCNEC (65).

The expression of the RB protein is lost in all cases in which the gene is mutated but also in 47% of cases in the wild type RB gene. Therefore, the evaluation of the real expression of the protein is more reliable to evaluate the inactivation rather than the analysis of the mutation itself. This is an important consideration given that protein expression is strongly de-regulated or lost in 72% of LCNECs (66). It is also necessary to take into account the close relationship between the RB protein and the P16 protein, an inhibitor of CDK4 / 6 kinases that normally phosphorylate RB by activating it. The expression of P16 and the inactivation of RB are closely related and mutually exclusive in LCNEC, between 46% and 78% of cases. Of note, patients with LCNEC tumors that harbor a wild-type and/or express *RB1* have superior overall survival when treated with NSCLC-chemotherapy (platinum + gemcitabine or taxanes) compared with SCLC-chemotherapy (platinum-etoposide) (66).

Tumors with SCLC-like molecular characteristics were seen to be more proliferating, with substantial histological overlap, underlining that these molecular subtypes cannot be accurately predicted by routine morphological examination in individual cases. On the other hand, evaluating the RB1 alteration, a key characteristic that defines the "SCLC-like" group, it

was seen that it can be precisely identified by the IHC, which was also detected in few cases with loss of pRB proteins in the absence of genetic mutations, which could be mediated by mechanisms such as hypermethylation of the promoter, or epigenetics. Therefore, in a case with LCNEC morphology, the expression of intact pRb IHC status could serve as a marker of the NSCLC-like subtype, even in the absence of molecular tests. Conversely, loss of pRb expression, although favoring the SCLC-like subset, would require molecular confirmation of the mutation in TP53, given the rare possibility of pRb loss in the absence of a TP53 mutation. Overall, pending further validation, the data suggest that the IHC could be used to predict the molecular subtype of LCNEC in at least a subset of cases at the time of histopathological evaluation (43) (**Figure 3**, source (55).

Furthermore, SCLC-like LCNEC patients have a shorter overall survival than those NSCLC-like, despite higher chemotherapy response rates. Thus, genomic subtyping might be useful for the purpose of prognosis and therapeutic decisions in LCNEC patients, since the molecular features of pulmonary carcinoid tumors and LCNEC subtypes seem to have key management implications (65–67).

Small cell lung carcinoma

SCLC accounts for approximately 15% of all lung cancer and is the leading cause of cancer death among men and the second leading cause of cancer death among women worldwide (68,69). Also, SCLC is the most common NEN of the lung. It is characterized by rapid growth and early distant metastasis, already at time of diagnosis of the primary tumor. The prognosis of patients with SCLC is dismal with a 5-year survival rate of less than 5% and an average overall survival period of only 2–4 months for patients not receiving any active treatment (70).

SCLC is defined by light microscopy as a tumor with cells that have a small size, a round-to-fusiform shape, scant cytoplasm, finely granular nuclear chromatin and absent or inconspicuous nucleoli. Nuclear molding is frequent. Crush artifact can cause smearing or streaming of nuclear chromatin. Necrosis is frequent and often extensive. Mitotic rates are high, with an average of 80 mitoses per 2-mm^2 area. In small biopsies, mitoses may be difficult to identify, and necrosis may be absent because of limited sampling. The tumor usually grows in diffuse sheets, but rosettes, peripheral palisading, organoid nesting, streams, ribbons and rarely, tubules or ductules that fall short of glandular differentiation may be present (51).

SCLCs harbor several mutations that are enriched in those that encode kinases, G-protein coupled receptors and chromatin-modifying proteins, genes encoding histone modifiers (*CREBBP, EP300* and *MLL*), as well as several members of the SOX family (61,71).
A whole genome sequencing study in nine cases of SCLC transformation was able to reconstruct the clonal evolutionary history and to detect genetic predictors for SCLC transformation (72). In fact, the authors identified that epidermal growth factor receptor tyrosine kinase inhibitors (EGFR TKI)- resistant lung adenocarcinomas and SCLCs share a common clonal origin and undergo branched evolutionary trajectories. The clonal divergence of SCLC ancestors from the lung adenocarcinoma cells occurred before the first EGFR TKI

treatments, and the complete inactivation of both *RB1* and *TP53* were observed from the early lung adenocarcinoma stages in sequenced tumors, hence, the evaluation of RB1 and TP53 status in EGFR TKI-treated adenocarcinomas is informative in predicting small-cell transformation (72).

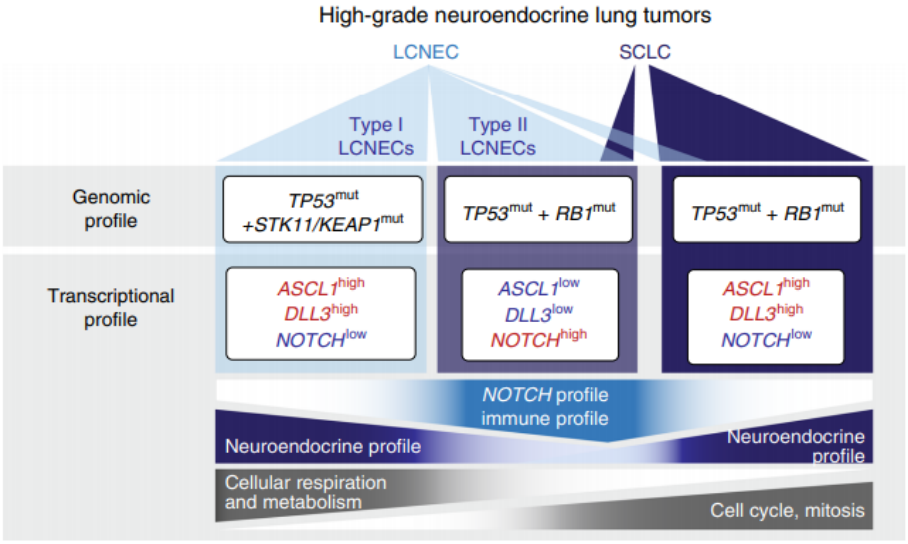

Figure 4. *Schematic overview of somatic alterations and expression profiles in high-grade neuroendocrine lung tumors. Significantly mutated genes are shown in black and differentially expressed genes are highlighted in red and blue, describing higher and lower expression, respectively. Upregulated expression profiles and signaling pathways are indicated by color gradients* (55).

Moreover, through the link between susceptibility to infection by a picornavirus (SVV) and SCLC cells, it was possible to understand the relative expression and existence of two different transcription factors: ASCL1 (or HASH1) and NEUROD1 (73), later to be understood responsible for NE differentiation in SCLC (74) (**Figure 4,** source (55).

ASCL1 activates NE differentiation, and regulates stemness, cell cycle progression, and mitosis. ASCL1 expression is limited to dormant progenitor pulmonary NE cells in mature lung but its reactivation in NE carcinomas maintains tumor development and survival. Its targets are *MYCL1*, *RET*, *SOX2*, *BCL2* and nuclear factor I B (*NFIB*) oncogenes, as well as NOTCH ligand *DLL3*. Of note, *NKX2-1* (also called *TTF1*) gene expression is also positively regulated by ASCL1 (75) as well as *BRN2* (brain-2; also known as *POU3F2*) (76). In contrast, NEUROD1 promotes neurogenic differentiation of cells during development and malignant behavior in SCLC cell lines. It targets *MYC* (77) and oncogenic Myc^{T58A} promotes the development of slow growing NE tumors (78). Of note, both ASCL1-high and NEUROD1-high SCLCs express insulinoma associated protein 1 (*INSM1*), which is a driver of NE differentiation in many organs and tissues (79).

Beside ASCL1expression in high-grade pulmonary neoplasms (80–83), evidence also suggests that it is present in a significant fraction (70%) of extrapulmonary NECs (84), and it is reported to be an effective therapy target for pulmonary NECs, by delivering ASH1-RNAi (oligonucleotides or adenovirus) (85). In addition, it could represent a target centered on *BCL2* gene activity, which is highly expressed by SCLC (81). Interestingly, lung cancer cells that are transfected with *ASCL1* gene were recently shown to be associated with the expression of various molecules including INSM1 and ISL1 transcription factors as well as SYT4, KTCD16 and SEZ6 that are related to neurosecretory functions (86).

For instance, in a study by La Rosa et al (84) an extensive series of 335 NENs of various origins and differentiation has been prompted for IHC and RT-PCR *ASCL1* analysis. This marker was identified in 82% and 70% of pulmonary and extrapulmonary NECs, respectively. Moreover, it demonstrated relatively high diagnostic sensitivity and specificity in distinguishing lung NECs from NETs. Furthermore, this marker has been recommended as an indicator of poor differentiation that may help to distinguish NECs from NETs in difficult cases, regardless of their site of origin. These data were confirmed in various studies (87,88) where, beside the role of ASCL1 in staining NE differentiated high-grade carcinomas, it was recommended as a useful tool in differential diagnosis with other non-NE lesions, such as squamous cell carcinomas or adenocarcinomas.

In particular, ASCL1 was observed to be expressed to a variable extent by SCLC with high NEUROD1 expression, therefore a low ratio of ASCL1 to NEUROD1 was a strong correlation of expression permissiveness. This initial dichotomy between "classic" SCLC, with a high ASCL1/NEUROD1 ratio and "variant" SCLC, demonstrating the opposite, made more clear that these two subtypes express different levels of these two transcription factors, one mostly *ASCL1* and the other *NEUROD1.*
Recent studies have provided biological insights into the role of *ASCL1* and *NEUROD1* and have identified other factors relevant to the subtype definition (82,89). In addition, several target genes regulated by these transcription factors have been identified such as *MYCL1, BCL2, SOX2, DDL3* for *ASCL1, MYC* for *NEUROD1,* and *INSMI* and *HE6* common to both.

A small fraction of SCLC expresses low levels of *ASCL1, NEUROD1* and *INSMI* expressing higher levels of markers such as *YAP1* and *POU2F3,* thus identifying two other subtypes. Different terminologies have been used to identify these different subtypes, the most recent therefore divides SCLC into four groups, based on the transcription factor expressed: SCLC-A, SCLC-N, SCLC-Y, SCLC-P (82). However, research in this regard is constantly evolving.
A classification has also been hypothesized by defining a score between NE and non-NE subtypes that distinguishes SCLC A and N from subtypes Y and P (**Figure 5**, source (82). Furthermore, the degree of expression of *ASCL1* is variable within SCLC-N and is still unclear what differences there are between tumors expressing multiple transcription regulators at different levels and tumors expressing one individually (82).

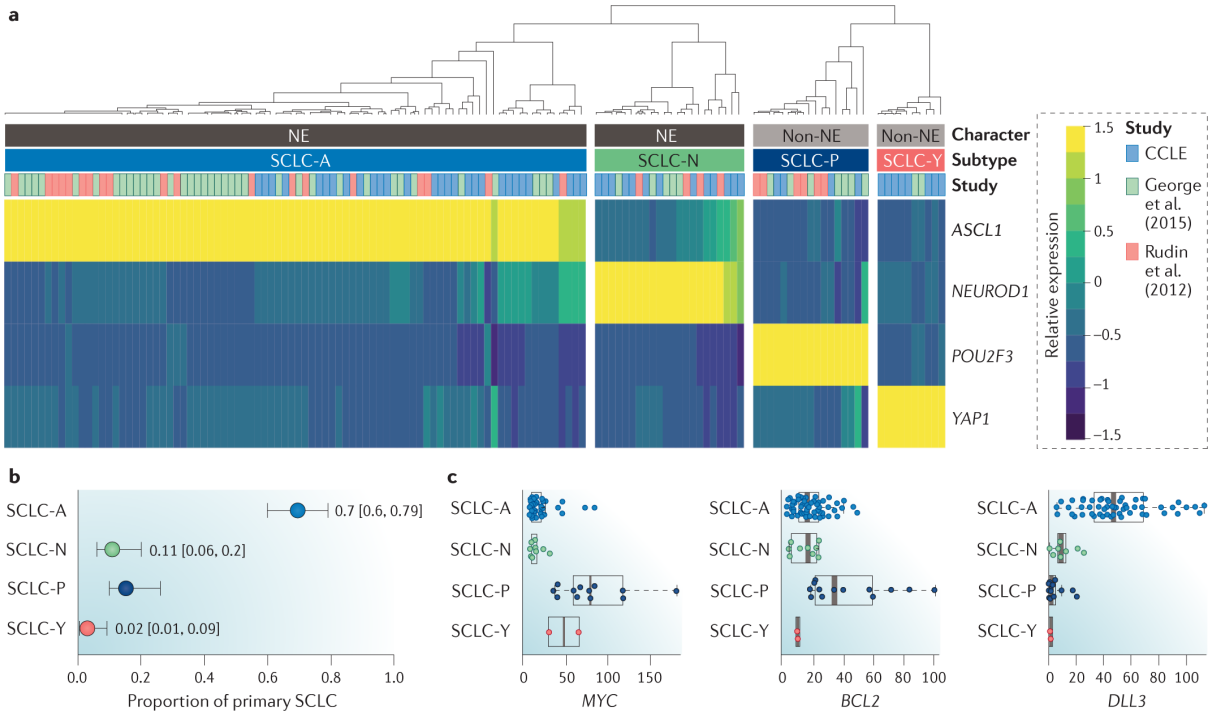

Figure 5. *(**a**) Hierarchical clustering of relative gene expression of four key transcription regulators defining subtypes in human small cell lung cancer. Clustering was performed using the R statistical computing environment, and the colour bar scale represents relative expression on a log scale. (**b**) Estimates of relative frequencies of the four subtypes based on representation in primary human tumour data sets with 95% CIs (n = 81). (**c**) Examples of differential expression of genes of interest (MYC, BCL2 and DLL3 are shown) among each subtype in primary human tumours (n = 81)* (82).

Understanding the different genetic pathways helps us to develop different targeted therapeutic strategies. Proteins such as DDL3 or BCL2, targets of ASCL1, therefore falling within the subtype of SCLC-A, are already being studied for target therapies. The activity of histone demethylase LSD1 involved in epigenetic modification is believed to play an important role in the SCLC subtype-A; its inhibition leads to an activation of NOTCH1 with final result of suppression of ASCL1 in SCLC. These inhibitors have already been tested in patients of this subtype. Another interesting study evaluates the role of the previously mentioned picornavirus SVV which has a marked tropism towards SCLC-N suggesting a strategy to increase immunotherapy, introducing the virus directly into tumor cells, thus stimulating its aggression by the *YES*. Other studies with IGF1R inhibitors have seen how the SCLC-P subtype is vulnerable to the absence of IGF1R, suggesting a re-evaluation of IGFR1 as target therapies for this subtype (82).

Despite the initial promising results with an antibody drug conjugate targeting DLL3, in the face of larger prospective studies that failed to replicate the efficacy of Rova-T in relapsed SCLC, this specific therapy now appears illusory. On the other hand, strategic pairing of DNA repair inhibitors, such as PARP inhibitors, with standard chemotherapy agents could lead to improvements in efficacy based on the results of early phase II study findings (70).

In comparison to the rest of lung cancers, data of PD-L1 expression and its clinical implications in lung NENs are limited but clinically worth exploring especially in the setting of life-threatening NECs. In fact, Tsuruoka et al. have mostly noted PD-L1 expression in high-grade lesions (10.4% of LCNEC and 5.8% of SCLC) showing median H-score of 45 (range 10-160), rather than carcinoid tumors where no reactivity was observed (90). In the same study, PD-L1 expression has been significantly correlated with age, only. In a different study, however, where 131 TCs and 37 ACs were investigated, PD-L1 expression was detected in 7% TCs tumors but no ACs (91), while in another paper none of the tested SCLCs and extrapulmonary small cell carcinomas stained positive for PD-L1 (92). These apparently contrasting findings document that differences in patients' selection or methodology procedures, including the choice of reagents or other assessment variables, might account for heterogeneity in the distribution of PD-L1 expression across the spectrum of lung NENs (33).

A better understanding of the biology of SCLC and the recent identification of above described molecular subtypes defined by differential expression of four key transcription regulators (82) may represent a significant step forward in defining a winning treatment strategy for SCLC.

Extra-pulmonary neuroendocrine neoplasms.

Even in extrapulmonary sites, NENs are divided into two groups based on morphology, number of mitoses, proliferation index: well-differentiated NETs (low or intermediate grade; G1 / G2) and poorly differentiated NEC (high grade; G3, large or small cell) (93). Only the latter will be described below.
This categorization is clinically relevant with respect to the impact on treatment and prognosis although it is not absolute, as a subset of low-grade appearance tumors may behave similarly to high-grade lesions.

Extra-pulmonary neuroendocrine carcinomas (EPNEC)

According to tumour cell morphology, two subtypes of NEC are recognised (94). The small cell type is defined by the presence of small-sized tumour cells, an elongated, hyperchromatic nucleus, devoid of visible nucleoli. The large cell type, first described in the lung, but later identified in most other body sites, is defined by the presence of large-sized tumour cells, containing a large, ovoid, vesicular nucleus with well visible nucleoli (44,55). Irrespective of their subtype, patients with NEC usually present with disseminated disease and have an adverse prognosis (95). The accurate diagnosis of small versus large cell EPNEC is challenging. The cytological, architectural and immunophenotypic characteristics have to be evaluated. In fact, small cell EPNECs have uniform morphological characteristics, similar to SCLC; on the contrary, those with large cells or mixed small-large cells differentiate with characteristics related to the site of origin. However, the distinction between SCC and LCNEC may seem superfluous, not only for the same clinical course, but also because very often many cases contain a mixed population of small and large cells. However, similar to what occurs in the lung, small cell EPNECs generally present with solid growth, finely granular nuclei and evident nucleoli. On the other hand, as mentioned above, large cell EPCNECs have a more structured architecture (solid, trabecular or organoid) with large nuclei and hyperchromatic nucleoli (96). However, the distinction between the two forms is not simple because there are no specific markers to discriminate small or large cell tumors, despite their specific characteristics. This is because both exhibit an epithelial immunoprofile with a broad spectrum of cytokeratins expression, although occasionally, particularly in SCCs, they have a para-nuclear “dot like” distribution. On the other hand, high molecular weight cytokeratins are generally absent in most NE tumors regardless of the anatomical site. There are also mixed NECs with a conventional non-NE component, very similar to their pulmonary counterparts (96).

While lung NEC are typically associated with a strong history of smoking, recent studies have suggested that the association with smoking for EPNEC is weaker (97). Also, compared to lung NEC, the incidence of brain metastases appear to be lower in EPNEC (98).
These tumors are virtually distributed throughout the body, but the most frequent sites are in the gastro-entero-pancreatic tract (GEP) including the esophagus, stomach, pancreas, colon and

rectum; in the prostate, bladder, cervix, skin (Merkel cell carcinoma), breast. An incidence of only 1.5 cases per 100 000 inhabitants per year is reported in Europe (99).
The gastrointestinal tract accounts for an estimated 35% to 55% of all EPNECs. The median overall survival for patients with localized disease is 38 months (100). However, 85% of the patients present with metastases, and their overall survival is only 5 months. In 5509 EPNECs of gastrointestinal origin in the Surveillance, Epidemiology, and End Results (SEER) database, esophageal NECs most commonly had a small cell morphologic makeup (74%), unlike gastric NECs (35%) or colorectal NECs (23%) (94).

There is insufficient data to assert that genetic molecular analysis allows an effective distinction between small and large cell EPNECs. As regards the NE markers, CgA and SYN are usually expressed, while NSE and CD56 are less specific. Interestingly, up to 80% of EPNEC express the thyroid- and lung-specific marker TTF-1, thus limiting its usefulness in the definition of the primary location in the cases of NEC of unknown primary origin (96,101,102) (**Figure 6**, source (96).

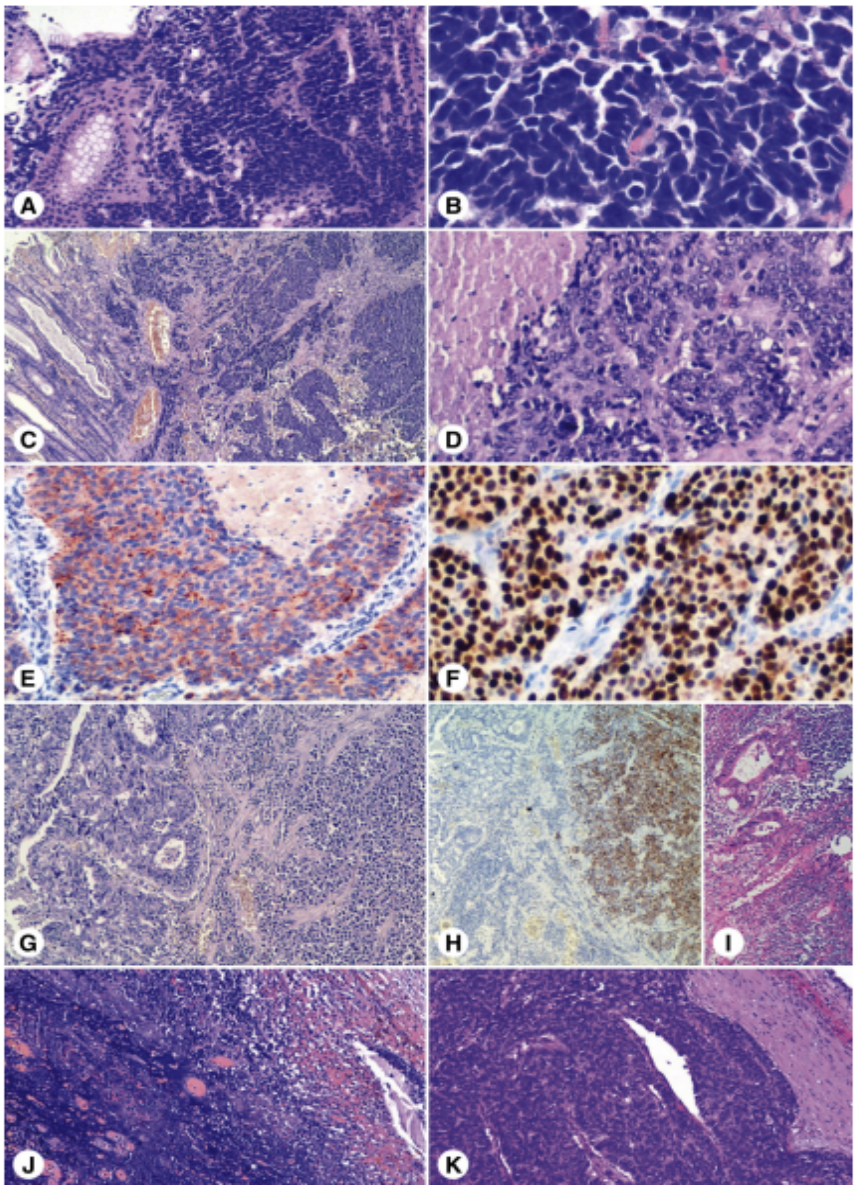

Figure 6. *A and B, A biopsy specimen of a small cell NEC of the stomach (H&E; original magnification ×200 and ×400 for A and B, respectively). C-F, A case of LCNEC of the rectum, deeply invasive (C), composed of large atypical cells with irregular nuclei having prominent nucleoli (D), typical dot-like patterned chromogranin A expression (E), and very high Ki-67 proliferation index (F) (C and D, H&E; E and F, immunoperoxidase; original magnification: C, ×100; D and F, ×400; E, ×200). G-I, A mixed adeno-NEC of the stomach showing two distinct tumor cell populations (G) with chromogranin A positivity restricted to the NE (large-cell) component (H) and a single lymph node micrometastasis from the adenocarcinomatous component (I) (G and I, H&E; H, immunoperoxidase; original magnification: G, ×200; H, ×100; I, ×400). J, A biopsy specimen of a case of small cell carcinoma of the bladder with extensive crushing artifacts (H&E; original magnification ×200). K, A case of LCNEC of the renal pelvis (H&E; original magnification ×200) (96).*

The differential diagnosis of EPNECs must first consider the poorly differentiated forms of the corresponding non-NECs or other hematological and mesenchymal malignancies. Especially regarding the component of non-neuroendocrine carcinomas often associated with EPNECs, it is necessary to rely on morphological parameters and an appropriate evaluation of immunohistochemistry. Most often the non-neuroendocrine component is completely separated from the neuroendocrine one but more often it is mixed with them, even if not immediately apparent (96).

First of all, it is necessary to identify the neuroendocrine component and then evaluate the relative proportions of the exocrine and endocrine components. This is important both for the clinical impact and for the response to therapies.

In the GEP area it is extremely important to identify the MANECs in 30% of the components, to define the tumors of mixed type. In the stomach, mixed tumors follow an intermediate behavior between pure LCNEC, the most aggressive, and conventional adenocarcinoma. In the colon and rectum, the extension of the neuroendocrine component does not predict clinical behavior and the prognosis between MANEC, and NEC is comparable. In the hepatobiliary system, on the other hand, few components of MANEC were found (96,103).

In the urogenital tract, both combined exocrine / neuroendocrine carcinomas and EPNECs are common. In the prostate, EPNECs appear either as pure SCC (57%) or combined with adenocarcinoma, with a high Gleason Score (> 8). Some SCCs can be confused with more usual and frequent poorly differentiated adenocarcinomas also due to their greater rarity. However, most undiagnosed cases are MANECs since very often the small cell component is considered as a more poorly differentiated area of adenocarcinoma (104).

In the bladder, both the mixed neuroendocrine forms with urothelial carcinoma and the pure forms of EPNEC show a poor prognosis compared to the pure non-neuroendocrine urothelial component. The bladder is the most frequent extra pulmonary site of SCC. The origin of the neuroendocrine component in these tumors is not clear, but studies suggest a metaplastic transformation from the urothelial carcinoma epithelium, and this would explain why in 50% of urothelial small cell NECs there are components of urothelial carcinoma (105) (Table 4, source (96). In the female genital tract, the most frequent site of EPNECs is the uterine cervix with a NE component mixed with squamous carcinoma. As for the bladder, the NE component has a negative prognostic index (106).

Table 4. *Comparison of general characteristic of pulmonary and extrapulmonary (divided into GEP and urogenital tract locations) NECs* (96).

Location	Relative frequency as compared to NETs (carcinoids)	Most prevalent type (SCC *vs* LCNEC)	Frequency of mixed NE and non-NE features	Etiologic/ risk factors	Precursor lesions
Lung	More frequent	SCC	Very rare	Cigarette smoking	Unknown
GEP	Less frequent	LCNEC	Frequent	Unknown	Unknown (possibly divergent differentiation from adenocarcinoma)
Urogenital tract	More frequent	SCC	More than 50% of cases	Unknown	Unknown (possibly divergent differentiation from carcinoma subtypes)

In the skin, the rare example of EPNEC is Merkel cell carcinoma. The etiology of this tumor is partly attributable to the integration of the polyoma virus within Merkel cells. It is a high-grade and poorly differentiated tumor, being size of the tumor the fundamental prognostic factor. The spectrum of MCCs includes small cell, intermediate cell and large cell carcinomas, so there is no rigid diagnosis dichotomy between small and large cells (107).

Differential diagnosis with well-differentiated low-grade NENs (carcinoids) in some samples can be complex. In fact, cases of well-differentiated NE tumors (NETs) made of small cells do exist as either the result of artifactual cellular size changes (frequent in small biopsies or cytological specimens) or, more rarely, as a special small cell variant of such tumors. There may also be cases of NETs with a borderline number of mitosis and / or extensive necrosis, which can lead to the suspicion of EPNECs (96,108).

Currently, the correct approach consists of counting mitotic figures, supported by the evaluation of Ki67, which represents immunohistochemical gold-standard marker of correct differential diagnosis between well differentiated and high-grade neoplasms. In a small percentage of cases some NETs, show a Ki67 above 20%. In this case evaluation of the CgA immunohistochemical status may be of help, as it is generally focal and / or paranuclear in EPNEC, while it is uniform and cytoplasmic in NETs.

Recently, a revised classification of GEP NENs was proposed (93). The latest edition clearly stated the differences between NETs from NECs and introduced new entity, namely, G3 NET to encompass highly proliferating NENs with well differentiated morphology, restricting the definition of NEC to NENs with poorly differentiated morphology, only. In fact, G3 NETs represent about one third of all high grade GEP NENs, are most common in the pancreas, stomach, and rectum, have a significantly lower Ki67 index, and a longer survival than NECs of the same sites (67,109–112).

From the clinical point of view, the distinction between small and large cell EPNECs is important, above all, for the definition of new lines of personalized therapies. For now, the therapeutic approach for these tumors is the same as that used for lung NECs. Effective treatment options for patients with EPNEC are challenging for several reasons. This includes a lack of targetable molecular drivers, lack of availability of patient-relevant preclinical models to study biology and test novel therapeutics, and the absence of validated biomarkers to guide clinical management.

Currently, the treatment of small cell EPNEC does not differ from that for SCLC with a similar response rate and prognosis. Generally, the entire spectrum of these tumors, both small and large cell tumors, is subjected to the same treatment. However, although the chemotherapy protocols are similar, the response to therapy is different and the stability of the disease after completing the chemotherapy could take a different course (96).
The standard protocol recommended for EPNEC with metastatic disease is with Platinum (cisplatin or carboplatin) in combination with Etoposide, therefore the same as the SCLC,

however with a low duration of response. Sequential or concomitant chemo-radio therapy is recommended in patients with loco-regional disease. However, recent studies comparing the effectiveness of treatment in EPNECs as well as SCLC, latter demonstrating worse response; this could be explained by the different nature of the two tumors: pulmonary SCCs are completely undifferentiated, chemo-sensitive tumors, while EPNECs include a greater heterogeneity of subtypes.

It is also possible to establish predictive factors of response to therapy. The most important is the Ki67 proliferation index. In a study where GEP NEC is analyzed, a cut-off of Ki67 > 55% is a predictor of response to cisplatin in combination with etoposide therapy, but patients with a Ki67 < 55% have a longer survival than other patients (14 months vs 10 months) (113). A lack of response to antifolates such as Pemetrexed is seen in both pulmonary NECs and EPNECs as these tumors express high levels of thymidylate synthase, the most important target of these molecules. This is important to understand, in order to better evaluate the genetical make-up of these tumors to precisely define targeted therapeutic strategies and / or predict the response to certain therapies (96).

Neuroblastoma.

Neuroblastoma is the most common extracranial solid tumor in children, originating from sympathetic nervous tissue typically affecting the adrenal gland and paraspinal ganglia (114,115). The most important clinical and biologic prognostic factors currently used to determine treatment are the age of the patient at diagnosis, stage of disease, *MYC-N* amplification status, DNA ploidy and Shimada histology (116). Approximately 80% of all neuroblastomas occur within the abdomen, while other grow in the mediastinum, at cervical level and other rare sites (117–119). Neuroblastoma differs from other NE solid tumors due to its biological heterogeneity and range of clinical behavior spanning from spontaneous regression to cases of highly aggressive metastatic disease unresponsive to standard and investigational anti-cancer treatment.

As may be expected with a disease of developing tissues, neuroblastomas generally occur in very young children; the median age at diagnosis is 17 months (120). The clinical presentation is highly variable, ranging from a mass that causes no symptoms to a primary tumor that causes critical illness due to local invasion, widely disseminated disease, or both. The incidence of neuroblastoma is 10.2 cases per million children under 15 years of age; it is the most common cancer diagnosed during the first year of life (121). The age at diagnosis is considered a surrogate for underlying biologic characteristics. In fact, younger patients are more likely to have tumors with biologic features that are associated with a benign clinical course. Although age is a continuous variable in terms of prognosis, it has been established, for clinical purposes, to use a cut-off point of 12 or 18 months of age (120). The stage of the disease, as formulated in the International Neuroblastoma Staging System (122), can also be considered a surrogate marker of the tumor burden and underlying tumor biology.

International Neuroblastoma Staging System and risk groups.

In detail, small, localized tumors that are completely resected are considered Stage 1 lesions. Stage 2 tumors are small, may or may not have had lymph node involvement, but could not be completely resected. Stage 3 lesions are large tumors that crossed the anatomical midline of the patient and could not be completely resected. Lastly, Stage 4 and 4S metastatic tumors are differentiated by the fact that 4S patients are found in patients less than 1 year of age with metastatic disease located in liver, skin and less than 10% of the bone marrow (122,123) (**Table 5**).

Table 5. *The International Neuroblastoma Staging System.*

Stage/Prognostic Group	Description
Stage 1	Localized tumor with complete gross excision, with or without microscopic residual disease; representative ipsilateral lymph nodes negative for tumor microscopically (i.e., nodes attached to and removed with the primary tumor may be positive).
Stage 2A	Localized tumor with incomplete gross excision; representative ipsilateral nonadherent lymph nodes negative for tumor microscopically.
Stage 2B	Localized tumor with or without complete gross excision, with ipsilateral nonadherent lymph nodes positive for tumor. Enlarged contralateral lymph nodes must be negative microscopically.
Stage 3	Unresectable unilateral tumor infiltrating across the midline, with or without regional lymph node involvement; or localized unilateral tumor with contralateral regional lymph node involvement; or midline tumor with bilateral extension by infiltration (unresectable) or by lymph node involvement. The midline is defined as the vertebral column. Tumors originating on one side and crossing the midline must infiltrate to or beyond the opposite side of the vertebral column.
Stage 4	Any primary tumor with dissemination to distant lymph nodes, bone, bone marrow, liver, skin, and/or other organs, except as defined for stage 4S.
Stage 4S	Localized primary tumor, as defined for stage 1, 2A, or 2B, with dissemination limited to skin, liver, and/or bone marrow (limited to infants younger than 12 months). Marrow involvement should be minimal (i.e., <10% of total nucleated cells identified as malignant by bone biopsy or by bone marrow aspirate). More extensive bone marrow involvement would be considered stage 4 disease. The results of the MIBG scan, if performed, should be negative for disease in the bone marrow.

During the last two decades, there have been major advances in understanding the genetics of neuroblastoma. Although the unfavorable prognostic factor, *MYCN* amplification, (124) is used by all cooperative groups for risk-group stratification and therapeutic decisions, while other prognostically significant genetic features (125−128) have not been consistently incorporated into risk classification schemes. Using overall and event-free survival rates combined with histological and biological criteria, patients with neuroblastoma can be assigned a pre-treatment risk classification (129). In fact, by combining the results of Omics data and available clinical/biological parameters, the International Neuroblastoma Risk Group (INRG) guidelines established a stratification system of neuroblastoma patients taking into

consideration diverse prognostic factors (i.e., clinical stage, patient's age at diagnosis, tumour histology (Shimada system) (130), grade of tumour differentiation, MYCN oncogene amplification, 11q deletion and DNA ploidy). Based on these criteria, neuroblastoma patients are currently subdivided into low-, intermediate-, and high-risk groups. Nowadays, about half of all diagnosed cases are classified as high-risk for disease relapse, while overall survival rates still show only modest improvement, less than 40% at 5 years (131).

Role of MYCN oncogene.

In detail, *MYCN* oncogene plays a major role in neuroblastoma tumorigenesis and defines an aggressive subset of tumors. Amplification of *MYCN* (defined as more than 10 copies) is found in about 20% of cases overall and confers a particularly poor prognosis.
Expression of the *MYCN* oncogene in a transgenic mouse model causes it development of neuroblastoma with characteristics similar to human neuroblastoma, demonstrating the key role of *MYCN* in the onset and development of this tumor (132,133). In the same animal model, the reduction of *MYCN* expression by the use of antisense oligonucleotides causes a reduction in proliferation and induces neuronal differentiation of neuroblastoma cells (134). Experiments conducted in human neuroblastoma cells have shown that, the reduction of *MYCN* levels causes a reduction in the time it takes to proceed through the various phases of the cell cycle, reduction of proliferation and adhesion to extracellular matrix (135).
Furthermore, *MYCN* appears to play a role in the regulation of the expression of miRNAs (136). Schulte and collaborators, employing a microarray analysis, performed on 384 different miRNAs, identified 7 miRNAs induced by *MYCN* in vitro and overexpressed in primary neuroblastoma with *MYCN* amplified. Three of the seven miRNAs belong to the miR-106a and miR-17 clusters and are in turn regulated by c-MYC. The polycistron miR-17-92 acts as an oncogene in hematopoietic progenitor cells. The same authors have identified another miRNA induced by MYCN: miR-221. These considerations have contributed to the hypothesis that *MYCN* represses the expression of many target genes through the induction of different miRNAs (136).

Treatment of neuroblastoma.

Neuroblastoma treatment recommendations range from observation only to intensive, multi-modal therapy and have been based on the event free and overall survival of patients enrolled on large, cooperative group clinical trials. Although the histological and biological characteristics used within classification schemes continue to evolve based on new scientific data, they are used to divide patients according to the risk groups. In general, those with low-risk disease have excellent event free and overall survival rates with regular check-ups only or minimal therapeutic interventions.

In 2012, Nuchtern et al noted that in patients <6 months of age with small, localized adrenal lesions, observation alone was a safe treatment option. Specifically, of the 84 patients whose lesions were initially observed, 81% spontaneously regressed, and the overall 3-year disease free survival was 97.7% (137). The outcome of patients with intermediate risk disease,

using primarily surgery and chemotherapy, have improved to the point where many groups are focused on using biological markers to help further decrease of therapy in specific subpopulations of children (138). Patients with high-risk disease, comprising approximately half of all new neuroblastoma cases each year, require treatment with multi-modal therapy using induction chemotherapy, surgery, radiotherapy, high-dose chemotherapy with autologous stem cell rescue, biologic and immunotherapeutic maintenance therapy in order to improve their survival odds (139). In the update by Yu et al to their 2010 report of the Phase III study randomizing patients to cis-retinoic acid alone vs cis-retinoic acid, Interleukin-2 (IL-2), granulocyte-macrophage colony-stimulating factor (GM-CSF) and a chimeric monoclonal antibody targeting GD2 (ch14.18), the use of immunotherapy is associated with an improvement in the 4-year event-free survival (140) of 48% vs. 59% and OS of 59% vs. 74%, respectively.

Project 1: Molecular subtypes of extra-pulmonary neuroendocrine carcinomas identified by the expression of neuroendocrine lineage-specific transcription factors

ABSTRACT

Extra-pulmonary neuroendocrine carcinomas (EPNEC) represent a group of rare and heterogenous neoplasms with adverse clinical outcome, whose molecular profile is largely unexplored. Our aim was to investigate if the major transcriptional drivers recently characterized in high-grade neuroendocrine carcinomas of the lung are expressed in EPNEC and characterize distinct molecular and clinical subgroups. Gene expression of principal transcriptional regulators of neuroendocrine differentiation, including *ASCL1, NEUROD1, DLL3, NOTCH1, INSM1, MYCL1, POU2F3* and *YAP1*, was investigated in a series of 54 EPNEC (including 10 cases with mixed components analyzed separately) and in a control group of 48 large cell neuroendocrine carcinomas of the lung whose gene expression profiles are partially depicted for these targets. Unsupervised hierarchical cluster analysis classified the whole series into four major clusters. Pulmonary large cell neuroendocrine carcinomas were classified into two major clusters, the first with high *ASCL1/DLL3/INSM1* expression and the second (that included four EPNEC) with low *ASCL1/DLL3* but high *INSM1* expression. The remaining EPNEC were sub-classified, irrespective of tumor location or cell type, into two other clusters similar but independent from pulmonary large cell carcinomas, the first with high *INSM1* and alternative ASCL1/DLL3 or *NEUROD1* expression, whereas the second characterized mainly by *MYCL1* and *YAP1* overexpression. In the ten cases with mixed histology, *ASCL1, DLL3, INSM1* and *NEUROD1* genes were significantly upregulated in the neuroendocrine component. Higher gene expression levels of *NOTCH1* and *INSM1* were associated with lower pT stage and negative nodal status. Moreover, low *INSM1* expression was associated with shorter overall survival in the entire case series (p=0.0017) and with a trend towards significance in EPNEC examined as a separate group (p=0.06). In summary, our results show that EPNEC possess distinct neuroendocrine-lineage specific transcriptional profiles; moreover, low *INSM1* expression represents a novel potential prognostic marker in high-grade neuroendocrine carcinomas including those in extra-pulmonary location.

SPECIFIC BACKGROUND

In recent years, small cell lung carcinoma has been characterized both at the genomic and transcriptional level, leading to the definition of molecular subgroups associated with different expression of neuroendocrine markers and to a potentially different pathogenesis. Major transcriptional drivers were initially indicated in *ASCL1* and *NEUROD1* with an apparent, at least partially, mutually exclusive activity in the regulation of neuroendocrine differentiation (77). More recently, alternative transcriptional patterns have been identified in small cell lung cancer (SCLC) and four major clusters were defined by the preferential expression of *ASCL1*, *NEUROD1*, *POU2F3* or *YAP1* genes (82). Specific transcriptional profiles were also very recently associated with functional activity in SCLC cells. In fact, *ASCL1* has been shown to orchestrate an IGFBP5-dependent mechanism that suppresses IGF-1 signaling (141), thus proving that molecular subtypes have distinct biological (and possibly clinical) characteristics. Data on pulmonary large cell neuroendocrine carcinomas (P-LCNEC) are more limited. Genomic studies clearly showed that they are in part similar to SCLC but also to non-small cell lung cancers and to a lower extent to carcinoids (43). However, despite sharing some genomic alterations with adenocarcinomas and squamous cell carcinomas, P-LCNEC have no transcriptional relationship with these histotypes and can be classified – likewise SCLC - into two molecular subgroups. They are characterized alternatively by high *ASCL1*/*DLL3* and low *NOTCH1* expression or by low *ASCL1*/*DLL3* and high *NOTCH1* expression, this latter group also showing a reduced neuroendocrine marker expression (55). However, the expression of other transcriptional regulators in P-LCNEC was not explored in detail, so far.

All the above data open a list of key questions in terms of both pathogenesis, biological and clinical properties of tumors belonging to the different molecular categories. For example, if distinct transcriptional profiles are acting, it might be questioned if in the lung small cell and large cell neuroendocrine carcinomas originate from a single or different stem cell, or are the consequence of alternative mechanisms including those driven by specific therapies (i.e. secondary neuroendocrine carcinomas arising from previously treated adenocarcinomas).
Since neuroendocrine carcinomas occur in a variety of extra-pulmonary locations, the molecular data obtained from the lung might correspond to tumors from extra-pulmonary sites or might be organ specific, with a significant impact in terms of clinical implications. As a matter of fact, although neuroendocrine carcinomas in extra-pulmonary locations are much rarer than their pulmonary counterparts, being 1/10 of all neuroendocrine carcinomas (94), they are usually considered similar and consequently treated as SCLC (142).

Although at the protein level some of the above-mentioned transcriptional regulators (i.e. *ASCL1* and *INSM1* protein products) have been tested as immunohistochemical markers of neuroendocrine differentiation in neuroendocrine carcinomas outside the lung (84,143–145), a detailed molecular characterization of neuroendocrine lineage-specific transcriptional markers has never been investigated in these lesions, so far.
Moreover, extra-pulmonary neuroendocrine carcinomas (EPNEC) may occur either as pure forms of small or large cell neuroendocrine carcinomas, or, rather frequently, as combined carcinomas having a more or less extensive neuroendocrine component admixed with a

conventional exocrine component of the adenocarcinoma, squamous or urothelial type. The biological behavior and, consequently, the most appropriate clinical management of combined carcinomas is even more heterogeneous and unpredictable than pure small or large cell neuroendocrine carcinomas. Apart from few genomic studies showing almost stable genotypes of the two components (146,147) the molecular mechanisms acting in the bi-directional clonal evolution of these tumors are largely unexplored.

AIM

Based on the aforementioned data, the aims of the present study were to evaluate the expression of key regulators of neuroendocrine differentiation (including *ASCL1*, *NEUROD1*, *DLL3*, *NOTCH1*, *INSM1*, *MYCL1*, *POU2F3* and *YAP1*) in a series of EPNEC (both pure and mixed) from various organs as well as in a control group of P-LCNEC, and to correlate their molecular signatures with pathological and clinical parameters.

MATERIALS AND METHODS

Case series.

Fifty-four cases of EPNEC were retrieved from the pathology files of the San Luigi (Orbassano, Turin, Italy) and at the "Città della Salute e della Scienza" (Turin, Italy) University Hospitals. A control series of 48 P-LCNEC was also collected from the same Institutions. Eligibility criteria were: a) confirmed histological diagnosis after blind revision following the appropriate WHO classifications (20,93,148,149); b) availability of residual paraffin material for molecular analysis. In cases of unknown primary tumor, the 2019 WHO classification of the gastrointestinal tract was adopted. Whenever available, immunohistochemical markers performed at the time of diagnosis were re-evaluated. In cases with incomplete baseline immunohistochemical assessment, epithelial (pan-cytokeratin cocktails) and neuroendocrine markers (chromogranin A and synaptophysin) were performed according to standard protocols in use for diagnostics. All pathological and clinical information available were also collected. All P-LCNEC were surgically resected specimens. By contrast, in EPNEC, 21 cases were large biopsies or metastasectomies, therefore pT and pN stages were missing. Survival data were available for 39 EPNEC and 44 P-LCNEC. In 20 cases of EPNEC, Ki-67 was not evaluable due to lack of positivity in internal control cells. Before review, a pathology staff member not involved in the study anonymized all cases and cases were investigated through coded data.

RNA extraction from formalin-fixed paraffin-embedded tissues and gene expression analyses.

Ten μm thick sections were cut in RNase-free conditions from paraffin-embedded tissues following microdissection using a scalpel at a magnification of 100x from hematoxylin-eosin-stained slides. In 10 cases with mixed neuroendocrine and non-neuroendocrine components, the two populations were separately dissected and analyzed. Total RNA isolation was performed by commercially available RNA extraction kits designed for paraffin material according to the manufacturer's instructions (miRNeasy FFPE kit; Qiagen, Hilden, Germany). RT reactions were performed using 10ng total RNA in a volume of 15 μl with the following conditions: 16°C for 30 min, 42°C for 30 min, 85°C for 5 min, and 4°C for 5 mi. Expression levels of all genes studied and internal reference were examined using a fluorescence-based real-time detection method (ABI PRISM 7900 Sequence Detection System—Taqman; Applied Biosystems, Foster City, CA,). The following TaqMan gene expression assays (Applied Biosystems) were used according to the manufacturer's instructions: *ASCL1* (HS00269932_m1), *DLL3* (HS01085096_m1), *INSM1* (Hs00357871_s1), *MYCL1* (Hs00420495_m1), *NEUROD1* (HS01922995_s1), *NOTCH1* (Hs01062014_m1), *POU2F3* (Hs00205009_m1), *YAP1* (Hs00902712_g1). *ACTB* (Hs01060665_g1) assay served as references for gene analyses.
Each measurement was performed in duplicate. The ΔΔCt values were calculated subtracting ΔCt values of sample and ΔCt value of Stratagene (a pool of RNA derived from normal different tissues; Stratagene, CA), and converted to ratio by the following formula: $2^{-\Delta\Delta Ct.}$

Statistical analyses.

Rows and columns were clustered using the hierarchal clustering tool in Morpheus (https://software. broadinstitute.org/morpheus/documentation.htm) using the one minus Pearson correlation matrix and the average linkage method. The log2 fold change values were z-score adjusted before clustering. Correlation among gene expression was assessed by means of Spearman's correlation test. Mann-Whitney test was used to test the association between gene expression and clinical pathological variables, as appropriate. Overall survival endpoint was defined as the time between diagnosis and patients' death. Univariate analysis was performed with Kaplan-Meier curve estimation and the significance was verified by the log-rank test. Median values were used as cut offs for low and high gene expression. Multivariate analysis was performed using a Cox proportional hazard model. All analyses were performed using GraphPad software (Graphpad Software Inc., La Jolla, CA) and SPSS software (IBM corporation, Armonk, USA). A p value lower than 0.05 was considered statistically significant in all analyses.

RESULTS

EPNEC locations.

The major clinical and pathological features of the cases analyzed are summarized in **Table 1**. In the gastro-entero-pancreatic group, 11 cases were from the colon, four cases, each, from stomach and esophagus, three cases from the duodenum, two cases from the anal canal and one case, each, from the pancreas and ileum. In the genito-urinary group, all cases were from the bladder except for two cases from the renal pelvis and one case, each, from the cervix and ovary. The primary origin of the remaining 6 cases was unknown. Of the ten cases with mixed neuroendocrine and non-neuroendocrine histology, 6 were from the bladder (with a urothelial carcinoma component) and four were from the gastrointestinal tract (two from the duodenum, one from the left colon and one from the stomach) (with an adenocarcinoma component).

Table 1. *Major clinical and pathological features of the cases investigated.*

Parameter	**EPNEC [#54]**	**P-LCNEC [#48]**
Sex (M/F)	36/18	40/8
Age, median (range)	73 (37-88)	67 (48-82)
Location		
GEP system	26	/
GU tract	22	/
unknown	6	/
NEC Histology		
Small cell type (%)	26 (48%)	/
Large cell type (%)	28 (52%)	48
Mixed non-NE component (%)	10 (18%)	/
Stage T3-4 (%)	25 (75%)*	15 (31%)
Positive nodal status (%)	16 (57%)**	13 (27%)
Ki-67, mean %	68	57
Ki-67 >55% (%)	22 (65%)***	30 (62%)
Died of disease (%)	27 (69%)****	20 (45%)^
Mean overall survival, months	21	40

*GEP: gastro-entero-pancreatic; GU: genito-urinary; EPNEC: extra-pulmonary neuroendocrine carcinoma; P-LCNEC: pulmonary large cell neuroendocrine carcinoma; NE: neuroendocrine; DOD: died of disease; *: 21 missing; **: 26 missing; ***: 20 missing; ****: 15 missing; ^: 4 missing*

Gene expression patterns.

A strong reciprocal positive correlation was observed in the whole series between *INSM1*, *ASCL1* and *DLL3* expression. *INSM1* was also positively associated with *NOTCH1*. *MYCL1* was strongly negatively correlated with *NOTCH1* and *INSM1*, whereas *POU2F3* and *YAP1* were inversely correlated with *ASCL1* and *DLL3* and *ASCL1* alone, respectively (**Table 2**).

***Table 2**. Reciprocal correlation among the genes tested.*

	ASCL1	***DLL3***	***NEUROD1***	***INSM1***	***POU2F3***	***MYCL1***	***YAP1***
NOTCH1	R: -0.17 p: 0.07	R: 0.25 p: 0.006	R: -0.23 p: 0.01	R: 0.45 p: <0.0001	R: 0.06 p: 0.49	R: -0.48 p: <0.0001	R: 0.27 p: 0.003
ASCL1	-	R: 0.67 p: <0.0001	R: 0.15 p: 0.11	R: 0.40 p: <0.0001	R: -0.25 p: 0.007	R: 0.18 p: 0.06	R: -0.49 p: <0.0001
DLL3	-	-	R: 0.05 p: 0.59	R: 0.60 p: <0.0001	R: -0.30 p: 0.0014	R: -0.11 p: 0.24	R: -0.21 p: 0.02
NEUROD1	-	-	-	R: 0.16 p: 0.10	R: -0.12 p: 0.19	R: 0.09 p: 0.35	R: -0.18 p: 0.06
INSM1	-	-	-	-	R: -0.17 p: 0.06	R: -0.32 p: 0.0006	R: -0.22 p: 0.02
POU2F3	-	-	-	-	-	R: 0.22 p: 0.02	R: 0.17 p: 0.06
MYCL1	-	-	-	-	-	-	R: -0.08 p: 0.40

R: Spearman's correlation value.

By using unsupervised cluster analysis, patterns of gene expression were able to stratify independently the cases into major subgroups (**Figure 1**). P-LCNEC were all, but one case classified into two major clusters. The first was composed exclusively by this tumor type and was characterized by overexpression of *ASCL1*, *DLL3* and *INSM1*. A second cluster was more heterogeneous, included four cases of EPNEC and was characterized by low expression of *ASCL1* and *DLL3* but overexpression of *INSM1* associated with variable overexpression of *POU2F3*, *NOTCH1* and *YAP1*. EPNEC were similarly sub-divided into two clusters. A first cluster composed exclusively of EPNECs, mirrored in part the first cluster of P-LCNEC and was characterized by *INSM1* overexpression and alternative overexpression of *ASCL1* and *DLL3* or *NEUROD1*. The second cluster was more heterogeneous, included one case of P-LCNEC and was characterized mainly by *MYCL1* and *YAP1* overexpression. In both clusters including EPNEC, there was no significant impact for classification neither of the tumor location nor of the cell type (large vs small).

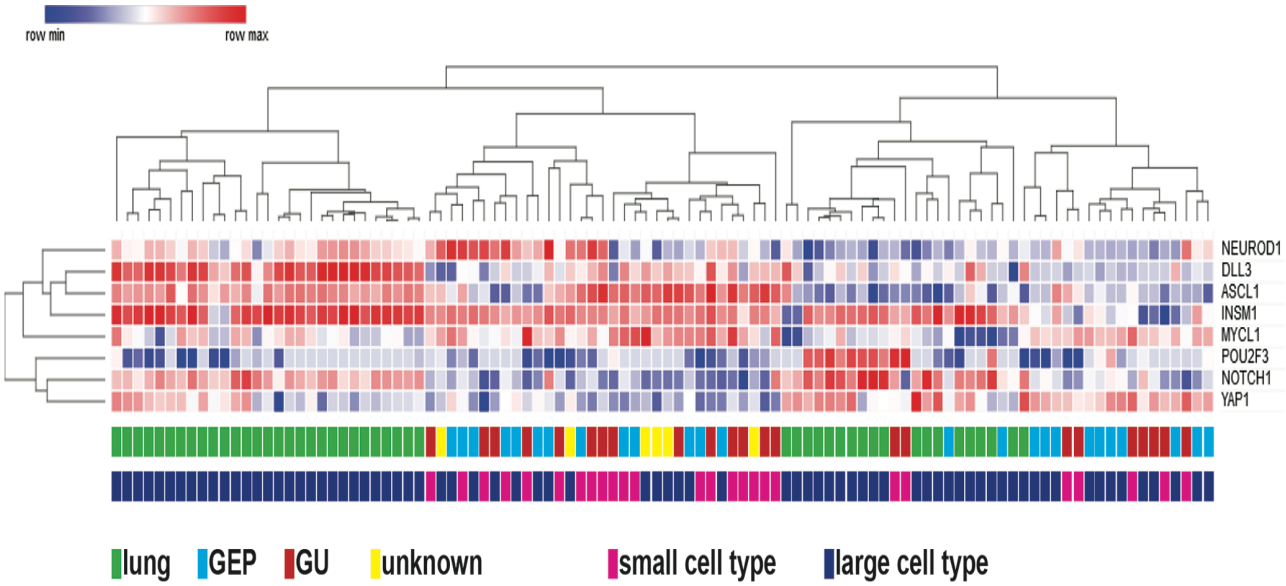

Figure 1. *Unsupervised cluster analysis of the entire cohort based on gene expression patterns. GEP: gatro-entero-pancreatic system; GU: genito-urinary tract.*

Clinical and pathological correlations.

The eight genes separately analyzed were heterogeneously distributed in the different locations (**Table 3**). Significantly different site-specific expression levels were observed for all but *NEUROD1* and *POU2F3*. In particular, P-LCNEC displayed higher gene expression levels of *NOTCH1*, *DLL3*, *YAP1* and *INSM1* and lower gene expression of *MYCL1*, as compared to the other locations. *ASCL1* and *MYCL1* gene expression was the highest in neuroendocrine carcinomas from the genitourinary tract. In EPNEC, cell type was not associated with significantly different gene expression levels, except for higher gene expression levels of *ASCL1* and lower gene expression levels of *YAP1* in small cell type. Higher gene expression levels of both *NOTCH1* and *INSM1* were strongly associated with lower pT stage and negative nodal status. A less strong statistical association was observed for higher and lower gene expression levels of *ASCL1* and *DLL3*, respectively, with high pT stage, and lower expression of *YAP1* with positive nodal status.

Table 3. *Correlation of gene expression with major clinical and pathological variables.*

		NOTCH1	***ASCL1***	***DLL3***	***NEUROD1***	***INSM1***	***POU2F3***	***MYCL1***	***YAP1***
Location	lung	6.744	31.28	118.9	10.99	128721	10.66	33.09	0.4887
	GEP	0.4079	23.30	3.00	144.2	6618	0.3908	204.5	0.2871
	GU	0.3963	144.5	5.742	57.03	6281	12.54	554.1	0.2368
	unknown	0.1500	121.3	10.35	38.78	13629	0.3375	151.8	0.1020
	P value	*<0.0001*	*0.02*	*<0.0001*	*0.11*	*<0.0001*	*0.697*	*< 0.0001*	*0.006*
Cell type	Small	0.3286	128.4	7.082	116.0	7464	10.84	654.9	0.1818
	large	0.3941	45.33	3.696	88.68	7335	0.3356	153.4	0.2950
	P value	*0.11*	*0.016*	*0.14*	*0.57*	*0.67*	*0.76*	*0.35*	*0.007*
pT stage	pT1-2	5.014	40.84	103.6	59.68	82231	8.828	384.1	0.3323
	pT3-4	2.221	51.50	26.62	43.68	63909	4.116	248.7	0.4005
	P value	*0.002*	*0.03*	*0.017*	*0.96*	*0.007*	*0.50*	*0.17*	*0.76*
pN stage	pN0	6.123	33.49	99.35	12.51	101191	12.87	84.15	0.4328
	pN+	1.950	43.75	32.19	110.1	50266	18.32	78.38	0.2890
	P value	*0.0012*	*0.45*	*0.2*	*0.14*	*0.013*	*0.986*	*0.071*	*0.041*

GEP: gastro-entero-pancreatic; GU: genito-urinary

Gene expression levels in neuroendocrine vs non-neuroendocrine components of cases with mixed histology.

In ten cases with mixed histology, the expression of target genes was analyzed independently in neuroendocrine and non-neuroendocrine components (**Figure 2**). *ASCL1*, *DLL3*, *INSM1* and *NEUROD1* genes displayed an upregulation in most cases in the neuroendocrine component as compared to the non-neuroendocrine micro-dissected population. For all but *ASCL1*, this result was independent from the location, whereas for *ASCL1* this observation was restricted to cases of the genito-urinary tract, only. By contrast, *NOTCH1*, *POU2F3*, *MYCL1* and *YAP1* genes did not show significant modifications (except for single cases) of their gene expression in the neuroendocrine vs non-neuroendocrine components. Indeed, the two latter genes showed even a trend to down regulation in the neuroendocrine as compared to the non-neuroendocrine population.

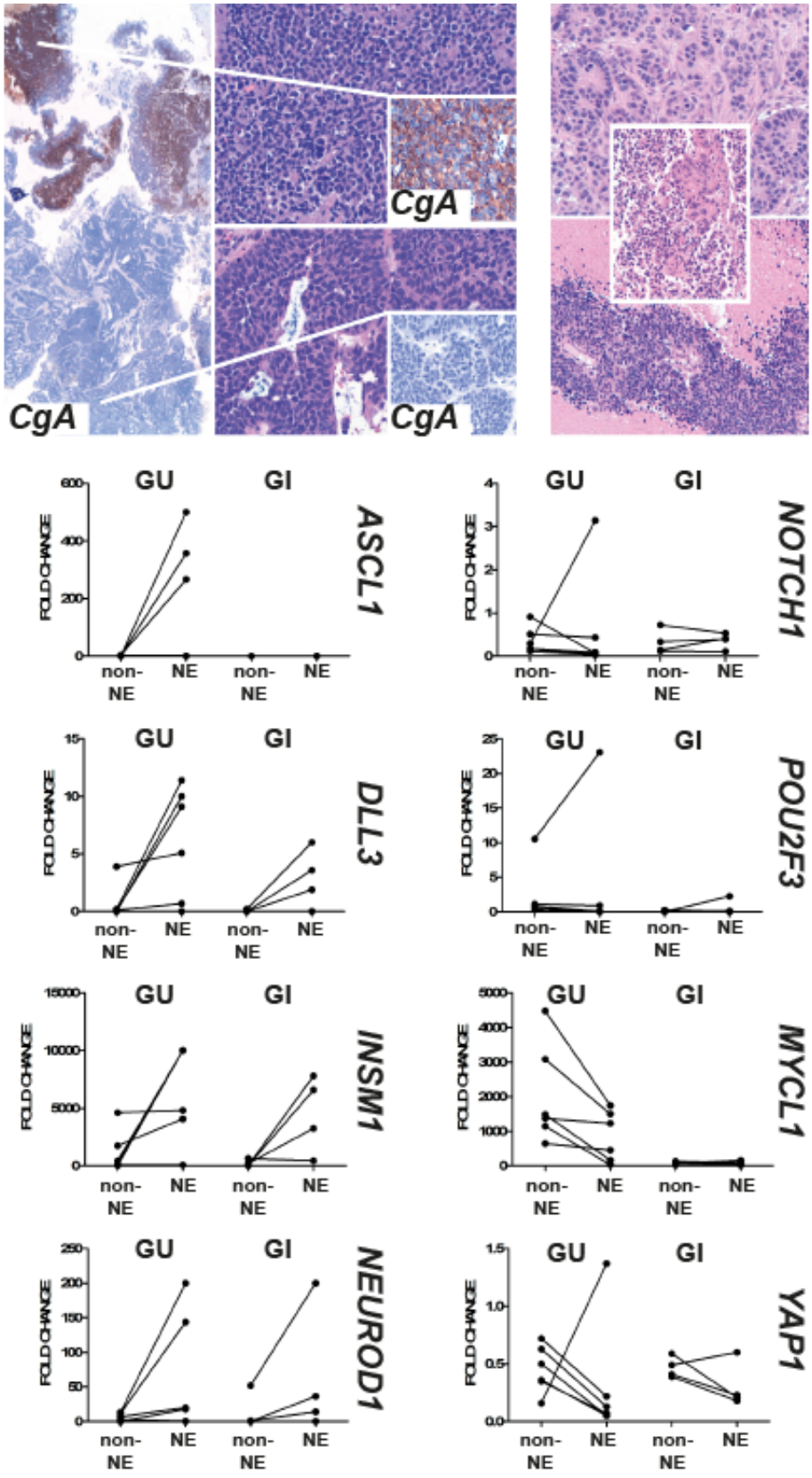

Figure 2. *Gene expression patterns in neuroendocrine and non-neuroendocrine microdissected tumor cell populations of ten cases. Top left: a case of bladder carcinoma (transurethral resection specimen) with mixed histology composed of high-grade urothelial carcinoma and small cell neuroendocrine carcinoma (highlighted by chromogranin A – CgA staining). Top right: a case of mixed adenocarcinoma (upper panel) admixed (inset) with small cell carcinoma (lower panel) of the stomach. NE: neuroendocrine. GU: genito-urinary tract. GI: gastrointestinal tract.*

Survival analyses.

By means of univariate overall survival analysis in the whole population, site of tumor (all other locations vs lung primary), pT3-4 stage, and positive nodal status were associated with significantly shorter survivals (**Table 4**) (**Figure 3**). As to concern the genes tested, all but *INSM1* did not show any significant association with survival, neither in the entire cohort nor in P-LCNEC or EPNEC series analyzed separately. By contrast, *INSM1* low expression was associated with shorter overall survival in the whole population and with a trend towards significance in EPNEC examined as a separate group (not shown in Table 4; median survival: 12.10 vs 44.10 months, Hazard Ratio 2.22, confidence intervals 0.94-5.25, p=0.06) (**Figure 4**), but not in the group of P-LCNEC. At multivariable analysis in the whole population, pN stage, only, retained statistical significance (coefficient 0.77, p=0.0169).

Table 4*. Univariate survival analysis.*

Parameter	**Median survival (months)**	**HR [CI]**	**p**
Location (lung vs others)	64.9 vs 14.5	0.3783 [0.18-0.78]	0.0082
Cell type (small vs large)**	14.5-16.6	1.233 [0.51 - 2.99]	0.6441
pT stage (pT3-4 vs pT1-2)	12.2 vs 91.3	2.88 [1.39-6.0]	0.0046
pN stage (pN+ vs pN0)	14.6 vs 91.3	3.58 [1.55-8.26]	0.0027^
NOTCH1* low vs high	44.1 vs 75.0	1.084 [0.53-2.20]	0.82
ASCL1* low vs high	31.9 vs 44.1	1.4 [0.76-2.58]	0.28
DLL3* low vs high	35.3 vs 32.3	1.05 [0.38- 1.29]	0.87
NEUROD1* low vs high	31.9 vs 44.1	0.95 [0.52- 1.75]	0.88
INSM1* low vs high	14.5 vs 91.3	2.808 [1.47- 5.35]	0.0017
YAP1* low vs high	18.3 vs 61.2	1.25 [0.67- 2.32]	0.48
POU2F3* low vs high	31.9 vs 44.1	1.0 [0.55-1.84]	0.99
MYCL1* low vs high	61.2 vs 31.9	0.69 [0.38- 1.29]	0.25

HR: hazard ration; CI: confidence Intervals; *: according to the median level; **: extra-pulmonary neuroendocrine carcinomas, only.

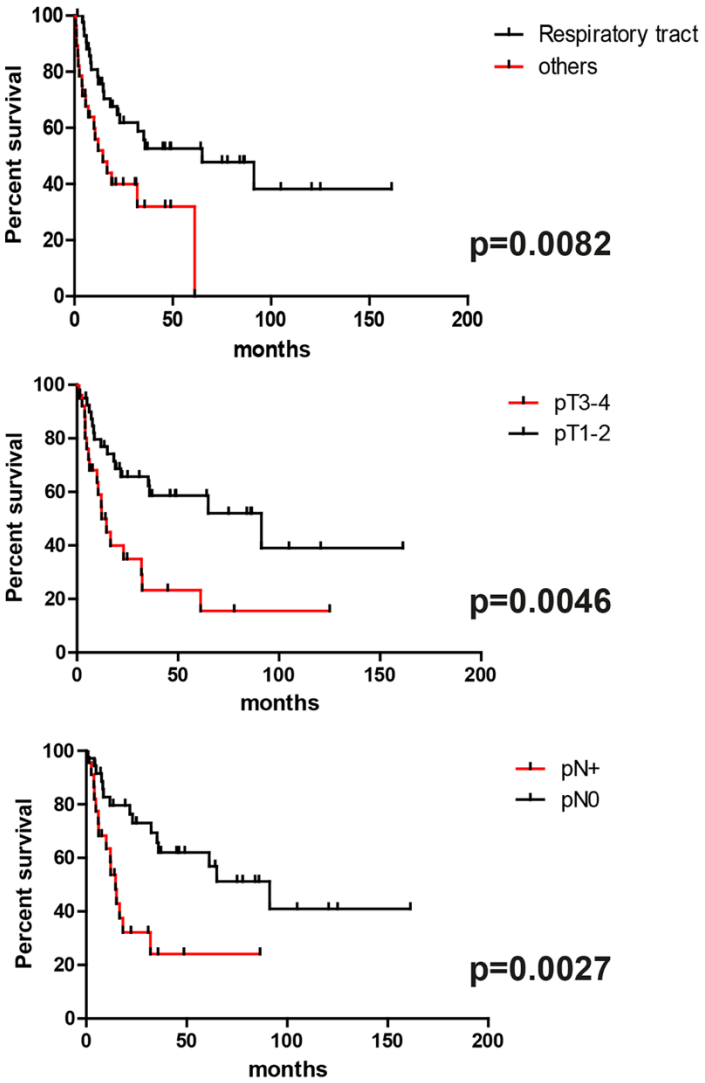

Figure 3. *Overall survival curves in the entire cohort according to site, T stage and nodal status.*

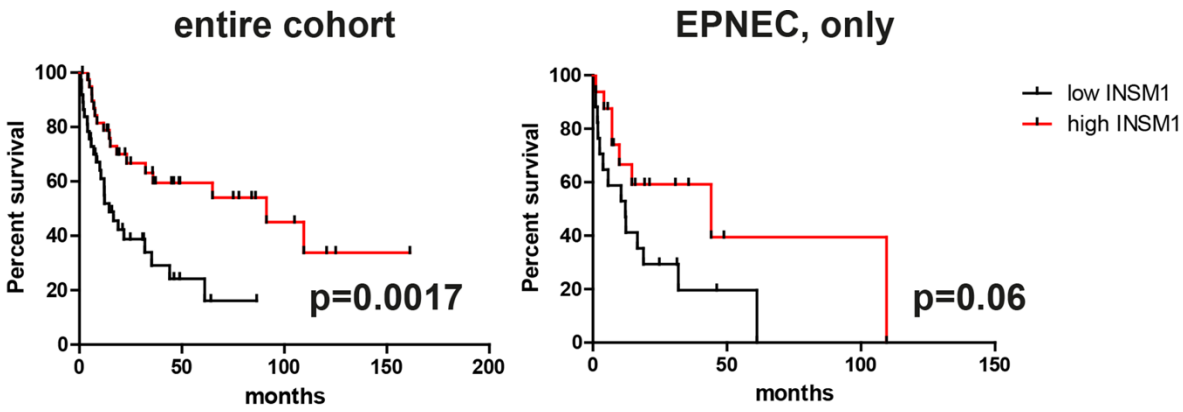

Figure 4. *Overall survival curves in the entire cohort and in EPNEC, only, according to INSM1 expression (low and high as determined by median values).*

DISCUSSION

In the present study, we analyzed the expression of a panel of transcriptional regulators of neuroendocrine differentiation in EPNEC as compared to a series of P-LCNEC.
The project stemmed from the growing evidence of the impact of lineage-specific transcription factor expression in stratifying SCLC into different molecular subgroups. Our data clearly demonstrated that EPNEC can be classified into molecular transcriptional subclasses partially overlapping those described in SCLC. In parallel, we also tested the same transcription factors (such as *INSM1*, *YAP1*, *POU2F3*, *MYCL* and *NEUROD1* genes) in P-LCNEC that have so far incompletely investigated in this respect.

Irrespective of the classification system specific for each location, EPNEC are diagnosed by the presence of an appropriate morphology and the expression of at least one neuroendocrine marker. From a pure morphological standpoint, EPNEC of the large or small cell type resemble their pulmonary counterpart and in the clinical practice they are managed and treated as such. However, some recent genomic data claimed that, at least in the gastro-entero-pancreatic system, they are molecularly closer to the respective adenocarcinoma counterpart than to well differentiated neuroendocrine tumors of the same locations (147). By contrast, in the lung either genomic (40) or transcriptional (39) data link small and large cell carcinomas more closely to carcinoids, for some Authors even within a hypothetical evolutionary context (150).

In this scenario, we might have expected gene expression patterns of transcriptional regulators different from those of the lung, and organ specific. Indeed, this was evident only in part. In fact, cluster analysis strongly segregated P-LCNEC from EPNEC, but at the same time these latter were further divided into two clusters that at least partially mirrored the lung cases. One cluster in particular was characterized by a high *INSM1* expression, and further sub-classified by the alternative expression of *ASCL1*/*DLL3* or *NEUROD1* as described in SCLC (77,82). A second group of P-LCNEC was clustered with a small number of EPNEC, and similarly to SCLC, it was characterized by preferential expression of *POU2F3* and/or *YAP1* in the presence of *INSM1* over-expression but with low expression of *ASCL1*, *DLL3* and *NEUROD1*. A fourth cluster (including EPNEC, only, except for one case) was particularly enriched for *YAP1* expressing cases with low expression of all other markers except for *MYCL1*. Interestingly, despite cluster analysis and the correlation of individual genes with location sharply took pulmonary apart from extra-pulmonary cases, site of origin as well as cell type (small vs large) were not influencing the sub-classification of EPNEC nor were associated with significant gene expression levels, with only few exceptions.

Cases with mixed neuroendocrine and non-neuroendocrine histology were randomly distributed in the three clusters containing EPNEC cases. Moreover, the modulation of the different genes in neuroendocrine carcinoma components was heterogeneous. In fact, up-regulation was evident in neuroendocrine cell population for *ASCL1*, *DLL3*, *NEUROD1* and *INSM1* in most cases. All genes were up-modulated in mixed cases irrespective of the tumor location, except for *ASCL1* that was not modulated in mixed cases of the gastro-intestinal tract, in agreement with its lower expression in cases from the gastro-entero-pancreatic system, as

demonstrated in our series and in the literature (84). By contrast, transcriptional regulators of SCLC associated to a lower expression of neuroendocrine markers (in particular *YAP1*, *NOTCH1* and *POU2F3*) were not modulated (if not negatively regulated in some instances) in neuroendocrine components of mixed cases.

As to concern clinical and pathological correlations, none of the genes investigated was reported to clearly impact on clinical aggressiveness or to be associated to specific characteristics of SCLC or, whenever tested, of P-LCNEC. *ASCL1* has been found to be associated with lack of EGFR mutations and a poor immune cell infiltration with no programmed cell death ligand 1 protein expression in adenocarcinomas with neuroendocrine differentiation (151), but not to clearly define subsets of SCLC with a distinctive clinical outcome. Also in our series, most genes were not associated with stage of disease or survival, with some exceptions.

DLL3, although never associated in the literature with clinical or pathological characteristics in either SCLC or P-LCNEC, was expressed to a higher extent in cases with lower tumor stage. More interestingly, the expression of DLL3 also in EPNEC paves the way to the potential use of specific therapies targeting this molecule (152), as also recently suggested for P-LCNEC (153). Moreover, DLL3 was identified in a subset of small cell carcinomas of the bladder as a negative prognostic biomarker, and the *in vivo* efficacy of a DLL3-targeting conjugated antibody was demonstrated in a PDX model (154).

Decreased expression of *NOTCH1* in our series was also characteristic of cases with higher pT stage and positive nodal status. This result is possibly explained by the inhibitory effect of the NOTCH pathway on cell growth demonstrated some years ago in SCLC cells (155).

INSM1 has been mostly investigated as a diagnostic immunohistochemical marker for neuroendocrine neoplasms in different organs and settings, but its comparative expression with other transcriptional regulators of the neuroendocrine phenotype has not been assessed if not for SCLC. Our data clearly confirm that *INSM1* is highly expressed in neuroendocrine carcinomas of different sites although its low expression defined a subset of cases of extra-pulmonary origin. Moreover, with all the possible limitations due to the relatively small sample size and heterogeneity of the case series, *INSM1* low expression characterized a subset of cases with more aggressive clinical features and worse outcome. Data on the prognostic role or association with clinical features of *INSM1* expression in EPNEC are missing. The presently observed adverse prognostic effect of low *INSM1* expression is partly in contrast with some data available in SCLC of a negative prognostic association of *INSM1* expression, as determined by immunohistochemistry in tumor samples (156), and by its capability to promote cell growth *in vitro* (157). By contrast, a negative prognostic impact of *INSM1* low expression in SCLC in terms of overall survival and lower rates of response to chemotherapy was reported by McColl and coworkers (158). Moreover, our results were supported by both survival analysis and the association with pT and pN stages. Whether *INSM1* expression reflects specific genomic profiles or a less differentiated phenotype associated with worse outcome has to be elucidated in future studies. Moreover, due to lack of robust information, we could not speculate if the prognostic impact of INSM1 was attributable to an influence in chemotherapy response.

CONCLUSION

In summary, our results show that EPNEC possess distinct neuroendocrine-lineage specific transcriptional profiles that in part mirror those described for pulmonary small and large cell carcinomas and are independent from the site of origin of the tumor. Moreover, decreased expression of *INSM1* was associated with characteristics of aggressive disease and shorter overall survival, and *INSM1* potential prognostic role in EPNEC merits validation in larger and independent series.

Project 2: Overexpression of a subset of neuroendocrine-lineage transcription factors is associated with adverse clinical outcome in pediatric neuroblastoma.

ABSTRACT

Pediatric neuroblastoma, responsible for approximately 8-10% of pediatric tumors, originates from developing sympathetic nervous system. Our aim was to investigate if the major neuroendocrine-associated transcriptional drivers, including *ASCL1, NEUROD1, DLL3, NOTCH1, INSM1, MYCL1, POU2F3* and *YAP1* are correlated with specific clinico-pathological characteristics. We selected a retrospective series of 46 primary pediatric neuroblastoma, composed of 30 treatment-naïve and 16 post-chemotherapy cases. In addition, in 4 treatment-naïve cases, a post-treatment specimen was available. Gene expression levels were explored by means of RT-PCR. An increased expression of *NOTCH1* (p=0.005), *NEUROD1* (p=0.0059), and *YAP1* (p=0.0008) was found in stage IV tumors, while highest levels of *MYCL1* and *ASCL1* were seen in stages IVS and III, respectively (p=0.0182 and p=0.0134). A higher level of *NOTCH1* (p=0.0079) and *YAP1* (p=0.0026) was found in cases with differentiating morphology, while high mitosis-karyorrhexis index cases demonstrated significantly lower levels of *POU2F3* (p=0.0277). By means of univariate analysis, stage IV (p=0.043) and high expression of *NOTCH1* (p=0.008), *NEUROD1* (p=0.026), *INSM1* (p=0.010) and *YAP1* (p=0.005) were associated with adverse prognosis in terms of DFI. Preliminary data on gene expression levels in pre- and post- treatment samples of 4 patients, demonstrated a decrease of *ASCL1, INSM1, DLL3* and an increase of *YAP1* and *NOTCH1* in all 4 cases, whereas *POU2F3, MYCL1, NEUROD1* demonstrated a more heterogenous gene expression levels. In conclusion, assessing gene expression levels of neural/neuroendocrine-lineage transcription factors might help to identify neuroblastoma patients with the risk of relapse.

SPECIFIC BACKGROUND

Neuroblastic tumors represent the most common extra-cranial solid malignancy in the pediatric age. Neuroblastoma is a tumor arising from developing sympathetic nervous system and is responsible for approximately 8-10% of pediatric tumors. Despite advances in molecular profiling and therapeutic options, survival of high-risk neuroblastoma patients remains poor.

Neuroblastoma development mechanisms are incompletely understood, but linked to oncogene mutations and/or amplifications, including *MYCN*, one of the most important driver genes in neuroblastoma (159–162). Moreover, basic helix-loop-helix (bHLH) class of transcription factors plays a pivotal role in tissue-specific differentiation and their dysregulation is associated to solid tumor development. Neuronal and neuroendocrine (NE) cell growth and differentiation, as well as their related tumors, are regulated by genes of the Notch, NEUROD and Achaete Scute families (77,86,163). In particular, in high grade NE small cell carcinomas, mostly of the lung, a complex genetic regulation has been recently reported with several pathways differentially activated in subgroups of such tumors. Among relevant regulators of NE growth and differentiation are Notch family genes, *ASCL1*, *NEUROD1*, *HES1*, *INSM1*, *POU2F3*, *YAP1*, *MYCL1* (81,82,164,165). In large cell NE carcinomas of the lung, two different molecular profiles were also identified, partly overlapping with those of small cell lung cancer or sharing gene alterations seen in non-small lung carcinomas (43,55–57). Some of these genetic differences were linked to different outcome and response to specific therapies in both types of pulmonary high grade NE carcinomas (164,166). In addition, some of these transcription factors are also express in extra-pulmonary NE carcinomas of various locations and are used as markers of NE differentiation (84,167,168).

Some genes belonging to the above-mentioned families have been individually investigated in neuroblastoma and found to be overexpressed and involved in response to specific therapies. In particular *MYCN* gene is pivotal in neuroblastoma development and progression (159–162). Central (intracranial) and peripheral neuroectodermal tumors and cell lines are known to express *NEUROD1* and *ASCL1* genes (169). Transcriptional regulators of these two genes were recently identified in neuroblastoma, including the neuronal differentiation markers of Purkinje cells *PCP4/PEP19* (170), and *ERK* (171). *NEUROD1* seems to act mainly through *ALK* to favor neuroblastoma cell proliferation, directly binding to the promoter region of this gene (172). *ASCL1* is downregulated during neuroblastoma cell differentiation along with upregulation of several genes including *IGF2* (173); moreover, the negative correlation of *ASCL1* expression with neuronal differentiation is independent from *MYCN* gene expression, suggesting that targeting *ASCL1* might increase the efficacy of retinoic acid-based differentiating therapies in neuroblastoma (174). More recently, other regulatory genes were investigated, including *INSM1* that is activated by *MYCN* gene, expressed in a large fraction of neuroblastomas and associated to a shorter survival (175–178).

AIM

Neuroblastic tumors encompass a spectrum of lesions with different pathological features, response to therapies and outcome. We studied the role of major drivers of neuroendocrine-associated transcriptional clustering in a retrospective series of surgically resected pediatric neuroblastomas, with the aim of exploring the correlation with specific pathological and clinical characteristics including response to treatment and survival.

MATERIALS AND METHODS

Case series.

We selected a retrospective series of 46 cases of pediatric neuroblastoma, all primitive, operated from 2007 to 2019 at "Città della Salute e della Scienza", Turin, and treated at the Pediatric Oncology Division of the "Regina Margherita" Children's Hospital, with sufficient residual histological material for molecular and immunohistochemical analyses. The case series was composed 30 treatment-naïve and 16 post-chemotherapy cases. The chemotherapy consisted of combination treatment, including carboplatin and etoposide. In addition, in 4 treatment-naïve cases a post-treatment specimen was also available, that was used for additional analyses, making it a total of 50 specimens included in the study.

Clinicopathological data such as age at diagnosis, sex, tumor location, stage, International Neuroblastoma Pathology classification (INPC) category (179), mitosis-karyorrhexis index (MKI) according to Shimada classification (130), presence of necrosis, calcifications and follow-up data were collected from clinical charts and inserted in a dedicated database.

Before the study started, all cases were de-identified and coded by a pathology staff member not involved in the study, and all data were accessed anonymously. The study was approved by the Institutional Board review of Città della Salute e della Scienza, Turin, Italy (n° 966/2011). The study was conducted in accordance with The Code of Ethics of the World Medical Association (Declaration of Helsinki).

RNA extraction from formalin-fixed paraffin-embedded tissues and gene expression analyses.

Ten µm thick sections were cut were cut from formalin fixed paraffin embedded blocks of the tumor in RNase-free conditions, following microdissection using a scalpel at a magnification of 100x from hematoxylin-eosin (H&E) stained slides. The suitability of the material was evaluated by hematoxylin and eosin staining, and care was taken to select tumor areas. Total RNA isolation was performed by commercially available RNA extraction kits designed for paraffin material according to the manufacturer's instructions (miRNeasy FFPE kit; Qiagen, Hilden, Germany).

RT reactions were performed using 10ng total RNA in a volume of 15 µl with the following conditions: 16°C for 30 min, 42°C for 30 min, 85°C for 5 min, and 4°C for 5 min. Expression

levels of all genes studied and internal reference were examined using a fluorescence-based real-time detection method (ABI PRISM 7900 Sequence Detection System—Taqman; Applied Biosystems, Foster City, CA,). The following TaqMan gene expression assays (Applied Biosystems) were used according to the manufacturer's instructions: *ASCL1* (HS00269932_m1), *DLL3* (HS01085096_m1), *INSM1* (Hs00357871_s1), *MYCL1* (Hs00420495_m1), *NEUROD1* (HS01922995_s1), *NOTCH1* (Hs01062014_m1), *POU2F3* (Hs00205009_m1), *YAP1* (Hs00902712_g1), *ACTB* (Hs01060665_g1) assay served as housekeeping reference gene for the analyses.
Each measurement was performed in duplicate. The ΔΔCt values were calculated subtracting ΔCt values of sample and ΔCt value of Stratagene (a pool of RNA derived from normal different tissues; Stratagene, CA), and converted to ratio by the following formula: $2^{-\Delta\Delta Ct}$.

Statistical analysis.

Statistical analyses were carried out using Stata 15.0 software (StataCorp, College Station, TX, U.S.A.). The differences in the distribution of the variables evaluated based on clinical-pathological parameters were analyzed using parametric and non-parametric tests (Student's t test, Pearson's chi-square test and Bonferroni's correction, Wilcoxon's rank test).
Time to relapse (Disease Free Interval - DFI) was assessed from the date of diagnosis to the date of relapse or the date of the last checkup. All dead patients were considered as events. Survival analysis was determined by the Kaplan-Meier curves and Mantel log-rank test was used to compare statistical differences. Cox regression analyses were carried out on DFI to calculate HRs and 95 % CIs for the different study groups. All statistical tests were two sided. P-values < 0.05 were considered significant.

RESULTS

Clinico-pathological characteristics of the study group.

The clinical and pathological features of 46 neuroblastoma cases are summarized in **Table 1.** In brief, the case series was composed of 20 females (43.5%) and 26 male patients (56.5%), 27 of them aged <18 months (58.7%) and 19 patients ≥18 months (41.3%). Stages I-II, III, IV and IVS were diagnosed in 15 (32.6%), 5 (10.9%), 18 (39.1%) and 8 (17.4%) cases, respectively. The poorly differentiated subtype (according to INPC) was present in the majority of cases (26/46, 56.5%), while undifferentiated and differentiated forms were seen in 17/46 (37%) and 3/46 (6.5%) cases, respectively. Low, intermediate, and high MKI were present in 21 (45.7%), 20 (43.5%) and 5 (10.8%) cases, respectively. Both calcifications and necrosis were noted in 28/46 cases (60.9%). Relapse occurred in 19/46 (41.3%) patients and 8/46 died of disease (17.4%).

Table 1. *Clinico-pathological characteristics of a 46 neuroblastoma case series.*

		Total #46
Sex	F	20 (43.5%)
	M	26 (56.5%)
Age	<18 months	27 (58.7%)
	≥ 18 months	19 (41.3%)
Treatment	Treatment-naive	30 (65.2%)
	Post-treatment	16 (34.8%)
Site	Adrenal gland	38 (82.6%)
	Other*	8 (17.4%)
Stage	I/II	15 (32.6%)
	III	5 (10.9%)
	IV	18 (39.1%)
	IVS	8 (17.4%)
INPC classification	Undifferentiated	17 (37%)
	Poorly differentiated	26 (56.5%)
	Differentiated	3 (6.5%)
Shimada classification	Low MKI°	21 (45.7%)
	Intermediate MKI	20 (43.5%)
	High MKI	5 (10.8%)
Calcifications	No	18 (39.1%)
	Yes	28 (60.9%)
Necrosis	No	18 (39.1%)
	Yes	28 (60.9%)
Relapse	No	27 (58.7%)
	Yes	19 (41.3%)
Died of disease	No	38 (82.6%)
	Yes	8 (17.4%)

*Mediastinal, pelvic, and cervical localization; °MKI: mitosis-karyorrhexis index.

Gene expression profiles and correlations with clinical-pathological features.

A strong reciprocal positive correlation was observed across the series between *NOTCH1* and *ASCL1* (p=0.0014), *NEUROD1* (p=0.0004), *INSM1* (p=0.0008) and *YAP1* (p<0.0001). Moreover, *ASCL1* was found significantly correlated with *DLL3* (p=0.0117), *NEUROD1* (p=0.0062) and *INSM1* (p<0.0001). Furthermore, *NEUROD1* was significantly correlated with *MYCL1* (p=0.0452), *YAP1* (p=0.0002), while *INSM1* resulted significantly correlated with *YAP1* (p=0.0257) (**Table 2**).

Table 2. *Reciprocal correlation among the genes tested across the case-series.*

	ASCL1	***DLL3***	***NEUROD1***	***INSM1***	***POU2F3***	***MYCL1***	***YAP1***
NOTCH1	R: 0.4561 p: 0.0014	R: 0.054 p: 0.7193	R: 0.4982 p: 0.0004	R: 0.4763 p: 0.0008	R: 0.2095 p: 0.1623	R: -0.0231 p: 0.8787	R: 0.8475 p: <0.0001
ASCL1	-	R: 0.3685 p: 0.0117	R: 0.3976 p: 0.0062	R: 0.5996 p: <0.0001	R: -0.0633 p: 0.6758	R: -0.1566 p: 0.2987	R: 0.2877 p: 0.0525
DLL3	-	-	R: 0.4173 p: 0.0039	R: 0.2937 p: 0.0476	R: 0.1029 p: 0.4961	R: -0.2786 p: 0.0608	R: 0.0117 p: 0.9387
NEUROD1	-	-	-	R: 0.2839 p: 0.0559	R: 0.2126 p: 0.1561	R: -0.2968 p: 0.0452	R: 0.5290 p: 0.0002
INSM1	-	-	-	-	R: 0.0422 p: 0.7804	R: 0.0979 p: 0.5176	R: 0.3286 p: 0.0257
POU2F3	-	-	-	-	-	R: -0.1093 p: 0.4695	R: 0.1574 p: 0.2960
MYCL1	-	-	-	-	-	-	R: -0.0958 p: 0.5266

Clinical and pathological correlations with gene expression levels are demonstrated in **Table 3**. As shown, *NOTCH1, NEUROD1, MYCL1* and *YAP1* were found significantly correlated with tumor stage. In detail, *NOTCH1* (p=0.005), *NEUROD1* (p=0.0059), and *YAP1* (p=0.0008) were more expressed in stage IV tumors, while highest levels of *MYCL1* and *ASCL1* were seen in stages IVS and III, respectively (p=0.0182 and p=0.0134). Moreover, a higher level of both *NOTCH1* (p=0.0079) and *YAP1* (p=0.0026) were found in cases with differentiating morphology according to INPC classification. Finally, cases with high MKI according to Shimada demonstrated significantly lower levels of *POU2F3* (p= 0.0277).

Table 3. *Correlation of gene expression levels with major clinical and pathological variables.*

		NOTCH1	***ASCL1***	***DLL3***	***NEUROD1***	***INSM1***	***POU2F3***	***MYCL1***	***YAP1***
Age	<18 months	1.11	103.2	1.25	0.001	998.7	0.03	103.2	1.70
	≥18 months	2.39	74.4	2.13	0.01	2771.2	0.03	74.4	2.93
	P value	*0.1901*	*0.6426*	*0.6586*	*0.1682*	*0.5214*	*0.6113*	*0.2874*	*0.1547*
Stage	I/II	0.96	25.6	0.15	0.0002	789.5	0.01	129.3	1.43
	III	1.11	604.3	15.9	0.01	843.9	0.39	37.5	1.60
	IV	3.56	203.8	3.80	0.065	4845.8	0.03	56.1	6.48
	IVS	1.41	87.5	3.01	0.002	731.4	0.10	253.5	3.12
	P value	*0.005*	*0.0134*	*0.4071*	*0.0059*	*0.1145*	*0.3413*	*0.0182*	*0.0008*
INPC^	Undifferentiated	2.89	389.9	4.09	0.03	3609.8	0.03	46.1	3.09
	Poorly differentiated	1.08	55.4	0.39	0.001	753.3	0.03	105.9	1.44
	Differentiated	3.52	134.4	8.91	0.149	907.4	0.02	9.63	14.7
	P value	*0.0079*	*0.0521*	*0.3671*	*0.1130*	*0.2048*	*0.7854*	*0.0607*	*0.0026*
Shimada classification	Low MKI*	1.30	119.6	2.12	0.0006	998.8	0.02	129.3	1.79
	Intermedium MKI	2.51	84.7	0.79	0.03	1174.3	0.10	76.3	2.98
	High MKI	1.48	91.9	5.60	0.002	986.4	0.001	29.0	2.33
	P value	*0.3757*	*0.6618*	*0.7353*	*0.2160*	*0.6670*	*0.0277*	*0.1662*	*0.4839*

*MK: mitosis-karyorrhexis index; ^ INPC: International Neuroblastoma Pathology classification

Gene expression levels and survival analyses.

Considering 30 treatment-naïve specimens only, we observed significantly higher gene expression levels of *ASCL1* (p=0.0007), *INSM1* (p=0.0016) and *DLL3* (p=0.0064) in cases that relapsed during the follow-up (**Table 4**). On the other hand, the same analyses on post-treatment group did not give significant result for any tested gene (**Supplementary Table 1**). In **Figure 1** we present the gene expression profile of the entire cohort, according to the median gene expression levels of *INSM1, NOTCH1, NEUROD1*, *YAP1, DLL3, ASCL1* and *POU2F3* and recurrent disease status. As depicted, the cases with a median higher gene expression level of *NOTCH1* (P <0.001), *INSM1* (P=0.001), *NEUROD1* (P=0.037) and *YAP1* (P=0.003) demonstrated more frequently recurrence of the disease.

Table 4. *Gene expression levels according to the follow up status in 30 treatment-naïve cases.*

mean±SD value	Total	Disease free (25)	Relapse (5)	*P* value
YAP1	2.70±3.11	2.67±3.34	2.88±1.21	0.891
MYCL	186.2±229.6	231.7±240.6	48.7±81.8	0.145
ASCL1	379.2±662.61	208.8±378.7	1231.2±110.7	**0.0007**
POU2F3	0.27±0.58	0.29±0.62	0.19±0.37	0.744
DLL3	20.4±49.1	9.90±23.3	72.0±100.4	**0.0064**
INSM1	2862.1±5349.5	1565.4±2369.1	9345.1±10523.1	**0.0016**
NEUROD1	0.16±0.46	0.10±0.28	0.49±0.95	0.08
NOTCH1	1.62±1.44	1.53±1.51	2.06±1.01	0.456

Figure 1. *Gene expression patterns of the entire cohort according to the recurrent disease status.*

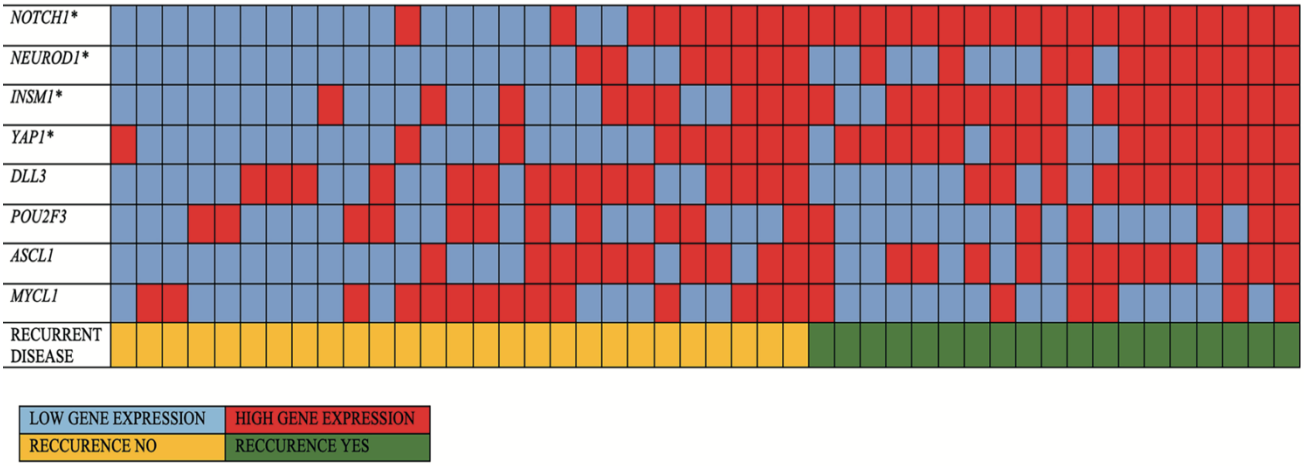

Fisher exact test: NOTCH1: p<0.001, NEUROD1: p= 0.037, INSM1: p=0.001, YAP1: p=0.003.

In detail, as shown in **Figure 2**, higher levels of *INSM1* were significantly correlated with shorter disease-free interval (DFI) in the whole group (**Figure 2A**, p=0.0012), as well as when separately analyzed in the treatment-naïve (**Figure 2B**, p=0.0147) and the post-chemotherapy groups of patients (**Figure 2C**, p=0.0365). Moreover, the patients with higher levels of *NOTCH1* had a shorter DFI, both in the whole cohort (**Figure 2D**, p=0.0001) and in the 30 treatment naïve patients (**Figure 2E**, p=0.0085), (but not in the 16 post-chemotherapy patients (**Figure 2F**, p=0.158). In addition, considering the whole case series, patients with high expression of *YAP1* and *NEUROD1* had shorter DFI, compared to those with low expression (**Supplementary Figure 1**. A (p=0.0007) and B (p=0.0128), respectively). However, no significance was observed when stratified according to the chemotherapy status (data not shown).

Furthermore, as shown in **Table 5**, univariate analysis of whole series indicated that, considering clinic-pathological features, stage IV (HR 8.57; CI 1.1-68.6 p=0.043) and high expression of *NOTCH1* (HR 15.6; CI 2.05-118.7, p=0.008), *NEUROD1* (HR 3.17;1.14-8.78, p=0.026), *INSM1* (HR 5.24, CI 1.49-18.5, p=0.010) and *YAP1* (HR 8.57, CI 1.93-37.9, p=0.005) where associated with adverse prognosis in terms of DFI. Moreover, poorly differentiated forms (HR 0.24; 0.06-0.98, p=0.048) of disease were significantly associated to better DFI survival compared to undifferentiating lesions.

Furthermore, preliminary analyses of gene expression levels in the pre- and post- treatment samples of 4 patient with available materials, demonstrated a decrease of *ASCL1, INSM1, DLL3* (**Figure 3A-C**) and an increase of *YAP1* and *NOTCH1* (**Figure 3D/3E**) in all 4 cases, whereas *POU2F3, MYCL1, NEUROD1* (**Figure 3F-H**) demonstrated a more heterogenous gene expression profile.

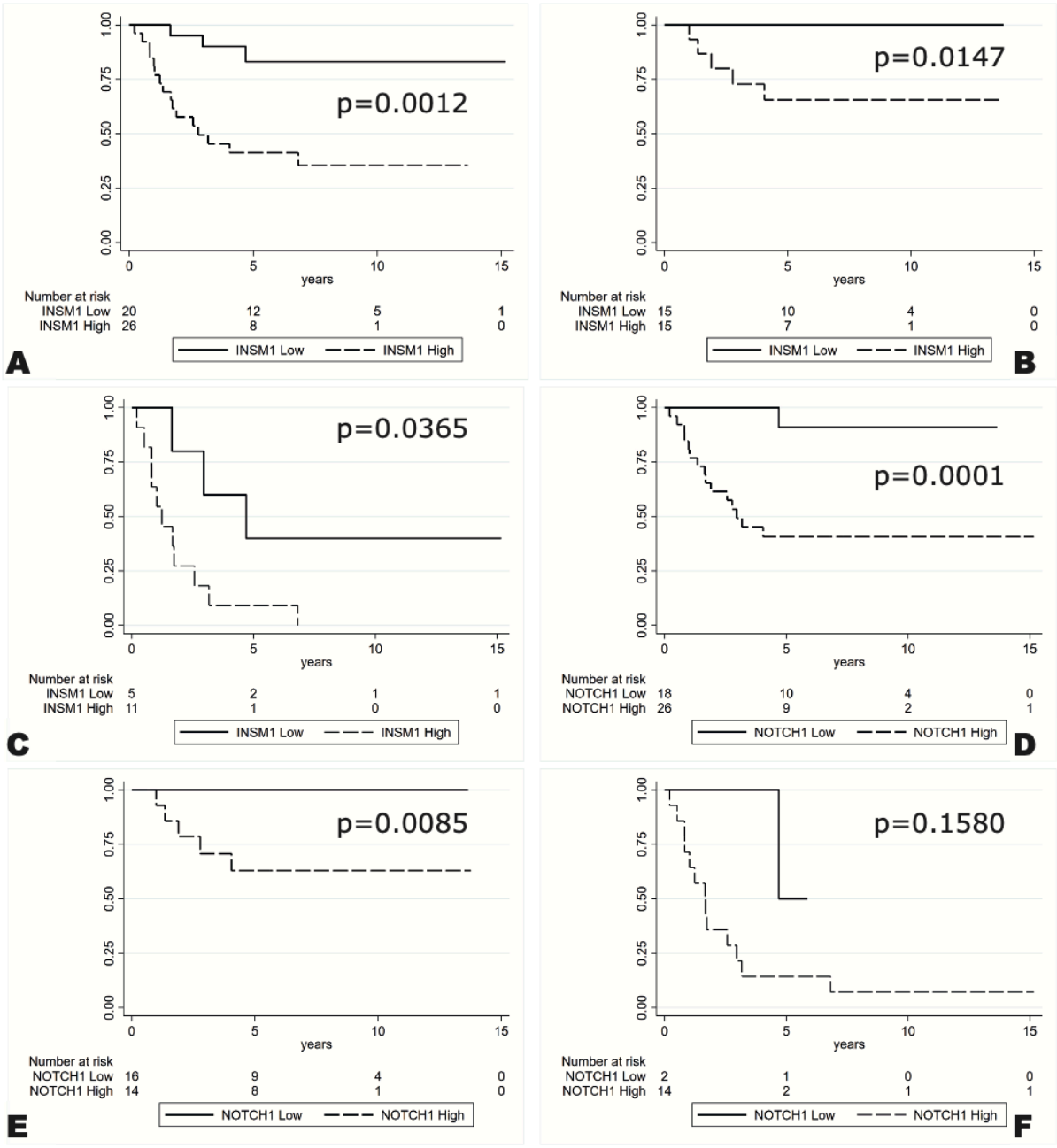

Figure 2. *Kaplan-Meier estimates of DFI according to the INSM1 gene expression level in the whole series (A: p=0.0012) and in treatment naïve (B: p=0.0147) and post-chemotherapy cases (C: p=0.0365). Kaplan-Meier estimates of DFI according to the NOTCH1 gene expression level in the whole series (D: p=0.0001) and in treatment naïve (E: p=0.0085) and post-chemotherapy cases (F: p=0.1580).*

***Table 5**. DFI Univariate survival analysis whole series (#46).*

Parameter		**HR [CI]**	**P value**
Age	(<18 vs ≥18 months)	3.97 [0.0-inf]	1.000
Stage	I/II[a]	1	
	III[b]	5.16 [0.0-inf]	1.000
	IV[c]	8.57 [1.1-68.6]	**0.043**
	IVS[d]	4.91 [0.0-inf]	1.000
INPC^	Undifferentiated	1	
	Poorly differentiated	0.24 [0.06-0.98]	**0.048**
	Differentiated	0.52 [0.06-4.47]	0.549
Shimada classification	Low MKI*	1	
	Intermediate MKI	1.90 [0.54-6.65]	0.315
	High MKI	8.24 [- -]	-
NOTCH1	low vs high	15.6 [2.05-118.7]	**0.008**
ASCL1	low vs high	2.09 [0.76-5.78]	0.153
DLL3	low vs high	1.26 [0.46-3.49]	0.649
NEUROD1	low vs high	3.17 [1.14-8.78]	**0.026**
INSM1	low vs high	5.24 [1.49-18.5]	**0.010**
YAP1	low vs high	8.57 [1.93-37.9]	**0.005**
POU2F3	low vs high	0.61 [0.16-2.32]	0.473
MYCL1	low vs high	0.34 [0.11-1.08]	0.069

Abbreviations: *MKI: mitosis-karyorrhexis index; HR: hazard ration; CI: confidence intervals; ^INPC: International Neuroblastoma Pathology classification.

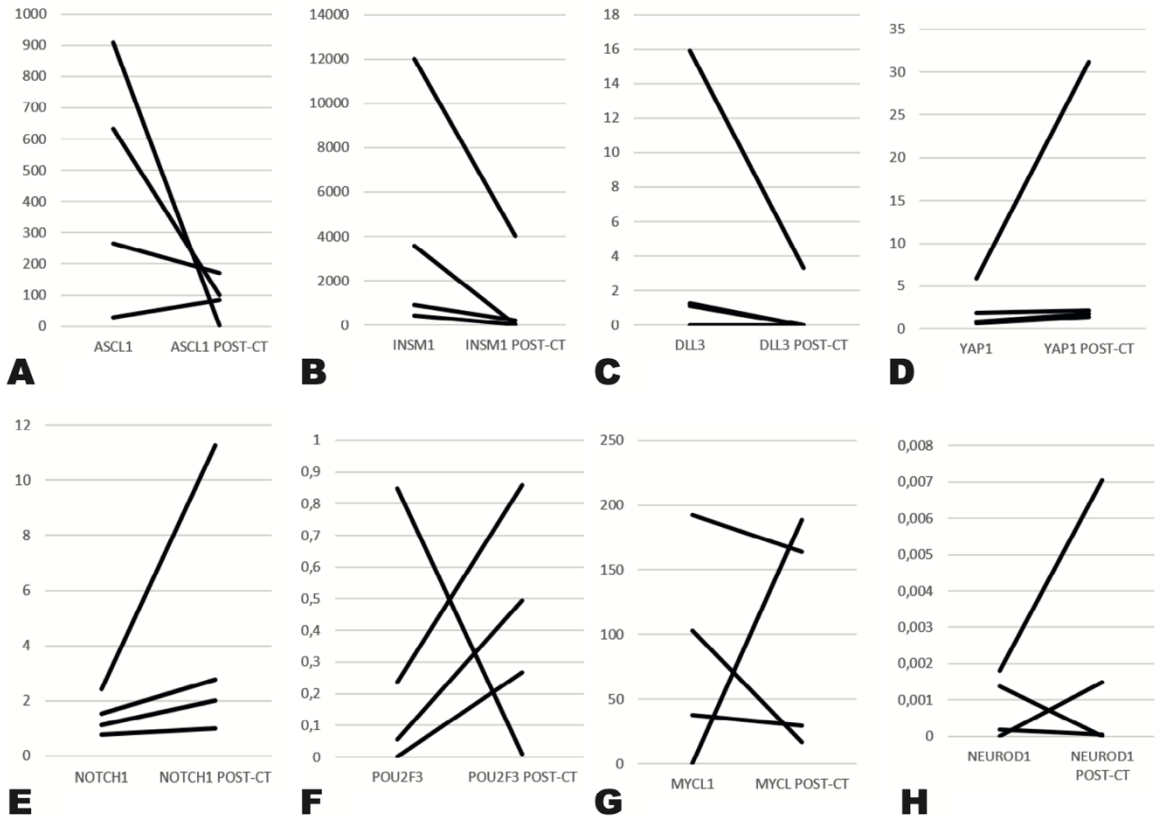

Figure 3. *Gene expression levels in the pre- and post- treatment samples of 4 patient with available materials, showing a decrease of ASCL1, INSM1, DLL3 (3A-C) and an increase of YAP1 and NOTCH1 (3D/3E) in all 4 cases, whereas POU2F3, MYCL1 and NEUROD1 (3F-H) demonstrated a more heterogenous genetic makeup.*

Gene combination analyses.

Considering the different combinations of *INSM1, NOTCH1, NEUROD1*, and *YAP1* gene expression levels according to the recurrent disease status (**Table 6**), patients with low expression of all four genes did not experience recurrent disease while patients with high levels of at least one of the forementioned genes demonstrated significantly more frequent recurrences (p=0.003).

Moreover, we observed a statistically significant increase in the odds of the patients with the high levels of ≥3 above indicated genes when considering the whole case series (OR:8.75, 95% CI: 2.19-34.81, p=0.002). However, when stratified according to the treatment status, no significance was observed the treatment naïve group (OR:4.75, 95%CI: 0.63-35.48, p=0.129) and post-chemotherapy group of patients (OR:2.75, 95% CI: 0.16-46.79, p=0.484) analyzed separately (**Supplementary Table 2**).

Table 6. *Gene combination analyses INSM1, NOTCH1, NEUROD1, and YAP1 according to recurrent disease status.*

Recurrent disease	None[a]	1-gene-high levels[b]	2-genes-high levels[c]	3-genes-high levels[d]	4-genes-high levels[e]	*P* value
No	11	6	3	5	3	0.003
Yes	0	1	3	5	9	
Total	11	7	6	10	12	

*Bonferroni correction e vs a p=0.001; e vs b p=0.038

DISCUSSION

We demonstrated in a series of 46 pediatric neuroblastomas that neuroendocrine-lineage transcriptional genes are expressed in neuroblastoma and that their profiles of expression may identify subgroups of patients with increased risk of recurrence and/or shorter survival. The study design focused on gene expression analysis and not immunohistochemical determination of the corresponding protein expression due to the following considerations. First, reliable, and robust antibodies are not available for all molecules. Second, tissue material available was limited in some cases preventing the possibility to perform both RNA extraction and subsequent sectioning for a multi-target immunohistochemical procedure. Moreover, even in the more extensively investigated small cell lung cancer model gene expression data have been used for molecular classification purposes (82,165), whereas no study clearly demonstrated a linear correlation between protein and mRNA expression for these targets. The strength of the transcriptional data observed in this study is proven by the very high positive reciprocal correlation among most of the markers investigated, being *NOTCH1* the one showing the correlation with the highest number of genes. Interestingly, at variance with other models in which these transcription factors are active, such as small cell lung carcinoma (82,165), the expression of the genes here investigated did not segregate neuroblastoma cases into different families characterized by alterative transcriptional profiles, since no inverse correlation among any of the genes tested was identified.

Our data on the association of gene expression profiles with aggressive clinical outcome and survival represent the first global evidence that the expression of neuroendocrine differentiation transcriptional drivers may be used to further characterize neuroblastoma patients, and several preclinical evidence exist supporting their role as potentially relevant clinical prognostic biomarkers.

Among all genes, four of them – *NOTCH1*, *INSM1*, *YAP1* and *NEUROD1* – emerge as the most significant, being associated with both shorter disease-free interval and high tumor stage and/or risk of recurrence.

The association of *NOTCH1* overexpression with adverse clinical outcome in our series is expanding previous data obtained by means of the immunohistochemical analysis of Notch1 protein in a large series of neuroblastomas (180). At variance with such previous series, we did not compare the expression of *NOTCH1* (and of all other genes) with *MYCN* amplification status, and this limitation should be considered in future studies. Interestingly, in a translational view, the demonstration of *NOTCH1* expression in neuroblastoma and its positive correlation with aggressiveness is paralleled by in vitro data on the efficacy of Notch1 inhibition in neuroblastoma cells. In a study on a variety of neuroblastoma cell lines, gamma-secretase inhibition (in particular GSI-I) was shown to impair cell proliferation and to promote apoptosis in vitro and in vivo through targeting Notch signaling (181). Moreover, the Notch1 inhibitor NSI-1 has recently shown to suppress the viability of SH-SY5Y neuroblastoma cells characterized by a constitutive Notch1 activation (182). The impact of *NOTCH1* overexpression in the adverse clinical behavior of neuroblastoma patients in our series is to be further validated in a biological perspective. However, among the possible mechanisms,

Notch1 has been shown to actively maintain a stem cell phenotype in neuroblastoma cells that confer highly tumorigenic properties (183).

INSM1 transcription factor has emerged *in vitro* as a neuroblastoma biomarker that plays critical role in facilitating tumor cell growth and transformation (177). Its protein nuclear expression has been documented in 84% of neuroblastomas, with a suggested association with clinical outcome, being the three INSM1-negative neuroblastoma patients in the published study all alive with a median survival of 15 years as opposed to a median of 5 years in 9 out of 13 INSM1-positive neuroblastoma patients (178). No definitive data are present in the literature on its possible role as prognostic biomarker in neuroblastoma. However, in other tumor models - such as pulmonary high grade neuroendocrine carcinoma - positive INSM1 protein expression has been associated with a dismal prognosis (184) in line with the data on *INSM1* gene expression levels from the present study.

Among other markers associated with neuroblastoma aggressiveness in our series, *NEUROD1* was already shown to promote cell growth in vitro (172) and tumor formation *in vivo* (185) in neuroblastoma cells. YAP1 expression has been reported to significantly increase cell proliferation and growth through inhibition of 27^{Kip1} activity in neuroblastoma cell lines SH-SY5Y and SK-N-SH (186). Moreover, YAP1 overexpression has been associated to the increased resistance to platinum-based (187) and MEK-inhibiting (188) therapeutic strategies. The preliminary data on gene expression levels of pre- and post-chemotherapy samples of the same patients indicated that the therapy induces varied expression of genes, generally characterized by a decrease of *ASCL1, INSM1, DLL3* and an increase of *YAP1* and *NOTCH1*. However, further studies are needed to validate this observation.

In terms of correlation with differentiation, *NOTCH1* and *YAP1* expression was significantly higher in differentiating as compared to poorly differentiated tumors according to the INPC classification. This observation cannot find a clear explanation in the current literature. A previous *in vitro* study is partly in contrast with our findings and shows that Notch1 inhibition prevents neurite formation in neuroblastoma cells (189). Moreover, these data are apparently in contrast with the adverse impact on clinical outcome for both markers in our same series and might more probably represent a bias related to the limited number of cases in the differentiation group.

CONCLUSIONS

The gene expression levels of our target genes were also shown to be significantly modulated by chemotherapy, since all genes were de-regulated in the majority of cases. However, this part of the study is explorative only, due to the small number of cases with both pre- and post-treatment samples available, and no definite data on regulatory profiles can be determined.
In conclusion, we identify a strong prognostic impact of neuroendocrine-lineage transcriptional profiles in neuroblastoma, and suggest that the evaluation of *NOTCH1*, *INSM1*, *YAP1* and *NEUROD1* might help to further characterize the risk of relapse in neuroblastoma patients.

SUPPLEMENTARY MATERIAL

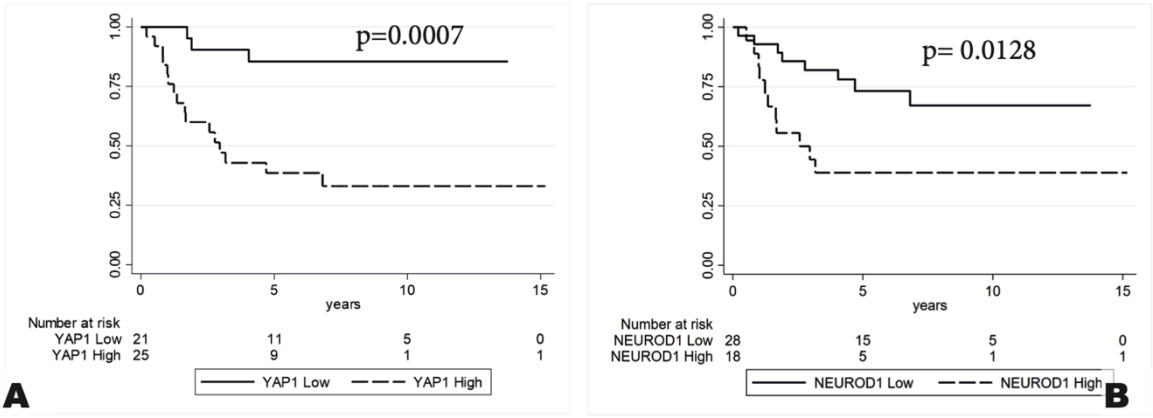

Supplementary Figure 1. Kaplan–Meier estimates of DFI according to *YAP1* (A: p=0.0007) and *NEUROD1* (B: p=0.0128) gene levels expression in the whole series.

Supplementary Table 1. Gene expression levels according to the relapse in 16 post- treatment case.

mean±SD	Total	Disease free cases (3)	Relapsed cases (13)	*P* value
YAP1	28.8±85.3	6.18±7.45	34.1±94.5	0.626
MYCL	93.6±83.3	45.0±21.7	104.8±88.7	0.277
ASCL1	415.2±766.7	204.4±216.6	463.8±844.6	0.614
POU2F3	1.84±4.51	0.35±0.57	2.19±4.96	0.543
DLL3	18.9±29.9	28.7±36.3	16.7±29.4	0.552
INSM1	17567.3±33322.6	8250.9±13453.17	19717.23±36484.7	0.608
NEUROD1	7.02±26.2	0.05±0.08	8.63±29.0	0.626
NOTCH1	3.76±2.22	3.95±4.21	3.73±1.79	0.879

Supplementary Table 2. OR and 95% CI regarding different gene expression levels of *INSM1, NOTCH, NEUROD1* and *YAP1*.

Recurrent disease	OR	95% CI	*P* value
Whole cohort #46			
≥ 3 markers with high gene expression	8.75	2.19-34.81	0.002
30 treatment naïve			
≥ 3 markers with high gene expression	4.75	0.63-35.48	0.129
16 post-chemotherapy			
≥ 3 markers with high gene expression	2.75	0.16-46.79	0.484

OR: Odds ratio; CI: Confidence Interval.

CHAPTER 2: IMMUNE-RELATED GENE EXPRESSION PROFILES OF ONCOCYTIC AND NON-ONCOCYTIC POORLY DIFFERENTIATED THYROID CARCINOMAS; CORRELATION WITH CLINICO-PATHOLOGICAL CHARACTERISTICS.

This chapter is based on the following papers:

Metovic J, Vignale C, Annaratone L, Osella-Abate S, Maletta F, Rapa I, Cabutti F, Patriarca S, Gallo M, Nikiforov YE, Volante M, Papotti M. The Oncocytic Variant of Poorly Differentiated Thyroid Carcinoma Shows a Specific Immune-Related Gene Expression Profile. J Clin Endocrinol Metab. 2020 Dec 1;105(12):dgaa655. doi: 10.1210/clinem/dgaa655. PMID: 32936917

Metovic J, Cabutti F, Osella-Abate S, Orlando G, Tampieri C, Napoli F, Maletta F, Daniele L, Volante M, Papotti M. Papillary thyroid carcinoma: clinico-pathological characterization and gene expression profiling of aggressive and non-aggressive forms (manuscript submitted).

INTRODUCTION

Thyroid cancer

Thyroid cancer comprises a group of tumours with remarkably different features. These neoplasms are the most common malignant tumors of the endocrine system (190), occurring around 3 times more often in women than in men (191). The incidence in the last few decades has been continuously increasing. This trend has been observed in various geographical areas, particularly in the Western world such as the United States (192), Canada and Europe (193,194).

SEER data indicate that the 5-year survival rate remained stable over the period between 2003 and 2012, amounting to 97.9% (195). The most significant prognostic factor is represented by the histotype: the survival rate for papillary thyroid carcinomas (PTC) at 20 years is 98-99%, for follicular thyroid carcinomas (FTC) 80-90%, dropping to 50-75% at 10 years for medullary thyroid carcinomas (MTC) and is less than 20% at 1 year for the anaplastic thyroid carcinomas (ATC) (196).

Risk factors.

Exposure to ionizing radiation is one of the risk risk factor for which it has been demonstrated a correlation with the development of thyroid carcinomas; especially for the papillary histotype and if the exposure occurred under 15 years of age, even for doses <0.1 Gy (197). The underlying mechanisms are a consequence of an interaction between the ionizing radiations with the cellular genome that it can involve rearrangements of the oncogenes such as *RET* and *TRK*; this would also explain their high presence in papillary forms (198).

Of note, iodine deficiency favors the development of thyroid cancer in the experimental animal models, likely following an increase in circulating TSH levels; however, in the low-iodine areas this correlation was not shown (199). The iodine deficiency is also a predisposing factor for development of papillary carcinomas in the case of exposure to ionizing radiation (200). It has been hypothesized that Hashimoto's thyroiditis may be a risk factor for development of thyroid cancer through two process-mediated mechanisms, autoimmune and TSH. TSH positively correlates with the risk of developing cancer of the thyroid gland (201–203); thyroid autoimmunity may play a role in carcinogenesis through the production of proinflammatory cytokines and oxidative stress (202), however no significant correlation was found between the presence of anti-thyroid antibodies and the risk of develop thyroid cancer (202,204).

A history of pre-existing benign thyroid nodular disease, adenoma, or goiter multinodular is another strong risk factor for the development of thyroid cancer. The risk is higher for adenomas than for non-toxic goiter and is higher in the first 10 years after diagnosis, but remains elevated even afterwards (205,206).

The risk of thyroid cancer in first-degree relatives of patients with carcinomas originating from follicular cells is 4 to 10 times higher than the general population (207). In patients with familial adenomatous polyposis of the colon, a syndrome caused by a germline mutation of the adenomatous polyposis coli (*APC*) gene on 5q21, thyroid cancer typically occurs in women in the third decade of life; most of the neoplasms that arise in these patients are papillary carcinomas, and 20-40% of these are morular cribriform variants (208). In individuals with Cowden syndrome, due to mutation of *PTEN* tumor suppressor gene on the chromosome 10q23.31, mainly follicular adenomas and carcinomas are observed (209). Cowden's disease is associated with goiter in 40% of patients and with thyroid carcinoma in 10% of patients. Some patients also have familiar PTC or FTC without other tumors. MTC is often familial and may occur in association with the multiple endocrine neoplasia syndromes (MEN) type 2A and 2B or without other endocrinopathies (210).

Classification

The primary thyroid cancers in more than 95% of cases originate from thyroid follicular cells, while 2-3% originate from C cells and includes medullary histotype carcinomas.
Carcinomas that originate from the follicular cells of the thyroid are PTC, FTC, Hürthle cell carcinoma (HCC), PDTC and ATC. PDTC and ATC are thought to be in many cases the result of a de-differentiation of well differentiated carcinomas, however some cases may arise *de novo* (179).

The main classes of thyroid carcinomas according to the WHO are as follows (179):

- PTC: constitutes from 63% (Ireland) to 93% (Japan and Korea) of all thyroid carcinomas, its main variants are: classic papillary carcinoma, follicular variant of PTC, encapsulated variant, tall cell carcinoma, hobnail variant, papillary microcarcinoma, columnar and oncocytic variant.

- FTC: constitutes from 6 in 10% of all thyroid cancers, its variants are: minimally invasive FTC, encapsulated angioinvasive FTC, and widely invasive FTC;

- HCC (oncocytic) constitutes about 3% of all thyroid cancers

- PDTC: it is rare, constituting 1-5% of all thyroid cancers.

- ATC: it is rare, constituting 1-2% of all thyroid carcinomas.

- MTC constitutes 2-3% of all carcinomas of the thyroid.

Well differentiated thyroid cancers (WDTC)

Papillary thyroid carcinomas

Macroscopic characteristics

Macroscopically, papillary carcinoma appears as an infiltrating neoplasm with poorly defined margins, hard consistency, white granular surface when cut and possible calcifications. Tumor diameter varies widely, averaging 2-3 cm (211).
The incidence of tumors less than 1.5 cm in size varies in the literature from 13.7% (212) to 64% (213). Necrosis is infrequent and its presence in the absence of previous fine needle aspiration, should point towards an alternative diagnosis of a more aggressive tumor or undifferentiated component within the tumor mass (179).

Microscopic characteristics

The two morphological cornerstones of PTC are the papillary type architecture and the nuclear alterations. The neoplastic papillae consist of a central fibrovascular axis lined with tumor cells and they can be presented with various morphology, from elongated to arborescent (179). In some cases there is a strong predominance of papillary structures, but it is very rare that it is completely constituted by them (214). In most cases the papillae are interspersed with follicular structures consisting of neoplastic cells with similar nuclear characteristics (179). The nuclei of PTC cells show characteristic alterations that can be grouped into three categories: changes in shape and size, nuclear membrane irregularities and chromatin alterations (215). The nuclei are enlarged and elongated, with irregular margins, thickened chromatin on the inner side of the nuclear membrane. Because of this apposition of chromatin material in the periphery the nucleoplasm appears empty when observed in light microscopy (216–219).

The cytoplasm of PTC cells is slightly eosinophilic. Mitotic figures are absent or rare in conventional PTCs, but after fine-needle aspiration there may be exceptions to this rule (179). As an alternative to the follicular or papillary growth pattern, PTC can appear as solid or trabecular formation; in most cases this is a focal change but it can also involve the whole tumor mass (179).
Psammoma bodies, round calcified concretions with central lamination, are structures classically associated with PTC. These are observed in the 50% of cases and are frequently present in carcinomas with a prevalent pattern of papillary growth (220,221). Psammoma bodies are located in the stroma or lymphatic vessels (179).
Squamous metaplasia is common in PTCs and is reported in 20-40% of cases (222,223).
An abundant fibrous stroma is also common in these tumors, especially on the periphery of the neoplasm (214). In some cases this stromal reaction evokes desmoplastic reaction (224).
Rarely, it can acquire a morphology similar to fibromatosis, nodular fasciitis or myofibroblastic inflammatory tumors, to the point of hiding original neoplastic component (224,225).

Multinuclear giant cells of histiocytic nature, can be observed, which can be numerous in cytological preparations (226).
Cystic formations are often present and most of these are bordered by papillary neoplastic structures, but it is also possible that they are lined with a deceptively benign monolayer flat epithelium (179). Neoplastic embolization of blood vessels is not as common as in FTC but can be observed (223). Lymphatic vessel embolization is much more common (179).

Immunophenotype

PTC cells are positive for thyroglobulin, TTF1, PAX8 and cytokeratins (pancytokeratin, CK7, CAM5.5, AE1/AE3) (227–231). They are negative for CK20, calcitonin and NE markers (179). Mucin stains are positive to a considerable extent of PTC (232,233). Positivity is observed for HBME1 in conventional PTC and less frequently in the follicular variants (234,235). Galectin 3 is positive both at the cytoplasmic and nuclear level; it is observed in most PTCs but also in reactive benign cells as in Hashimoto's thyroiditis (236–238). CD56, absent in carcinomas but present in normal thyroid and benign tumors (239), it is the marker of more sensitive and specific malignancy, in comparison to CK19, the least specific marker of malignancy (240).

Variants

Papillary microcarcinoma

Papillary microcarcinoma is defined as a tumor with a diameter less than or equal to 1 centimeter (179). An autopsy incidence of papillary microcarcinoma has been reported in several studies in a range between 5% and 35.6%. The prevalence of this tumor increases rapidly from infancy to adulthood and then remains relatively constant (241–243).

Macroscopically, due to their small size, these tumors can pass unnoticed on gross examination of the surgical specimen (179). Microscopically, this variant has in general an irregular configuration, similar to a scar. Neoplastic cells are mostly represented in the periphery, while other non-cancerous elements are located in the center of the lesion. Some microcarcinomas are totally surrounded by an extremely thick fibrous capsule, which may be focally calcified. The typical features of PTC are present, including typical nuclear irregularities, fibrosis, psammomatous bodies and occasional well-formed papillae(179).

The prognosis of papillary microcarcinoma is excellent. In one study, 93% of patients were disease-free at follow-up, and there were no cases of distant metastasis (244,245). Despite this, some authors have highlighted how these neoplasms can exhibit a malignant behavior (246,247), especially in cases with the BRAF mutation (V600E) (248).

Encapsulated variant

The encapsulated variant accounts for 10% of PTCs (244,249,250). It demonstrates architecturally and cytologically classical PTC features, completely surrounded by a fibrous capsule, which may be intact or focally invaded by the neoplasm (179).

Encapsulated PTCs have an excellent prognosis. Locoregional lymph node metastases can be present, but distant metastatic depostis are rare and the survival rate is nearly 100% (249–251).

Follicular Variant (PTCFV)

This variant presents almost exclusively a follicular growth pattern (252,253). It can be encapsulated (with or without vascular or capsular invasion) or non-encapsulated (infiltrative). In its infiltrative form the variant has many features common in classical PTC; especially the nuclei of the cells that line the follicles present the classic alterations of the PTC (179). There are rare cases in which the neoplastic follicles are cystically dilated, simulating nodular hyperplasia (254–256), cases in which neoplastic follicles intersperse normal follicles (the so-called "sprinkling sign") (257) and even rarer cases in which there is diffuse tumour involvement of the whole thyroid gland, without formation of grossly discernible nodules (diffuse or multinodular follicular variant) (258,259).

Diffuse Sclerosing Variant

This uncommon variant occurs more frequently in women in the second or third decade of life (260). It is typically presented as diffuse enlargement of the thyroid gland. Elevated serum antithyroglobulin and antimicrosomal antibodies may mimic Hashimoto thyroiditis (261,262), while a hardened thyroid gland can mimic Riedel's thyroiditis (263).
Histologically there is a widespread involvement of the gland characterized by multiple neoplastic foci, dense sclerosis, numerous psammomatous bodies and background changes of chronic lymphocytic thyroiditis. Tumor nests appear solid with associated squamous metaplasia. The neoplastic cells have a tendency to invade intrathyroidal lymphatic spaces and to show extrathyroidal extension (179). Cancer cells are unevenly positive for thyroglobulin, TTF1 and CK19 (264,265). *RET / PTC* rearrangements are frequent, while mutation of *BRAF* is rare (266–268). Unlike classic PTC, this variant is associated with a higher rate of extrathyroidal extension, lymph node metastases and distant metastases (occurring in about 10-15% of cases, mainly to the lungs). Diffuse sclerosing variant is also associated with a shorter disease-free interval (269–271). Despite this, mortality is comparable to conventional PTC (272,273).

Tall Cell Variant

By definition, this variant is composed of cells that are two to three times as tall as they are wide, and that show abundant eosinophilic (oncocytic-like) cytoplasm. The typical cytologic alterations of PTC are present and and nuclear pseudoinclusions are usually easily found (179).

Because tall-cell areas are frequently present in otherwise conventional papillary carcinomas, tall cells must account for > 30% of all tumour cells for the diagnosis of the tall cell variant (274,275).

The tall cell variant is more common in elderly patients and is considered aggressive, with frequent metastases and invasion of extrathyroidal tissues compared to classic PTC (276). However, the prognosis is also less favorable in tall-cell PTC variant confined to the thyroid gland (277). Furthermore, the tall cell variant of PTC accounts for a substantial proportion of radioiodine-refractory thyroid carcinomas (278). Mutations of *BRAF* and the *TERT* promoter are frequently present (279).

Hobnail variant

This rare variant is defined by the presence of more than 30% of cells with hobnail features (280–284). Histologically it presents complex micropapillary structures lined with follicular cells characterized by eosinophilic cytoplasm, apical nuclei with prominent nucleoli that have a decreased N:C ratio and loss of cellular cohesion (285). These features t can be associated with a follicular or solid growth pattern. Psammomatous bodies are present but not numerous (285). Necrosis, mitosis, vascular and lymphatic invasion and extrathyroidal extension are common. Recurrence and metastasis to lymph nodes and distant organs are frequent (281,285). Cancer cells have the same immunohistochemical profile as classic PTC: they are typically positive for TTF1, variably positive for thyroglobulin and more than 25% of the nuclei are positive for p53 (285). The neoplastic cells have a mean proliferative index Ki-67 of 10% (285). *BRAF* V600E mutations are the most common genetic alterations, followed by those of *TP53* (286–288)

Solid-Trabecular Variant

It is not uncommon for PTC, especially in pediatric malignancies, to have foci with solid and / or trabecular growth. The term "solid variant" is used when all or most of the tumor has solid, trabecular or insular (nested) architecture (179).
The solid variant constitutes 1 to 3% of all PTCs (289,290); it's more common in young patients and with a history of exposure to ionizing radiation (291,292). This neoplasm appears to be more frequently associated with lung metastases and it may be associated with slightly higher mortality (approximately 10%) (290,293). This variant is frequently associated with *RET / PTC* fusions in pediatric and radiation-related cases (294), but not in cancers in the adult population (290).

Oncocytic variant

In its pure form, this variant is extremely rare. Examples include papillary tumours that are often encapsulated but invasive and that have oncocytic cell cytology throughout (295–298). This neoplasm must be distinguished from the tall cell variant (179).

Some PTC variants are presented in **Figure 1**, source (299).

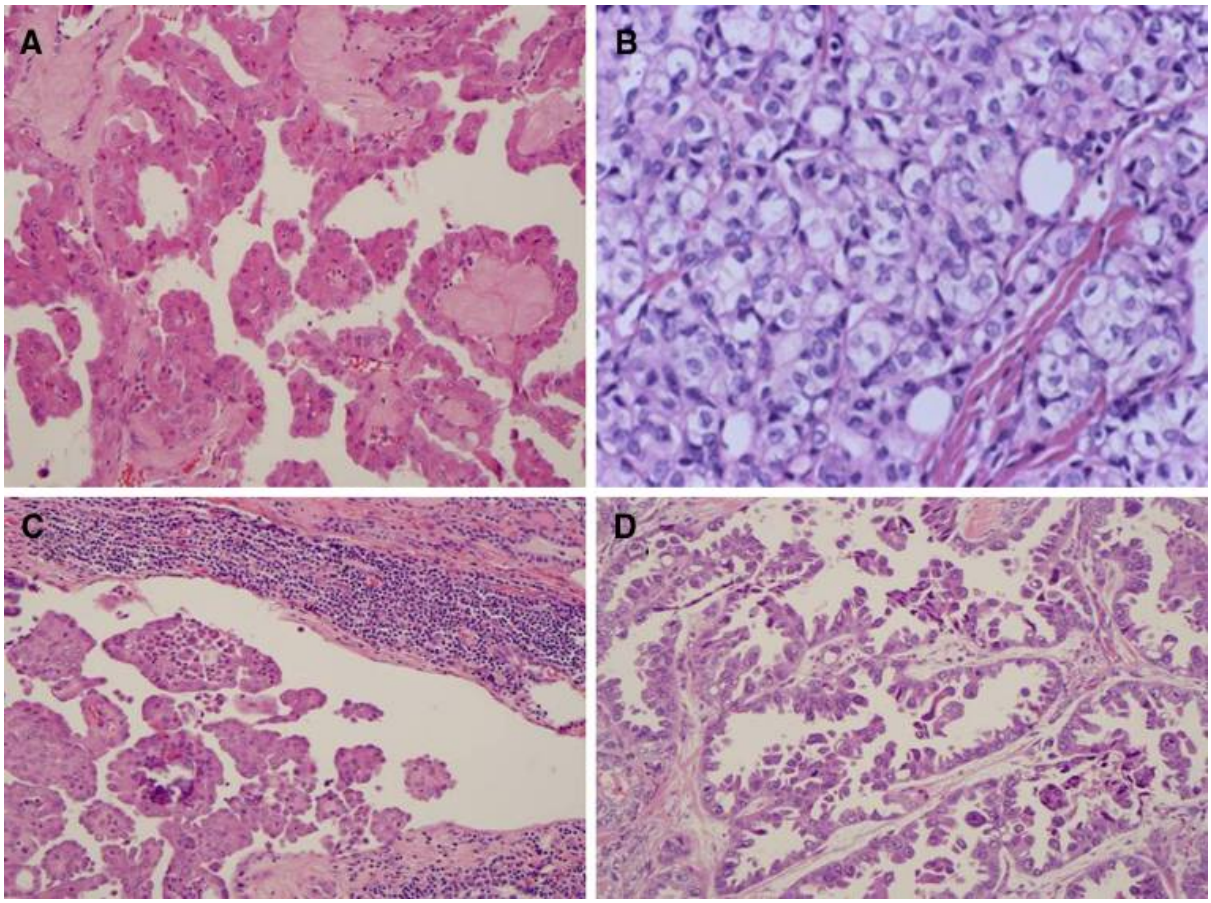

Figure 1. *Variants of papillary thyroid carcinoma.* ***A*** *Oncocytic variant with large cells showing abundant eosinophilic cytoplasm and nuclear features of papillary thyroid carcinoma.* ***B*** *Solid variant with sheets of tumor cells with abundant cytoplasm and nuclear features of papillary thyroid carcinoma including cytoplasmic invagination into nuclei.* ***C*** *Diffuse sclerosing variant showing abundant psammoma bodies, and squamoid changes in the tumor cells. A prominent lymphocytic infiltrate is present in the background.* ***D*** *Papillary thyroid carcinoma with prominent hobnail features. The tumor consists of hobnail cells with loss of polarity and high grade cytologic features including prominent nucleoli and increased mitotic activity*

Genetic profile

The *BRAF* V600E mutation is the most common driver mutation (found in about 69% of PTCs) typically present in classical PTC and in the tall cell variant (266,300–302). Other less frequent changes in *BRAF* include the mutation point K601E, small insertions or deletions in the vicinity of codon 600 (303,304) and chromosomal rearrangements such as *AKAP9-BRAF* fusion (305,306). Mutations of *NRAS, KRAS* and *HRAS* are also common (305), especially in the follicular variants (307). The *EIF1AX* mutation can also be found in the follicular variants. *RET / PTC* chromosomal rearrangement is the most common (found in 6.8% of PTCs) followed by rearrangements of *NTRK3, NTRK1* and *ALK* (305).
The progression of the neoplasm is associated with the accumulation of mutations in other genes, such as *TP53, PIK3CA* and *AKT1* (173,174). Mutations of *TERT* (C228T and C250T) are present in more advanced stages of PTCs and are associated with a higher risk of distant metastases, cancer-related recurrence and mortality (308–310).

Follicular thyroid carcinoma

Macroscopic characteristics

FTCs range from solid lesions enclosed by thick capsule (with possible calcifications) to tumors mimicking follicular adenomas, although the capsule is usually more evident compared to the latter. Foci of capsular invasion can rarely be observed. Moreover, extrathyroidal extension can be observed in widely invasive tumors (179).

Microscopic characteristics

FTC is a neoplasm of follicular cells surrounded by capsule with the presence of vascular and / or capsular invasion. According to these criteria it is further classified into: (1) minimally invasive (capsular invasion only), (2) encapsulated angioinvasive, and (3) widely invasive (311,312).

The cytoarchitectural features of the FTC are the same as the follicular adenoma: cuboidal or polygonal cells; round nuclei, located at the base of the cells, with defined margins, uniform and finely dispersed chromatin; rare mitotic figures; and possible stromal reaction (179).

FTC is enclosed in a thick capsule, which can be calcified. For many authors in order for the tumor to be considered invasive, the capsule must be invaded at a full thickness (313,314). A tumor that infiltrates vessels of any size near or beyond the tumor capsule is considered angioinvasive. Intravascular neoplastic cells are adherent to the vessel walls, usually lined with endothelium (313). The neoplasms with limited vascular invasion (less than 4 vessels) have a better prognosis than the more invasive ones (315). Lymphatic invasion and lymph node metastases by FTC are very rare (179).

Extensively invasive FTC is associated with extensive extrathyroidal infiltration, and it is often large (316). From a prognostic point of view, the extent of vascular invasion is associated with an adverse of prognosis, and it has greater impact on prognosis in comparison to extrathyroidal extension (314).

Immunophenotype

Like other follicular-cell-derived thyroid diseases, FTC expresses lineage-specific markers such as thyroglobulin and TTF1. PAX8 is usually positive (179). For the diagnosis of malignancy some studies suggest the use of combinations of markers such as CK19, galectin 3 and HBME1 (317).

Genetic profile

Cytogenetic alterations were observed in approximately 65% of FTCs (318,319). Mutations of the RAS family are present in 30-50% of these neoplasms (320,321). Rearrangements of *PPARG, PAX8-PPARG* or *CREB3L2-PPARG* are observed in 20-30% of follicular carcinomas (322,323). Also, mutations affecting the *PI3K / PTEN / AKT* pathway occur in FTCs: *PI3KCA* and *PTEN* mutations are observed in approximately 10% of these neoplasms (324,325). *TSRH* activating mutations can be observed, especially in hyperfunctioning carcinomas (326). Mutations of the *TERT* promoter are present in 20% of FTC and are associated with more aggressive tumor behavior (310,327).

Hürthle cell carcinoma (oncocytic)

HCC are neoplasms composed of oncocytic cells; non-invasive cases are called Hürthle cell adenomas while neoplasms with evidence of vascular and / or capsular invasion are called HCC (179). Oncocytic cell tumors are considered to be neoplasms formed of more than 75% of this cell-type (328).

Macroscopic characteristics

When cut, Hürthle cell tumors show a variable brown color intensity. A capsule is normally present and that of adenomas tends to be less thick than carcinomas. Calcifications may be present in the capsule and in the tumor mass (179).

Microscopic characteristics

Hürthle cells are large cells with eosinophilic granular cytoplasm, centrally located nuclei and prominent nucleoli. The cytoplasm, which resembles that of normal hepatocytes, is completely filled with mitochondria of abnormal size, with loss of cell polarity (329,330).

Oncocytic cell carcinoma is distinguished from adenoma by the presence of invasion capsular and / or vascular (203); moreover, a growth pattern is more frequent trabecular and solid in carcinomas compared to adenomas, in which it is prevalent a follicular architecture. Fibrous bands can be observed, delimiting nests of neoplastic cells (179).
Due to the presence of scarce stroma, this tumor may exhibit pseudopapillary architecture. Cases with true papillae formation have also been reported. The nuclear characteristics make it possible to distinguish HCC wiht papillary growth pattern from oncocytic variant of PTC (179).

Calcifications can be observed in Hürthle cell neoplasms, typically in the colloid of the follicles (179). Hürthle cell tumours have a propensity to undergo infarction due to minor trauma such as fine-needle aspiration or core biopsy (331).

Unlike FTC, HCC can metastasize to the locoregional lymph nodes (332), but also give distant metastatic deposits to liver, lungs and bones (333). It is possible for the carcinoma to metastasize, forming neoplastic thrombi at the level of cervical veins, which can be confused with lymph node metastases (332).

Immunophenotype

Oncocytic cell carcinoma cells are positive for TTF-1 and thyroglobulin. In cases of poorly differentiated HCC, these two markers can be negative, causing diagnostic difficulties and confusion of these lesions with tumors of non-thyroid origin (334).

Genetic Profile

HCC have a higher frequency of mitochondrial DNA mutations versus non-Hürthle neoplasms, in the form of point mutations, deletions and insertions of various magnitudes (335–337). The biochemical, metabolic, and structural (accumulation of mitochondria in the cytoplasm) alterations of oncocytic lesions are caused by defects in genes coding for subunits of the five multimeric complexes of the inner mitochondrial membrane that constitute the oxidative phosphorylation system. If these subunits are missing or defective due to a mutation, the multimeric complex does not assemble properly, oxidative phosphorylation is impaired, and there is a compensatory accumulation of mitochondria (338,339). More than 50% of mutations involve mitochondrial coding genes (336,340), while mutations of the complex I subunit encoded by the *NOUFA1*3 nuclear gene (also called *GRIM19*) are the only nuclear gene mutations specific to oncocytic tumours reported to date. (341). Hürthle cell neoplasms of the thyroid have a lower frequency of *RAS* mutations and *PAX8-PPARG* rearrangements versus non-oxyphilic thyroid tumors (321,342,343). TP53 mutations have been observed in 10-20% HCC are (326,344) often associated with *PTEN* mutations (345). Aneuploidies are common in oncocytic carcinomas and are associated with aggressive behavior and poor prognosis (346).

Poorly differentiated thyroid cancer

Poorly differentiated thyroid carcinoma (PDTC) was first proposed as a distinct subtype of thyroid malignancy by Carcangiu et al (347). These authors reinterpreted the original observation made in 1907 by Langhans, who described a locally aggressive tumor with a peculiar architecture: tumor cells arranged in large, round to oval formations, the so-called "insulae."
PDTC is a follicular cell neoplasm that shows limited evidence of follicular cell differentiation and is morphologically and behaviourally intermediate between differentiated (follicular and papillary) carcinomas and anaplastic carcinoma (179).
PDTC accounts for a small proportion of all thyroid cancers, less than 1% of all thyroid malignancies in Japan, 1.8% in the United States and up to 6.7% in northern Italy (179,348,349).
This subtype of thyroid cancer can progress from well-differentiated forms or occur *de novo* (179). PDTC has a more aggressive behavior than well differentiated cancers but less severe than ATC (350). They can coexist with other thyroid tumor histotypes, such as tall cell variant of PTCs (278,351). Some cases have a predominantly oncocytic structure (352), others may show tall cell component, mucinous differentiation (353), rhabdoid (353) or signet ring cells (354).

PDTCs are often present at an advanced stage, have a propensity for local recurrence, and tend to metastasize to regional lymph nodes, lung, and bones. The mean 5-year survival of patients with PDTC is approximately 50% (179,355). Well differentiated thyroid carcinomas with a focal (10% or greater) PDTC component follow a more aggressive clinical course than standard well differentiated carcinomas of the thyroid (356).

Macroscopic characteristics

The tumor is usually around 5 cm in the diameter, having a solid consistency with a light brown-grey color, or may have a soft consistency accompanied by necrosis. The growth margins are often pushing, and the tumour may be partially encapsulated. Satellite nodules are often present within the parenchyma; In some cases, the multi-nodular tumors can mimic thyroid goiter (179).

Microscopic characteristics

The microscopic features described by Carcangiu et al (347) include "nests" of solid tumor formations formed by cells containing a variable number of follicles, often clearly separated by artificially created clefts.

In Turin in 2006, thanks to the collaboration of 12 pathologists from Europe, Asia and the USA, the standard diagnostic criteria were established for the diagnosis of PDTC (357). These criteria included:

1. Growth pattern (solid, trabecular, insular).
2. Absence of the typical nuclear characteristics of papillary carcinoma.
3. Presence of at least one of the following characteristics:
    - presence of irregular, convoluted nuclei
    - mitotic figures ≥3x10 HPF
    - presence of necrosis

The tumour cells are small and uniform, with round hyperchromatic nuclei, or may have convoluted nuclei reminiscent of those seen in papillary carcinoma. Mitoses are common. Extensive necrosis can result in a peritheliomatous appearance (179). Vascular invasion can occur either in a mild form with the number of affected vessels ≤ 3 or in a more aggressive form with a number of vascular foci greater than 4 (349,357). It is an event that is observed in almost all PDTCs (179).

Asioli et al (349) based on the Turin Proposal (357) considered 152 cases of PDTC and detected mitotic activity ≥ 3x10 HPF in 94% of cases, atypical mitosis in 20% of cases and presence of necrosis in 70% of cases.

Growth pattern

PDTC in general present solid- trabecular and/or insular growth patterns (179,357).
Solid forms show small and dark cells that grow in compact nests, with irregular contours; there is a loss of the ground glass structure and nuclear pseudo-inclusions, typical of PTC (357). It is necessary to distinguish this type of tumor from the solid variant of PTCs, which are common in pediatric age, presenting well-delineated oval-shaped cells containing nuclear pseudo-inclusions, and showing vascular invasion in the > 40% of cases and absence of necrosis (290,355,357,358). The prevalence of solid, trabecular, and insular architecture shows distinctive geographical distribution (359) which may underestimate the diagnosis of PDTC in certain geographical areas. Furthermore, a solid pattern of growth (defined by Nikiforov *et al*. as solid/trabecular/insular pattern) (290) may not be representative of tumor aggressiveness in PDTC based on studies of solid variant of PTC.
Insular variant consists of well-defined solid nests of cells, which may contain microfollicles containing dense colloid; tumor cells are small and uniform, with rounded or irregular hyperchromatic nuclei (179). In this variant cellular islets are located in the perivascular area and are surrounded by large areas of tumor necrosis (179,357). Insular carcinoma, in some circumstances can coexist with a classic PTC or its follicular variant (360).

Oncocytic variant

The oncocytic variant of PDTC is a controversial topic. It is characterized by a large number of mitochondria within the neoplastic cells, which give it an eosinophilic color (352). In 1996, Papotti et al (352) investigated the trabecular/insular pattern, cellular features, p53 and Bcl2 expression in a series of oncocytic thyroid carcinomas, and reported 20 well-documented cases

of oncocytic variant of PDTC. Although it was excluded from the Turin consensus, the literature mostly concurs on the existence and importance of the oncocytic variant based on large series and case reports (349,357,361,362). Although oncocytic PDTCs are generally considered more aggressive than their nononcocytic counterparts (334,352,363), they are essentially regarded as a variant of classical PDTC.

The different growth patterns of PDTC are presented in **Figure 2**, source (362).

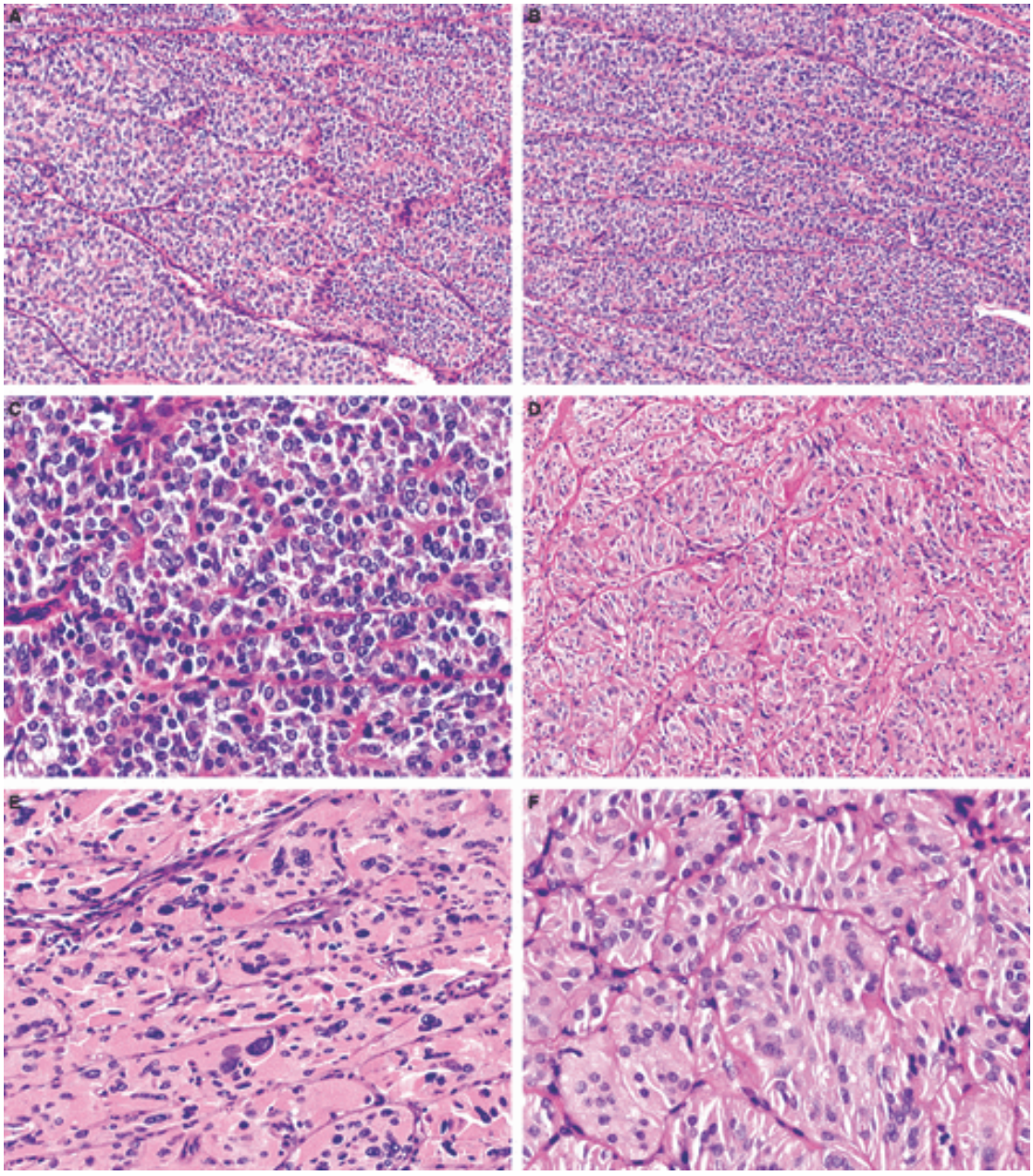

Figure 2. ***A****, Conventional poorly differentiated thyroid carcinoma (PDTC), insular growth pattern (H&E).* ***B****, Conventional PDTC, trabecular growth pattern (H&E).* ***C,*** *Conventional PDTC, increased mitotic rate, solid growth pattern (H&E).* ***D****, Oncocytic PDTC, insular growth pattern (H&E).* ***E****, Oncocytic PDTC, frank endocrine atypia may be present (H&E).* ***F****, Oncocytic PDTC, increased mitotic rate (H&E).*

Immunophenotype

PDTC tumor cells are positive for high molecular weight cytokeratins, in particular for CK7 with a positivity of 86% of cases, however they show absence of staining for CK20 (179).
In PDTCs, thyroglobulin is positive but in a lower percentage compared to PTC (showing positive staining in 57% of PDTCs and 100% of PTCs). Moreover, PDTCs are positive for the transcription factors TTF1, TTF2 and PAX-8 (179,227,364).
P53 is a nuclear marker involved in the control of cell cycle and apoptosis (365). During the formation of thyroid cancer, the p53 gene plays an important role, since its inactivation occurs which causes an increase in cell proliferation in thyroid tumors. In a study by Soares et al (366), a positivity was observed in 20 % of FTCs, 16% of PDTCs (16.1%) and 83% of ATCs (83.3%), however, no correlation with tumor aggressiveness was found.

Genetic profile

Genetical make up of PDTC includes alterations that are early driver events in thyroid carcinogenesis (i.e. RAS family) and BRAF mutations, ALK fusions and others that typically occur as late events associated with tumour dedifferentiation (i.e. mutations of TP53), TERT, CTNNB1, and AKT1 (367). PDTCs have a mutation load intermediate between that of anaplastic and well-differentiated papillary carcinomas. They carry multiple genetic alterations more frequently than do well-differentiated tumours: usually one of the early changes in combination with late alterations. Activating AKT1 mutations have been reported in 19% of aggressive, radioiodine refractory PDTCs, nearly always in combination with BRAF V600E mutation. In composite tumours, in which a well differentiated component is associated with poorly differentiated or undifferentiated areas, early alterations are typically found in both components, whereas late changes appear to be restricted to the less-differentiated areas. TERT mutations are clonal in PDTCs and ATCs, whereas they are typically subclonal in well-differentiated PTCs. Disruption of the SWI/ SNF chromatin remodelling complex, mutation of histone methyltransferases, and inactivation of the DNA mismatch repair system each occurs in as many as 5-10% of PDTCs, and in a higher proportion of ATCs. These data support a multiple genetic hits model, which is seen in many types of aggressive cancer, indicating a multistep progression from well-differentiated to poorly differentiated or anaplastic carcinoma. Some rearrangements frequently found in well-differentiated tumours are uncommon: RETJPTC and PAXB/PPARG are detected in about 10% and 5% of cases respectively, suggesting that they do not promote dedifferentiation to PDTC or ATC (179).

BRAF V600E

BRAF is the gene that codes tyrosine kinase, a potential predictor of prognosis. About 5-15% of PDTCs carry the BRAF mutation (179). BRAF V600E, previously associated with PTCs, was also noted in PDTCs, in particular those deriving from PTCs (365,368).
This mutation is related to lymph node metastases (369), therefore its presence is associated with an increased mortality (365). Mutated BRAF is associated with the silencing of the iodine transport gene in thyroid tumors (368).

RAS

The RAS genes encode G proteins, a family of 150 types of cytoplasmic proteins binding guanosine triphosphate (GTP), with the function of transducing the extracellular signal. These proteins regulate the pathways responsible for cell proliferation and survival. In tumors, RAS proteins remain blocked in their active form, causing the continuous transmission of the cell growth activating signal, thus undergoing hyper-proliferation (365).
The prevalence of RAS mutations (N-RAS, K-RAS and H-RAS) is around 18-55% in PDTCs (179,368). Unlike the BRAF mutation, the mutation of the RAS genes is linked to systemic metastases (369).

TP53

TP53 is a tumor suppressor gene and performs its action on the cell cycle, on apoptosis and on the maintenance of genetic stability. This gene also encodes the transcription factor p53, which is involved in the regulation of the cell cycle (365).The mutated TP53 gene is rarely found in WDTCs (2%), unlike PDTC, where it has been found in 10-26% of cases (368,369). This gene plays an important role in late tumor evolution, in particular from WDTC to PDTC (369).

RET

The RET gene encodes the membrane receptor with tyrosine kinase activity, involved in signal transduction (365). This gene occurs more commonly in PTC than in PDTC where it can only be found in 13-17% of cases. Its presence often indicates a coexistence with PTC (368). However, this gene was not related to increased aggression or reduced patient survival in PDTC patients (365,368).

TERT

The TERT gene encodes a component of the telomerase enzyme (368). The TERT promoter mutation is associated with aggressive PDTC behavior. It has a prevalence of 40%, intermediate between 10% of PTCs and 73% of ATCs (369).

Therapy of thyroid cancers

Surgery

Regarding well-differentiated thyroid carcinoma, in cases with tumor diameter larger than 4 cm the initial surgery must include total thyroidectomy and complete gross tumor removal. In case of tumor dimensions between 1 and 4 cm the recommended intervention is a total or subtotal thyroidectomy while in carcinomas less than 1 cm in size, along with the absence of clear indications for removal of the contralateral lobe, lobectomy is recommended (370).
On the other hand, because of their poor clinical prognosis, PDTCs are usually managed more aggressively than well differentiated thyroid carcinomas. Unlike well-differentiated thyroid carcinomas, treatment of PDTC has not been standardized due to the rarity of the disease and heterogeneity of inclusion criteria. Therapeutic decisions on PDTC have thus been mainly extrapolated from the treatment experience on well differentiated carcinomas (371). In addition, central and/or lateral neck dissection should be performed if there is clinical or radiological evidence of enlarged lymph nodes.
Surgery is the treatment of choice for PDTC, whereby the extent of surgery is determined by preoperative assessment with appropriate imaging studies and intraoperative findings. Total thyroidectomy and clearance of all gross disease can achieve satisfactory locoregional control (five-year locoregional control in up to 81% of PDTC patients) (372).

Cervical lymphadenectomy

The emptying of the recurrent lymph nodes should be performed in case of confirmed metastases, but it can also be taken into consideration in case of clinical doubt as 30-50% of PTC patients have metastases at this level. The prophylactic central neck is a controversial topic as in patients without lymph node metastases due to its unclear effects on oncologic results and quality of life of patients and as increased rates of post-operative complications (373). Laterocervical lymph node surgery is to be performed only in the case of ascertained metastases operatively (374).

Radiometabolic treatment

Regarding adjuvant treatment, its indications and effectiveness in PDTC are not clear. When compared to well differentiated forms, PDTC does not usually respond as well to the same modalities of adjuvant treatment. Radioiodine avidity of PDTC is variable (375), likely due to variation in tumor heterogeneity and variable admixtures of well and less well differentiated tumor components. Older age and extrathyroidal extension and/or extranodal extension are associated with aggressive biology and loss of radioiodine avidity in well differentiated thyroid cancers (376). PDTC often presents at an older age and at an advanced stage (377) which are

both manifestation of a more aggressive biology and thus can be accompanied by loss of radioiodine avidity. The role of postoperative external beam radiation therapy (EBRT) in PDTC is equally controversial. EBRT can be beneficial in patients with well differentiated tumors who are at high risk for locoregional recurrence (378). Similar criteria could be applied to PDTC whereby EBRT has been recommended in PDTC patients with T3 and T4 tumors and in patients with neck node involvement (359). However, no significant survival improvement has been recorded in PDTC patients following EBRT (359,379). Although reports of EBRT benefits on local control of PDTC are inconclusive, it may still be considered in high-risk settings due to a low toxicity profile with intensity-modulated radiotherapy (IMRT). Regarding chemotherapy in PDTC, reports have been scarce. There is level III evidence (nonrandomized trials with contemporaneous controls according to Sackett *et al.)* (380) with short follow-up that patients with inoperable PDTC who received chemotherapy regimen with or without EBRT became operable or were free of disease (381).

Regarding well differentiated tumors, in low-risk patients (for instance, T1, non-aggressive papillary histology) adjuvant therapy with radioiodine is not indicated (370,382–385). On the other hand, there is an indication for treatment when the tumor has a diameter greater than 1 cm or less than 1 cm, but with aggressive histology (383,384); also in tumors larger than 4 cm; in forms with extrathyroid extension; in the presence of lymph node metastases; in aggressive histological forms (370).

Hormone therapy

Thyroid hormone replacement therapy is the mainstay of long-term medical management. Patients treated with total thyroidectomy and some who undergo lobectomy alone require thyroid hormone therapy to restore euthyroidism with normal serum TSH levels. Because TSH acts as a growth factor for thyroid follicular cells (including those that are neoplastic), it can potentially affect the onset and/or progression of follicular-cell derived thyroid cancer (386).
Of note, levothyroxine hormone therapy reduces the relapse rate and improves survival, by blocking the action of TSH on neoplastic cells (370).

Immunotherapy

To date, no immunotherapy has been approved for advanced thyroid carcinoma. However, preclinical studies, a few case reports, and clinical trials, are starting to produce indications for their use. Characterization of the immune phenotype of cancers has gained interest for its potential immunotherapeutic implications. In this regard, few recent studies analyzed the immune expression profile of thyroid carcinomas (387,388).

Immune escape represents the last step of a process that starts with the development of transformed cells that are resistant to immune surveillance and progresses through the Immunoediting phase where, due to genetic or epigenetic changes in the transformed cell, but above all due to the modifications of the tumor microenvironment (TME) and of the

interactions between the tumor cells and the TME, the developing cancer acquires an increasing refractoriness to the effects of the immune system (389).

Recently published results obtained in 22 patients affected by advanced PTCs or FTCs, included in the phase Ib KEYNOTE-028 trial conducted to evaluate safety and antitumor activity of pembrolizumab as monotherapy in advanced solid tumors, showed two partial responses, for an overall response rate of 9%. Response duration was 8 and 20 months (390).

Combination of immune checkpoint inhibitors with strategies to normalize the tumor vasculature and stroma might represent a very promising approach in PDTCs that have a dominant prevalence of altered-excluded and cold immune coordination profiles. In ATCs and advanced PDTCs, a phase II clinical trial is ongoing that foresees in BRAF and RAS-negative patients the combination of atezolizumab, chemotherapy and bevacizumab (NCT03181100) (391).

Patients with PDTC often rapidly acquire a form of resistance to therapies, therefore it is necessary to act with combined strategies, aimed at targeting different aspects of the tumor microenvironment including immune cells, blood vessels, the endothelium or the cancer cells themselves. This strategy could provide a benefit on the patient's prognosis (392).

Programmed cell death-1 (PD-1) is an immune checkpoint molecule whose role is to suppress the CD8+ T-cell response upon interaction with its ligand, PD-L1(393). PD-1 is expressed on T-cells (as well as some other immune cells) in response to stimuli, such as interferon gamma, and upon interaction with PD-L1 (a membrane protein expressed on a variety of immune cells and which can be induced on cancer cells), results in T-cell anergy and apoptosis (394). There has been extensive research on disrupting this axis (through inhibition of PD-1 or PD-L1) in order to reactivate the immune response for cytotoxic T cell killing. Three of these drugs have received FDA approval for treatment of several malignancies and are considered candidate first- or second-line therapies for a variety of cancers including melanoma (395), non-small cell lung carcinoma (396), head and neck squamous cell carcinoma (397), and Merkel cell carcinoma (398).

The critical role of the PD-L1/PD-1 interaction has been demonstrated in both preclinical models and in clinical trials across many solid cancers. However, investigation into its use as a treatment option for thyroid cancer has been limited to date (399,400). Cunha et. al. demonstrated higher levels of PD-L1 expression in papillary thyroid cancers compared to normal and benign lesions and showed a positive correlation between PDL-1 levels and infiltration of CD8+, CD4+, FoxP3+ lymphocytes, as well as tumor-associated macrophages (401). In a preclinical study of ATC, PD-L1 blockade was shown to be effective only when combined with a BRAF inhibitor (392). A recent case report also showed dramatic and durable response of an ATC patient to combined vemurafenib and PD-L1 inhibitor treatment (402). The therapeutic effect of blocking either PD-1 or PD-L1 has not been previously tested in patients with thyroid cancer, but a multicenter clinical trial sponsored by International Thyroid

Oncology Group (ITOG) has recently opened to examine the efficacy of PD-1 inhibitor therapy (NCT #02688608).

In a more recent study, the expression of PD-L1 and IDO1 in PDTC was reported. PD-L1 expression was found to be relatively common in a series of tested PDTC, and a subset co-expressed IDO1. These findings provide a promising rationale to further explore immune checkpoint inhibitors as either monotherapy or in combination in PDTC patients who have limited effective treatment options (403).

Project 3: The oncocytic variant of poorly differentiated thyroid carcinoma shows a specific immune-related gene expression profile

ABSTRACT

Poorly differentiated thyroid cancer (PDTC) is a rare, follicular cell-derived neoplasm with unfavorable prognosis. The oncocytic variant of PDTC may be associated with even more adverse outcome than classical PDTC cases, but its specific molecular features are largely unknown. Our aim was to explore the immune-related gene expression profile of oncocytic and classical PDTC, in correlation with clinical and pathological characteristics (including PD-L1 expression) and outcome, and in comparison, with a control group of well differentiated follicular carcinomas (WDFC), including conventional follicular carcinomas (FTC) and Hürthle cell carcinomas (HCC).

A retrospective series of 48 PDTC and 24 WDFC was analyzed by means of NanoString technology employing nCounter PanCancer Immune Profiling panel. Gene expression data were validated using quantitative real time PCR.

Oncocytic PDTC showed a specific immune-related gene expression profile, with higher expression of *LAIR2, CD274, DEFB1, IRAK1, CAMP, LCN2, LY96,* and *APOE,* and lower expression of *NOD1,* as compared to conventional PDTCs. This molecular signature was associated with increased intra-tumoral lymphocytic infiltration, PD-L1 expression and adverse outcome. Three of these genes, *CD274, DEFB1, IRAK1,* as well as PD-L1 expression, were also the hallmarks of HCCs as compared to FTCs. By contrast, the panel of genes differentially regulated in PDTCs as compared to WDFCs was unrelated to the oncocytic phenotype.

Our results revealed a distinctive immune-related gene expression profile of oncocytic PDTC and confirmed a more aggressive outcome in this cancer subtype. These findings may provide guidance when exploring novel immunotherapeutic options for oncocytic PDTC patients.

SPECIFIC BACKGROUND

Poorly differentiated thyroid carcinomas (PDTC) represent a group of neoplasms with morphological and clinical features intermediate between follicular and papillary thyroid carcinomas on the one end, and anaplastic thyroid carcinomas on the other (179,404).

PDTC was recognized by World Health Organization (WHO) classification of thyroid tumors as a separate pathologic entity since the 2004 edition, only, although the diagnostic criteria were still ambiguous and hardly applicable in the routine diagnostic practice (179,405). Current WHO classification criteria are based on the results of a consensus conference held in Turin in 2006, that defined PDTC as a malignant follicular-derived tumor with solid, insular, or trabecular growth pattern, absence of typical nuclear features of papillary thyroid carcinoma (PTC), increased mitotic activity (≥3/10 HPF), tumor necrosis, and/or presence of convoluted nuclei (357).

PDTC can show oncocytic features (334,352,362,363), defined as cellular enlargement characterized by a voluminous, granular and eosinophilic cytoplasm, reflecting altered mitochondrion accumulation (329,406). Although oncocytic PDTC are generally considered more aggressive than their non-oncocytic counterpart (334,352,362,363), they are essentially regarded as a variant of classical PDTC. Otherwise, the oncocytic variant of follicular carcinoma (FTC), by virtue of its diverse intrinsic profile and clinically more aggressive behavior compared with other well differentiated thyroid carcinomas, has been recognized as a distinct entity and named Hürthle cell carcinoma (HCC) (179,407,408).
Oncocytic changes in thyroid neoplasms are considered a cellular adaptation process related to mitochondrial adaptive homeostasis involving reprogramming of stem cells. Defective mitochondrial ATP synthesis has been reported in oncocytic thyroid neoplasms, suggesting that impaired oxidative phosphorylation might induce mitochondrial hyperplasia and proliferation in these tumors as a compensatory mechanism (329). Disruptive mitochondrial DNA (mtDNA) mutations in different complex subunits of the respiratory chain have also been reported in oncocytic thyroid neoplasms (409). Moreover, somatic and germline missense mutations in a non-mitochondrial gene (GRIM-19), that is involved in the maintenance of mitochondrial membrane potential by controlling normal electron transfer activity of complex I, have been linked to oncocytic thyroid tumors (341).

Recently, integrated molecular analysis of HCC identified additional recurrent mutations in *DAXX*, *TP53*, *NRAS*, *NF1*, *CDKN1A*, *ARHGAP35* and the *TERT* promoter and widespread loss of chromosomes, culminating in near-haploid chromosomal content, in a large fraction of cases, a molecular signature which is maintained during metastatic spread (410).
However, the specific molecular signature of oncocytic PDTC as compared to the conventional one or to well-differentiated histotypes is largely unexplored, with a single study showing upregulation of miR-221 and miR-885-5p in oncocytic PDTC (411). This lack of information might partly explain the poor advances in therapeutic strategies for PDTC, either conventional or oncocytic. In fact, radioiodine-refractory disease in PDTCs was reported to reach up to 50% of cases (412), possibly due to tumor heterogeneity and reduced competence in iodine uptake

(350,352,372). The potential application of novel therapies, such as immunotherapy, implies the need of characterizing tumor microenvironment and immune related gene expression, an approach that in thyroid cancer is to date principally confined to preclinical investigation or clinical studies with limited sample sizes.

AIM

Based on the above, we designed the present study to explore the immune-related gene expression profile of both oncocytic variant and classical PDTC as well as of a control group of well differentiated follicular tumors. Gene expression data were correlated with clinical and pathological characteristics of PDTC, including PD-L1 expression.

MATERIALS AND METHODS

Case selection.

PDTC cases were retrieved from the pathology files of the "Città della Salute e della Scienza" and "San Luigi Gonzaga" University Hospitals of Torino in years 2000-2017. Inclusion criteria were: 1) a confirmed diagnosis of PDTC according to the WHO 2017 classification, after re-evaluation of all conventional H&E slides available; 2) availability of clinical and follow data; 3) sufficient residual tumor tissue material for molecular and immunohistochemical analyses. In total, 48 cases were selected, consisting of 25 classical PDTC and 23 PDTC oncocytic variant. A control group of 24 cases of well differentiated follicular carcinomas (WDFC) (12 classical FTC and 12 HCC cases) were retrieved from the same pathology files and time frame. The diagnosis of oncocytic PDTC and HCC was rendered when >75% tumor cells displayed oncocytic features. Clinical pathological data, including age at diagnosis, sex, tumor location, bilateral involvement, type of surgery, tumor size, pTN stage, presence of capsular and/or vascular invasion, presence of necrosis, number of mitoses, surgical margin status, extra-thyroidal extension, intra-tumoral fibrosis, concomitant presence of goiter, and follow up data were collected from clinical reports. The percentage of tumor infiltrating lymphocytes (TILs) was evaluated in intra-tumoral areas, only. Before the study started, all cases were de-identified and coded by a pathology staff member not involved in the study, and all data were accessed anonymously. The study was approved by the local Ethical Committee (#610, date December 20th, 2017), and conducted in accordance with the principles set out in the Declaration of Helsinki. Considering the retrospective nature of this research protocol and that it had no impact on patients' care, no specific written informed consent was required.

Gene expression analysis by NanoString technology.

Two 10-µm-thick formalin fixed paraffin embedded (FFPE) tissue sections were obtained from each tissue block and the tumor tissue was collected in sterile Eppendorf tube by means of manual microdissection, excluding normal parenchyma or necrotic areas.

RNA isolation was performed using the FFPE RNA Isolation Kit (Roche Diagnostics GmbH, Mannheim, Germany), according to the manufacturer's protocols. Total RNA concentration was assessed using a NanoDrop spectrophotometer (Thermo Fisher Scientific, Inc., Wilmington, DE, USA). NanoString nCounter technology was used to measure relative expression levels of immune genes within the tumor microenvironment: 300 ng of total RNA from each sample were hybridized to the nCounter PanCancer Immune Profiling panel, according to the manufacturer's instructions (NanoString Technologies, Seattle, WA, USA). This panel detects the expression of 770 mRNA targets: 730 immune related genes and 40 housekeeping genes. The analyses were set up according to the protocol provided by the manufacturer. Expression data were normalized and analyzed with the nSolver Analysis Software (version 4.0.62). For background correction, the mean count of negative controls plus two times the standard deviation was subtracted from the counts for each gene. The means of the supplied positive controls and the geometric mean of the housekeeping genes were used to normalize the measured expression values. Both positive and negative controls were included in the panel, according to manufacturer's instructions. Additionally, the Advanced Analysis module (version 2.0.115) was used to perform differential expression analyses. Briefly, by the differential expression analysis tool (nSolver Advanced Analysis module), for each gene a single linear regression was fit using all selected covariates to predict expression. A volcano plot was generated to display each gene's -log10 (p-value) and log2 fold change with the selected covariate. Highly statistically significant genes fell at the top of the plot above the horizontal lines, and highly differentially expressed genes fell to either side. Horizontal lines indicated various p-value thresholds. In addition, by the nSolver Advanced Analysis module, genes previously shown to be characteristic of various cell populations were used to measure these populations' abundance. Covariates plots were generated to compare raw cell type abundance measurements to covariates. In addition, by the nSolver Advanced Analysis module, genes previously shown to be characteristic of various cell populations were used to measure these populations' abundance (413). Covariates plots were generated to compare raw cell type abundance measurements to covariates. To run the Cell Type Profiling Module included in the nSolver Advanced Analysis module a p-value of 0.05 was set to see results (and calculate relative cell scores) only for cell types whose quantification was supported by our data. Cell types whose evidence for cell type-specific expression did not meet this level of confidence were discarded.

Quantitative real time PCR.

RT reactions of 1µg of total RNA were performed using M-MLV Reverse Transcriptase kit (Invitrogen, Carlsbad, US) in a volume of 20 µl with the following conditions: 37°C for 50 min, 70°C for 15 min.

Relative expression levels of all genes validated and internal reference were examined using a fluorescence-based real-time detection method (ABI PRISM 7900 Sequence Detection System—Taqman; Applied Biosystems, Foster City,US). For gene expression quantifications SensiFAST Probe Hi-ROX kit (Bioline, Taunton, MA) and the following TaqMan gene expression assays (Applied Biosystems, Foster City, US) were used according to the manufacturer's instructions: *ITGAL* (Hs00158218_m1), *LAIR2* (Hs00430498_m1), *DEFB1*

(Hs00608345_m1), *IRAK1* (Hs00155570_m1), *CAMP* (Hs00189038_m1), *PSMD7* (Hs00427396_m1), *LCN2* (Hs01008571_m1), *LY96* (Hs00209770_m1), *APOE* (Hs00171168_m1), *NOD1* (Hs01036720_m1), *CD68* (Hs02836816_g1), *CD163* (Hs00174705_m1). *ACTB* (Hs01060665_g1) assay was used as references for gene analyses. SensiFAST Probe Hi-ROX Kit.
Each measurement was performed in duplicate. The ΔΔCt values were calculated subtracting ΔCt values of sample and ΔCt value of a pool of RNA derived from normal different tissues and converted to ratio by the following formula: $2^{-\Delta\Delta C}$.

Immunohistochemistry.

Immunohistochemistry was performed by an automated platform (Ventana BenchMark AutoStainer, Ventana Medical Systems, Tucson, AZ, USA) using PD-L1 mouse monoclonal antibody (22C3, diluted 1:50, Dako Agilent, Santa Clara, USA). For statistical purposes, PD-L1 cut off was set at 1% of positive tumor cells with a membranous pattern. Appropriate positive (normal placenta) and negative controls were included for each immunohistochemical run.

Statistical analyses.

All analyses were performed using Stata/MP 15.0 Statistical Software (STATA, College Station, TX). Continuous variables were summarized as the mean and standard deviation (SD), whereas for categorical variables the frequency was provided. The patient's characteristics were compared using the Chi-square test for categorical variables and the T-test or ANOVA test for continuous variables, according to Bonferroni corrections. All statistical tests were two sided. Moreover, univariate/multivariate binary logistic regression models were performed using oncocytic feature as the dependent variable (yes or no) and tumour characteristics as covariates. Odds ratios and 95% CIs were estimated. The Hosmer–Lemeshow goodness-of-fit statistics were used to determine whether the model adequately described the data. Spearman's correlation test was applied to test the reciprocal correlation among genes analyzed by means of quantitative real time PCR. P-values <0.05 were considered significant. Disease-specific survival (DSS) was calculated from the surgical excision date of the primary tumor to the date of thyroid cancer death or last check-up. The disease-free interval (DFI) was calculated from the date of surgical excision of the primary tumor to the date of the first relapse or last check-up. Survival curves between different groups were plotted using the Kaplan-Meier method and the statistical comparisons were performed with Log-rank test.

RESULTS

Clinical and pathological characteristics of oncocytic PDTC.

As shown in **Table 1,** oncocytic PDTC subtype was significantly correlated with extensive angioinvasion (p=0.012), presence of necrosis (p=0.030), and presence of tumor infiltrating lymphocytes (p=0.030). Although not reaching statistical significance, fatal outcome was more frequent in oncocytic PDTC patients (p=0.080). Furthermore, Kaplan-Meier survival analysis demonstrated that oncocytic PDTC cases have a shorter DSS (**Fig. 1**; p=0.042) as compared to the classical PDTC.

Moreover, PD-L1 expression was observed more frequently in oncocytic PDTC (14/23, 61%) as compared to conventional ones (4/25, 16%) (p<0.001) and a positive PD-L1 expression was associated with a worse DFI in PDTC cases (p=0.033) (**Fig. 2**). However, PD-L1 expression was not significantly associated with clinical or pathological features of aggressiveness except for the presence and extent of necrosis in the whole series of PDTC (**Table 2**). No association of PD-L1 expression and clinical and pathological variables was identified in oncocytic PDTC, only (not shown).

At univariate analysis (**Table 3**), logistic regression highlighted a significant association between oncocytic variant and PD-L1 expression and necrosis. Multivariate logistic regression analyses confirmed the significant association between PD-L1 expression (OR 5.54, CI 1.30-23.6) and oncocytic variant also when adjusting for age, sex and necrosis. The Hosmer-Lemeshow goodness-of-fit statistics (p value=0.9190) indicated that the model adequately describes the data.

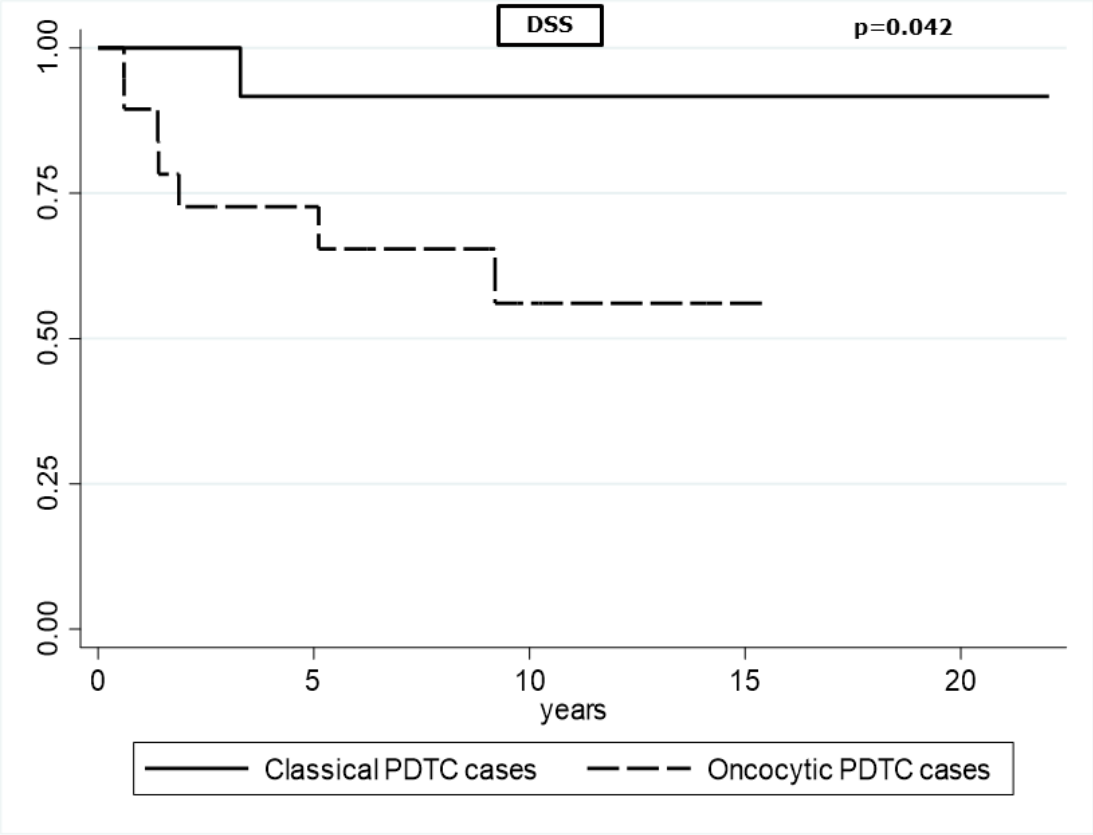

***Figure 1**. Kaplan–Meier estimates of DSS in oncocytic compared to classical PDTC cases (log-rank test p=0.042).*

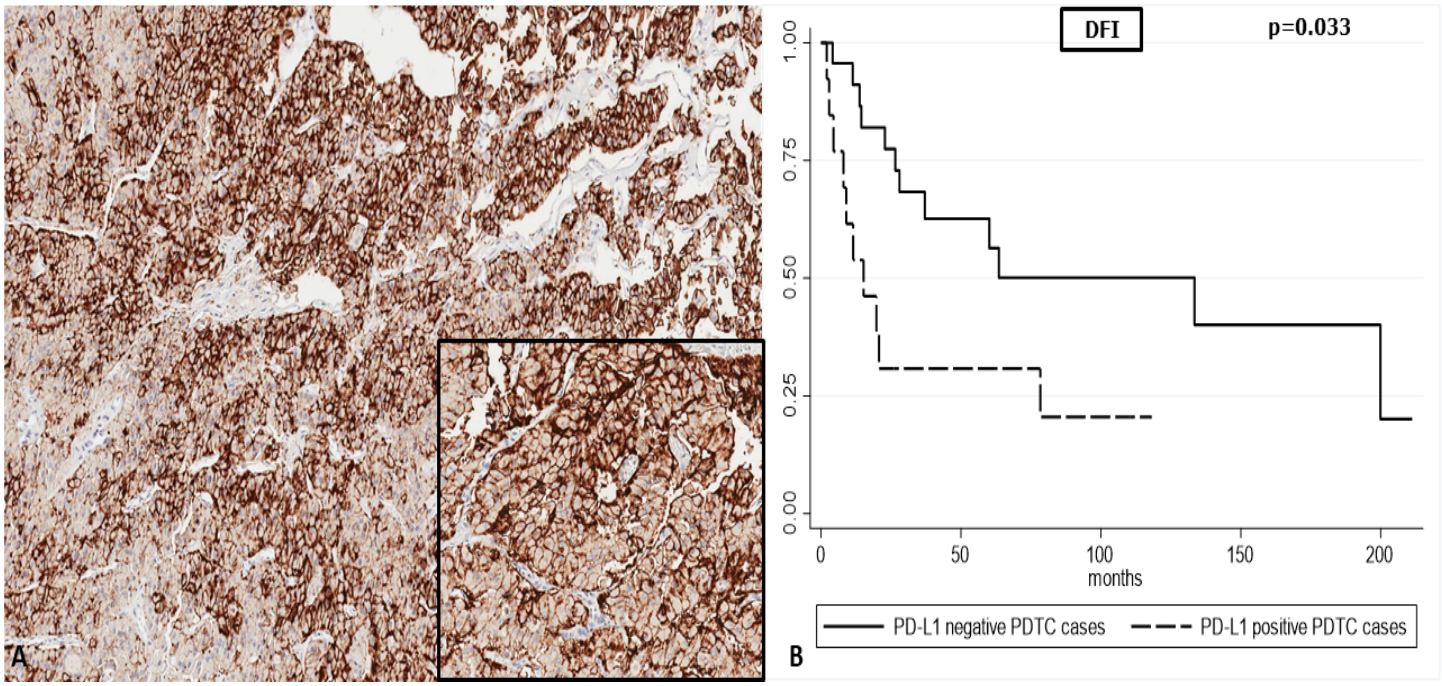

Figure 2. *Strong PD-L1 immunoreactivity in a case of oncocytic poorly differentiated thyroid carcinoma (100x; insert 200x) (**A**). Kaplan–Meier estimates of DFI in PD-L1 positive vs negative poorly differentiated thyroid carcinomas (log-rank test p=0.033) (**B**).*

Table 1. *Clinical-pathological characteristics and PD-L1 expression in 48 poorly differentiated thyroid carcinomas, with or without predominant oncocytic features.*

		Total	**Oncocytic variant**		
		#48	**NO [#25]**	**YES [#23]**	P* (Bonferroni corrections)
Age	<55	12	7	5	0.617
	≥55	36	18	18	
Sex	F	28	16	12	0.406
	M	20	9	11	
Type of surgery	total thyroidectomy	16	9	7	0.839
	total thyroidectomy and lymphadenectomy	25	12	13	
	other*	7	4	3	
Lymphadenectomy	no	21	11	10	0.971
	yes	27	14	13	
Stage	I	9	4	5	0.601
	II	24	11	13	
	III	3	2	1	
	IV	12	8	4	
Stage groups	I-II	33	15	18	0.173
	III-IV	15	10	5	
Bilateral involvement	no	46	25	21	0.132
	yes	2	0	2	
Size (cm)	≤2	2	1	1	0.703
	>2 to ≤4	14	6	8	
	>4	32	18	14	
Angioinvasion	<4 vessels	6	6	0	0.012
	≥4 vessels	42	19	23	
Necrosis	absent	8	7	1	0.030
	focal	9	6	3	
	extensive	31	12	19	
Mitoses (x10HPF)	<4	28	15	13	0.807
	≥4	20	10	10	
Surgical margins status	negative	25	14	11	0.571
	positive	23	11	12	
Extrathyroidal extension	absent	20	11	9	0.732
	present	28	14	14	
Capsular penetration	absent	13	9	4	0.147
	present	35	16	19	
Tumor infiltrating lymphocytes	absent	41	24	17	0.030
	present	7	1	6	
Intratumoral fibrosis	absent	10	5	5	0.987
	mild	23	12	11	
	extensive	15	8	7	

Synchronous metastasis	no	27	15	12	0.585
	yes	21	10	11	
Reccurent disease/progression	no	19	11	8	0.514
	yes	29	14	15	
Died of disease	no	33	20	13	0.080
	yes	15	5	10	
PD-L1	negative	30	21	9	<0.001
	positive	18	4	14	

Legend: *hemithyroidectomy, hemithyroidectomy and lymphadenectomy

Table 2. *Association of clinical and pathological characteristics of 48 poorly differentiated thyroid carcinomas with PD-L1 expression.*

		Total	**PD-L1 IHC**		
		# 48	Negative #30	Positive #18	p* (Bonferroni corrections)
Age (years)	<55	12	8	4	0.731
	≥55	36	22	14	
Sex	Female	28	18	10	0.762
	Male	20	12	8	
Type of surgery	total thyroidectomy	16	11	6	0.798
	total thyroidectomy and lymphoadenectomy	24	14	10	
	other*	7	5	2	
Lymphoadenectomy	no	22	14	8	0.881
	yes	26	16	10	
Stage	I	9	6	3	0.981
	II	24	15	9	
	III	3	2	1	
	IV	12	7	5	
Bilateral involvement	no	46	29	17	0.709
	yes	2	1	1	
Tumor size (cm)	≤2	2	1	1	0.690
	>2 to ≤4	14	10	4	
	>4	32	19	13	
Angioinvasion	<4 vessels	6	4	2	0.822
	≥4	42	26	16	
Necrosis	absent	8	8	0	**0.016**
	present	40	22	18	
Extent of necrosis	absent[a]	8	8	0	**0.016 c vs a 0.019**
	focal[b]	9	7	2	
	extensive[c]	31	15	16	
Mitoses/10HPF	<4	28	18	10	0.762
	≥4	20	12	8	
Surgical margins status	negative	25	15	10	0.709
	positive	23	15	8	
Extrathyroidal extension	absent	20	14	6	0.364
	present	28	16	12	
Capsular penetration	present	35	20	15	0.208
	absent	13	10	3	
Tumor infiltrating lymphocytes	absent	41	27	14	0.245
	present	7	3	4	
Intratumoral fibrosis	absent	10	8	2	0.292
	mild	23	12	11	
	extensive	15	10	5	
Synchronous metastasis	no	27	19	8	0.202
	yes	21	11	10	
Recurrent disease/progression	no	19	13	6	0.493
	yes	29	17	12	
Died of disease	no	33	22	11	0.376
	yes	15	8	7	

Legend: *hemithyroidectomy, hemithyroidectomy and lymphadenectomy

Table 3. *Uni- and multivariate logistic regression analyses*

Univariate binary logistic regression		**Oncocytic features**		
		OR	CI	p
Age	≥55	1.4	0.37-5.24	0.618
Sex	M VS F	1.63	0.51-5.18	0.408
Stage	III-IV vs I-II	0.42	0.11-1.49	0.178
Size	>4 vs other	0.69	0.25-1.92	0.484
Angioinvasion	>4 vessels vs ≤4 vessels	6.94	0.77-62.9	0.085
Necrosis	Extensive vs other	3.28	1.25-8.55	**0.015**
Mitosis	≥4 vs <4	1.15	0.36-3.63	0.807
Tumor infiltrating lymphocites	Present vs absent	8.47	0.93-76.9	0.058
Intratumoral fibrosis	Extensive vs other	0.94	0.42-2.07	0.873
PD-L1	Positive vs negative	8.17	2.1-31.75	**0.002**
Multivariate binary logistic regression		**Oncocytic features**		
		OR	CI	p
Age	≥55	1.16	0.24-5.47	0.854
Sex	M VS F	1.46	0.38-5.69	0.582
Necrosis	Extensive vs other	2.13	0.76-5.98	0.151
PD-L1	Positive vs negative	5.54	1.30-23.6	**0.021**

(Hosmer-Lemeshow, goodness-of-fit test p=0.9190)

Immune-related gene expression profile of oncocytic vs non oncocytic PDTC.

Immune-related genes differentially expressed in our series according to major histotypes and clinical and pathological features are summarized in **Table 4**.

Several immune response-related genes were found up- or downregulated in the oncocytic variant of PDTC as compared to the classical type. There was a significantly higher expression ($p<0.01$) in 10/730 genes (1.4%), namely, *ITGAL, LAIR2, CD274, DEFB1, IRAK1, CAMP, PSMD7, LCN2, LY96,* and *APOE* in samples pertaining to the PDTC oncocytic variant (**Fig. 3,** solid line rectangle). On the other hand, a single gene, *NOD1,* was found downregulated (1/730, 0.1%) (**Fig. 3,** dashed line rectangle). Fold change data and confidence intervals related to Fig. 3 are indicated in **Table 5a**.

Clustering genes based on their biological function, oncocytic PDTC cases had an increased expression of genes linked to the macrophage functions (nSolver Macrophage Functions pathway score). Moreover, in single gene exploration analysis, *CD68* (p=0.0015) and *CD163* (p=0.0264) were found to be significantly overexpressed in oncocytic PDTCs (**Fig. 4**).

Table 4. *Summary of genes differentially expressed in our series according to major clinical and pathological characteristics.*

Parameter	**Significantly up regulated genes (p<0.01)**	**Significantly down regulated genes (p<0.01)**
Oncocytic vs classical PDTCs	*ITGAL, LAIR2, CD274, DEFB1, IRAK1, CAMP, PSMD7, LCN2, LY96, APOE*	*NOD1*
pN0 *vs* pN1	*CAMP*	None found
pM0 *vs* pM1	None found	*ITGAL*
PD-L1 positive *vs* negative PDTC cases	*ITGAL*, *CD79B*, *LY96*, *[CD274]*, *LAIR2*	None found
PDTC vs WDFC	*CD79B, TNFSF15, NUP107, CD8A, LTB*	*CD7, PPARG, CCL14, TOLLIP, TNF, LILRB3, EBI3*
HCC vs FTC	*ECSIT, PSMB7, TP53, GPI, CD274, IRAK1, ICAM3, DEFB1, RRAD*	*ITGB3, ENTPD1, CD44, CXCL2, CREB1, IKBKB, DOCK9, MYD88, CD47*

*PDTC: poorly differentiated thyroid carcinoma; WDFC**:** well-differentiated follicular carcinoma; HCC: Hürthle cell carcinoma; FTC: follicular thyroid carcinoma.*

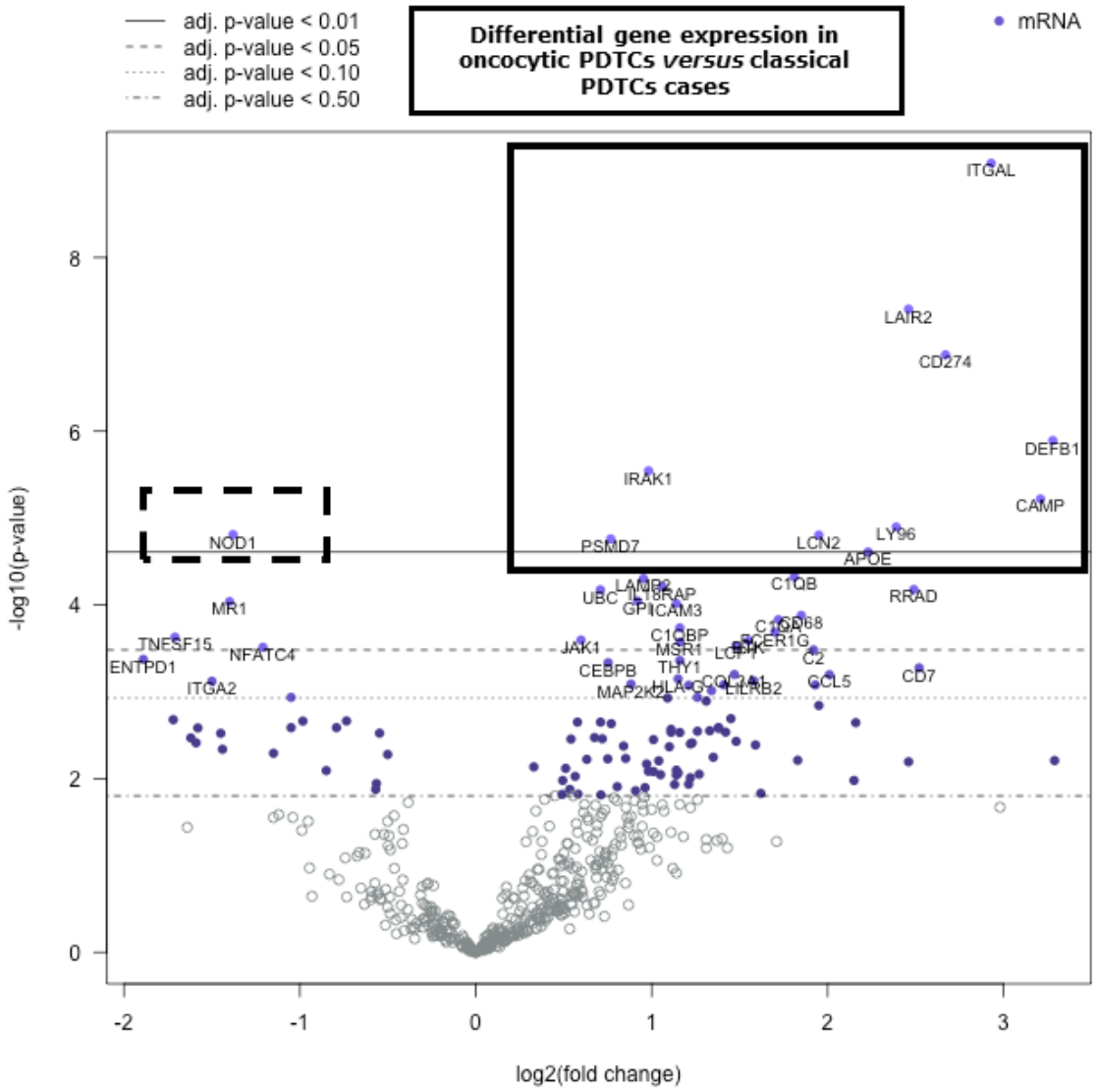

Figure 3. *Different immune-related gene expression profile of oncocytic PDTC cases compared to classical histotype. Upregulated genes are marked by the solid line rectangle, whereas downregulated genes are marked by the dashed line rectangle.*

Table 5. *Fold change data and confidence intervals corresponding to the volcano representation plots of Figure 3 (a), Figure 6A (b) and Figure 6B (c).*

a	Log2 fold change	std error (log2)	Lower confidence limit (log2)	Upper confidence limit (log2)	P-value	*BY P-value
ITGAL-mRNA	0.147917	0.262500	0.095833	0.171528	8.21e-10	3.07e-06
LAIR2-mRNA	0.115278	0.259028	0.092361	0.138194	3.93e-08	7.36e-05
CD274-mRNA	0.129861	0.297917	0.099306	0.160417	1.32e-07	0.000164
DEFB1-mRNA	0.144444	0.407639	0.092361	0.196528	1.28e-06	0.0012
IRAK1-mRNA	0.681944	0.127778	0.431250	0.065278	2.86e-06	0.00214
CAMP-mRNA	0.139583	0.435417	0.109722	0.197222	6.03e-06	0.00376
LY96-mRNA	0.110417	0.339583	0.071528	0.149306	1.27e-05	0.00651
LCN2-mRNA	0.107639	0.279861	0.052778	0.134722	1.57e-05	0.00651
PSMD7-mRNA	0.532639	0.011111	0.315278	0.047222	1.74e-05	0.00652
APOE-mRNA	0.099306	0.330556	0.043750	0.136806	2.46e-05	0.00837
NOD1-mRNA	-1.38	0.198611	-1.94	-0.821	1.55e-05	0.00651

b	Log2 fold change	std error (log2)	Lower confidence limit (log2)	Upper confidence limit (log2)	P-value	*BY P-value
ECSIT-mRNA	0.102083	0.147222	0.073611	0.103472	1.1e-08	4.09e-05
PSMB7-mRNA	0.005556	0.070833	0.004167	1.000000	8.35e-08	8.74e-05
TP53-mRNA	0.060417	0.113194	0.659028	0.082639	9.27e-08	8.74e-05
GPI-mRNA	0.091667	0.153472	0.061111	0.093750	9.42e-08	8.74e-05
CD274-mRNA	0.147222	0.300000	0.115972	0.177778	1.18e-07	8.78e-05
IRAK1-mRNA	0.075694	0.158333	0.044444	0.106944	1.41e-06	0.000874
ICAM3-mRNA	0.106944	0.244444	0.059028	0.127083	1.58e-05	0.00532
DEFB1-mRNA	0.145139	0.426389	0.089583	0.200694	2.59e-05	0.0064
RRAD-mRNA	0.100694	0.025000	0.051389	0.121528	3.8e-05	0.00783
ITGB3-mRNA	-3.17	0.036111	-4.19	-2.15	3.91e-06	0.00207
ENTPD1-mRNA	-3.62	0.428472	-4.82	-2.41	6.67e-06	0.00279
CD44-mRNA	-2.87	0.339583	-3.82	-1.91	6.77e-06	0.00279
CD47-mRNA	-0.899	0.112500	-1.22	-0.582	1.37e-05	0.00508
CXCL2-mRNA	-2.65	0.345833	-3.63	-1.68	2.41e-05	0.0064
CREB1-mRNA	-1.23	0.161111	-1.68	-0.777	2.47e-05	0.0064
IKBKB-mRNA	-0.94	0.122917	-1.29	-0.593	2.5e-05	0.0064
DOCK9-mRNA	-1.01	0.133333	-1.38	-0.629	2.95e-05	0.00684
MYD88-mRNA	-1.4	0.186806	-1.93	-0.873	3.19e-05	0.00697
RRAD-mRNA	0.100694	0.025000	0.051389	0.121528	3.8e-05	0.00783

c	Log2 fold change	std error (log2)	Lower confidence limit (log2)	Upper confidence limit (log2)	P-value	*BY P-value
CD79B-mRNA	0.130556	0.265278	0.106250	0.154861	9.64e-09	3.58e-05
TNFSF15-mRNA	0.104861	0.295833	0.074306	0.134722	2.11e-06	0.00196
NUP107-mRNA	0.371528	0.075000	0.223611	0.518750	1.09e-05	0.00468
CD8A-mRNA	0.116667	0.353472	0.075000	0.158333	1.32e-05	0.0049
LTB-mRNA	0.144444	0.468750	0.107639	0.170833	1.51e-05	0.00509
CD7-mRNA	-0.847	0.088194	-1.1	-0.598	3.37e-08	6.25e-05
PPARG-mRNA	-3.36	0.384028	-4.44	-2.28	2.19e-07	0.00027
CCL14-mRNA	-1.86	0.246528	-2.56	-1.17	3.76e-06	0.00239
TOLLIP-mRNA	-0.673	0.088889	-0.925	-0.422	3.86e-06	0.00239
TNF-mRNA	-0.772	0.103472	-1.06	-0.479	5.27e-06	0.00279
LILRB3-mRNA	-0.655	0.092361	-0.915	-0.395	1.14e-05	0.00468
EBI3-mRNA	-0.709	0.102778	-0.999	-0.419	1.86e-05	0.00575

Legend: *Benjamini-Yekutieli method.

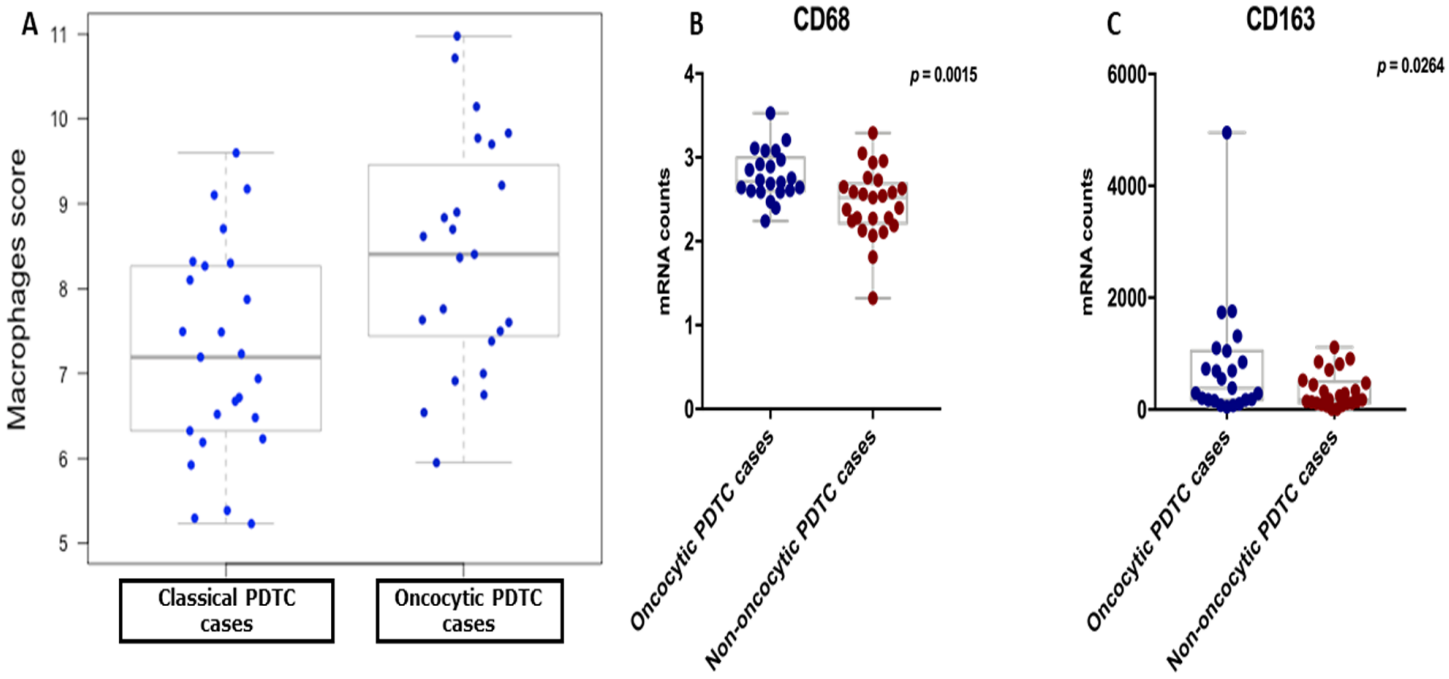

Figure 4. *Oncocytic PDTC cases demonstrated an increased expression of genes linked to the macrophage functions (nSolver Macrophage Functions pathway score) (**A**); Single gene analyses showed CD68 (p=0.0015) (**B**) and CD163 (p=0.0264) (**C**) upregulation in oncocytic PDTC.*

Gene expression validation by means of quantitative real time PCR.

All significant genes discovered by NanoString analysis to be significantly different in oncocytic as compared to non-oncocytic PDTC were analyzed independently by means of quantitative real time PCR. *CD274* gene was excluded since validated at the protein level by using PD-L1 immunohistochemistry (see below). All but one case (belonging to the non-oncocytic group) were adequate for the analysis. *LAIR2* gene was excluded due to the poor efficiency of probes available. Among the 11 genes analyzed, 7 were differentially expressed in oncocytic as compared to non-oncocytic PDTC with statistical significance, and included *CAMP, DEFB1, NOD1, IRAK1, LCN2, CD68* and *CD163* **(Fig. 5**), following the same distribution observed in NanoString analysis. Two other genes showed borderline statistical significance (*LY96* and *APOE,* p=0.07 and p=0.17, respectively). Two remaining genes (*PSDM7* and *ITGAL*) were not significant (p=0.69 and p=0.63, respectively). However, for these latter two genes, correlation between raw data obtained in NanoString analysis and quantitative real time PCR were strongly correlated (data not shown), thus showing that the loss of statistical significance was not associated to a methodological issue of gene expression analysis but rather to the heterogeneous distribution of values among cases (including different ranges of values in the population) and the presence of outliers. A further validation was obtained performing Spearman's correlation analysis among genes. A strong correlation was observed between *CD163* and *CD68,* and between both genes and all other genes except for *NOD1* and *IRAK1*, whereas *ITGAL* showed a low statistical significance (**Table 6**).

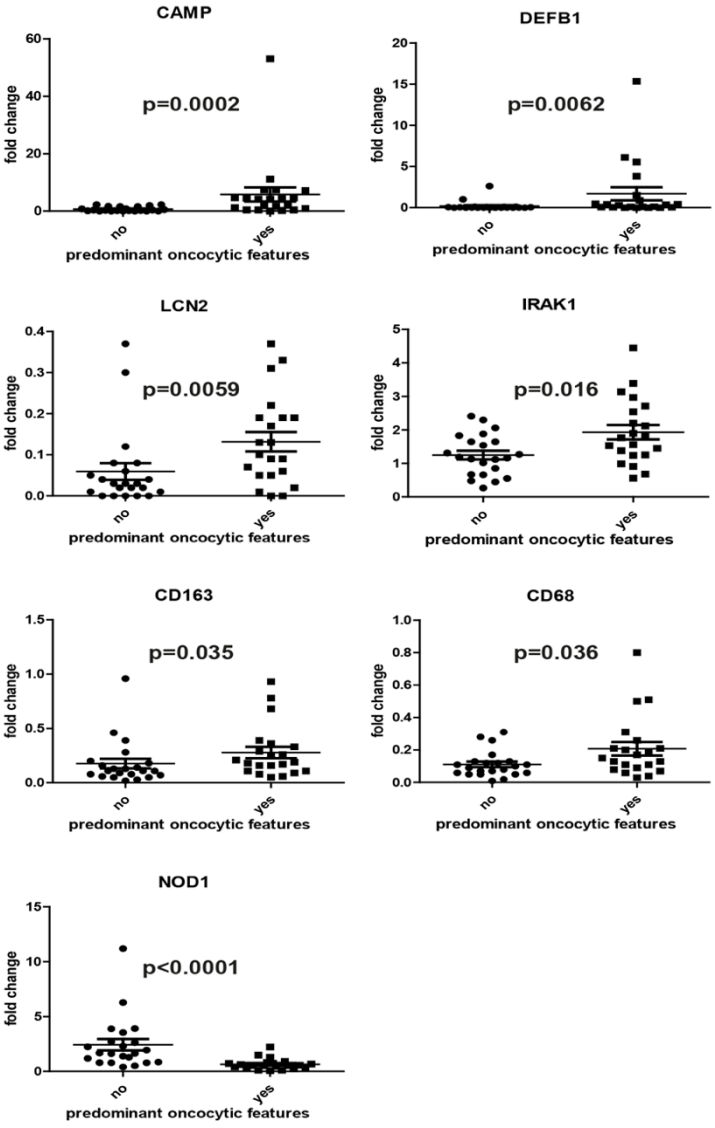

Figure 5*. Distribution of 7 genes with significantly different gene expression in oncocytic as compared to non-oncocytic PDTC according to quantitative real time PCR analysis.*

***Table 6**. Correlation among the 11 genes validated by means of quantitative real time PCR.*

	PSDM7	***DEFB1***	***ITGAL***	***APOE***	***NOD1***	***IRAK1***	***LCN2***	***LY96***	***CD163***	***CD68***
CAMP	R: 0.13 p: 0.37	***R: 0.53 p: 0.0001***	R: 0.06 p: 0.68	R: 0.22 p: 0.14	R: -0.26 p: 0.07	***R: 0.38 p: 0.008***	***R: 0.49 p: 0.0004***	***R: 0.34 p: 0.02***	***R: 0.34 p: 0.02***	***R: 0.31 p: 0.03***
PSDM7	/	***R: 0.40 p: 0.005***	R: -0.004 p: 0.98	***R: 0.45 p: 0.002***	***R: 0.29 p: 0.04***	R: 0.02 p: 0.89	R: 0.16 p: 0.29	***R: 0.76 p: <0.0001***	***R: 0.39 p: 0.007***	***R: 0.42 p: 0.003***
DEFB1	/	/	R: 0.25 p: 0.09	***R: 0.43 p: 0.002***	R: -0.06 p: 0.68	R: 0.05 p: 0.73	***R: 0.52 p: 0.0002***	***R: 0.60 p: <0.0001***	***R: 0.55 p: <0.0001***	***R: 0.55 p: <0.0001***
ITGAL	/	/	/	***R: 0.34 p: 0.02***	R: -0.02 p: 0.91	R: 0.22 p: 0.14	R: 0.05 p: 0.75	R: 0.22 p: 0.13	***R: 0.34 p: 0.02***	R: 0.27 p: 0.06
APOE	/	/	/	/	R: 0.05 p: 0.71	R: 0.01 p: 0.93	R: 0.16 p: 0.29	***R: 0.50 p: 0.0003***	***R: 0.54 p: <0.0001***	***R: 0.54 p: <0.0001***
NOD1	/	/	/	/	/	***R: -0.35 p: 0.016***	R: 0.06 p: 0.69	R: 0.15 p: 0.31	R: -0.07 p: 0.64	R: 0.21 p: 0.16
IRAK1	/	/	/	/	/	/	R: 0.07 p: 0.61	R: -0.04 p: 0.79	R: 0.23 p: 0.12	R: -0.04 p: 0.80
LCN2	/	/	/	/	/	/	/	***R: 0.37 p: 0.01***	***R: 0.37 p: 0.01***	***R: 0.49 p: 0.0004***
LY96	/	/	/	/	/	/	/	/	***R: 0.52 p: 0.0002***	***R: 0.64 p: <0.0001***
CD163	/	/	/	/	/	/	/	/	/	***R: 0.71 p: <0.0001***

Immune-related gene expression profile as compared to clinical and pathological characteristics in PDTC.

Among the genes investigated, none resulted significantly associated with specific clinical or pathological characteristics, except for *CAMP* which had a higher expression in patients with lymph node metastases ($p<0.01$) and *ITGAL* which was downregulated in patients with distant metastases at diagnosis ($p<0.01$) (**Table 4**). Moreover, *ITGAL, CD79B, LY96, CD274* and *LAIR2* genes were significantly upregulated in PD-L1 positive PDTC. Noteworthy, considering the high number of oncocytic PDTC cases showing PD-L1 immunoreactivity, all the above genes - except *CD79B* – were also among those found to be upregulated in oncocytic PDTCs.

Clinical pathological associations, PD-L1 expression and differential gene expression profile in HCC vs classical FTC cases

Clinical and pathological characteristics and PD-L1 immunoreactivity of 24 WDFCs are shown in **Table 7.** The HCC cases were more frequently assigned to a higher stage ($p=0.016$), associated with concomitant goiter ($p=0.004$) and intratumoral fibrosis ($p=0.035$). Of note, as in PDTC cases, PD-L1 expression was significantly more frequent in HCC (9/12, 75%) than FTC (1/12, 8%) cases ($p<0.001$).

As shown in **Fig. 6A,** *ECSIT, PSMB7, TP53, GPI, CD274, IRAK1, ICAM3, DEFB1, RRAD* genes were found up-regulated **(**$p<0.01$) (9/730 genes, 1.2%; solid line rectangle), whereas *ITGB3, ENTPD1, CD44, CXCL2, CREB1, IKBKB, DOCK9, MYD88* and *CD47* were downregulated **(**$p<0.01$) (9/730 genes, 1.2%; dashed line rectangle) in HCC as compared to FTC cases. Three of these upregulated genes, namely *DEFB1, IRAK, CD274,* were also up regulated in oncocytic vs classical PDTC cases. Fold change data and confidence intervals related to **Fig. 6A** are indicated in **Table 5b**.

Immune-related gene expression differences between PDTCs and a control group of WDFCs.

Finally, we explored differential gene expression levels between PDTCs and WDFCs. All cases of WDFCs were compared with 24 PDTCs matched for the absence or presence of oncocytic features, sex, age and pT stage. In the PDTC group, significant up-regulation of *CD79B, TNFSF15, NUP107, CD8A, LTB* genes ($p<0.01$) (**Fig. 6B,** solid line rectangle) (5/730 genes, 0.7%), and downregulation of *CD7, PPARG, CCL14, TOLLIP, TNF, LILRB3, EBI3* genes were detected (**Fig. 6B,** dashed line rectangle) (7/730 genes, 1%) ($p<0.01$). Fold change data and confidence intervals related to **Fig. 6B** are indicated in **Table 5c**.

Table 7. *Clinical and pathological characteristics and PD-L1 expression of 24 well differentiated follicular thyroid carcinomas.*

		Total	FTC [#12]	HCC [#12]	P (Bonferroni corrections)
Age	<55	6	5	1	0.059
	≥55	18	7	11	
Sex	F	14	9	5	0.098
	M	10	3	7	
Type of surgery	total thyroidectomy	9	6	3	0.403
	total thyroidectomy and lymphadenectomy	11	4	7	
	hemithyroidectomy*	4	2	2	
Stage	I	6	5	1	0.016 (II vs I 0.031)
	II	13	3	10	
	IV	5	4	1	
Bilateral involvement	no	21	10	11	0.537
	yes	3	2	1	
Diameter	≤2	2	1	1	0.824
	>2 to ≤4	3	1	2	
	>4	19	10	9	
Angioinvasion	<4 vessels	9	6	3	0.206
	≥4 vessels	15	6	9	
Necrosis	absent	20	10	10	1.000
	present	4	2	2	
Surgical margins status	negative	18	10	8	0.346
	positive	6	2	4	
Extrathyroidal extension	absent	16	8	8	1.000
	present	8	4	4	
Capsular penetration	absent	1	1	0	0.307
	present	23	11	12	
Presence of concomitant goiter	no	11	9	2	0.004
	yes	13	3	10	
Tumor infiltrating lymphocytes	absent	18	9	9	1.000
	present	6	3	3	
Intratumoral fibrosis	absent	9	2	7	0.035
	present	15	10	5	
Synchronous metastasis	no	19	8	11	0.132
	yes	5	4	1	
Recurrent disease/progression	no	20	9	11	0.273
	yes	4	3	1	
Died of disease	no	23	11	12	0.307
	yes	1	1	0	
PD-L1	negative	14	11	3	0.001
	positive	10	1	9	

Legend: FTC: follicular thyroid carcinoma; HCC: Hürthle cell carcinoma; *: with or without lymphadenectomy

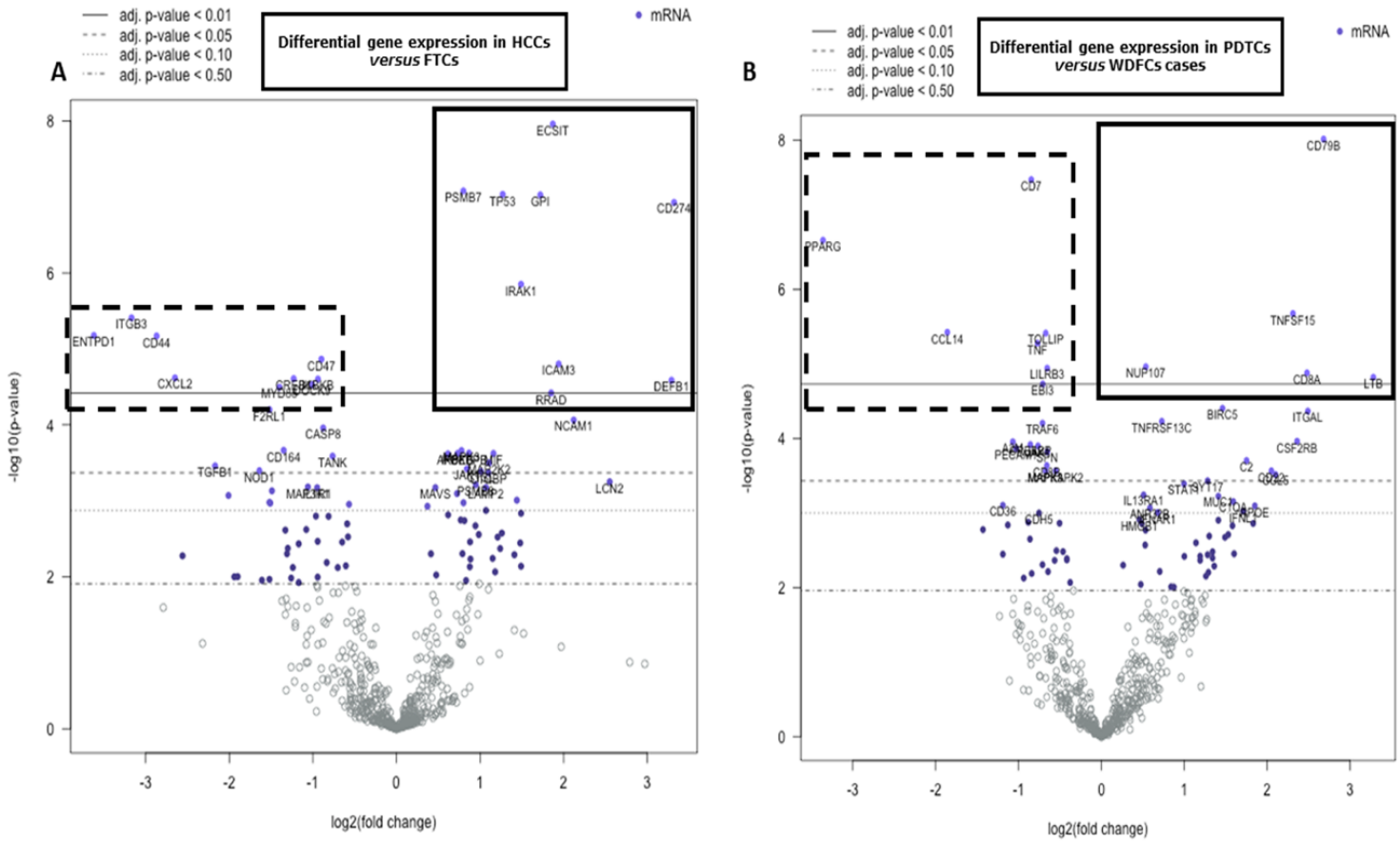

Figure 6. *Different immune-related gene expression profile in HCC as compared to FTC (**A**) and in PDTC as compared to WDFC (**B**).*

DISCUSSION

The immune network in thyroid cancer is a complex and dynamic system characterized by multiple interactions between tumor cells and various immune cell types. Tumor-associated macrophages, M2 macrophages, tumor-associated mast cells, monocytes, polymorphonuclear-myeloid-derived suppressor cells, monocyte-derived suppressor cells, T regulatory cells, tumor-associated neutrophils, and immature dendritic cells have been shown to play pro-tumorigenic roles in thyroid cancer, whereas M1 macrophages, cytotoxic $CD8^+$ T cells, natural killer cells, Th1 cells, mature dendritic cells and their mediators are anti-tumorigenic (414). In this complex scenario, the correlation between immune related gene expression signatures and pathological or clinical characteristics has never been explored in PDTC.

In the present study, we show that oncocytic PDTC possesses peculiar pathological, clinical and molecular features as compared to conventional PDTC and well differentiated thyroid carcinomas. The specific immune related gene and protein (namely PD-L1) expression profile in oncocytic PDTC may partly explain their more aggressive behavior as compared to conventional PDTC and potentially paves the way to the development of novel therapeutic strategies aimed at impairing their tumor escape mechanisms from the immune system. In fact, at first glance, oncocytic PDTCs have a high expression of PD-L1 gene (*CD274*) and protein as compared to conventional ones. The significant activation of PD-L1-mediated tumor escape mechanism is associated to increased presence of tumor infiltrating lymphocytes, thus depicting a microenvironment that might fit with the observed shorter DSS of oncocytic PDTC as compared with classical cases. Moreover, PD-L1 expression was an adverse prognostic factor in PDTC cases, as a whole.

PD-L1 expression has been largely investigated in thyroid cancer especially in papillary carcinoma, where it is associated with aggressive disease features and more adverse prognosis (415,416). Moreover, PD-L1 targeting has shown promising results in anaplastic thyroid cancer (417). To the best of our knowledge, a single study in the literature tested PD-L1 expression (at the protein level, only) in PDTC, describing a positive rate of 25% using a 5% cut-off, with a significant association with aggressive features but not quoting the presence or absence of oncocytic variant PDTC cases (403). Overall, all these data claim a potential role of PD-L1 as a biomarker of aggressiveness and a potential target in PDTC.

A growing body of evidence suggests that the tumor biological behavior is significantly impacted by its immune microenvironment. Although there is not enough evidence for testing immune check point molecules in these tumors in the routine workout, our results demonstrate that a subset of PDTC and HCC upregulate immune checkpoint molecules, providing a rationale for investigating checkpoint targets in thyroid neoplasms that currently lack effective treatment options in advanced stage tumors. In fact, a significant up-regulation of innate immunity-related genes (*DEFB1, IRAK1, LCN2, LY96)* was observed. Components of innate immunity and their role in thyroid cancer have been investigated in several studies. In particular, the expression of *DEFB1* mRNA has been already described in both well differentiated and undifferentiated thyroid cancer cell lines as a favoring factor of cell proliferation, viability and migratory characteristics (418). *IRAK1*, has been recently demonstrated to be a target of miR146a, mainly upregulated in HCC and related to tumor development and progression (419). In other cancer models, *IRAK1* was shown to increase

cancer stemness and drug resistance (420), including resistance to radiotherapy (421), and to be a novel potential therapeutic target (422). Interestingly, both genes were specifically associated in our study to the oncocytic phenotype, both in PDTC and WDFC groups. As for the other up-regulated genes, *LCN2* had been found as an independent predictor of extra-thyroidal extension in well-differentiated thyroid carcinomas (423) and its protein expression had been shown to increase along the spectrum of thyroid cancers from well differentiated to anaplastic histotypes (424). The oncocytic PDTC gene profile, harboring overall 11 upregulated and 1 downregulated gene, is mainly related to the circuits of innate immunity, that plays a critical part in regulating cancer pathogenesis (425,426). We suggest that complex intercellular interactions within the tumor microenvironment may be influenced by innate immune pathways, paving the way for exploring more successful patient-tailored cancer immunotherapy, and eventually enhancing the immune control of tumors. The role of immunity-related genes in oncocytic transformation is probably not relevant, but certainly the immune response modalities of cells thus modified, despite the many mitochondria, with borderline energy status are particular and associated with a fragility and reduced compliance of these stress cells metabolic or environmental (427). Furthermore, *NOD1*, the single downregulated gene in the present series of oncocytic PDTC, was found to be inversely correlated with tumor growth in breast cancer (428) and renal cell carcinoma (429) models. All these data are supportive of our general interpretation that oncocytic phenotype in PDTC is associated to a more aggressive molecular phenotype.

It would be worth to compare the gene expression levels obtained in the present study, with special reference to oncocytic PDTC cases, with the corresponding genomic background. However, the genomic data we have for a subset of the 48 cases analyzed were not enough to enable any statistical correlation. In fact, among 17 cases informative using a wide next-generation sequencing approach, only 9 harbored any kind of alteration, being TP53 and RAS mutations the most frequent but indeed each being present in 4 out of 17 cases, only (data not shown). Therefore, although the issue is relevant and of great interest, it cannot be addressed in the present explorative study, despite its relatively high number of cases for such a rare thyroid tumor histotype. The lack of validation is a general limitation of this study that we aim to address planning a large multi-institutional collection of oncocytic PDTC with detailed clinical and pathological annotates.

In our study, we also observed a generally increased expression of mRNAs related to macrophage functions in oncocytic PDTC group as compared to the classical type. Several studies have reported a correlation between poor patient prognosis and a high intratumoral macrophage content (430,431). These latter include M1 polarized macrophages that possess anti-tumor functions, and M2 tumor associated macrophages that exert immunosuppressive and pro-tumorigenic role (432). In a study by Mazzoni et al. (433), it has been reported that both senescent thyrocytes and thyroid tumor cell lines trigger M2-like macrophage polarization that is related to PGE2 secretion, suggesting that the interaction within microenvironment occurs at both early and late thyroid tumor stages and favors tumor progression. In our study, single gene analyses revealed that *CD68* and *CD163* have increased expression in oncocytic PDTC, further supporting the notion that a specific microenvironment exists in oncocytic PDTC, that favors a higher biological aggressiveness. CD68 is not completely specific since it might be expressed by a variety of cells of the mononuclear phagocyte lineage (including

macrophages, microglia, osteoclasts, and myeloid dendritic cells) is generally used as pan-macrophage marker (434). Conversely, *CD163* is considered an indicator of M2 macrophage lineage (435). Interestingly, all genes up-regulated in oncocytic PDTC, except for *IRAK1*, were positively correlated with both *CD68* and *CD163*, thus supporting a direct association with macrophage related functions. With all the limitations due to the sample size and lack of tissue localization of these markers, these results pave the way for future studies on larger series aimed at further profiling immune cells other than tumor-associated lymphocytes in PDTC, and oncocytic PDTC in particular.

Finally, we compared gene expression of PDTC with WDFC, either conventional or oncocytic/Hürthle cell types.

Our findings integrate the data of a single study on thyroid cancer that applied a similar methodological approach, although in a different design setting (388). In fact, using our same gene expression panel, Giannini and coworkers explored the immune related gene profiles of different thyroid cancer histotypes, showing that immune-related genes are significantly upregulated in anaplastic and papillary thyroid cancers as opposed to PDTC (14 cases tested, not known if the oncocytic variant was included). In our series, twelve genes only were differentially (either up or down-) regulated between PDTC and WDFC, thus showing a more consistent immune signature in these two groups, than that observed by Giannini and coworkers comparing anaplastic and papillary carcinomas with PDTC and normal thyroid. As a matter of fact, our data further claim that the PDTC-like phenotype described by these Authors might better fit with conventional PDTC rather than the oncocytic variant.

CONCLUSIONS

In conclusion, to the best of our knowledge, this is the first study that explored gene expression profiles in a relatively large series of oncocytic variant PDTC by NanoString technology. Overall, our study has revealed several insights into the molecular background of oncocytic PDTC, identifying specific alterations of innate immunity and tumor microenvironment that favor tumor escape, and might be responsible for their more aggressive behavior reported in the literature and confirmed in our study. These findings may be useful when developing novel treatment options for oncocytic PDTC patients.

Project 4: Papillary thyroid carcinoma: clinico-pathological characterization and gene expression profiling of aggressive and non-aggressive forms.

ABSTRACT

Papillary thyroid carcinoma (PTC) derives from follicular cells, and is the most common thyroid malignancy, comprising more than 80% of all malignant thyroid tumors. PTC is generally considered a tumor with indolent behavior, slow progression, and low mortality rates, however, in some instances these tumors can demonstrate aggressive clinical behavior.

We aimed to identify clinico-pathological and genetic prognostic biomarkers that could be restricted to aggressive forms of PTCs, by depicting clinico-morphological aspects of the case series included in the study and by comprehensive probe-based gene expression analyses of canonical pathways by employing NanoString nCounter® technology.

Methods: We selected 43 cases of aggressive PTC and 43 controls that resulted free of disease during the clinical follow up, matching them according to age, sex, and T and N parameters of the TNM staging system. Twenty-four pairs (a total of 48 cases) were studied using nCounter PanCancer Pathways Panel, along with 6 normal thyroid tissues.

Aggressive PTCs showed more aggressive clinical and morphological features, such as multifocal presentation, absence of tumor capsule, presence of tumor infiltrating lymphocytes and extensive fibro-sclerotic changes within the tumor bulk. Of note, at follow-up, 11/43 (25.6%) patients with aggressive PTC died (8 of their PTC, and 4 due to other causes), compared to 4/43 (9.3%) patients with non-aggressive who died of other causes, not related to their PTC) ($p=0.047$). The genes related to DNA Damage – Repair, namely, *POLD4, H2AFX, POLR2J, ATM, MAD2L2, PRKDC,* were found upregulated in non-aggressive PTC cases, only ($p<0.01$). Analysis of MAPK pathway revealed an overlap of *TGFB1, PPP3CB, CACNB3, DUSP4, HSB1,* and *PDGFA*. On the other hand, *KRAS, MAP3K1, SOS2, DUSP5, RAC2,* and *CDC25B* were found upregulated only in the non-aggressive cases. Also, *CACNA2D1* and *JUN* were found downregulated in the same group ($p<0.01$). Considering RAS pathway, there was a difference in overexpression of *PDGFC, KRAS, RAC2, SOS2,* and *PIK3R2* genes, being overexpressed in non-aggressive cases, with an overlap regarding other differentially overexpressed genes ($p<0.01$), namely, *RASA4, MET, PDGFA, RIN1, TIAM1, LAT, BCL2L1.*

In conclusion, to the best of our knowledge, this is the first study to investigate gene expression profiles of aggressive and non-aggressive PTC cases, by exploring canonical pathways through NanoString technology. Overall, our study has revealed several insights into the molecular background of both groups, in particular related to DNA Damage and Repair, MAPK and RAS pathways, as well as morphological features, that may be useful in order to identify more aggressive behaviour of a subset of PTC patients. Moreover, these findings may be useful when developing novel, tailored treatment options for these patients.

SPECIFIC BACKGROUND

Papillary thyroid carcinoma (PTC) derives from follicular cells, and is the most common thyroid malignancy, comprising more than 80% of all malignant thyroid tumors (370,436,437). PTC is generally considered a tumor with indolent behavior, slow progression, and low mortality rates (438).
Compared to the classical PTCs, there are more aggressive histotypes, in particular, hobnail, tall cell, columnar, and solid variant (179,439).
Clinical features, morphological and gene alterations allow us, up to a certain extent, to predict the aggressive behavior of this tumor (440). Prognosis is worsened by higher disease stages, tumor size above 3-4 cm, presence of distant metastases, extrathyroidal extension of the neoplasm, neoplastic infiltration of the resection margins, and/or older age at diagnosis (179,315,441,442).
Various studies attempted to better characterize the genetic make-up of these neoplasms (388,443–445).

The BRAF V600E mutation is the most common one (found in approximately 70% of PTCs) and typically present in classical and tall cell variants (266,300,301,308). The presence of the BRAF V600E mutation in PTC is one of the best-defined prognostic markers to date, strongly related to disease aggressiveness and a reliable preoperative prognostic factor that facilitates the choice of surgical treatment. (446,447). Other less frequent alterations of BRAF include the K601E point mutation, small insertions, or deletions in the vicinity of codon 600, and chromosomal rearrangements such as the AKAP9-BRAF fusion (306). Mutations of NRAS, KRAS and HRAS are also common (305), especially in follicular variants (307).
Cancer progression is associated with accumulation of mutations in other genes, such as TP53, PIK3CA and AKT1 (326,448) TERT mutations (C228T and C250T) are present in more advanced PTCs and are associated with a higher risk of distant metastasis, recurrence, and cancer-related mortality (308–310,449).
More recently, molecular biomarkers with strongly altered expression levels in PTC, including TIMP1, c-KIT, c-MET, and TPO (450–453) have been proposed to be predictive of PTC behavior. Of note, the BRAFV600E mutation exhibited correlation with changes in TIMP1 and TPO expression levels in PTC (450).
Moreover, *RET*/PTC rearrangements (454) identified almost exclusively in thyroid lesions, were correlated, in particular *RET*/PTC3 (455), with a more aggressive PTC phenotype and advance disease stages (454). RET/PTC induces RAS-dependent BRAF activation and RAS- and BRAF-dependent ERK activation (302). Several studies suggested that the oncogenic effects of RET/PTC require signalling along the MAPK pathway and the presence of the functional BRAF kinase (456–458).

Nevertheless, the therapeutic options are still limited. Surgery and radiotherapy are the first choices in the case of local recurrence. External beam radiotherapy can be an alternative in inoperable and/or is iodine-refractory tumors (459–462). Alternative therapeutic approaches, such as molecular target therapies, are currently being explored.

AIM

We therefore aimed to test the profiles of gene expression through the NanoString nCounter® technology in a series of well-characterized clinically aggressive PTC, matched with non-aggressive PTC cases, to identify molecular biomarkers potentially predictive of aggressive clinical course that might be integrated with the current pathological characterization.

MATERIAL AND METHODS

Case selection.

A group of 43 cases with aggressive clinical behavior, defined based on presence of metastasis atdiagnosis, development of distant metastases during follow-up, and/or biochemical recurrence (>2 ng/ml levels of thyroglobulin after TSH stimulation) was selected from a large series of PTC undergoing thyroidectomy from 2002 to 2017 at "Città della Salute e della Scienza" Hospital (Turin, Italy), San Luigi Gonzaga Hospital (Orbassano, Turin, Italy) and Mauriziano Hospital (Turin, Italy). These cases were matched for age, sex, and T and N parameters with 43 controls that resulted free of disease during the clinical follow up (median follow up 12.1 years, range 4.4 – 19 years).
Representative hematoxylin & eosin (H&E) stained slides we re-evaluated for all cases enrolled in the study by three of us (FM, MV, MP). The following parameters were re-assessed and recorded: histological type, TNM stage, tumor diameter, uni- or multifocal presentation (including bilaterality), presence of tumor capsule, presence and extent of extrathyroidal invasion, presence of vascular invasion, status of surgical margins, presence of necrosis, presence of tumor infiltrating lymphocytes (TILs) and presence of fibro-sclerotic changes.
A pool of normal thyroid tissues from patients operated due to benign thyroid conditions was used as the baseline for gene expression testing, and consisted of 3 female (aged 33, 50 and 71) and 3 male patients (aged 40, 50 and 69) (see below).
Before the study started, all cases were de-identified and coded by a pathology staff member not involved in the study, and all data were accessed anonymously. The study was approved by the local Ethical Committee (#610, date December 20th, 2017), and conducted in accordance with the principles set out in the Declaration of Helsinki. Considering the retrospective nature of this research protocol and that it had no impact on patients' care, no specific written informed consent was required.

Molecular analyses

From the resulting database of PTC cases, the subgroup with available archival formalin-fixed-paraffin-embedded (FFPE) material, consisting of 24 pairs of aggressive and their non-aggressive match, was analyzed by means of gene expression profiling, making it a total of 48 tested cases, along with 6 samples of normal thyroid tissue.
Two 10-µm-thick FFPE tissue sections were obtained from each tissue block and were collected in sterile Eppendorf tube by means of manual microdissection. The same procedure

was adopted for normal thyroid tissues, making sure that only healthy/unaltered parenchymal areas were dissected.
RNA isolation was performed using the FFPE RNA Isolation Kit (Roche Diagnostics GmbH, Mannheim, Germany), according to the manufacturer's protocols. Total RNA concentration was assessed using a NanoDrop spectrophotometer (Thermo Fisher Scientific, Inc., Wilmington, DE, USA). NanoString nCounter technology was used to measure relative expression levels of immune genes within the tumor microenvironment: 300 ng of total RNA from each sample were hybridized to the nCounter PanCancer Pathways Panel, according to the manufacturer's instructions (NanoString Technologies, Seattle, WA, USA). The nCounter PanCancer Pathways panel includes 730 genes from 13 canonical pathways and 40 selected reference genes.

The analyses were set up according to the protocol provided by the manufacturer. Expression data were normalized and analyzed with the nSolver Analysis Software (version 4.0.62). For background correction, the mean count of negative controls plus two times the standard deviation was subtracted from the counts for each gene. The means of the supplied positive controls and the geometric mean of the housekeeping genes were used to normalize the measured expression values. Both positive and negative controls were included in the panel, according to manufacturer's instructions. Additionally, the Advanced Analysis module (version 2.0.134) was used to perform differential expression analyses. Briefly, by the differential expression analysis tool (nSolver Advanced Analysis module), for each gene a single linear regression was fit using all selected covariates to predict expression. A volcano plot was generated to display each gene's -log10 (p-value) and log2 fold change with the selected covariate. Highly statistically significant genes fell at the top of the plot above the horizontal lines, and highly differentially expressed genes fell to either side. Horizontal lines indicated various p-value thresholds. In addition, by the nSolver Advanced Analysis module, genes previously shown to be characteristic of various cell populations were used to measure these populations' abundance. Covariates plots were generated to compare raw cell type abundance measurements to covariates. The results of differential expression testing were also summarized at the gene set level.

Statistical analyses.
All analyses were performed using Stata/MP 15.0 Statistical Software (STATA, College Station, TX). The differences in the distribution of the variables evaluated based on clinical-pathological parameters were analyzed using parametric and non-parametric tests (Student's t test, Pearson's chi-square test and Bonferroni's correction, Wilcoxon's rank test). Overall survival (OS) was calculated from the surgical excision date of the primary tumor to the date of thyroid cancer death or last check-up. The disease-free survival (DFS) was calculated from the date of surgical excision of the primary tumor to the date of the first relapse or last check-up. Survival curves between different groups were plotted using the Kaplan-Meier method and the statistical comparisons were performed with Log-rank test.
Cox regression analyses were carried out on DFS and OS to calculate HRs and 95 % CIs for the different study groups. All statistical tests were two sided. P-values < 0.05 were considered significant.

RESULTS

Clinical and pathological characteristics of PTC case series.

As shown in **Table 1**, aggressive PTC were more frequently multifocal (27/43, 62.8%) as compared to the non-aggressive cases (16/43, 37.2%) (p=0.031). The tumor capsule was absent in more than half of aggressive cases (29/43, 67.4%), and in only 17/43 (39.5%) of non-aggressive ones (p=0.015). Furthermore, aggressive PTCs had more frequently TILs (26/43, 60.5%), compared to only 11/43 (25.6%) cases in the non-aggressive group (p=0.001). Only 10/43 (23.3%) non-aggressive PTCs had extensive fibro-sclerotic changes, compared to 21/43 (48.8%) of aggressive cases (p=0.047). Of note, at follow-up, 11/43 (25.6%) patients with aggressive PTC died (8 of their PTC, and 4 due to other causes), compared to 4/43 (9.3%) patients with non-aggressive who died of other causes, not related to their PTC) (p=0.047). Although not statistically significant, vascular invasion was observed more commonly in aggressive (30/43, 69.8%) *versus* non-aggressive cases (21/43, 48.8%) (p=0.077).

By means of univariate analyses (**Table 2**), in terms of DFS, presence of vascular invasion (HR 1.99; CI 95% 1.12 – 3.55) (p=0.019), TILs (HR 2.81; CI 95% 1.50-5.27) (p=0.001), necrosis (HR 2.81; CI 95% 0.99-7.93) (p=0.050), extensive fibro-sclerotic changes (HR 2.29; CI 95% 1.05-5.02) (p=0.038) and higher mitotic counts (HR 2.06; CI 95% 1.37 – 3.10) (p=0.001), were all correlated with adverse prognosis. On the other hand, presence of complete tumor capsule was confirmed as a favorable morphologic feature (HR 0.20; CI 95% 0.05 – 0.85).

Regarding OS, age older than 55 (HR18.8, CI 95% 5.26-67.1) (p<0.001), pT3 descriptor (HR 5.36; CI 95% 1.27-22.6) (p=0.022) and pT4 descriptor (HR 13.9; CI 95% 2.22 – 87.5) (p=0.005), TNM stage II (HR 6.76; CI 95% 1.89 – 24.2) (p=0.003) and stages III and IV (HR 30.4; CI 95% 8.37-110.3) (p<0.001), tumor diameter larger than 4 cm (HR 11.1; CI 95% 2.11 – 58.5) (p=0.004), presence of necrosis (HR 12.9; CI 95% 3.85 – 43.6) (p<0.001) and higher mitotic index (HR 2.29; CI 95% 1.54 – 3.41) (p=0.001) were parameters correlated with unfavorable outcome.

Table 1. *Clinico-pathological features of the PTC case series (#86).*

Parameter		Total	Non-aggressive PTC	Aggressive PTC	P-value
Age	Median (interval)	86	40 (18-82)	46 (19-78)	/
Sex	M	32	16	16	/
	F.	54	27	27	
T	1	42	21	21	/
	2	22	11	11	
	3	18	9	9	
	4	4	2	2	
N	0	34	17	17	/
	1	52	26	26	
Histotype	Classic	27	13	14	0.579
	Classic + Follicular	20	10	10	
	Follicular	14	8	6	
	Oncocytic	5	3	2	
	Tall cell	5	1	4	
	Hobnail	7	2	5	
	Solid	4	3	1	
	Cystic	2	2	0	
	Diffuse sclerosing	2	1	1	
Histotype (dichotomized)	Classic/Follicular	61	31	30	0.812
	Other histotypes	25	12	13	
TNM Stage	1	71	38	33	0.209
	2	9	4	5	
	3/4	6	1	5	
Tumor diameter (cm)	≤1	17	10	7	0.322
	> 1 - ≤ 2	37	16	21	
	> 2 - ≤ 4	25	15	10	
	> 4	7	2	5	
Multifocal presentation	no	44	27	17	0.031
	yes	42	16	26	
Bilateral presentation	no	57	32	25	0.110
	yes	29	11	18	
Tumor capsule	absent	46	17	29	0.015
	incomplete	29	17	12	
	complete	11	9	2	
Extrathyroidal extension	no	38	22	16	0.193
	yes	48	21	27	
Vascular invasion	no	34	21	13	0.077
	yes	52	22	30	
Surgical margins	negative	61	33	28	0.235
	positive	25	10	15	
Necrosis	no	81	42	39	0.167
	yes	5	1	4	
Mitosis	0	8	6	2	0.255
	1	72	36	36	
	2	3	1	2	
	3	2	0	2	
	5	1	0	1	
Tumor infiltrating lymphocytes	no	49	32	17	0.001
	yes	37	11	26	
Fibro-sclerotic changes	absent	24	13	9	0.047
	mild	33	20	13	
	extensive	31	10	21	
Follow-up status	alive	71	39	32	0.047
	dead	15	4	11	

Table 2. *Univariate analyses.*

		DFS			OS		
	Parameter	HR	CI	p	HR	CI	p
Age	>55	1.46	0.73-2.91	0.278	18.8	5.26-67.1	**<0.001**
Sex	F VS M	1.00	0.54-1.87	0.982	0.72	0.26-1.98	0.521
T	1	0			1		
	2	0.89	0.43-1.85	0.765	4.10	0.96-17.5	0.056
	3	0.98	0.43-2.21	0.956	5.36	1.27-22.6	**0.022**
	4	1.15	0.27-4.93	0.845	13.9	2.22-87.5	**0.005**
N	1 VS 0	1.10	0.59-2.05	0.764	1.13	0.40-3.17	0.821
TNM Stage	1	1			1		
	2	1.56	0.61-4.03	0.353	6.76	1.89-24.2	**0.003**
	3/4	2.40	0.93-6.17	0.070	30.4	8.37-110.3	**<0.001**
Tumor diameter (cm)	≤1	1			1		
	1 - 2	1.43	0.60-3.39	0.412	0.44	0.06-3.10	0.407
	> 2 - 4	0.91	0.35-2.38	0.844	2.56	0.51-12.7	0.251
	>4	2.55	0.81-8.04	0.111	11.1	2.11-58.5	**0.004**
Multifocal presentation	Multi vs uni	1.84	0.99-3.43	0.051	0.74	0.26-2.09	0.571
Bilateral presentation	Yes vs no	1.44	0.78-2.66	0.245	1.05	0.36-3.10	0.922
Tumor capsule	absent	1			1		
	incomplete	0.52	0.26-1.03	0.061	0.99	0.32-3.04	0.986
	complete	0.20	0.05-0.85	**0.029**	1.24	0.26-5.84	0.789
Extrathyroidal extension	Yes vs no	1.66	0.89-3.10	0.110	0.77	0.28-2.12	0.614
Vascular invasion	Yes vs no	1.99	1.12-3.55	**0.019**	2.47	0.95-6.45	0.064
TILs	Yes vs no	2.81	1.50-5.27	**0.001**	0.30	0.08-1.06	0.061
Surgical margins	Positive vs negative	1.74	0.92-3.27	0.085	1.40	0.48-4.11	0.537
Necrosis	Yes vs no	2.81	0.99-7.93	**0.050**	12.9	3.85-43.6	**<0.001**
Fibro-sclerotic changes	absent	1			1		
	moderate	0.91	0.38-2.15	0.828	1.44	0.36-5.77	0.604
	extensive	2.29	1.05-5.02	**0.038**	1.46	0.36-5.86	0.589
Mitotic index	linear	2.06	1.37-3.10	**0.001**	2.29	1.54-3.41	**0.001**

In **Figure 1** we present the Kaplan-Meier estimate of OS, showing that patients affected by aggressive forms of disease were significantly correlated with an unfavorable prognosis (p=0.038).
In addition, we explored the impact of fibro-sclerotic changes on outcome. As shown in **Figure 2**, the presence of extensive fibro-sclerosis was correlated with a shorter DFS (p=0.0121).

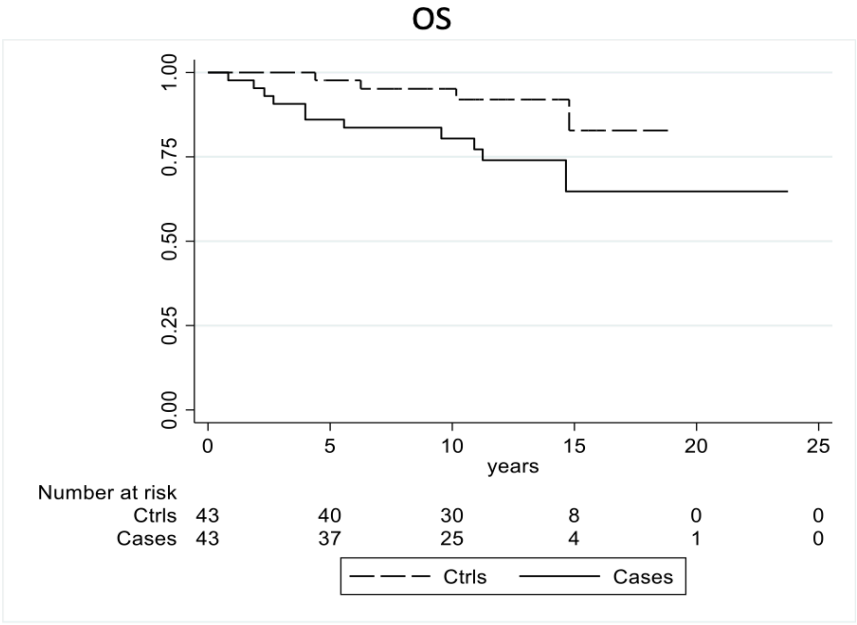

OS	CTRLS	Cases	P log rank test
1 years	97.7%	97.7%	0.0386
5 years	97.7%	83.6%	

Figure 1. *Kaplan-Maier estimates of overall survival (OS) of 43 aggressive cases of papillary thyroid carcinomas versus 43 non-aggressive ones (p=0.0386)..*

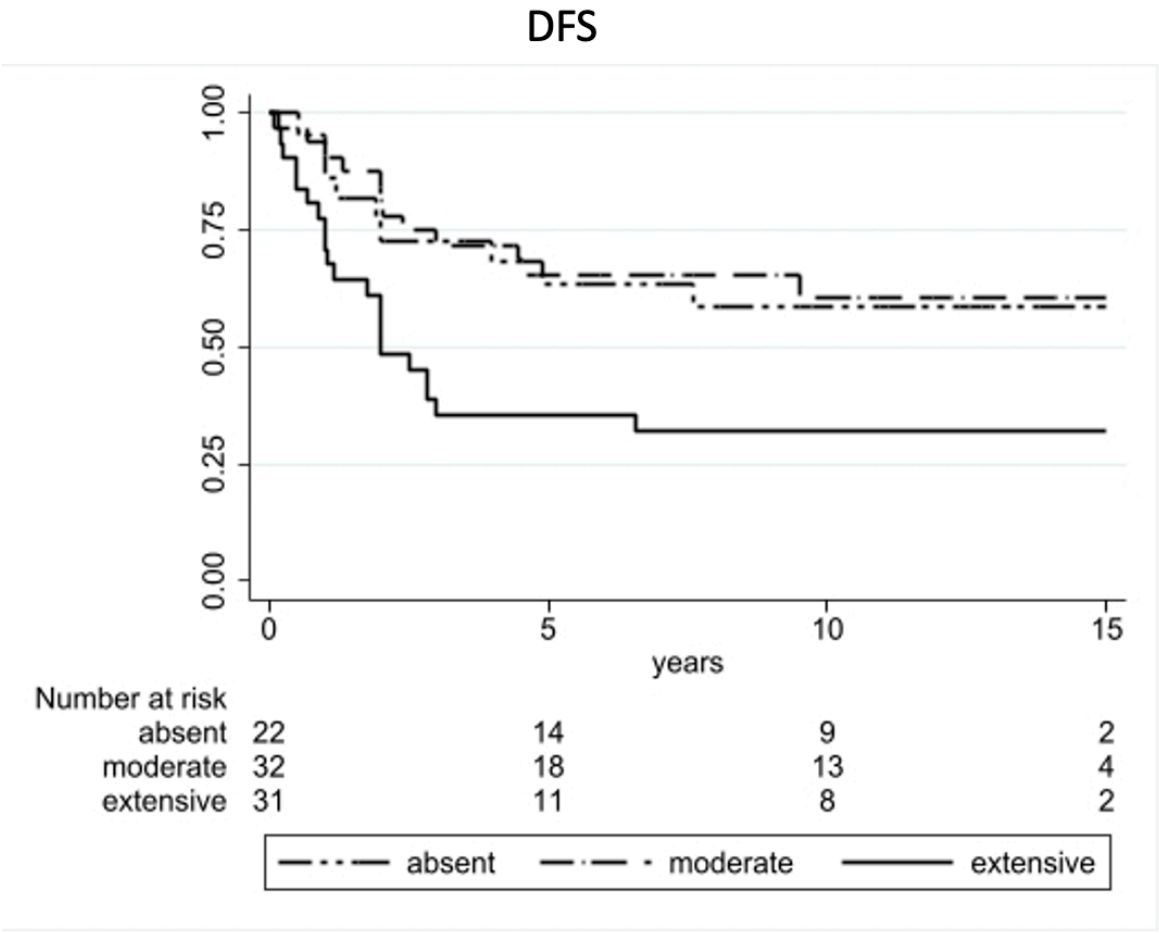

DFS	absent	moderate	extensive	P log rank test
1 year	95.4%	90.9%	77.4%	0.0121
5 years	63.6%	63.2%	35.5%	

Figure 2. *Kaplan-Meier estimates of disease-free survival (DFS) according to fibro-sclerotic changes within the tumor bulk (p=0.0121).*

Gene expression profile of aggressive and non-aggressive PTC cases

The clinico-pathological characteristics of the 48 analyzed patients are summarized in **Supplementary Table 1**.

In **Figure 3,** the gene expression differences of aggressive and nonaggressive PTC *versus* normal thyroid tissue, respectively, are shown.

Specifically, an upregulation of *RXRG, ATRX, COL1A1, EPOR, TGFB1, PML, PPP3CB, TRAF7, STK11, HMGA2, FN1, ETV4, RASA4, COMP, RIN1, LAMB3, CACNB3, DTX4, DUSP4, BCL2L1, BID, MET, INHBB, JAG2, SMAD2, HSPB1, PKMYT1, MCM7, WNT10A, TIAM1, LAT, SFN, TLR2, BAIAP3, CBL, PDGFA, ITGB4, RUNX1* ($p<0.01$) and downregulation of *HDAC4, GLI3, MLF1* ($p<0.01$*)* genes was found in aggressive PTC cases, as compared to the baseline of normal thyroid tissue (**Figure 3a**).

Moreover, *RXRG, RASA4, DUSP4, COL1A1, ATRX, PDGFC, CBL, RIN1, HMGA2, FN1, ETV4, INHBB, COMP, BCL2L1, GNAQ, TGFB1, SFN, BID, PDGFA, RUNX1, LAMB3, TRAF7, KRAS, LAT, PIK3R2, JAG2, PPP3CB, SMAD2, TLR2, PML, MCM7, MYD88, EPOR, TIAM1, COL1A2, DTX4, AMER1, CIC, CCND3, SP1, POLD4, CACNB3, MET, H2AFX, GSK3B, STK11, MAP3K1, SFRP4, SMAD3, ARID2, SPP1, SOS2, OSM, CDKN2D, POLR2J, SMARCB1, ATM, MAD2L2, PRKDC, ITGB4, VHL, CDK6, DUSP5, AXIN1, JAK3, RAC2, MEN1, PLAU, HMGA1, SGK2, ALK, PIM1, COL4A4, HDAC5, CDC25B, IL2RB, BAIAP3, HSPB1, ITGA2, LAMA5, COL3A1* genes were found upregulated ($p<0.01$) and *ASXL1, TPO, NUPR1, TSHR, FLT1, HDAC4, CACNA2D1, JUN, MLF1* genes downregulated ($p<0.01$) in non-aggressive PTC, as compared to the baseline of the normal thyroid tissue (**Figure 3b).**

The overlapping up- and down-regulated genes in aggressive and non-aggressive PTC, as compared to normal tissues are reported in **Figure 4.**

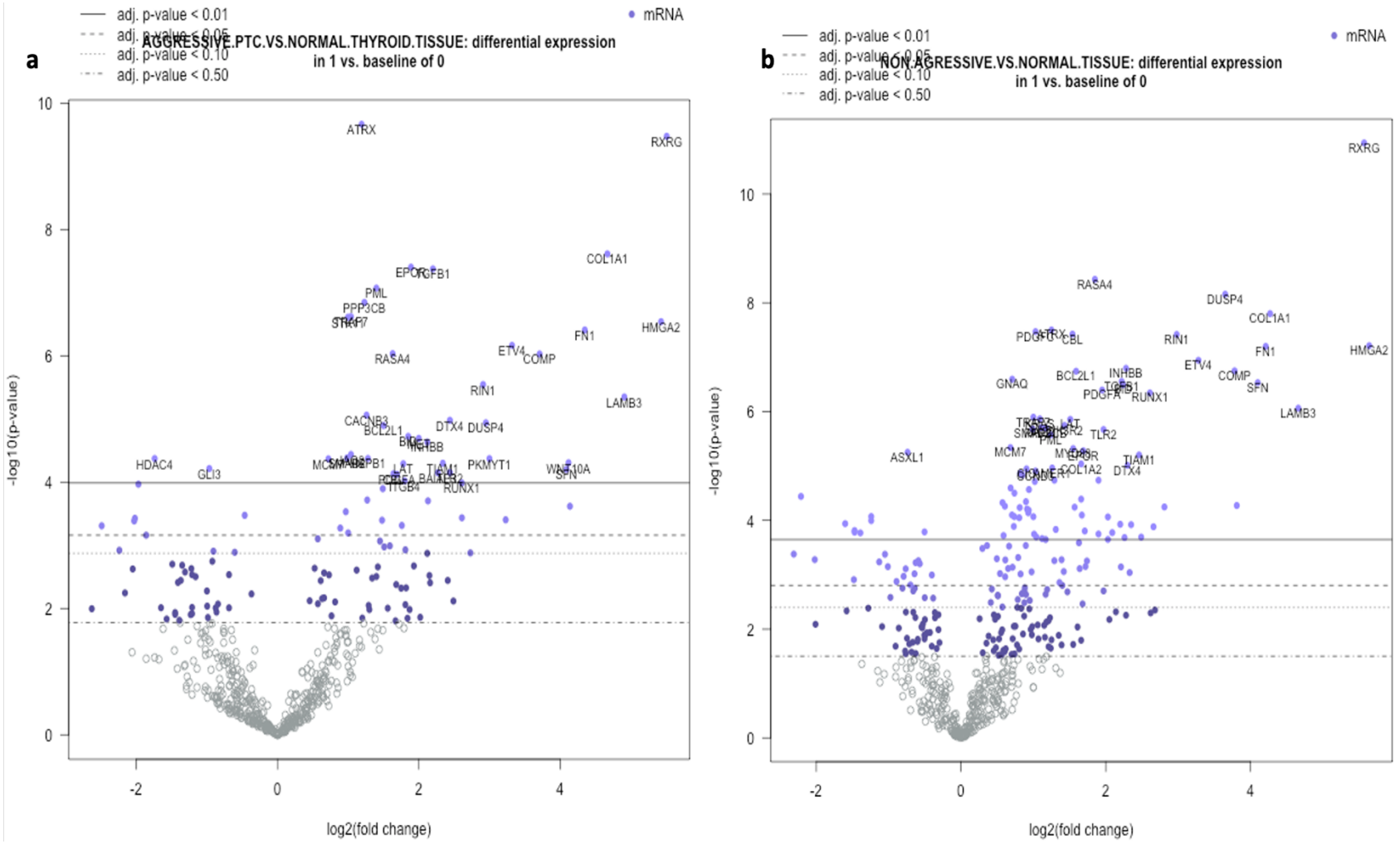

Figure 3. *Volcano plots representing gene expression differences of aggressive (a) and nonaggressive (b) PTC versus normal thyroid tissue.*

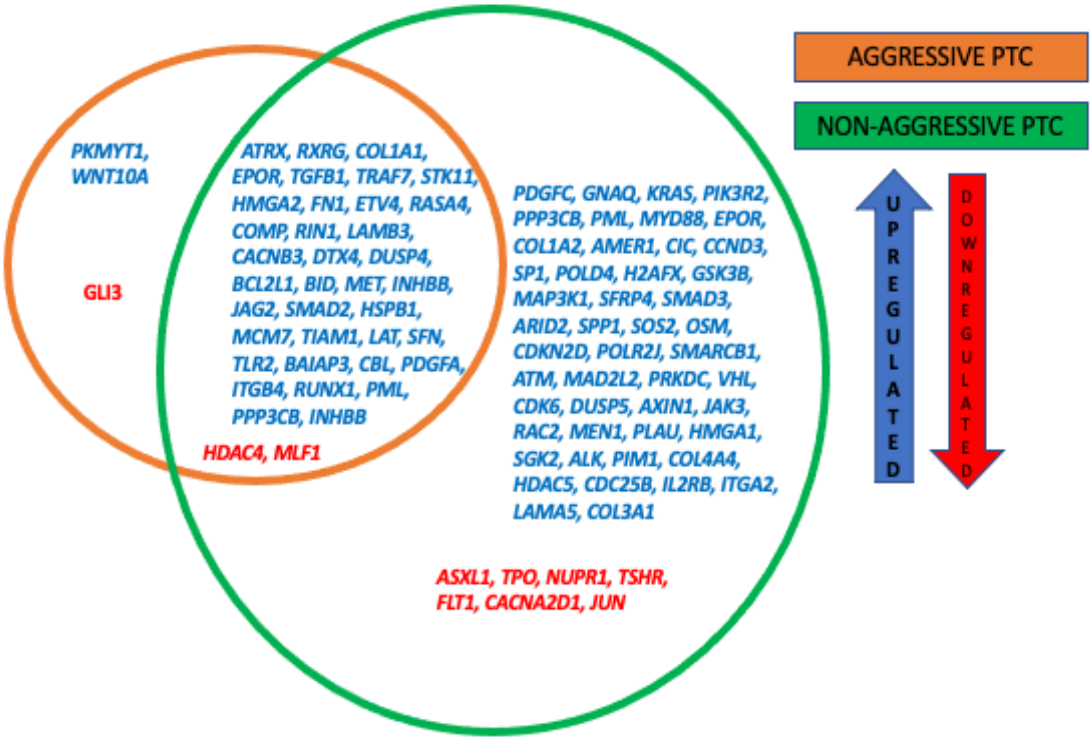

Figure 4. *The overlapping up- and down-regulated genes in aggressive and non-aggressive PTC.*

Canonical pathways.

In details, differential gene expression between aggressive and non-aggressive cases according to different pathways is presented in **Supplementary Figure 1**.

Of note, none of the genes *POLD4, H2AFX, POLR2J, ATM, MAD2L2, PRKDC,* related to DNA Damage - Repair and upregulated in non-aggressive PTC cases, was found differentially expressed in aggressive PTC ($p<0.01$) (**Supplementary Figure 1.a1/2**).

The same genes, *DTX2* and *JAG2,* related to NOTCH pathway were upregulated (**Supplementary Figure 1.b1/2**) in both test groups ($p<0.01$). Regarding Transcriptional misregulation, all genes found up or downregulated in aggressive PTC, were overlapping with those of non-aggressive cases. In addition, in non-aggressive cases only, also *SP1*, *ATM, MEN1* and *PLAU* genes were up- and *NUPR1* down-regulated ($p<0.01$). (**Supplementary Figure 1.c1/2**).

Regarding Hedgehog pathway, *WN10A* and *GLI3* were found up- and downregulated in aggressive PTCs, respectively ($p<0.01$). On the other hand, another gene, namely *GSK3B*, related to the same pathway, was found upregulated in non-aggressive PTCs ($p<0.01$) (**Supplementary Figure 1.d1/2**).

The analyses of another pathway, WNT, revealed overlap in only one gene between tested groups, namely, *PPP3CB*. In addition, several genes found upregulated in non-aggressive cases, *CCND3, GSK3B, SFRP4, SMAD3, AXIN1, RAC2*, and only one *JUN*, was found downregulated ($p<0.01$) (**Supplementary Figure 1.e1/2**).

Regarding JAK-STAT pathway, there was an overlap in the upregulation of *EPOR, BCL2L1, CBL* genes in both groups, while *PIK3R2, CCND3, SOS2, OSM, JAK3, PIM1* and *IL2RB* genes

were up- and *TPO* down- regulated in the non-aggressive group, only ($p<0.01$) (**Supplementary Figure 1.f1/2**).
Considering RAS pathway, there was a difference in overexpression of *PDGFC, KRAS, RAC2, SOS2,* and *PIK3R2* genes, being overexpressed in non-aggressive cases, with an overlap regarding other differentially overexpressed genes ($p<0.01$), namely, *RASA4, MET, PDGFA, RIN1, TIAM1, LAT* and *BCL2L1* (**Supplementary Figure 1.g1/2**).

Regarding the genes labeled as "driver genes", there was an overlap in *ATRX, TRAF7, STK11, MET, SMAD2, CBL* and *RUNX1*, between two tested groups ($p<0.01$) (**Supplementary Figure 1.h1/2**).

Analysis of MAPK pathway (**Supplementary Figure 1.k1/2),** revealed an overlap of *TGFB1, PPP3CB, CACNB3, DUSP4, HSB1,* and *PDGFA*. On the other hand*, KRAS, MAP3K1, SOS2, DUSP5, RAC2,* and *CDC25B* were found upregulated only in the non-aggressive cases. Also, *CACNA2D1* and *JUN* were found downregulated in the same group ($p<0.01$).

Genes related to PI3K pathway, namely *COL1A1, EPOR, STK11, FN1, COMP1, LAMB3, BCL2L1, MET, TLR2, PDGFA, ITGB4* were found upregulated in both, aggressive and non-aggressive cases. On the other hand, *PDGFC, KRAS, PIK3R2, COL1A2, CCND3, GSK3B, STK11, SPP1, SOS2, OSM, ITGB4, CDK6, JAK3, SGK2, COL4A4, IL2RB, ITGA2,* and *LAMA5*, were found upregulated in non-aggressive PTCs ($p<0.01$) (**Supplementary Figure 1.l1/2).**
To be considered, some of the genes are pertinent to different pathways.

Gene expression levels of patients with biochemical recurrence versus normal thyroid tissue.

We performed gene expression analyses on a subgroup of 6 patients that during the course of disease developed biochemical recurrence, only.
As shown in **Figure 5**, several genes, namely, *RXRG, TRAF7, ATRX, PPP3CB, TGFB1, COL1A1, GNA11, STK11,* and *EPOR* we found upregulated ($p<0.05$) (**Figure 5A**). Of these nine differentially expressed genes, four belong to the "driver gene" group (**Figure 5B**). Moreover, similarly to previous analyses on aggressive/non-aggressive cases (see **Figure 3A/B**), *RXRG* gene, pertinent to Transcriptional misregulation gene set was found as the most significant one. (**Figure 5C**).

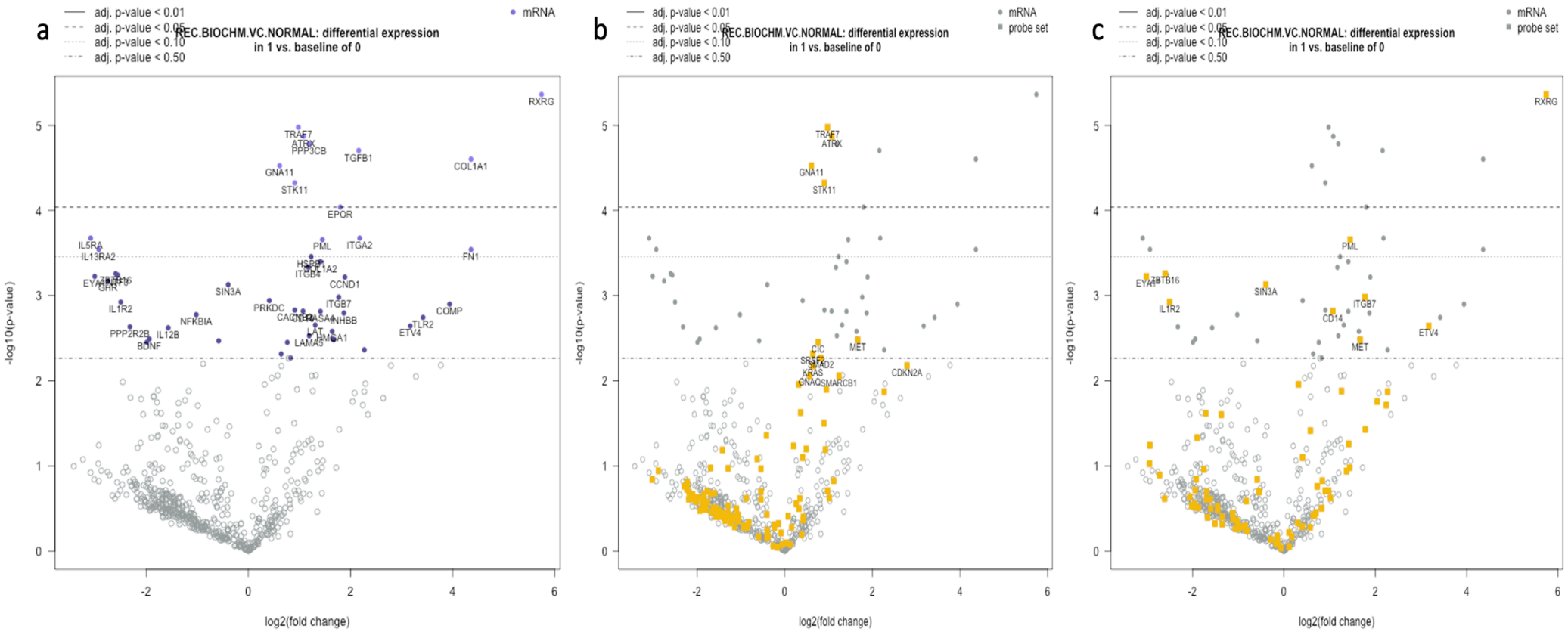

Figure 5. *Volcano plot rapresenting gene expression profile of patients that had biochemical reccurence only (a), mainly pertinent to 'driver genes' (b) and Transcriptional misregulation (c) gene categories.*

Differential gene expression levels of overlapping genes in aggressive vs non-aggressive cases

When taking into account all overlapping genes in aggressive and non-aggressive cases (see **Figure 4**), we found four genes, namely, *DUSP4* (p=0.009) *INHBB* (p=0.009), *JAG2* (p=0.042) and *MLF1* (p=0.041) significantly over-expressed in the group of non-aggressive cases, as compared to the aggressive ones (**Figure 6**).

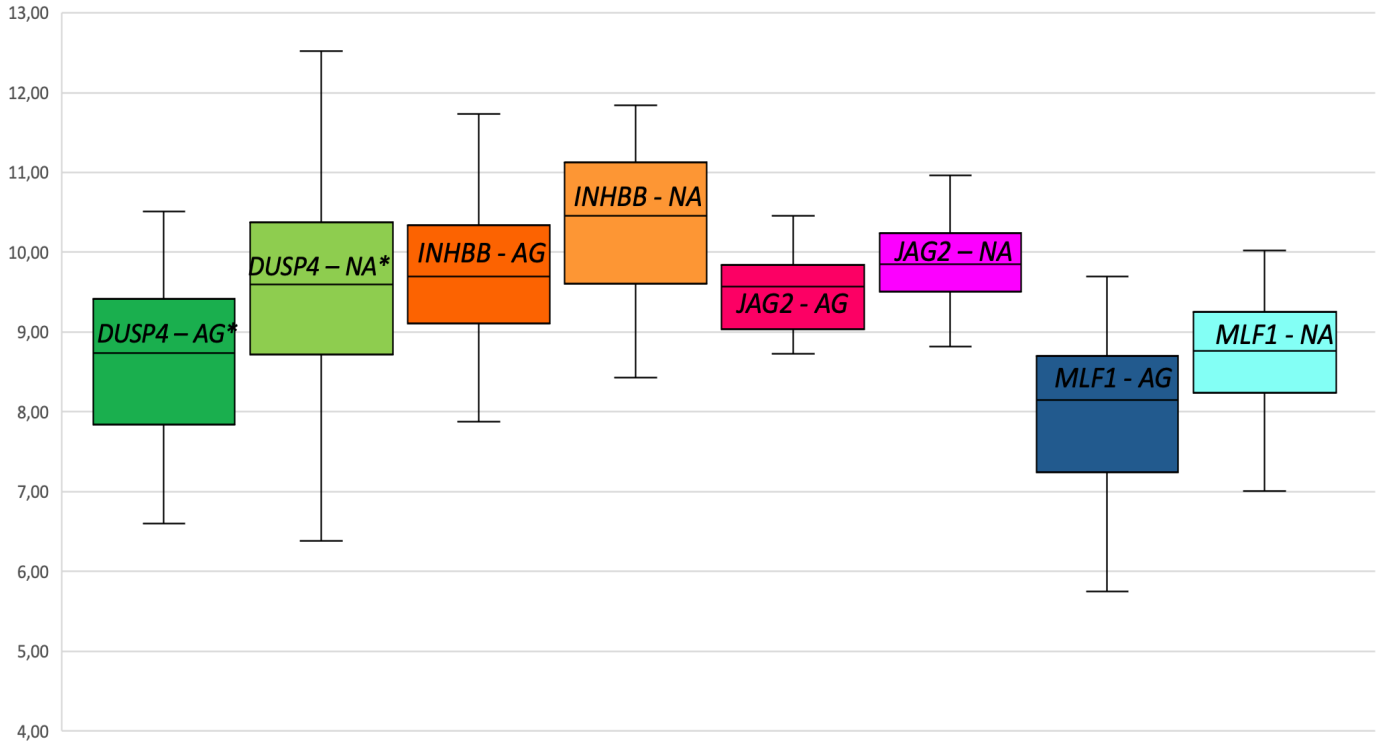

*AG- AGGRESSIVE
*NA – NON-AGGRESSIVE

		Total	AGGRESSIVE	NON-AGGRESSIVE	P-value
DUSP4	Median (interval)	9.2 (4.95-10.51)	8.74 (4,95-10.51)	9.59 (6,38-12,52)	0.009
INHBB	Median (interval)	10.0 (7.88-12.33)	9.7 (7.88-12.33)	10.5 (8.43-11.84)	0.009
JAG2	Median (interval)	9.7 (8.73-10.96)	9.57 (8.73-10.46)	9.85(8.82-10.96)	0.042
MLF1	Median (interval)	8.52(5.75-10.02)	8.15(5.75-9.7)	8.76 (7.01-10.02)	0.041

Figure 6. *Different gene expression levels of DUSP4 (p=0.009) INHBB (p=0.009), JAG2 (p=0.042) and MLF1 (p=0.041) (overlapping genes in aggressive and non-aggressive cases, see* ***Figure 4****), were found significantly over-expressed in the group of non-aggressive cases, as compared to the aggressive ones.*

DISCUSSION

In the present study, we reported that clinically aggressive PTC are associated with peculiar pathological features and gene expression profiles.

PTCs in general show indolent behavior with localized disease and typically do not recur or metastasize beyond local lymph nodes. A recent meta-analysis, using univariate comparisons, has identified male sex, advanced age, tumor size, multifocality, lymphovascular invasion, extrathyroidal extension and lymph node metastasis as risk factors for distant metastasis in well differentiated thyroid cancers (463).
Regarding morphological features, in line with literature data, we found TILs present more frequently in aggressive PTCs (26/43, 60.5%), as compared to non-aggressive cases 11/43 (25.6%) (p=0.001) (464). In another study, authors showed that Tregs are present in PTC and may promote more aggressive disease. Furthermore, the relative frequency of Tregs in comparison with total $CD4^+$ T cells and $CD8^+$ T cells may be a useful tool in predicting disease severity in PTC patients (465).

Moreover, another feature, extensive fibro-sclerotic tissue modification within the tumor bulk, was significantly more present in aggressive cases (21/43, 48.8%), as compared to non-aggressive PTCs (10/43, 23.3%). In fact, fibrosis has been reported to support cancer growth through a variety of mechanisms including direct cellular interactions, immune modulation, and extracellular matrix remodeling (466). Moreover, PTCs with intra-tumoral nodular fibrosis and heterotopic ossification were shown to have higher incidences of lymph node metastasis and extrathyroidal invasion than those without these features (467).

A second part of our study was focused on the definition of gene expression profiles in a subset of aggressive and non-aggressive PTC cases, selected from the pathological series and matched also for histological type. Several studies employed NanoString nCounter technology to explore genetical make up of thyroid malignances (388,444,445). However, to the best of our knowledge, this is the first study using nCounter® PanCancer Pathways Panel, exploring different canonical pathways.
Most thyroid cancers harbor mutations along the MAPK cellular signaling pathway (468). This pathway, activated by mutually exclusive *RET, BRAF*, and *RAS* mutations in thyroid cancer, transmits growth signals from the cell membrane to the nucleus. These mutational events, playing an important part in gene expression and cell regulation, initiate cancer development. In some but not all thyroid cancers, tumor initiation is followed by tumor progression, depending on the accumulation of more mutations. These somatic mutations enable the tumor to recruit further signal pathways (468).

Analysis of MAPK pathway (**Supplementary Figure 1.k1/2),** revealed an overlap of *TGFB1, PPP3CB, CACNB3, DUSP4, HSB1,* and *PDGFA*. On the other hand*, KRAS, MAP3K1, SOS2, DUSP5, RAC2,* and *CDC25B* were found upregulated only in the non-aggressive cases. Also, *CACNA2D1* and *JUN* were found downregulated in the same group ($p<0.01$).

In particular, *CACNA2D1* gene has been related to enhanced radio resistance in cancer stem-like cells of non-small cell lung cancer cell lines (469). Moreover, *CACNA2D1* expression at the protein level in a case series of ovarian cancer was suggested to play a crucial role in promoting aggressive ovarian cancer behavior and progression, and that it may serve as a novel predictive prognostic marker and a potential target for therapeutic intervention in these patients (470). Furthermore, *JUN* is a proto-oncogene, and its encoding product is the first discovered oncogenic transcription factor (471). Of note, *JUN* has been proposed as a specific diagnostic biomarker/therapeutic molecular target of PTC (472). In another setting, namely murine model of hepatocellular carcinomas it has been demonstrated that it could promote tumor formation and maintain tumor cell survival between the initiation and progression stages (473).
Interestingly, both genes, *CACNA2D1* and *JUN* were found downregulated in non-aggressive group of PTCs.

The development of more aggressive and de-differentiated thyroid tumors is believed to be associated with additional late-hit driver mutations (305,369). The most common and well-studied of those are TERT promoter mutations, which have been associated with recurrence and mortality, particularly when they concomitantly occur with a primary *BRAF* or *RAS* mutation (308,310,474). The initial *RAS* or *BRAF* mutation is central to the subsequent behavior of the tumors they give rise to. BRAF mutations confer strong activation of ERK, whereas RAS mutations provide weaker ERK activation, but allow activation of other relevant effectors involved in tumorigenesis such as PI3K (phosphatidylinositol 3-kinase) or RAC1 (Ras-related C3 botulinum toxin substrate 1) (305).

Considering RAS pathway, there was a difference in overexpression of *PDGFC, KRAS, RAC2, SOS2,* and *PIK3R2* genes, being overexpressed in non-aggressive cases, with an overlap regarding other differentially overexpressed genes ($p<0.01$) (**Supplementary Figure 1.g1/2**).
Interestingly, *PIK3R2* gene, found downregulated in non-aggressive PTC cases, was studied in tumor xenografts models of lung squamous cell carcinoma cell lines where authors examined the consequences of targeting *PIK3R2* expression. The authors demonstrate that the interference with *PIK3R2* expression in established squamous cell carcinoma xenografts reduced tumor survival. In particular, interference with *PIK3R2* expression triggered tumor shrinkage in all the cell lines with predominant p85β expression.
However, some of the genes pertinent only to non-aggressive cases in our study, such as *PDGFC* (475,476), *RAC2* (477) were labeled as oncogenic in different tumor models, promoting tumor growth and metastasis. Specifically, *RAC2* is involved in various aspects of host defense including integrin and immunoreceptor signaling, polarization to M2 macrophages and generation of *ROS* (478–480). *RAC2* knockout mice demonstrated a pronounced impairment in tumor growth, angiogenesis, and metastasis (479).

DNA damage is one of the major causes that trigger the development of tumors (481). DNA repair pathways are encoded by a class of proteins that detect DNA double stand breaks, chromosomal fragmentation, translocation and deletions, and can correct some alterations (482). The DNA damage response pathway responds to cellular damage by using signal sensors, transducers and effectors (483). Such mechanisms help the genome to tolerate or

correct damage on an ongoing basis. DNA repair mechanisms restore damaged DNA and may have a dual effect on the tumor: they prevent new somatic mutations and may restrict tumor development, but they also restore tumor cells with damaged DNA after chemo and radiation therapy (484). DNA repair genes can make tumor cells more sensitive to the therapy, but at the same time not-repaired damaged tumor cells can form more new clones of treatment resistant cells (485,486).

Of note, *POLD4, H2AFX, POLR2J, ATM, MAD2L2, PRKDC,* genes related to DNA Damage - Repair pathways were found upregulated in non-aggressive PTC cases, only.

ATM gene located on chromosome 11q22-23 spanning over 160 kb of genomic produces a protein that plays a key role in DNA damage response, especially for double-strand break (487). ATM belongs to the phosphoinositide 3-kinase (PI3-K) family and exists in the form of dimer or multimer (488). Once cells received radiation, *ATM* dimer will be dissociated and so activated, followed by a variety of downstream proteins phosphorylation (489,490). Malignancies that have been reported to be associated with specific *ATM* alleles mutation include breast, lung, thyroid, prostate cancer, and chronic lymphocytic leukemia (491–495). Studies previously suggested that low expression of *ATM* was related to poor differentiation of oral squamous cell carcinoma and gastric cancer and involved in lymph-node metastasis (496,497). A recent study also demonstrated that *ATM* facilitated invasion and lymph-node metastasis of breast cancer through the ATM-Snail pathway (498). Similar situation was found in neuroendocrine tumor in which ATM was downregulated in metastatic patients compared with nonmetastatic ones (499). The authors suggested that *ATM* down-regulation can lead to increased cell cycle regulatory genes such as *CDKN3* and *CCNB1*, and then increased *CDKN3* and *CCNB1* leading to increased cell division and cell proliferation.

Another gene, related to the same pathway, *H2AFX*, maps to chromosome 11 at position 11q23, in a region that frequently exhibits mutations or deletions in a large number of human cancers (500,501). Head and neck squamous cell carcinoma is often characterized by amplification of chromosomal region 11q13 as well as loss of distal 11q, the region containing *H2AFX* (502). The increased chromosomal instability seen in these cells indicates that loss of 11q and *H2AFX* may contribute to tumour development, progression and resistance to therapy in this cancer subtype. These findings have led to the intriguing proposal that human *H2AFX* may be an excellent candidate gene to indicate susceptibility to lymphomas, leukemia and other cancers (503,504). Additional evidence of the tumour-suppressing role of *H2AX* comes from a study involving gastrointestinal stromal tumour (GIST) cell lines. Imatinib mesylate, a clinically approved protein kinase inhibitor, has been shown to trigger apoptosis in GIST cell lines through upregulation of *H2AX* (505).

MAD2L2 was originally identified as a subunit of DNA polymerase ζ critical for DNA translesion synthesis (506) and a component of the mitotic spindle assembly checkpoint that inhibits the anaphase-promoting complex (507).
MAD2L2 has been reported to promote Elk-1 phosphorylation by c-Jun N-terminal protein kinase (JNK) and thus lead to the up-regulation of Elk-1 target genes in the presence of DNA

damage, which suggests that *MAD2L2* might be a central player in coordinating the cellular response to DNA damage (508). Moreover, *MAD2L2* has been reported to regulate the epigenetic reprogramming of germ cells (508,509) and the maintenance of pluripotency in embryonic stem cells (510), and promote the open chromatin configuration through *DPPA3* in embryonic stem cells (511). Accordingly, it is not surprising that dysregulation of *MAD2L2* has been found in multiple cancers. For instance, *MAD2L2* was overexpressed in glioma, epithelial ovarian cancer, and breast cancer (512–514), while inactivation of *MAD2L2* sensitized nasopharyngeal carcinoma cells to DNA-damaging agents (515).

Of note, in a study by Li et al (516), higher expression of *MAD2L2* was associated with lower tumor volume, earlier TNM stage, less invasion, and a smaller chance of distant metastasis in colorectal cancer patients, which suggested that *MAD2L2* was a suppressor of colorectal cancer growth and metastasis. Consistently, survival analysis indicated that *MAD2L2* suppressed colorectal cancer development.

CONCLUSIONS

In conclusion, we demonstrate that clinically aggressive PTC are characterized by peculiar pathological features, including an increased TILs infiltration and a more prevalent occurrence of intratumoral fibrosis, supporting the value of a careful reporting of these parameters in the PTC diagnostic work up. Moreover, although non-aggressive PTC in our series showed a larger number of deregulated genes as compared to aggressive PTC cases, the existence of a set of differentially regulated genes in the two groups suggests that different molecular mechanisms are active in promoting clinical aggressiveness in PTC with special reference to the impairment of the Hedgehog pathway.

SUPPLEMENTARY MATERIAL

Supplementary Table 1. *Clinico-pathological characteristics of cases included in nCounter Nanostring analyses (#48).*

Parameters		TOTAL	Non-aggressive PTCs	Aggressive PTCs	P value
Age median (interval)		38 (18-73)	37 (18-61)	40 (19-73)	/
Sex	M	16	8	8	/
	F	32	16	16	
Histotype	Classic/Follicular	38	19	19	/
	Other histotypes	10	5	5	
T	1	30	15	15	/
	2	16	8	8	
	3	2	1	1	
N	0	22	11	11	/
	1	26	13	13	
Histotype	Classic/ Follicular	38	19	19	1.000
	Other histotypes	10	5	5	
TNM Stage	1	47	23	24	0.312
	2	1	1	0	
Tumor diameter (cm)	≤1	10	6	4	0.702
	> 1 - ≤ 2	22	9	13	
	> 2 - ≤ 4	14	8	6	
	> 4	2	1	1	
Multifocal presentation	no	24	19	5	<0.001
	yes	24	5	19	
Bilateral presentation	no	33	20	13	0.029
	yes	15	4	11	
Tumor capsule	absent	22	7	15	0.064
	incomplete	19	12	7	
	complete	7	5	2	
Extrathyroidal extension	no	23	14	9	0.149
	yes	25	10	15	
Vascular invasion	no	22	14	8	0.082
	yes	26	10	16	
Surgical margins	negative	35	18	17	0.745
	positive	13	6	7	
Necrosis	no	47	23	24	0.312
	yes	1	1	0	
Mitosis	0	8	6	2	0.199
	1	39	18	21	
	2	1	0	1	
Tumor infiltrating lymphocytes	no	24	17	7	0.004
	yes	24	7	17	
Fibro-sclerotic changes	absent	16	10	6	0.040
	moderate	18	11	7	
	extensive	14	3	11	
Follow-up	alive	45	23	22	0.551
	dead	3	1	2	

Supplementary Figure 1. *Differential gene expression in aggressive and non-aggressive papillary thyroid carcinomas, according to different canonical pathways (continued at page 134 and 135).*

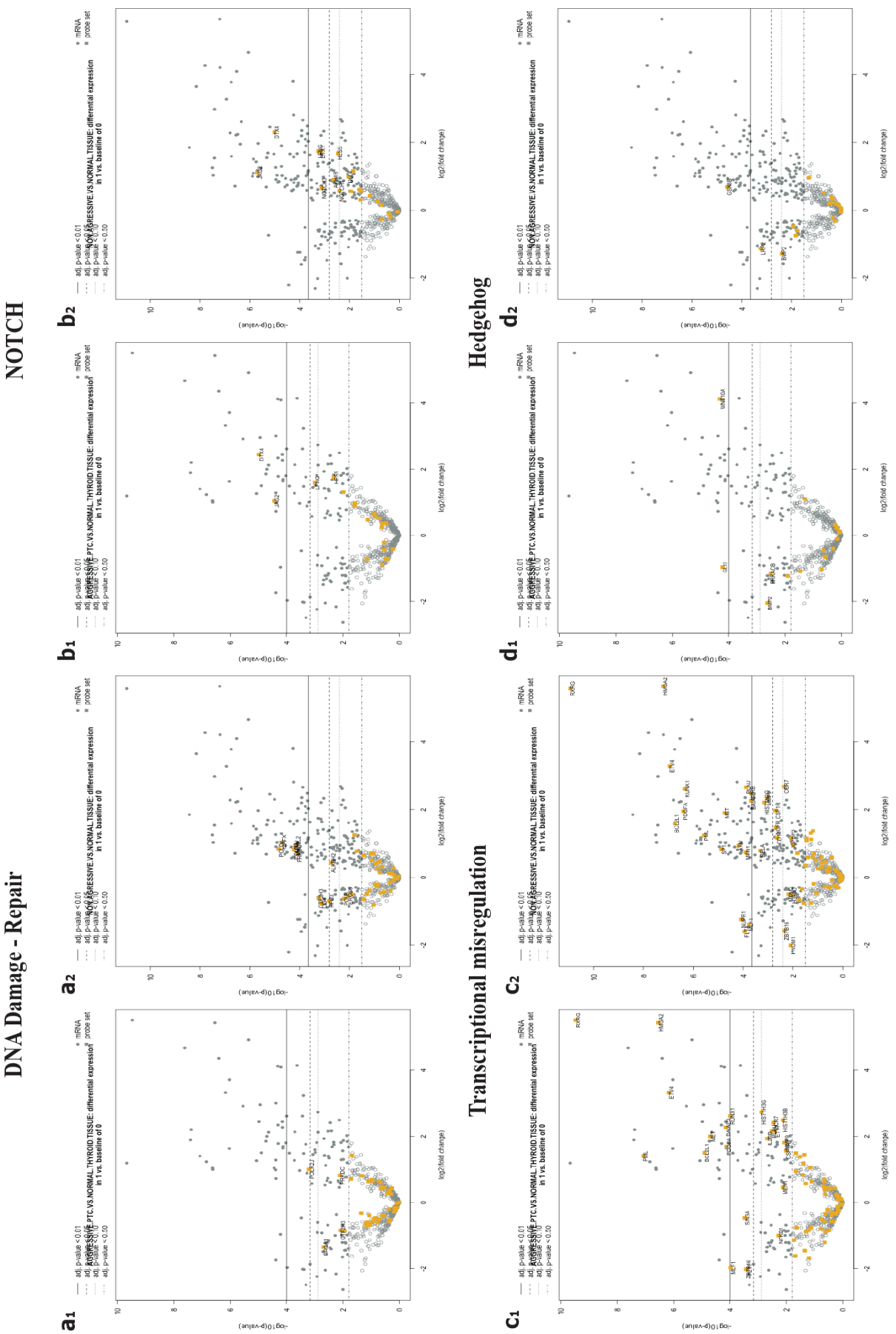

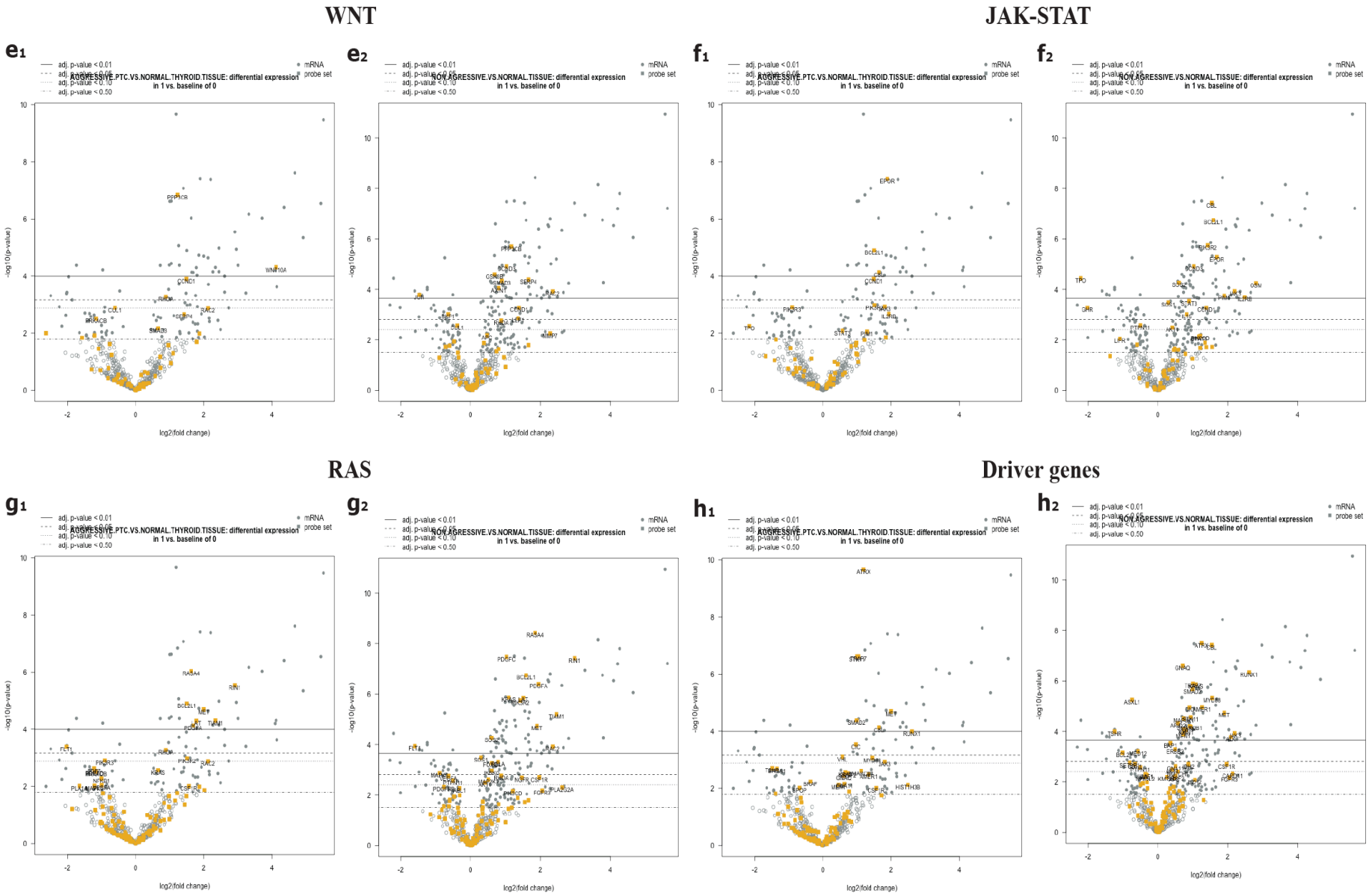
WNT
JAK-STAT
RAS
Driver genes
e1
e2
f1
f2
g1
g2
h1
h2
adj. p-value < 0.01
adj. p-value < 0.05
adj. p-value < 0.10
adj. p-value < 0.50
mRNA
probe set
AGGRESSIVE.PTC.VS.NORMAL.THYROID.TISSUE: differential expression in 1 vs. baseline of 0
NON.AGGRESSIVE.VS.NORMAL.TISSUE: differential expression in 1 vs. baseline of 0
-log10(p-value)
log2(fold change)

MAPK

PI3K

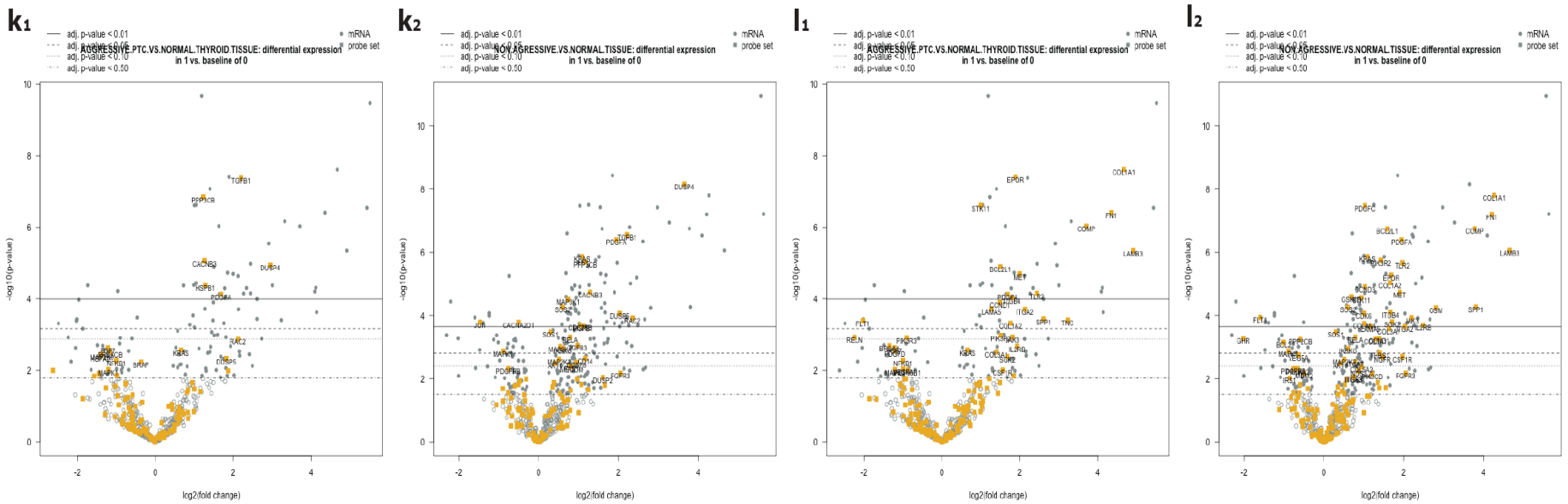
k1
k2
l1
l2
adj. p-value < 0.01
adj. p-value < 0.05
adj. p-value < 0.10
adj. p-value < 0.50
mRNA
probe set
AGGRESSIVE.PTC.VS.NORMAL.THYROID.TISSUE: differential expression in 1 vs. baseline of 0
NON.AGGRESSIVE.VS.NORMAL.TISSUE: differential expression in 1 vs. baseline of 0
-log10(p-value)
log2(fold change)

CHAPTER 3: MERKEL CELL CARCINOMA AND CHIMERIC ANTIGEN RECEPTOR (CAR) T- CELL THERAPY

INTRODUCTION

Merkel cell carcinoma (MCC) is a rare cancer. Data from the SEER program in the US and national registries in Europe, Australia and New Zealand estimate global incidence ranging between 0.1 and 1.6 cases per 100,000 inhabitants / year, with the peak recorded in Australia (517). Given the progressive aging of the population, it is expected that the incidence in the USA could rise from approximately 2500 cases per year in 2013 to more than 3000 cases per year by 2025 (518). This increase is most probably due to the diagnostic progress, aging of population, development of regional and national registers, and greater awareness and familiarity with this tumor by medical community.

The most affected are subjects with fair complexion, elderly and with significant previous sun exposure. The incidence is generally higher in men than in women (518). The most affected group of patients are older adults (median age of 75-80 years), while pediatric cases are extremely rare (519,520). In fact, an analysis of the data coming from over 9000 patients in the USA has shown a median age of 76 years and that only 12% of patients are under 60 years of age (521).
MCCs have a higher incidence in immunosuppressed individuals, which make 10% of patients (522). Immunosuppression is the risk of developing this disease and many reports show that tumor onset in these patients occurs at an earlier age compared to average values. Furthermore, immunosuppression is associated with a worst prognosis, regardless of the stage of the disease: the 3-year MCC-specific survival is half of that of immunocompetent patients (523,524). Moreover, reports have described MCC onset at an earlier age in immunosuppressed patients, particularly organ-transplant-recipients and patients with HIV/AIDS (525,526).

Cell of origin

The name for MCCs comes from the structural and immunohistochemical characteristics they share with Merkel cells. However, there has been an ongoing debate in the literature about the cells of origin of MCC, with various groups suggesting that MCCs do not arise from Merkel cells but instead arise from epidermal stem cells (527), dermal stem cells (528) or pre-/pro-B cells (529).

Histologically, MCC reveals distinctive subtypes, which are the intermediate (approximately 90%), the small cell and the trabecular type, which all express cytokeratin 20 (CK20), neural cell adhesion molecule (NCAM/CD56), Chromogranin A and Synaptophysin (107).

Even though MCCs share certain features with Merkel cells, emerging data suggest that Merkel cells are not the cells of origin (530). Merkel cells are oval shaped osmoreceptors and mechanoreceptors essential for light touch sensation (531). While MCCs share some markers with Merkel cells, there are important differences. For example, although CK20 is expressed in both Merkel cells and MCCs, its pattern of expression differs sharply. In Merkel cells, CK20 is loosely arranged, leading to diffuse CK20 immunohistochemical staining in the cytoplasm. In contrast, in MCCs, CK20 filaments are organized in characteristic whorl- or plaque-like arrangements, leading to the classic dot-like staining pattern in IHC (532). Moreover, MCCs express a number of markers, such as c-kit, CD171, and CD24 that are not expressed by Merkel cells (533). Of note, the frequent expression of B-lymphoid lineage markers in MCC and its sometimes difficult histological discrimination from lymphoid malignancies (534) contributed to the formulation of the hypothesis that MCC could originate from pre/pro B-cells (529,535). The pre/pro B-cell as the cellular origin of MCC would explain why most MCCs are located within the dermis and subcutis (536) without revealing contact to the epidermis, where Merkel cells or epidermal stem cells reside (529). The arguments in favor of a lymphocytic origin are: expression immunohistochemistry of B-cell markers (PAX5, TdT) and immunoglobulins (IgH and Igk), tumor regression following treatments with Idelalisib (normally used in the treatment of B-cell lymphoma) (537).
Furthermore, the lymphocytes (as well as the fibroblasts) are located in the dermal compartment, which is not very exposed to the action of ultraviolet rays. Therefore, UV-mediated MCCs are unlikely to originate from these cells.
A recent study (538) by Kervarrec and colleagues, based on the sequencing of a combined tumor consisting of a trichoblastoma and MCC, supports the hypothesis of an origin from epithelial progenitors. Finally, it seems that the dermal fibroblasts are able to support the viral replication of Merkel cell polyomavirus (MCPyV) (see below), representing the main host of infection in MCCs. It was demonstrated that the production of matrix metalloproteinases (MMPS), induced by molecular pathway WNT / β-catenin, promotes infection of fibroblasts by MCPyV (539) (**Figure 1**, source (533).

According to some authors it is also possible that MCCs have cells of multiple origin (530), with MCPyV-positive forms that could originate from dermal fibroblasts and the MCPyV-negative forms that could be connected to epidermal cells. However, this argument still remains controversial.

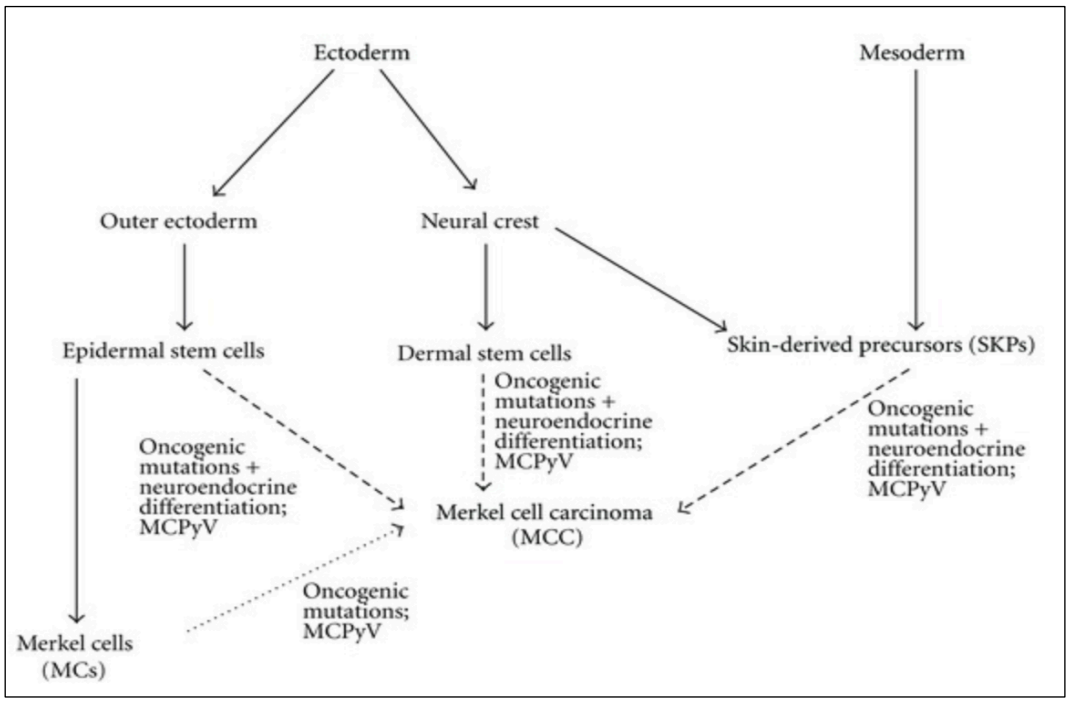

Figure 1. *Scheme of potential cells of origin of Merkel cell carcinoma (MCC), shown from an ontogenetic perspective. All arrows with a* scattered *line represent thus far hypothetic lineage relationships. However, whereas MCC derivation from Merkel cells is not very likely, there are hints implying epidermal stem cells in MCC genesis, and dermal stem cells as well as SKPs at least cannot be excluded as cells of origin for MCC. For each putative cell type of origin, an involvement of MCPyV in MCC genesis is highly probable, at least in a large fraction of MCCs (source 533).*

Clinical features

Clinically, MCC develops rapidly and asymptomatically over months (540). Heath and colleagues coined an acronym: **AEIOU** – according to the he most significant features can be summarized in **A**symptomatic/lack of tenderness, **E**xpanding rapidly, **I**mmune suppression, **O**lder than age 50, and **UV**-exposed site on a person with fair skin (522). It usually manifests as solitary, firm, flesh-colored to red nodule with a smooth, shiny surface, sometimes with telangiectasia (541). The majority of MCCs arise on sun-exposed skin. The most frequently affected sites are the head and neck (50%) and extremities (40%) (541). Of note, metastatic disease may develop in absence of prior history of primary MCC. In such cases, primary tumor, may have spontaneously regressed (542).

Staging system and sentinel lymph node biopsy

Staging represents a fundamental step in the management of MCC. Following the histopathological confirmation of the diagnosis, MCC patients should undergo an evaluation for extra-primary disease. For this purpose, ultrasound examination of the regional, lymph nodes are generally recommended, along with CT / MRI and alternatively with PET-CT for the diagnosis of distant metastatic deposits. MCC generally spreads to loco-regional lymph nodes earlier than giving distant metastasis. Precisely for this reason the biopsy of the sentinel lymph node, represents an important staging procedure.
Regional node involvement has been reported in up to two-thirds of patients and can be apparent at initial presentation in one-third. It can take up to eight months for nodal metastases to become clinically apparent. Proper identification and staging of the nodal involvement could direct treatment algorithms for patients with MCC. These algorithms can include elective lymph nodal dissection or adjuvant treatment with radiation or chemotherapy (543). The eighth edition American Joint Committee on Cancer (AJCC) staging system provides important information for both management and prognosis of patients with MCC (544).

MCC staging is assigned based upon tumor, node, and metastasis assessment. These stages can be summarized as follows:

●Stage I – Primary tumors ≤2 cm in maximum dimension (T1), without evidence of regional lymph node involvement.
●Stage II – Primary tumors >2 cm (T2 or T3) or a primary tumor with invasion into bone, muscle, fascia, or cartilage (T4), without evidence of lymph node involvement. Stage II is further divided into two subgroups based upon the size and depth of invasion of the primary tumor.
●Stage III – Any primary tumor with in-transit metastasis or regional lymph node disease. Pathologic stage III is divided into subgroups based upon the extent of in-transit or regional lymph node involvement.
●Stage IV – Metastasis beyond the regional lymph nodes, regardless of the status of the primary tumor and regional node.

The diagnostic accuracy and usefulness of sentinel lymph node biopsy in MCC have been studied in detail. Gupta et al. analyzed 122 patients with clinical N0 staging and found that 32% harbored occult metastatic disease, compared to a 5% incidence rate in similarly staged melanoma (545). As expected, patients with positive sentinel lymph node biopsy (SLNB) were 3 times more likely to develop recurrent disease than with N0 patients. This study showed that SLNB changed the stage of one-third of MCC patients, altering their treatment course. Many other studies have shown that SLNB can be performed reliably and safely both in the head and neck region (546) and in the extremities (547) in order to identify occult regional disease.
A study from Memorial Sloan-Kettering in New York looking at recurrence and survival in MCC patients undergoing SLNB showed that the only predictors of SLNB positivity were primary tumour size (25% <2 cm versus 45% >2 cm) and the presence of lymphovascular

invasion (55% positive versus 4% negative). Interestingly, they found no difference in recurrence or death from MCC between SLNB-positive and -negative patients. Moreover, only lymphovascular invasion was associated with both recurrence and survival (548).

Schmalbach et al. studied 10 patients with MCC who had SLNB and found that the two patients with positive lymph nodes appeared negative on hematoxylin-eosin staining. MCC was identified using CK20 immunostaining (549). It should be noted that the clinical significance of submicroscopic lymph node metastases identified only by immunohistochemistry remains unclear.

Microscopic features

Microscopically, MCC belongs to the category of small blue round cell tumors. The mass develops intradermally but frequently extends subcutaneously and is generally made up of small, nodular aggregates of monomorphic cells characterized by scant cytoplasm, large basophilic nuclei with irregular outlines and indistinct nucleoli (**Figure 2**, source (550). An accurate histological analysis is essential for the diagnosis. In detail, MCC is composed of cells of uniform size with a round to oval nucleus and scant cytoplasm. Nuclear membranes are distinct, the chromatin is finely dispersed, and nucleoli are usually inconspicuous. Mitotic figures and nuclear fragments are numerous. Focal spindle cell differentiation may be present. The tumour is centered on the dermis and frequently extends into the subcutaneous fat. The epidermis may be involved in a pagetoid fashion and in exceptional cases the tumour cells are entirely limited to the epidermis. Ulceration of the epidermis occurs in a subset of cases. This neoplasm forms diffuse sheets and solid nests in the dermis. The dermis occasionally shows a desmoplastic response. Larger lesions may show focal necrosis and angiolymphatic involvement is commonly present (551). Three histological variants were described, although their prognostic significance has showed limited level of evidence. Trabecular is the rarest histological subtype, and if present it is usually focal. Some cases show so-called Homer-Wright-like pseudorosettes (550). Numerous mitotic figures scattered apoptotic cells and occasionally zones of geographic necrosis are observed. The intermediate subtype is the most common and is characterized by a high cellular mitotic activity. Finally, the third variant, small cell, is a form undifferentiated and has similar characteristics as small cell forms of other carcinomas.

Immunohistochemistry

Tumour cells express low molecular weight cytokeratins (detectable by specific or broad spectrum cytokeratins such as AE1/AE3, CAM5.2, pan-cytokeratin), epithelial membrane antigen and the epithelial marker BER-EP4. Cytokeratin 20 is a sensitive and quite specific marker for Merkel cell carcinoma (552). The staining pattern for low molecular weight cytokeratins and CK20 typically is as paranuclear dots, but may also show cap-like paranuclear or diffuse cytoplasmic staining (553). CK20 is useful in combination with thyroid-transcription factor-1 to differentiate between Merkel cell carcinoma (CK20 positive, TTF-1negative) and small cell carcinoma of the lung (<10% CK20 positive, TTF-1 positive) (554). CK20 and broad

spectrum cytokeratin are also useful for the detection of occult micro-metastases in sentinel lymph nodes (555). Markers of neuroendocrine differentiation include CgA, SYN, NSE, somatostatin, calcitonin, gastrin and others (Figure 2, source (550). Merkel cell carcinoma also expresses CD117, the KIT receptor tyrosine kinase (556), and in approximately a third of cases CD99 (557). The tumour cells are negative for leukocyte common antigen and S-100 (551). PAX-5 is expressed with variable intensity by 93% of MCC, while huntingtin-interacting protein 1 (HIP1) oncoprotein is detected in 90% of tumors (558). One third of the tumors stain for the p63 tumor protein; this is associated with a more negative prognosis (559). Recently, the insulinoma-associated protein (INSM1) has been shown to be a sensitive but not-specific nuclear marker (560).

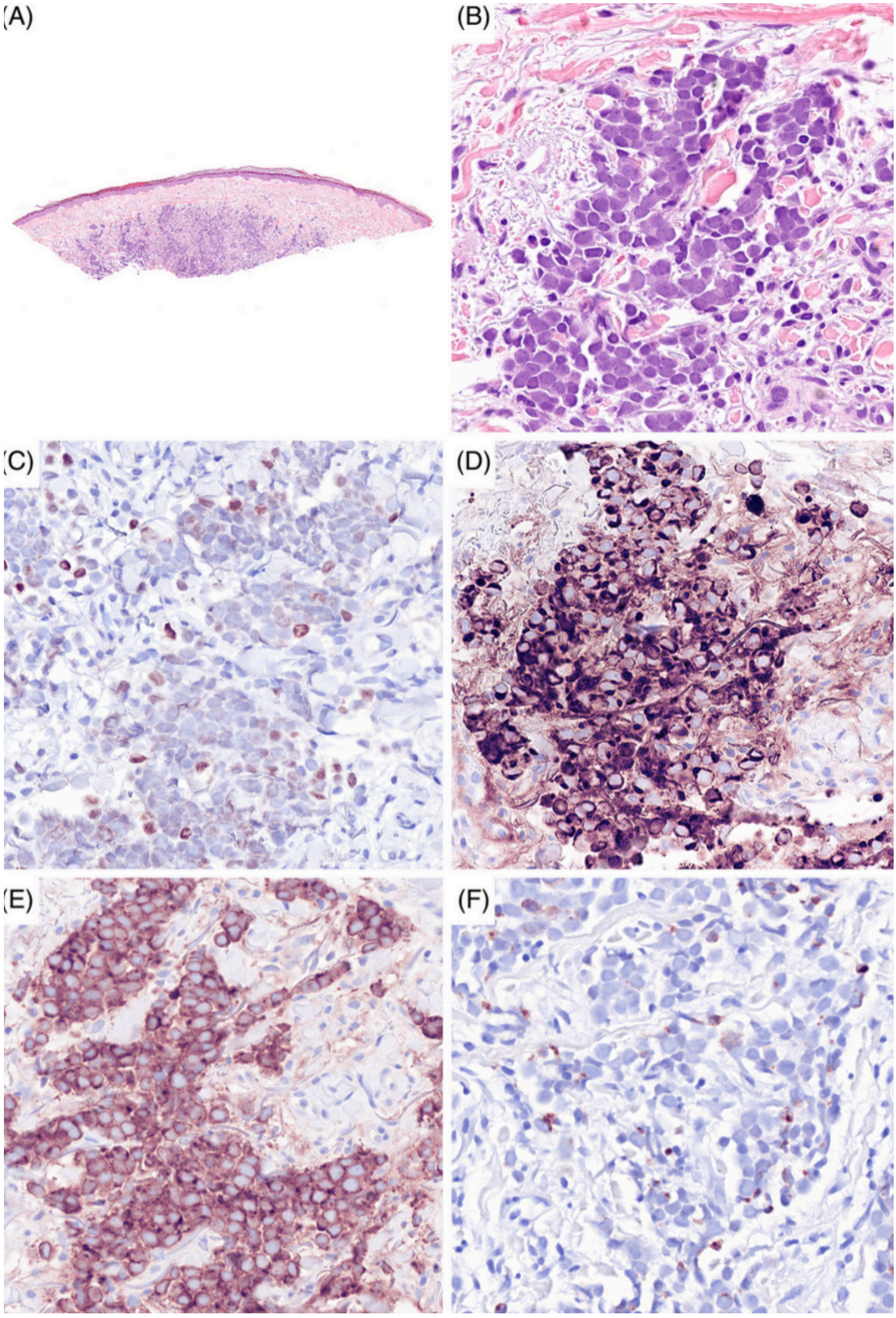

Figure 2. *Shave biopsy of skin displaying a Merkel cell carcinoma with pure neuroendocrine morphology at scanning, A, and high, B magnification. The neoplastic small blue round cells exhibit spotty nuclear positivity for Merkel cell polyomavirus, C, and cytoplasmic positivity for CK20 (paranuclear dot and circumferential patterns), D, synaptophysin (diffuse cytoplasmic pattern), E, and neurofilament (scant dot-like pattern), F(source 550).*

Merkel cell polyomavirus (MCPyV) and role in MCC

Merkel cell polyomavirus (MCPyV) is a naked double-stranded DNA virus belonging to the *Polyomaviridae* family (561). Its circular genome of ~5400 base-pairs (bp) encompassed three functional domains. The early region includes the "Tumor" (T) antigen gene locus (562), from which, alternatively-spliced RNA transcripts are produced. This region encodes for distinctive gene products: the large T (LT), small (sT), 57kT antigens and a product from an alternate frame of the LT open reading frame (ALTO) (563). The LT, sT and 57 kT antigens, due to alternative splicing, share a 78 amino acid sequence at their N-terminal region (564). The discovery of MCPyV in 2008 enabled the progress in the understanding of oncogenesis of this neoplasm (565).

The integration pattern of MCPyV suggests that viral infection and non-productive integration of the viral genome into the host cell occurs earlier then the proliferation of cancer cells. Furthermore, the continued expression of the T antigens is required for the survival of cancer cells. All together this evidence provides strong support for the causal role of MCPyV in development of the MCC. Although it is well defined as the clonal integration of viral genomic DNA in the host genome precedes the development of most cases of MCC, the mechanism by which infection contributes to tumor progression and many aspects of the process of the infectious cycle still remain unclear (539,566,567).

MCPyV-positive MCCs express a C-terminal truncated LT (tLT) due to nonsense mutations or frameshift mutations generating premature stop codons. Tumor-derived tLTs retain the DnaJ region and the RB binding domain, and sometimes the NLS, but lack the OBD and helicase/ATPase domain (568,569). The C-terminal region contains several elements fundamental for viral replication, hence tLT fails to support viral replication (570). As for other human PyVs, and in general for other tumor viruses, there is strong selective pressure within tumors to eliminate viral replication capacity (571).

Studies in mouse and human fibroblasts demonstrated that expression of a tumor-derived tLT has stronger growth promoting activities than wild-type LT and 57kT (572). Expression of full-length did not induce anchorage-independent growth, whereas tLT proteins induced aggregates in soft agar that did not grow into full colonies, suggesting that tLT has increased cell proliferative capacity compared with the wild-type LT. Expression of the C-terminal 100 amino acids residues inhibited the cell growth of fibroblasts and of the virus positive-MCC MKL-1 cell line (572). The mechanism by which this region inhibits cellular growth is not known but is likely to be independent of p53 since neither full-length LT nor 57 kT are able to bind p53. The C-terminal domain may interact with a yet unidentified cellular protein involved in growth regulation. Putative candidates are the cell cycle checkpoint kinase ATM, casein kinase 2β and phosphatidylinositol-5-phosphate 4-kinase type 2β, which are all involved in proliferation and were found to interact with MCPyV LT, but the biological importance of these interactions were not examined, nor was the region of LT required for interaction identified (573). CRISPR/Cas9 targeting of LT/57kT impaired MS-1 and WaGa

cell proliferation, decreased G1/S cell cycle progression and increased apoptosis. Additional targeting of sT did not enhance the effect in LT/57kT mutated cells (574,575).

Cell culture studies revealed that neither full-length nor tumor-derived tLT was able to trigger cellular transformation (576) but LT is required for growth of virus positive-MCC cells (577,578). The C-terminal domain of LT causes DNA damage and stimulates host DNA damage response, leading to p53 activation and inhibition of cellular proliferation. Phosphorylation of the C-terminus by ATM kinase induces apoptosis and inhibits proliferation (579,580). Thus, the C-terminus of LT contains anti-tumorigenic properties and may explain why this region is deleted in VP-MCC. To further elucidate the role of MCPyV LT in MCC tumorigenesis, cellular proteins that interact with LT were identified using different methods (573,581). However, the biological relevance of these interactions and possible implications for MCPyV-induced cancer have not always been studied.

Unlike other common episomal infections, genetic analyses have found that viral DNA is clonally integrated into the host cell genome. The etiology of over 80% of MCC tumors can be traced to MCPyV by the presence of integrated MCPyV genomic sequence in the cellular DNA
(582). Liu et al (567) in their recent study identified a cell culture model MCPyV infection which could facilitate understanding of the mechanisms oncogenic agents of viral DNA. They identified the dermal fibroblasts as the natural host skin cell that supports virus entry, gene expression and replication. This discovery arose after establishing in cell cultures the conditions that potentially mimicked cell growth in the skin. The cellular signaling associated with damage repair could induce the skin microenvironment to promote viral infection. Subsequently, proliferation of fibroblasts stimulated transcription and viral replication.
In this model, the induction of metalloprotease besides the WNT/ β-catenin pathway and other growth factors, such as EGF and FGF, stimulate MCPyV infection. This suggested that MCC risk factors, such as UV radiation and aging, which are known to stimulate WNT signaling and metalloprotease expression, may promote viral infection and thereby drive MCC tumorigenesis (567). Subsequent studies using PCR and/or immunohistochemistry targeting MCPyV large T antigen have at times provided disparate estimates of viral positivity in MCC, ranging from as low as 24% in some series to 100% in another (583,584). With wide variation in methods and populations, the remaining 10 of 12 major studies to address this question to date have estimated anywhere from 46% to 89% MCPyV positivity, with the aggregate estimate of all studies being 76% (453 of 595 unique MCCs) (565,583−593). At this time, there is currently no accepted standard method for determining MCC viral status, neither is there consensus on which single assay might be most appropriate for routine clinical application (594).
The most common methods for detection of MCPyV in MCC include PCR amplification of MCPyV DNA from DNA isolated from MCC tumors or immunohistochemistry staining for MCPyV LT using monoclonal antibodies CM2B4 and Ab3 (584,595).
The use of gene sequencing in recent studies has made it possible to characterize the genomic background of association-based MCC subtypes with the viral status. Several series have shown that MCPyV-negative tumors have a high mutational load, with the distinctive UV

radiation damage signature (CC> TT substitution), and more frequent mutations in oncogenic pathways such as p53 and RB as compared to the positive MCPyV counterpart (594,596).

Despite the significant differences in the tumor mutational burden between MCPyV-positive and MCPyV-negative MCC, there were few phenotypic differences in the two types of MCC. Based on histopathological features alone, two subtypes of MCC can be recognized: pure neuroendocrine tumors and combined tumors with neuroendocrine and divergent (mainly squamous) differentiation. Most pure tumors are MCPyV-positive and CK20-positive while combined tumors are uniformly MCPyV-negative and occasionally CK-20 negative (597,598). However, virus-negative MCC can also present as pure neuroendocrine-type MCC (599).

While genomic sequencing has revealed that virus-negative MCC has evidence for a high degree of UV damage, this does not exclude a role for UV exposure in the development of virus-positive MCC. The relative lack of UV damaged DNA in virus-positive MCC indicates that the etiologies are clearly different, suggesting that the precursor to virus-negative MCC was a recipient of lifelong intense UV exposure while the virus-positive MCC were not exposed to sunlight for the same degree or for as long. It was reported that the early promoter of MCPyV responds to UV exposure and that levels of small T antigen mRNA increased in UV exposed skin from a healthy human volunteer (600). Transient UV exposure could affect the immune response to virus-negative and virus-positive MCC etiology. The effect of UV radiation in the pathogenesis of MCC has been suggested to be more likely a result of immune modulation rather than direct effects on DNA itself (601).

Genetic landscape

With the advent of next-generation sequencing, the mutational profile of MCC has emerged. MCPyV-positive and MCPyV-negative MCC's have displayed unique mutational profiles. For MCPyV-negative patients, NGS and whole exome sequencing have revealed a high tumor mutational burden, with recurrent mutations in *TP53* and *RB1*. On the other hand, for MCPyV-positive patients a particularly low TMB has been noted, without a pattern of recurrent mutations (602–604).

In fact, the aforementioned data allowed genomic mapping to identify two distinct patterns of genomic alterations that support the theory of two different etiologies underlying MCPyV positive and MCPyV negative cases. However, MCC appears to exhibit dysregulation in common cell signaling pathways, regardless of viral status. The somatic mutations in the negative virus cases could, in fact, mimic the effects of viral oncoproteins. For example, Rb is inhibited by the LT antigen in virus cases positive and presents inactivating mutations in negative cases, converging genotypically in a G1 / S checkpoint dysregulation in both subtypes. Recently González-Vela et al evaluated transduction pathways in 48 cases potentially involved in MCC tumor development using genomic and immunohistochemical approach. In spite of the already highlighted important gene differences, both subgroups share the accumulation of factors of transcription such as NFAT, (activated T cell nuclear factor) / PCREB (protein phosphorylated ligand CRE) and P-STAT (activator of transcription-3 and transducer of the

signal). This evidence suggests a common deregulation of the pathogenetic mechanisms as a potential treatment target (596,603,604).

Moreover, mutations affecting *PIK3CA* and deregulated PI3K-mTOR activity have been observed in patient samples and cell lines (591,605), and alterations in NOTCH and RAS/mitogen-activated protein kinase signaling pathways (522) have been detected in MCCs. Although *TP53* and *RB1* rank as the 2 most common mutations in both subsets, the UV-driven subset harbors mutations in genes such as *KMT2C/D, FAT1*, and *LRP1B* at high frequency, akin to cutaneous squamous cell carcinoma (606–610). This may imply that MCPyV genes confer the same oncogenic properties as the suite of mutations enriched in the UV-driven subset. Conversely, the frequency of *PTEN* alterations is similar across both subsets, suggesting a common requirement for alterations in this key pathway.
However, these advances are not yet used to diagnose or treat the disease. Current treatment options mainly rely on surgical excision combined with loco-regional adjuvant radiation (611).

Main molecular features of Merkel cell carcinomas according to MCPyV status are presented in **Figure 3**, source (612).

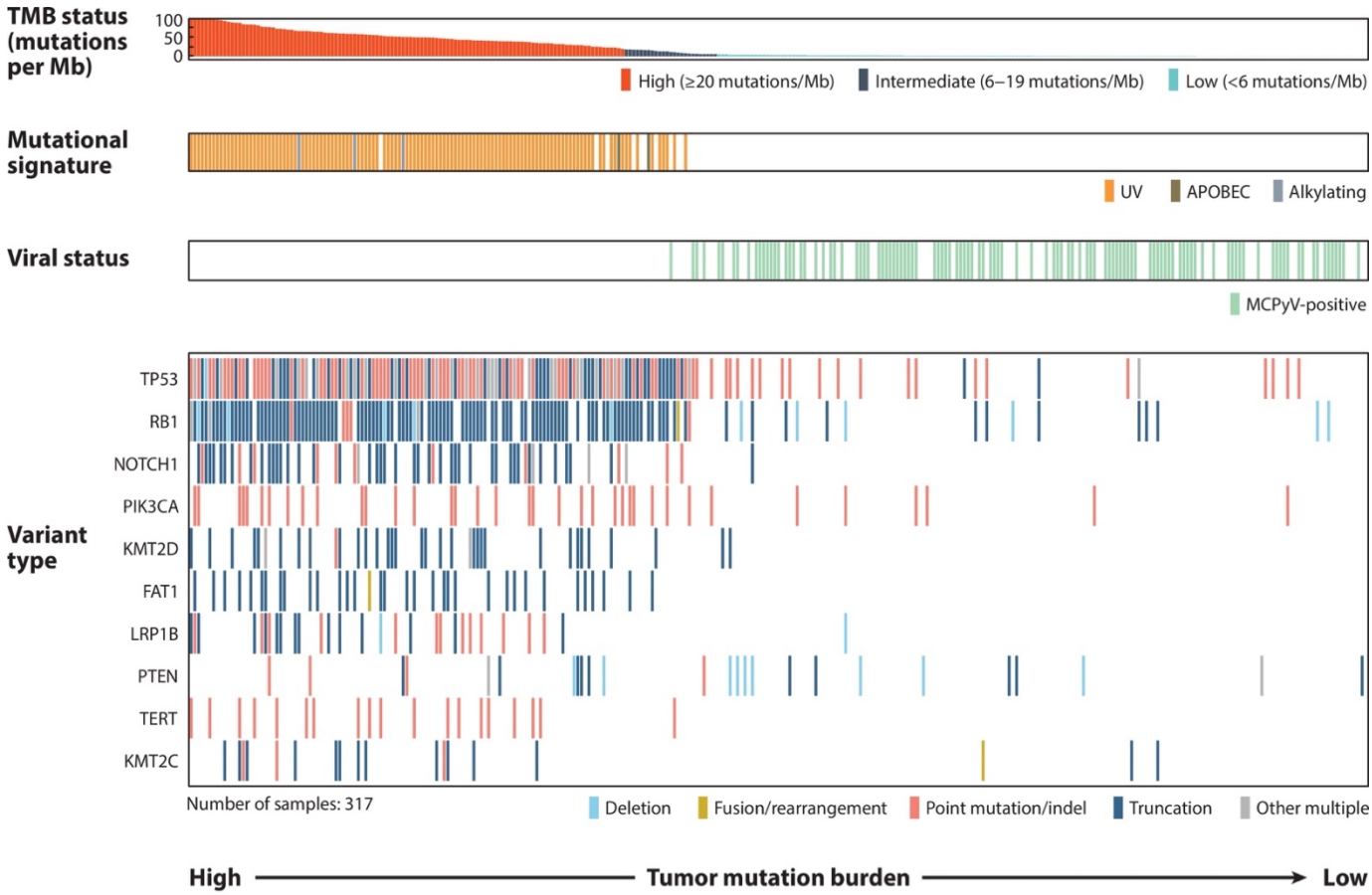

Figure 3. *Molecular subtypes of MCC, showing an oncoprint of co-occurrence of TMB status, dominant mutational signature, viral status, and most commonly altered genes demonstrating mutual exclusivity of MCPyV, APOBEC integration, and UV damage. Each column corresponds to one unique MCC tumor. Tumors are sorted in descending order by TMB from the left. Abbreviations: Mb, megabase; MCC, Merkel cell carcinoma; MCPyV, Merkel cell polyomavirus; TMB, tumor mutational burden.*

Treatment

The choice of treatment depends on certain characteristics of the disease, including its stage (with particular reference to the location of the primary tumor), the involvement of regional lymph nodes, comorbidities and patient clinical status (613). While the guidelines have defined the management of loco-regional disease, so far there was no consensus on therapeutic strategies in advanced disease.

Surgery

Surgery has typically been the first-line treatment for patients with locoregional primary MCC. However, just how much of the surrounding normal-appearing skin should be excised around the tumor during surgery is still controversial (521,614). Complete surgical excision, with the goal of establishing clear margins, is the mainstay to treat local MCC. Although surgical margins have not yet been defined, a wide excision with 1 to 3 cm of clinically free margins is generally recommended, regardless of tumor size (615). A correlation between margin size and the recurrence risk has not been established, with some studies suggesting that wide margins of 2–3 cm are associated with a reduction of recurrence risk (616–618) and others showing no difference in recurrence risk with margins that are > 1 cm (619). According to the current National Comprehensive Cancer Network (NCCN) guidelines, for local disease excision should be done with margins of 1–2 cm and down to the fascia or periosteum. Patients with lymph node involvement should be dissected and subsequently treated by radiotherapy (RT). In clinically negative lymph node disease, the sentinel lymph node exploration is widely recommended together with the operation of the primary surgery. If positive, patients should be candidates a lymphadenectomy and / or RT.
In a recently published retrospective trial (620), 188 stage I–II MCCs were analyzed. A total of 48 patients were treated with surgery alone and, among them, 35 had narrow margins (≤1 cm) while 13 had margin > 1 cm. In the first group of patients, 7 (20%) developed local recurrence, while in the second group, 0 patients developed local recurrence. A group of patients underwent surgery plus RT: this group tended to present higher-aggressiveness tumors or a higher-risk profile (e.g., immunosuppressed) but had less local recurrence than those who were treated with surgery alone (1% vs. 15%), regardless of surgical margins.

Radiotherapy

Merkel cell carcinoma is a radiosensitive tumor (621), and RT should be considered either as adjuvant treatment to surgery or as palliative treatment for inoperable cases of MCC. In some studies, adjuvant RT was recommended for patients with loco-regional tumor in order to reduce the recurrence rate, although the impact on the overall survival is still unclear (622–624). However, the outcomes of radiation monotherapy may be inferior to those of complete surgical resection (621,622,625). There are few published studies reporting the outcomes of RT and its effects on MCC relapse and disease-specific survival. A retrospective study of 57 inoperable

patients treated with localized RT reported an overall survival rate at 5 years of 39% (624); similar results have been reported in a retrospective study involving 43 patients in which an overall survival rate of 37% was reported (622). The NCCN guidelines recommend doses of 60–66 Gy for curative-intent radiation, with a wide treatment margin (5 cm) around the primary site (626). Radiation doses to the primary site after surgical resection should range from 50 to 60 Gy depending on the presence or absence of microscopically positive margins (521,626).

Chemotherapy

Although cytotoxic chemotherapy has been commonly used to treat patients with advanced MCC, its role remains unclear in the literature; responses are rarely durable, and few studies have shown a survival benefit. The most common regimens recommended in the NCCN guidelines are carboplatin (or cisplatin) and etoposide or a combination of cyclophosphamide, doxorubicin (or epirubicin) and vincristine. MCC is very sensitive to chemotherapy (627–630), and initial response rates range from 53 to 76%; however, this high response rate is not durable, and tumors often recur within 4–15 months. A retrospective study of 6908 patients found that chemotherapy was not associated with an overall survival benefit in patients who presented with either local or nodal MCC (631).

Immunotherapy

As described above, Merkel cell polyomavirus-encoded T-antigens are constitutively expressed in MCV-positive MCC malignancies (632). They are therefore attractive targets for TCR-based immunotherapy. The fact that immune-suppressed individuals are more likely to develop MCC indicates that host immune responses play an important role in preventing MCC tumorigenesis (523). This notion is supported by the higher rate of spontaneous regression than expected (12 in 400–700 cases or 1.7–3.0%) (633,634). Studies of regressing tumors demonstrated infiltration by $CD4^+$ and $CD8^+$ T cells suggesting that T-cell-mediated immunity plays a key role in tumor regression. Additionally, high intratumoral $CD8^+$ and $CD4^+$ lymphocyte infiltration predicts better survival (635,636). Although over 90% of the MCC patients are immune competent, they fail to clear MCC tumors that express non-self Merkel cell polyomavirus antigens. These observations suggest that Merkel cell polyomavirus-induced MCCs are capable of escaping immune surveillance.

However, not only T-cells play a role in the prognosis of MCC. Antibodies against MCPyV T antigens produced by B-cells correlate with disease burden and MCC recurrence (637). Anti-MCPyV T antibody titers decrease after successful treatment and upon recurrence they increase again. For these reasons, anti-MCPyV T antibody titer is used to monitor patients after MCC treatment. Unfortunately, seropositivity for MCPyV cannot be used for MCC screening or to distinguish MCPyV-positive from MCPyV-negative patients due to the high seropositivity levels in the healthy population.

As described above, the cancer evolves with strategies to suppress or evade the immune system, which conceal or protect the tumour cells from the immune cells. One example is the down-regulation of the expression of MHC I molecules on the surface of MCC cells (638). Another mechanism is the creation of an immune suppressive tumour micro-environment with the help of suppressive cytokines and chemokines such as TGF-β or IL-10 (639,640). Otherwise, an up-regulation of checkpoint proteins on the surface of T-cells, such as programmed cell death protein 1 (PD-1) (641) or cytotoxic T lymphocyte associated protein 4 (CTLA-4) (601), is detected. PD-L1 has been shown to be up-regulated in tumour cells and immune cells in the tumour microenvironment of MCC patients with a better overall survival, if PD-L1 is overexpressed (642,643)This suggests that these checkpoints are a good target for immunotherapy using checkpoint inhibitors, which is discussed below.

Pembrolizumab was the first immune checkpoint inhibitor to demonstrate objective tumor regressions in patients with MCC (644). In a phase 2, single-arm, multicenter study (ClinicalTrials.gov number NCT02267603), patients with advanced MCC who had not previously received systemic therapy were treated with pembrolizumab 2 mg/kg every three weeks for a maximum of two years or until disease progression, dose-limiting toxicity, or complete response. Out of 26 patients, 4 experienced a complete response (CR) and 10 had a partial response (PR), for an objective response rate (ORR) of 56%. At 6 months, the progression-free survival rate was 67% and the duration of response ranged from 2.2 months to at least 9.7 months. 86% of responses were ongoing at last follow-up. These results prompted the addition of pembrolizumab for the treatment of disseminated MCC to the National Comprehensive Cancer Network (NCCN) guidelines (615). Interestingly, objective regression was observed in both virus-positive and virus-negative tumors. PD-L1 expression did not seem to correlate with a higher likelihood of response to treatment as it has in other tumors (645). Until today, no predictive factors for anti-PD-L1/PD-1 therapy are accepted, although tumor PD-L1 expression, virus status, and some other factors may correlate.

The last update of this trial has been recently published and represents the longest observation of a cohort of patients treated with first-line anti-PD-1, with a median follow-up of 31.8 months (646). The ORR was 58%, with 15 patients achieving CR and 14 patients PR; median duration of response (DOR) was not reached. The majority of responses (90%) developed during the first 12 weeks from the start of treatment and after 3 years of observation 72.7% of responders maintained the response. Median progression-free survival (PFS) was 16.8 months and estimated 3-year PFS was 39.1%; median OS was not reached at the time of the analysis, while estimated 3-year OS was 59.4%. When considering only the cohort of responders, 3-year estimated OS reached 89.5%, suggesting that ORR could be considered as an early predictor of overall survival. Tumor PD-L1 expression (PD-L1 negative versus PD-L1 positive) seems to correlate with efficacy of immunotherapy, in line with results observed in other tumor types. However, no definite conclusions have been drawn (647).

Furthermore, cabozantinib is a multiple-kinase inhibitor, including c-MET and VEGFR-2, commonly used in the treatment of several metastatic solid cancer. Cabozantinib (648) was evaluated in a prospective phase II trial (NCT02036476) that enrolled eight metastatic or locally advanced platinum-resistant MCC patients. The trial was closed

prematurely due to poor tolerability and lack of activity of the study drug, which obtained a median PFS of 2.1 months and a median OS of 11.2 months. Notably, patients were not selected based on the presence of any mutation.

Somatostatin analogues (SSAs) are commonly used in low- and medium-grade NETs, but several studies support their possible use in MCC therapy. Lanreotide has been evaluated in a phase II study (NCT02351128) on 35 patients (649). Among them, seven (20%) obtained a disease control form more than 3 months. Pasireotide had also been evaluated among melanoma and MCC patients in a phase I trial (NCT01652547). However, no data are available for the MCC cohort (650). In a recently published retrospective trial (651), 40 patients were evaluated for somatostatin receptor (SRS) expression. A total of 33 patients (85%) had some degree of SRS uptake, and 19 patients were treated with SSAs. Among them, seven had a response-evaluable target lesion and three (43%) experienced disease control, with a median PFS of 237 days. The major limit of this study is the confounding effect induced by radiotherapy, which made several lesions not radiologically evaluable according to RECIST. Interestingly, the degree of SRS expression did not correlate significantly with the efficacy endpoints.

Combining targeted therapy and immunotherapy is known to be an interesting and promising strategy in several solid tumors (652,653). In MCC, a number of clinical trials are ongoing to assess such combination strategy. Combination between domatinostat and immunotherapy (pembrolizumab) has been subsequently evaluated in a phase II trial (654) that assessed the safety of this combination and the potentially ability of domatinostat to increase the antitumor activity of pembrolizumab.

Project 5: Engineering target CAR-Ts as a potential treatment of Merkel cell carcinoma

ABSTRACT

Merkel cell carcinoma (MCC) is a rare and aggressive skin cancer with a neuroendocrine phenotype and limited treatment options.

In the present study we aimed to (i) explore ALK and Merkel cell polyomavirus (MCPyV) immunoexpression in a retrospective series of MCC human tissue samples obtained from the pathology files of Città della Salute e della Scienza Hospital, Torino, Italy; (ii) investigate ALK, GD2 expression levels in MCC cell lines and assess *in vitro* their therapeutic potential by engineering ALK- and GD2.CAR-T cells; (iii) investigate major histocompatibility complex (MHC)-class I antigens - HLA-ABC expression levels in MCC cell lines; (iv) explore the effect of ALK inhibitors, lorlatinib and ceritinib, in MCC cell lines ; (iv) develop a MCC metastatic model using NOD/SCID/IL2Rγ−/− (NSG) mice.

We observed positive ALK immunoreaction in 135/155 (87.1%) MCCs, while 20/155 (12.9%) were ALK negative. MCPyV-positive status was seen in 105/155 (67.7%) cases. There was a significant correlation between ALK immunoexpression and MCPyV status, being majority of ALK positive cases also positive for MCPyV staining (p=0.0001).

MCC cell lines, WAGA and MKL1 were ALK positive, while MCC26 showed absence of ALK and were selected as test and negative control cell lines, respectively. Furthermore, all 3 cell lines showed low GD2 expression levels, as determined by flow cytometry. Regarding HLA class-I surface expression WAGA and MKL1 showed low to no expression, respectively, while MCC26 demonstrated high expression.

ALK.CAR-Ts efficiently eliminated most of the MKL1 and WAGA cells at the T cell to tumor cell ratio of 1:1, with or without the combination with lorlatinib. At higher T cell to tumor cell ratios, namely 1:5 and 1:10, variable killing effect was observed. No ALK.CAR-T killing was observed in MCC26. There was a modest killing activity observed in case of GD2.CAR.Ts across cell lines at ratio 1:1, in line with low GD2-expression levels, with or without combination with lorlatinib. This effect was not sustained at higher ratios. No effect of lorlatinib nor ceritinib on ALK pathway was observed, suggesting that ALK is expressed but likely not active in MCC cell lines. Finally, we developed a metastatic mouse model that will serve as a base of future experiments regarding ALK.CAR-T antitumor activity in vivo.

In conclusion, to the best of our knowledge, this is the first study to explore the potential therapeutic use of ALK- and GD2.CAR-Ts in MCC cell lines. Overall, our study has revealed several insights into the molecular background of MCCs, identifying specific alterations of immunity and tumor microenvironment that favor tumor escape, and that might be useful when developing novel treatment options for these patients.

SPECIFIC BACKGROUND

Merkel cell carcinoma (MCC) is a rare and aggressive form of skin cancer, which occurs more frequently in elderly patients and immunosuppressed (523). It is associated with a high rate of mortality and reduced over-all survival (655).
So far, there are limited treatment options for this rare tumor. In fact, despite being considered a chemosensitive neoplasm, the current use of cytotoxic therapies rarely allows lasting responses, with a median progression free survival of only 3 months, and it is burdened with significant toxicity, suggesting the need for alternative treatment options (656,657).

Oncogenesis and exact histogenesis have historically been poorly understood. However, evidence supporting the role of immunosurveillance in MCC has led the detection of the Merkel cell polyomavirus (MCPyV) in 2008, in approximately 80% the cases (565). The discovery of the integration of the viral genome into the host genome and the role of the virus in MCC tumorigenesis and more recent description of UV-induced mutations in MCPyV-negative cases have given great boost to knowledge on viral and molecular oncogenic mechanisms.

Virus-associated and MCPyV-negative MCCs possess distinct clinical and molecular characteristics, but to date there are no conclusive data on the clinical and therapeutic impact of these two distinctive groups (612). A recent publication indicated that the viral status can be used as a prognostic marker, and that MCPyV+ tumours are associated with a better overall survival, as well as recurrence free survival (658).
Nevertheless, it is known that MCPyV-negative MCCs are associated with a high tumour mutational burden, which could be useful for immunotherapy as more tumour neo-antigens can be used as targets (603). The MCPyV-negative MCC also shows a typically UV-mutational signature. In comparison to the non-viral MCC, the viral MCC does not have this UV-mutational signature and a low TMB (610).

In recent years, immune checkpoint inhibitors (ICIs) became one of the most promising immunotherapeutic type of drugs. So far, around 50% of MCC patients benefit from the development of ICIs, and their use is now approved as standard of care for metastatic MCC (659). Nghiem et al. showed that MCC patients without any previous treatment, receiving 2 mg/kg Pembrolizumab every three weeks, had an objective response rate of 56%. The progression free-survival rate at 6 months was 67%. However, 15% of patients showed grade 3 or 4 adverse events (myocarditis and elevated levels of aminotransferase). In general, the trial showed that Pembrolizumab as a first-line treatment in MCC patients is working and is only associated with adverse side effects in some patients (644). Even though the response rates of ICIs are quite good in MCC, still 50% of patients do not respond to the treatment. Reasons for resistance are manifold and all prevent an effective interaction of T-cells and tumour cells: if a patient has a priori no MCC-specific T-cells, a release of the inhibitory breaks cannot create a T-cell activity against the tumour (660,661).

Notably, intratumoral infiltration of $CD8^+$ T cells is associated with an improved prognosis (636). Unfortunately, strong intratumoral $CD8^+$ T-cell infiltration is a sporadic event in MCC, being present in only 5% of tumors (662). Lack of T-cell infiltration may reflect different immune escape strategies utilized by MCC cells such as inhibition of cellular immune

responses via PD1/PD-L1 signaling (601,643), and/or defects in classical human leukocyte antigens (HLA) class-I antigen expression (638). Similar to the observations in other virus-associated cancers.

The major histocompatibility complex class I (MHC-I) proteins in humans are termed as HLA-I and they are divided into classical and non-classical HLA-I subtypes (663). Classical type I HLA molecules (HLA-A, HLA-B, and HLA-C) function to present cellular antigens to T cells and are essential for immunosurveillance and cancer immunotherapy. It is now clear that loss of HLA-I function is an important escape mechanism for tumors from immunotherapy, by a variety of mechanisms (664–666). In fact, HLA class-I downregulation is an immune escape mechanism present in the majority of MCC tumors (636,667,668). Reduction of HLA class-I surface expression readily explains MCC's resistance to PD-1/PD-L1 blockade, as adaptive T-cell responses critically depend on MHC class-I-restricted antigen presentation (669).

Merkel cell polyomavirus-encoded T-antigens are constitutively expressed in MCV-positive MCC malignancies (632). They are therefore attractive targets for T cell receptors-based immunotherapy (670). Given the role of MCPyV in driving MCC carcinogenesis and the fact that immune-suppressed individuals are more likely to develop MCC indicates that host immune responses play an important role in preventing MCC tumorigenesis, a future treatment approach may involve administration of genetically modified Chimeric antigen receptor (CAR) T-cell therapy against MCPyV antigens (523).

Anaplastic lymphoma kinase (ALK) is a transmembrane receptor tyrosine kinase that belongs to the insulin receptor superfamily (671). Transforming rearrangements of the ALK gene have been reported in human hematologic and solid malignancies including anaplastic large-cell lymphoma, myofibrobalstic tumors as well as NSCLC, suggesting that ALK-mediated signaling might play a part in the development or progression of these tumors (672–674). Recently, ALK tumor expression, at both protein and RNA level, and its correlation with viral status as well as a longer survival was reported in MCC (675,676). However, despite in-depth analysis, no activating ALK mutations or fusion genes involving ALK have been discovered (675,677). A high ALK expression without an activating mutation or fusion of the *ALK* gene is also observed in Hepatocellular carcinoma (HCC) and it is correlated to presence of Hepatitis C Virus infection and earlier development of metastasis and lower survival (678). In addition to HCC, ALK overexpression or phosphorylation is linked to unfavorable course of disease also in inflammatory breast cancer (679) as well as neuroblastoma, where ALK phosphorylation is linked to activating mutations of the *ALK* gene (680). The positive effect of ALK inhibition in HCC *in vitro* was recently demonstrated by Yu and Zhao (681). Two approved inhibitors crizotinib and ceritinib suppressed the proliferation of HCC cell lines and inhibited the ALK phosphorylation; moreover, ceritinib treatment induced cell apoptosis (681). Therefore, it seems that in HCC ALK inhibition is beneficial, even though the mechanism of ALK activation is still unknown (682). Of note, Lorlatinib (Pfizer) is a novel third-generation ALK inhibitor, more potent than second-generation inhibitors having the broadest coverage of

ALK resistance mutations that have been identified (683–685). Lorlatinib was designed to cross the blood–brain barrier in order to achieve high exposures in the CNS (686,687). In phase 1 and 2 studies, lorlatinib had potent antitumor activity after the failure of previous ALK inhibitors (first-generation, second-generation, or both) (686,688). Because of its efficacy and safety, lorlatinib is a standard treatment option for *ALK*-positive patients in whom one or more ALK inhibitors have failed.

AIM

Considering this complex background the aim of the present study was to (i) explore ALK and Merkel cell polyomavirus (MCPyV) immunoexpression in a retrospective series of MCC human tissue samples obtained from the pathology files of Città della Salute e della Scienza Hospital, Torino, Italy; (ii) investigate ALK, GD2 expression levels in MCC cell lines and assess *in vitro* their therapeutic potential by engineering ALK- and GD2.CAR-T cells; (iii) investigate major histocompatibility complex (MHC)-class I antigens - HLA-ABC expression levels in MCC cell lines; (iv) explore the effect of ALK inhibitors, lorlatinib and ceritinib, in MCC cell lines ; (iv) develop a MCC metastatic model using NOD/SCID/IL2Rγ−/− (NSG) mice.

MATERIALS AND METHODS

Merkel cell carcinoma human tissue samples.

We selected 155 formalin-fixed and paraffin-embedded MCCs, obtained from the pathology files of the University of Turin (Città della Salute e della Scienza Hospital, Torino, Italy). These included 117 primitive skin and 38 extra-cutaneous tumors (35 lymph nodal and 3 visceral neoplasms). Available routinely stained hematoxylin and eosin (H&E) tumor slides were re-evaluated to select a representative block. MCPyV status was obtained from pathological charts. In case of absence of data, the IHC analyses was performed (see below). Before the study started, all cases were deidentified and coded by a pathology staff member not involved in the study, and all data were accessed anonymously.

Immunohistochemical analyses.

Four-µm-thick sections were cut from a representative FFPE tissue block of each case, collected onto charged slides and submitted to IHC testing. The IHC assessment was performed by an automated platform (Ventana BenchMark AutoStainer, Ventana Medical Systems, Tucson, AZ, USA) with the following primary antibodies: ALK (Rabbit Monoclonal Primary Antibody, clone D5F3, pre-diluted; Roche Diagnostics, Inc., Tucson, AZ, USA) and MCPyV large T-antigen (Mouse Monoclonal Antibody, clone CM2B4, diluted 1:50; Santa Cruz Biotechnology, Inc., Dallas, Texas, USA). Appropriate positive and negative controls were included for each IHC run.

Regarding ALK expression, the reaction was considered negative when staining was observed in < 1% of tumor cells; 1+ score was assigned to cases demonstrating very weak to moderate staining intensity in < 25% of tumor cells and were considered as low immunopositivity; 2+ score was given in case of weak to moderate staining intensity in > 25% of tumor cells, or when strong staining intensity was observed in < 25% of tumor cells and were considered as moderate immunopositivity; 3+ score was assigned to cases showing strong staining intensity in > 25% of tumor cells and were considered as strong immunopositive cases.
MCPyV status was interpreted according to Moshiri et al. (594); cases were considered negative when weak staining was observed in < 1% of tumor cells.

Cell Lines and Cell Culture.

Human MCC cell lines MCC26, MCC13, MKL1, WAGA, and UISO were purchased from American Type Culture Collection (ATCC). Human neuroblastoma cell lines, Kelly, NB1, SHSY5Y, IMR32, SKNFI and SKNSH were purchased from American Type Culture Collection (ATCC) and served as a control in different experiments. All cell lines were maintained in RPMI 1640 (Corning) supplemented with 10% fetal bovine serum (FBS) (Gibco), 100 U/mL of penicillin, 100 µg/mL of streptomycin (Corning), and 2 mM of L-glutamine (Corning). Cells were maintained at 37°C in humidified atmosphere with 5% CO_2. MCC cell lines were transduced with a retroviral vector encoding the GFP-Firefly-Luciferase (GFP-FFluc) gene. All cell lines were mycoplasma free. Lorlatinib was obtained from Pfizer. Ceritinib (LDK378) was obtained from Selleckchem.

Western Blot.

Whole-cell extracts were obtained using GST-FISH buffer (10 mM MgCl2, 150 mM NaCl, 1% NP-40, 2% Glycerol, 1 mM EDTA, 25 mM HEPES pH 7.5) supplemented with Protease Inhibitor Cocktail (Roche), 1 mM phenylmethanesulfonylfluoride (PMSF), 10 mM NaF and 1 mM Na3VO4. Extracts were cleared by centrifugation at 15,000 rpm for 20 min. The supernatants were collected and assayed for protein concentration using BCA protein assay method (Sigma). Equal amounts of protein lysates were resolved by Criterion gels (BIO-RAD), transferred on nitrocellulose membrane (GE Healthcare), and probed with the following primary antibodies: rabbit polyclonal β–actin (Sigma, #A5316), rabbit α-actinin (D6F6) XP (Cell Signaling Technology, #6487), rabbit ALK (D5F3) XP (Cell Signaling Technology, #3633), rabbit phospho-ALK (Tyr1604) (Cell Signaling Technology, #3341), rabbit phospho-Akt (Ser473) (Cell Signaling Technology, #9271), rabbit Akt (pan) (C67E7) (Cell Signaling Technology, #4691), rabbit phospho-STAT3 (Tyr705) (Cell Signaling Technology, #9131S), rabbit STAT3 (79D7) (Cell Signaling Technology, #4904S), rabbit phospho-p44/42 MAPK (Erk1/2) (Thr202/Tyr204) (Cell Signaling Technology, #9101) and rabbit p44/42 MAPK (Erk1/2) (Thr202/Tyr204) (D13.14.4E) XP (Cell Signaling Technology, #4695T). Membranes were developed with ECL solution (GE Healthcare).

CAR-T and Plasmid Construction.

The variable regions of the heavy and light chains of the ALK.1, ALK.2, ALK.3, ALK.4, ALK.5, ALK.6, and ALK.7 mAbs were obtained by Celldex Therapeutics and cloned as a scFv fragment into previously validated CAR formats that include the murine CD8α hinge and transmembrane domain, CD28 intracellular costimulatory domain, and CD3ζ intracellular signaling domain from a previous validation in mice T cells (data not show).
The ALK.CAR cassettes were cloned into the retroviral vector SFG. For the human version of the ALK.CAR used in this project, murine CD8α, CD28, and CD3ζ were replaced by human CD8α, CD28, and CD3ζ, and the ALK scFv was modified to generate a humanized version (ALK.CAR) (689). Since Merkel carcinoma cells do not express CD19, we used human CD19.CAR-Ts (690) as negative control. After exploring GD2 expression levels in MCC cell lines, we also explored the effect of GD2.CAR-Ts. All three constructs were based on the same CAR expressing the human CD28 costimulatory endodomain. The scFv specific for CD19 and GD2 were previously reported (690,691).

Retrovirus Production for CAR-T Transduction.

For the preparation of retroviral supernatants used for the transduction of human T cells, 2×10^6 293T cells were seeded in 10 cm cell culture dish and transfected with the plasmid mixture of the retroviral vector, the Peg-Pam-e plasmid encoding MoMLV gag-pol, and the RDF plasmid encoding the RD114 envelope, using the GeneJuice transfection reagent (Merck Millipore), according to the manufacturer's instructions. Supernatants containing the retrovirus were collected 48 and 72 hours after transfection and filtered with 0.45 μm filters.

Transduction and Expansion of Human T Cells.

Apheresis leukoreduction collars from healthy donors were obtained from the Boston Children's Hospital Blood Donor Center, Boston, MA. On day 0, lymphocytes were isolated with Ficoll-Paque Plus density separation (GE Healthcare), T cells isolated with EasySep Human T Cell Isolation Kit (Stemcell) and activated with Dynabeads Human T-Activator CD3/CD28 (Gibco), according to the manufacturer's instructions. On day 2, T lymphocytes were transduced with retroviral supernatants using retronectin-coated plates (Takara Bio Inc., Shiga, Japan). Briefly, non-tissue culture treated 24-well plates are coated overnight with 7 μg/mL retronectin (500 μL/well) in the cold room, washed once with 1 mL medium, coated with 1 mL of the retroviral supernatant per well, and centrifuged at 2,000 g for 90 min. After removal of the supernatant, 5 x 105 activated T cells are plated and centrifuged at 1,000 g for 10 min. Three days later, T cells are collected and expanded in complete medium (45% RPMI-1640 and 45% Click's medium (Irvine Scientific), 10% FBS (Gibco), 2 mM GlutaMAX (Gibco), 100 unit/mL of penicillin and 100 μg/mL of streptomycin (Corning)) with rhIL-7 (10 ng/mL; PeproTech) and rhIL-15 (5 ng/mL; PeproTech), changing medium every 2-3 days. On day 12-14, cells are collected for in vitro and in vivo experiments. T cells were cultured in rhIL-7/IL-15 depleted medium for two days prior to being used in in vitro functional assays.

Co-culture Experiments with hCAR-T and Bioluminescence Imaging Analysis.

GFP-Firefly-Luciferase tumor cells were seeded in black 96-well plates at a concentration of 5 x 104 cells/well 24 hours before co-culture. T cells were added to the culture at different ratios (E:T of 1:1, 1:5, 1:10) without adding exogenous cytokines. Remaining luciferase activity was subsequently measured on day 3 by bioluminescence imaging using IVIS Spectrum in vivo imaging system (PerkinElmer). Percentage residual tumor cells was calculated by the following equation: Percentage = [(target cells total flux [p/s] / (target cells only total flux [p/s])] × 100.

Flow Cytometry.

We performed flow cytometry with following antibodies: anti-human disialoganglioside GD2, Clone 14.G2a, Alexa Fluor® 647 (RUO) (562096, BD Pharmigen) and anti-human HLA-ABC-PE, Clone W6/32, Alexa Fluor® 700 (RUO) (Biolegend, 307604) according to the manufacturer's instructions. Samples were acquired with BD FACSCelesta flow cytometer using the BD Diva software (BD Biosciences). A minimum of 10,000 events were acquired for each sample, and data were analyzed using FlowJo 10.

In Vivo Mouse Studies.

Female 6 - 8 weeks old NOD/SCID/IL2Rγ−/− (Strain #:005557, NSG) mice were purchased from Jackson Laboratories. All the mice were housed in the Animal Core Facility at Boston Children's Hospital. All mouse experiments were performed under protocols approved by the Institutional Animal Care and Use Committee (IACUC) of Boston Children's Hospital.

Merkel Cell Carcinoma Metastatic Models.

Six - eight weeks old female NSG mice were injected i.v. with the tumor cell lines FFluc-MKL1 (2×10^6 cells/mouse) and FFluc-Waga (2×10^6 cells/mouse). Tumor growth was monitored by bioluminescence imaging using IVIS Spectrum *in vivo* imaging system (PerkinElmer). Animals were imaged 10 minutes after Luciferin injection to ensure consistent photon flux. Mice were euthanized when the investigators detected signs of discomfort or as recommended by the veterinarian.

Quantification and Statistical Analysis.

The two-tailed unpaired or paired t-test were used to measure differences between two groups. One-way ANOVA and Tukey post hoc tests were used for multiple group comparisons. P value < 0.05 indicates a significant difference (*$P < 0.05$, **$P < 0.01$, ***$P < 0.001$, ****$P < 0.0001$). Graph generation and statistical analyses were performed using the GraphPad Prism v8 software (GraphPad Software Inc.).

RESULTS

Expression of ALK in Merkel cell carcinoma in human tissues and correlation with polyoma virus

We observed the positive immunoreaction in 135/155 (87.1%) MCCs, while 20/155 (12.9%) showed absence of staining (**Figure 1**). In detail, 33 cases (21.3%) showing ALK positive immunoexpression were labeled as low, 42 (27.1%) as moderate and 60 (38.7%) as high ALK-positive cases (**Figure 2**).

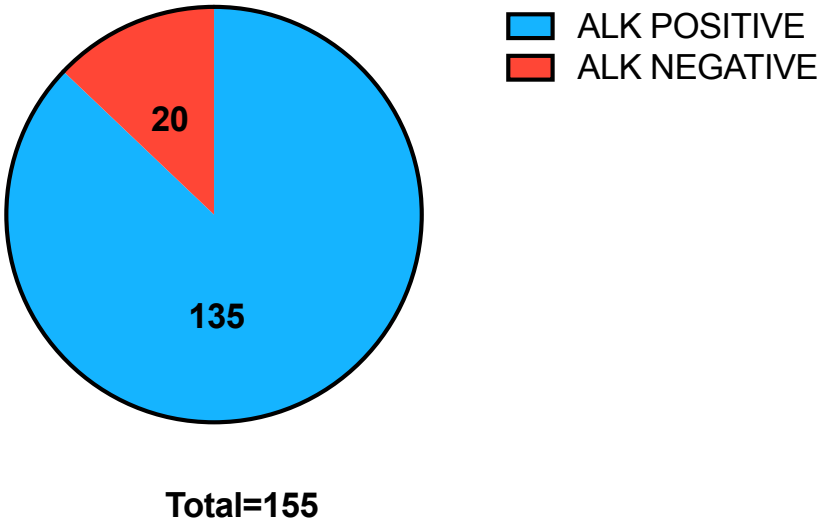

***Figure 1**. ALK immunoexpression in human samples of Merkel cell carcinomas.*

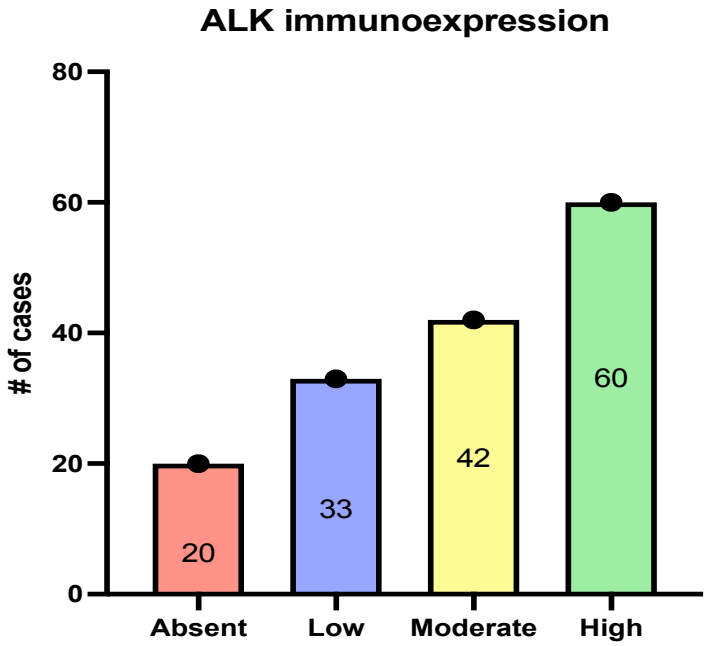

***Figure 2**. ALK immunoexpression according to different categories, namely, absence of staining, low, moderate, and high.*

We found 105/155 (67.7%) MCPyV-positive samples, while 50/155 (32.3%) were MCPyV-negtive. Furthermore, there was a positive correlation between ALK immunoexpression and MCPyV status, being majority of ALK positive cases also positive for MCPyV staining (p=0.0001) (**Figure 3**).

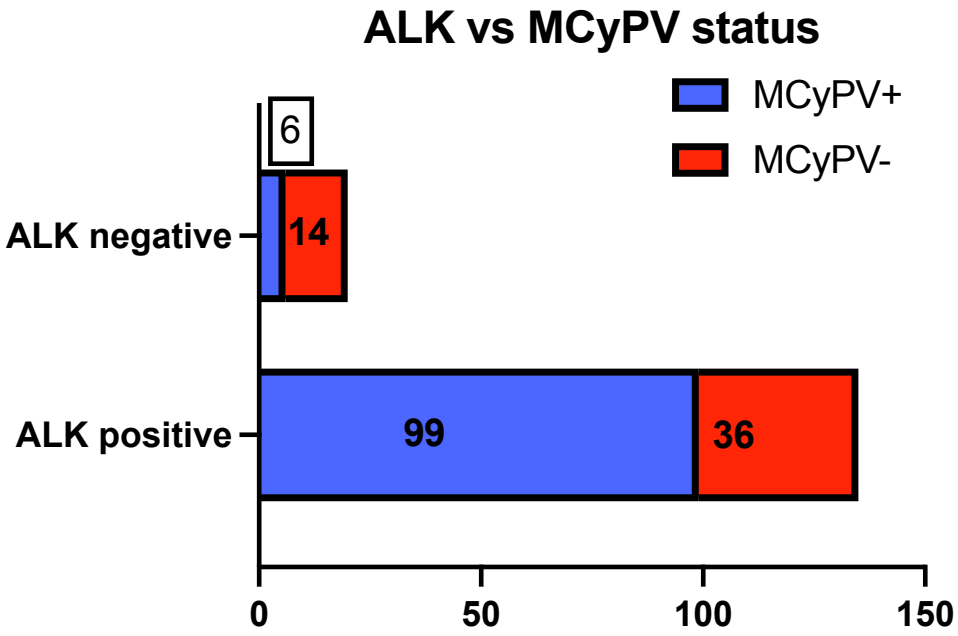

Figure 3. *Graph representing positive correlation between ALK and MCyPV status.*

ALK pathway in Merkel cell carcinoma cell lines

The expression of proteins, namely, ALK, ERK and STAT3 and their phosphorylated forms were determined by means of Western blot analyses. The expression levels are shown in **Figure 4**. Specifically, ALK expression was found in MKL-1 and WAGA cell lines, while MCC26, MCC13, and UISO did not show ALK expression. The phosphorylated form of ALK was not found in any of these cell lines. All cell lines showed high levels of expression of STAT3, phosphorylated form of STAT3 and ERK. Regarding phosphorylated form of ERK, UISO was the cell line demonstrating complete absence, WAGA very low expression, while the remaining cell lines (MCC26, MCC13 and UISO) were showing relatively high expression. Kelly, SHSY5Y and NB1 served as control cell lines.

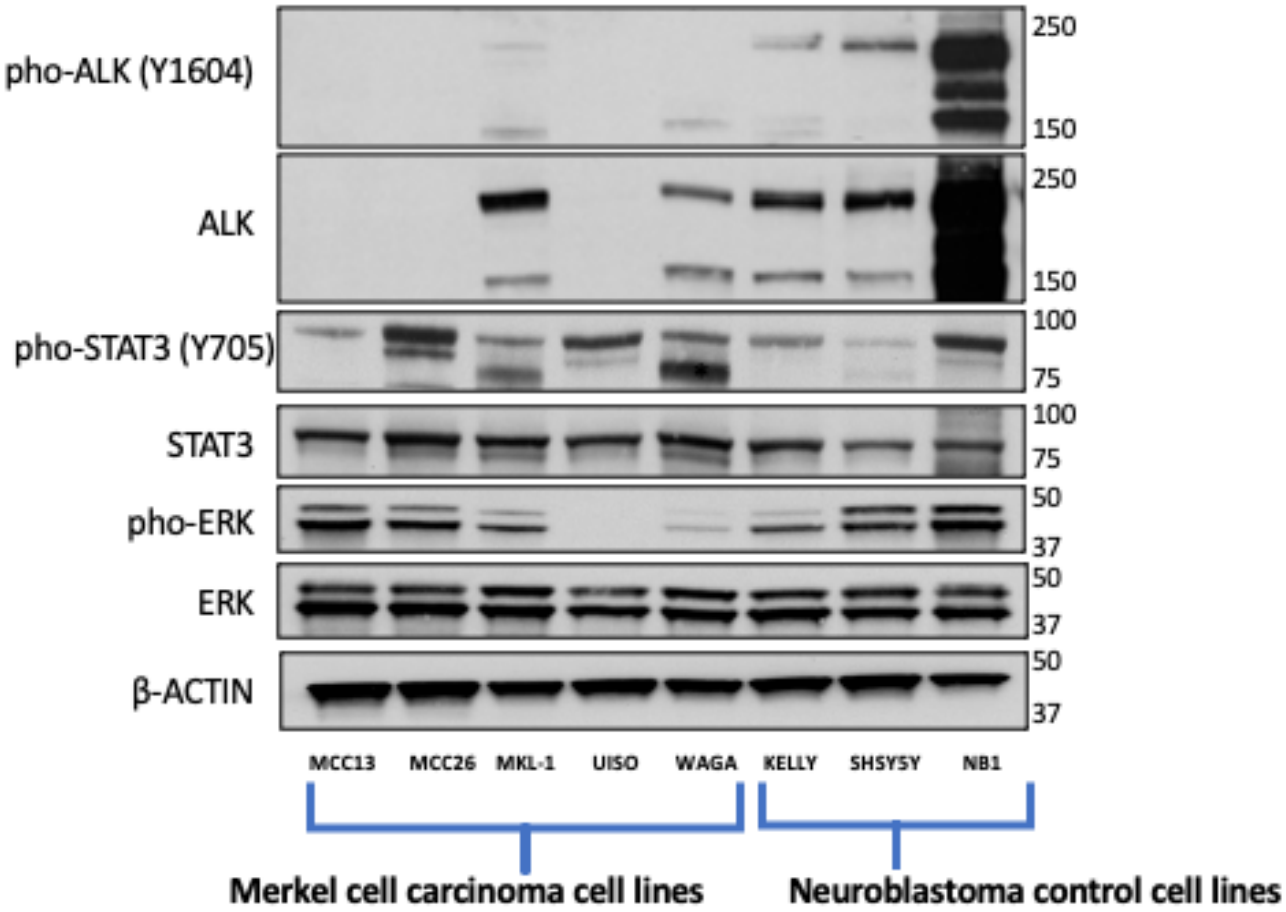

Figure 4. *Western blot analyses of ALK pathway.*

Immunohistochemical analysis of ALK in Merkel cell carcinoma cell lines

The expression of ALK in cell lines was also confirmed by means of immunohistochemical analyses. MKL1 and WAGA showed homogenous and intense immunoexpression in virtually all cells. MCC26 and MCC13 demonstrated complete absence of staining, while rare positive cells were found in UISO cell line (**Figure 5**).

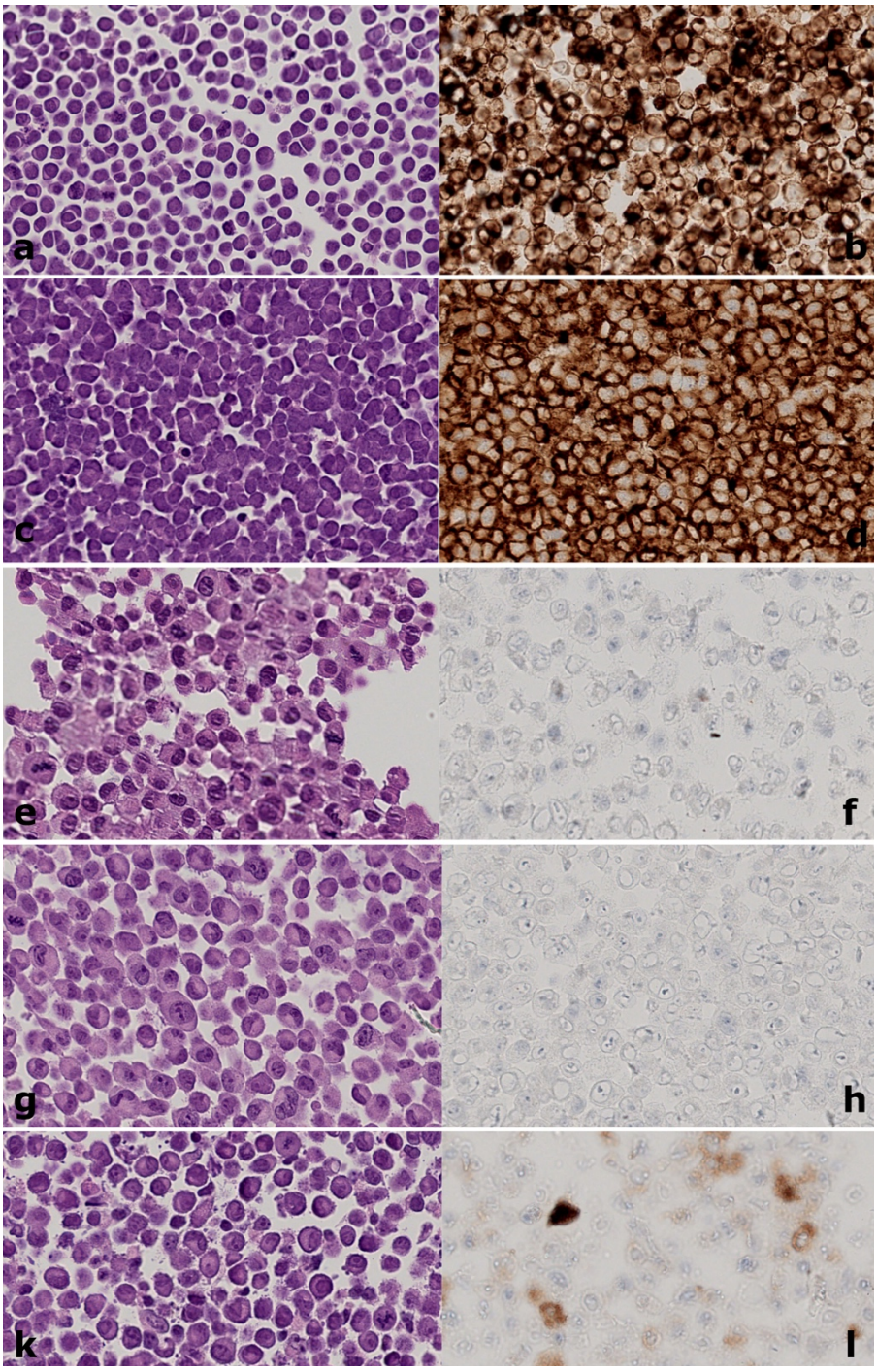

Figure 5. *Hematoxylin and eosin staining and ALK immunoexpression of Merkel cell carcinoma cell lines, namely, WAGA (a/b, 400x), MKL1 (c/d, 400x), MCC26 (e/f, 400x), MCC13 (g/h, 400x), and UISO (k/l, 400x).*

Based on the ALK expression, by means of Western-blot and immunohistochemical analyses for further experimental purposes MKL1, WAGA were included as the test cell lines and MCC26 was considered a negative control.

GD2 expression in test and control cell lines

GD2 expression was determined by means of flow cytometry. The expression levels are shown in **Figure 6**. In detail, all 3 test cell lines, WAGA, MKL1 and MCC26 showed low GD2 levels, comparable to negative control (SKNFI neuroblastoma cell line). IMR32 neuroblastoma cell line served as a high-GD2 control cell line.

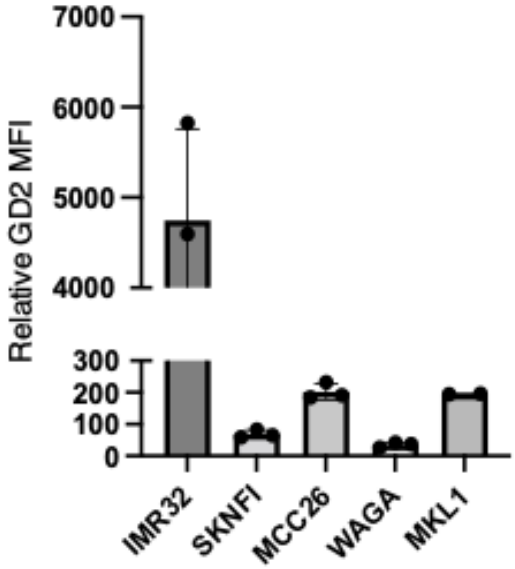

***Figure 6**. GD2 expression levels as determined by flow-cytometry.*

MCC cell lines are characterized by a various levels of HLA class-I expression

We analyzed test (MKL1 and Waga) and control (MCC26) cell lines for their HLA class-I surface expression with an HLA-A, -B and -C detecting antibody (clone W6/32) by flow cytometry revealing differential expression levels of HLA class-I. Waga and MKL1 showed low to no expression, respectively, while MCC26 demonstrated high HLA class-I surface expression (**Figure 7**).

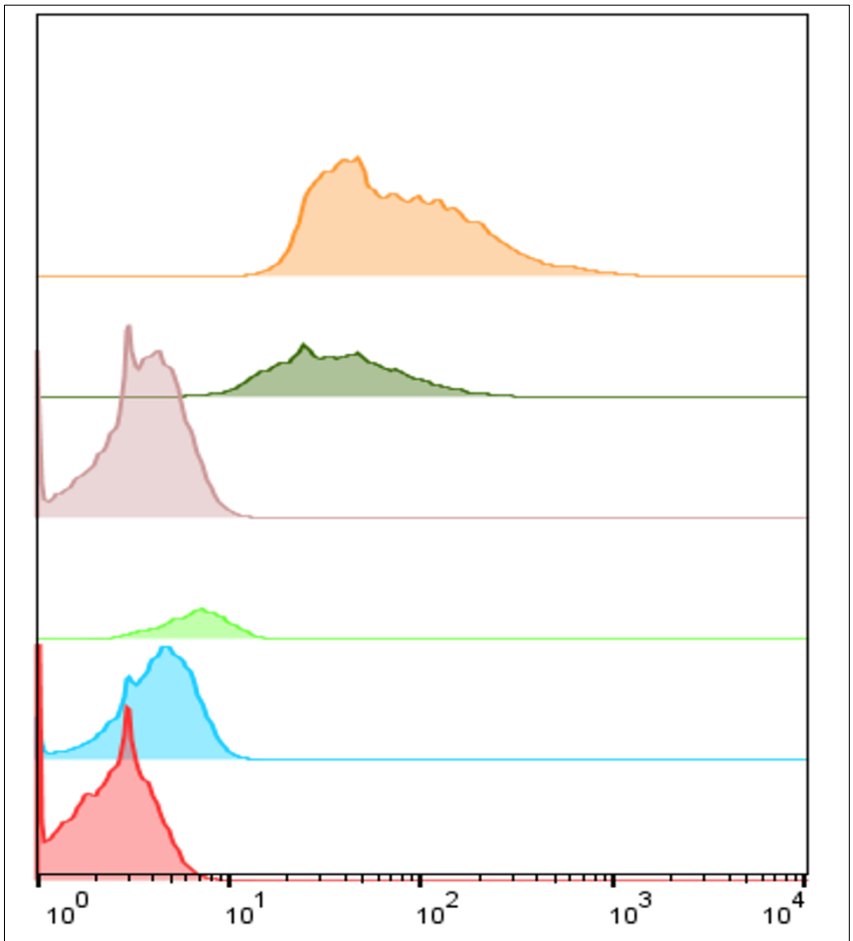

	Sample Name	Subset Name	Count	Mean : PE-A
	MCC26 HLA-I_3_11_22	Single Cells	12839	112
	NB1_3_11_22	Single Cells	4793	48.3
	WAGA HLA-I_3_11_22	Single Cells	11457	3.86
	MKL1 HLA-I_3_11_22	Single Cells	1555	7.07
	KELLY_3_11_22	Single Cells	6936	4.60
	KELLY UNST_3_11_22	Single Cells	10064	2.71

Figure 7. *HLA class-I surface expression levels as determined by flow cytometry.*

Human ALK.CAR-Ts efficiency against human Merkel cell carcinoma cells

MCC cell lines were co-cultured at different T cell to tumor cell ratios (1:1, 1:5, 1:10) with control untransduced T cells (UT), CD19.CAR-Ts (negative control), GD2.CAR-Ts, and ALK.CAR-Ts, alone and in combination with lorlatinib.
ALK.CAR-Ts efficiently eliminated most of the MKL1 and WAGA cells at the T cell to tumor cell ratio of 1:1, with or without the combination with lorlatinib (**Figure 8A/B**).

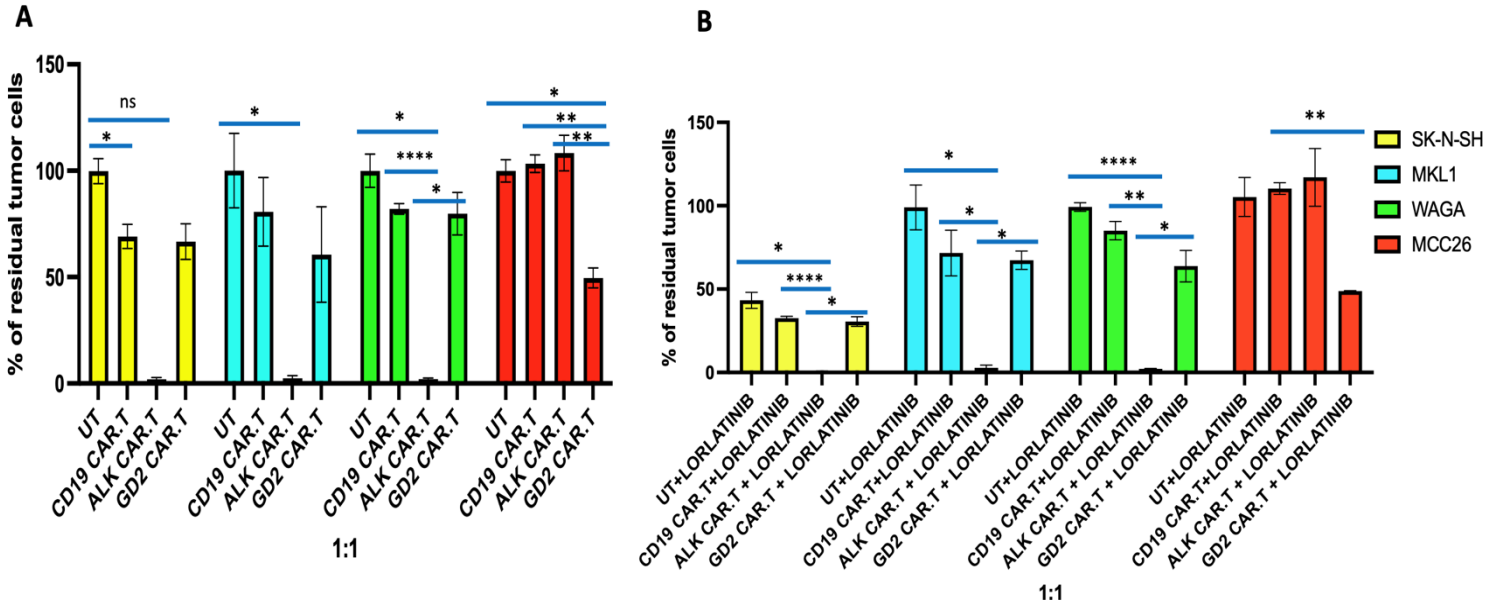

Figure 8. *Co-culture experiment using T cell to tumor ratio 1:1, employing untransduced T cells (UT), CD19.CAR-Ts (negative control), GD2.CAR-Ts, and ALK.CAR-Ts alone (A) and in combination with lorlatinib (B).*

At higher T cell to tumor cell ratios, namely 1:5 (**Figure 9**) and 1:10 (**Figure 10**), variable killing effect was observed. ALK.CAR-Ts were still efficient against WAGA at the ratio 1:5 with or without lorlatinib, however killing effect was considerably low at 1:10 ratio, and only combination with lorlatinib gave significant effect. In case of MKL1, at 1:5 ratio only ALK.CAR-Ts combined with lorlatinib gave significant killing effect. No significant effect was seen in other modalities. No ALK.CAR-T killing was observed in MCC26.

There was a modest killing activity observed in case of GD2.CAR.Ts across cell lines at ratio 1:1 (**Figure 8**), with or without combination with lorlatinib. This effect was not sustained at higher ratios (**Figure 9 and 10**).

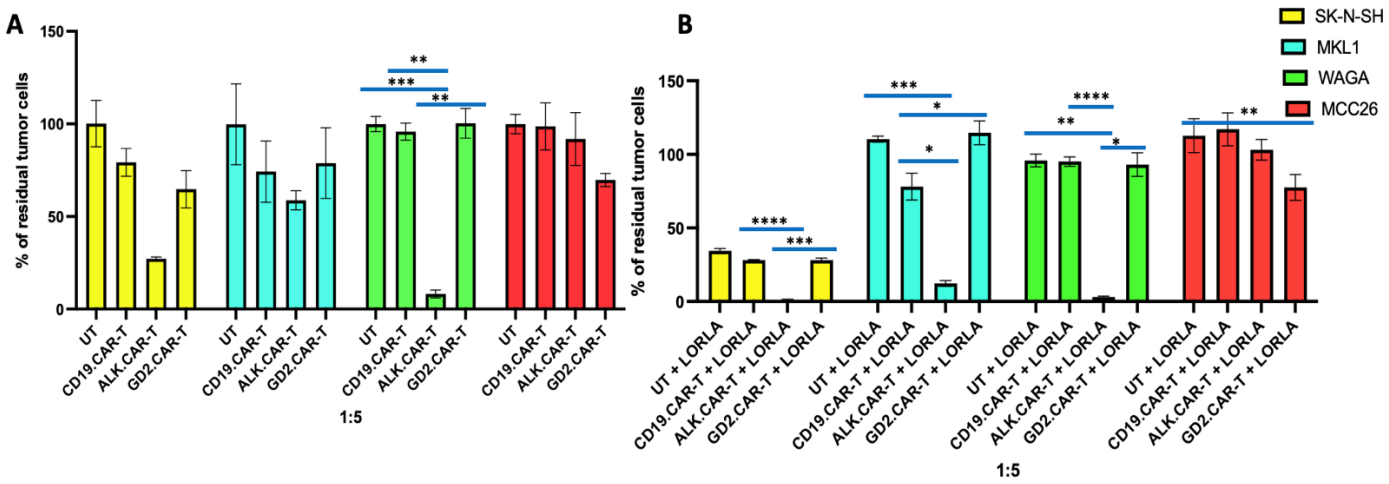

Figure 9. *Co-culture experiment using T cell to tumor ratio 1:5, employing untransduced T cells (UT), CD19.CAR-Ts (negative control), GD2.CAR-Ts, and ALK.CAR-Ts alone (A) and in combination with lorlatinib (B).*

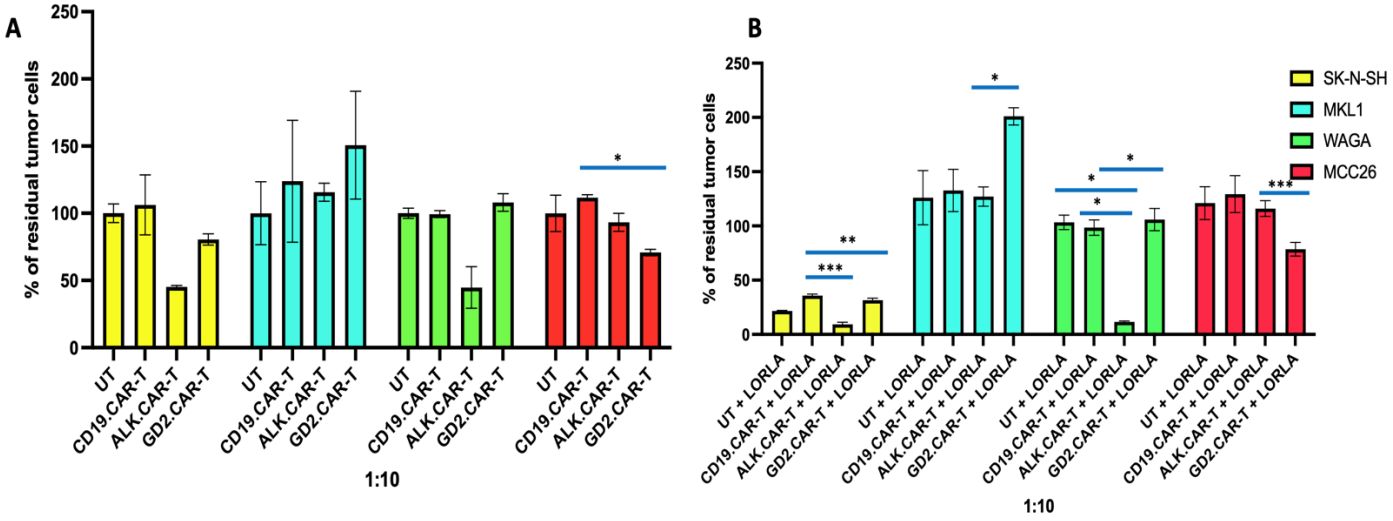

Figure 10. *Co-culture experiment using T cell to tumor ratio 1:10, employing untransduced T cells (UT), CD19.CAR-Ts (negative control), GD2.CAR-Ts, and ALK.CAR-Ts alone (A) and in combination with lorlatinib (B).*

Effect of ALK inhibitors, lorlatinib and ceritinib, in MCC cell lines

We performed 4-hour-treatment of WAGA, MKL1 and MCC26 with ALK-inhibitors, namely, lorlatinib (concentration 10nM and 100nM), and ceritinib (concentration 200nM).
As determined by western blot analysis, no effect of lorlatinib nor ceritinib on ALK pathway was observed (**Figure 11**), suggesting that ALK is expressed but likely not active in MCC cell lines. NB1 and Kelly neuroblastoma cell lines served as a control cell lines.

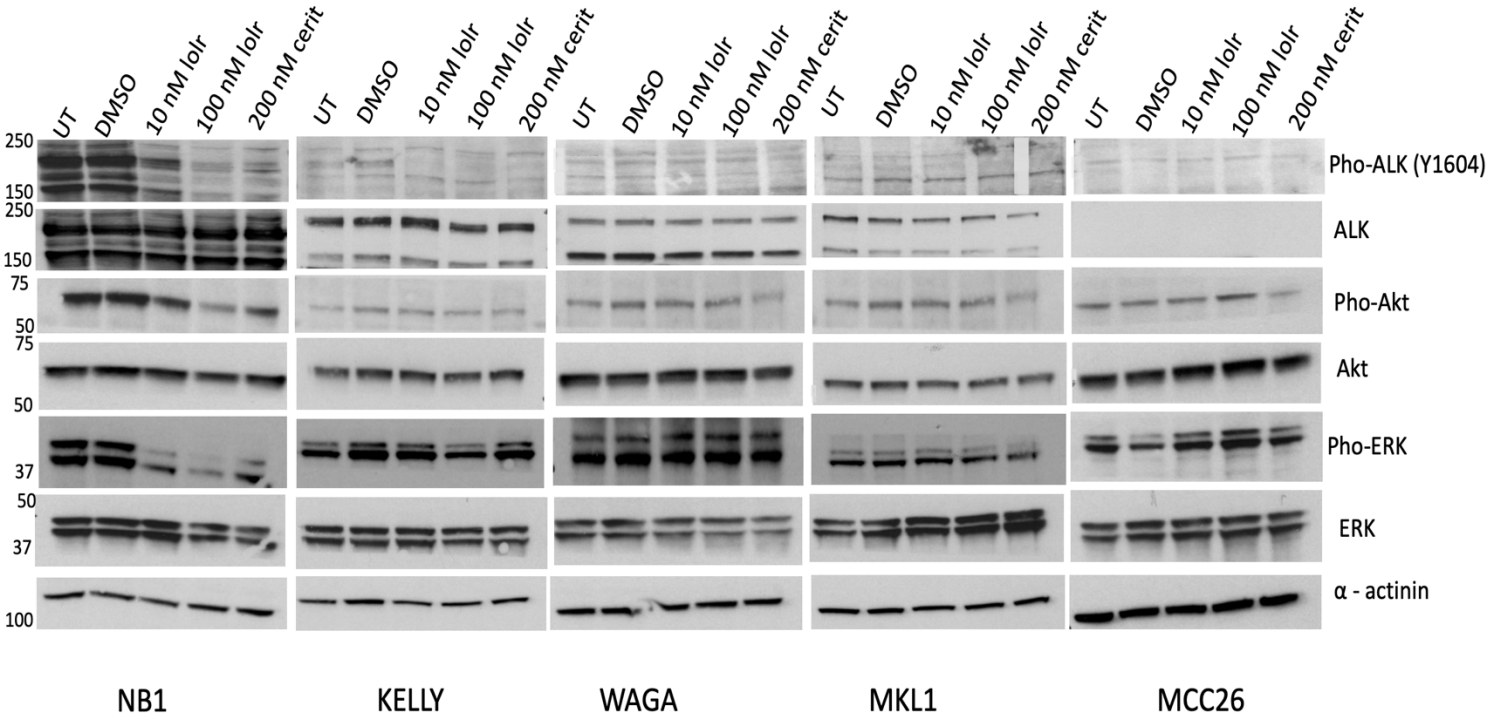

Figure 11. *Western blot analyses of ALK pathway performed after 4-hour-treatment of WAGA, MKL1 and MCC26 with ALK-inhibitors, lorlatinib (concentration 10nM and 100nM), and ceritinib (concentration 200nM). NB1 and Kelly neuroblastoma cell lines served as a control cell lines.*

Merkel cell carcinoma metastatic model

We developed metastatic models of Merkel cell carcinoma by injecting Ffluc-transduced MKL1 and WAGA cell lines with relatively high ALK expression, i.v. into NOD/SCID/IL2Rγ−/− (NSG) mice. We monitored tumor growth by bioluminescence imaging using IVIS Spectrum *in vivo* imaging system (PerkinElmer) at day 8, 15, 22, 29 (for both cell lines) and day 54 for WAGA cell line, since the i.v. inoculation (**Figure 12**).
In this model, tumor deposits emerged on day 22, to be clearly detected on day 29 since inoculation. MKL1 (panel A) and WAGA (panel B) were detected at lymph nodal and lymph nodal/liver level, respectively (**Figure 12**).

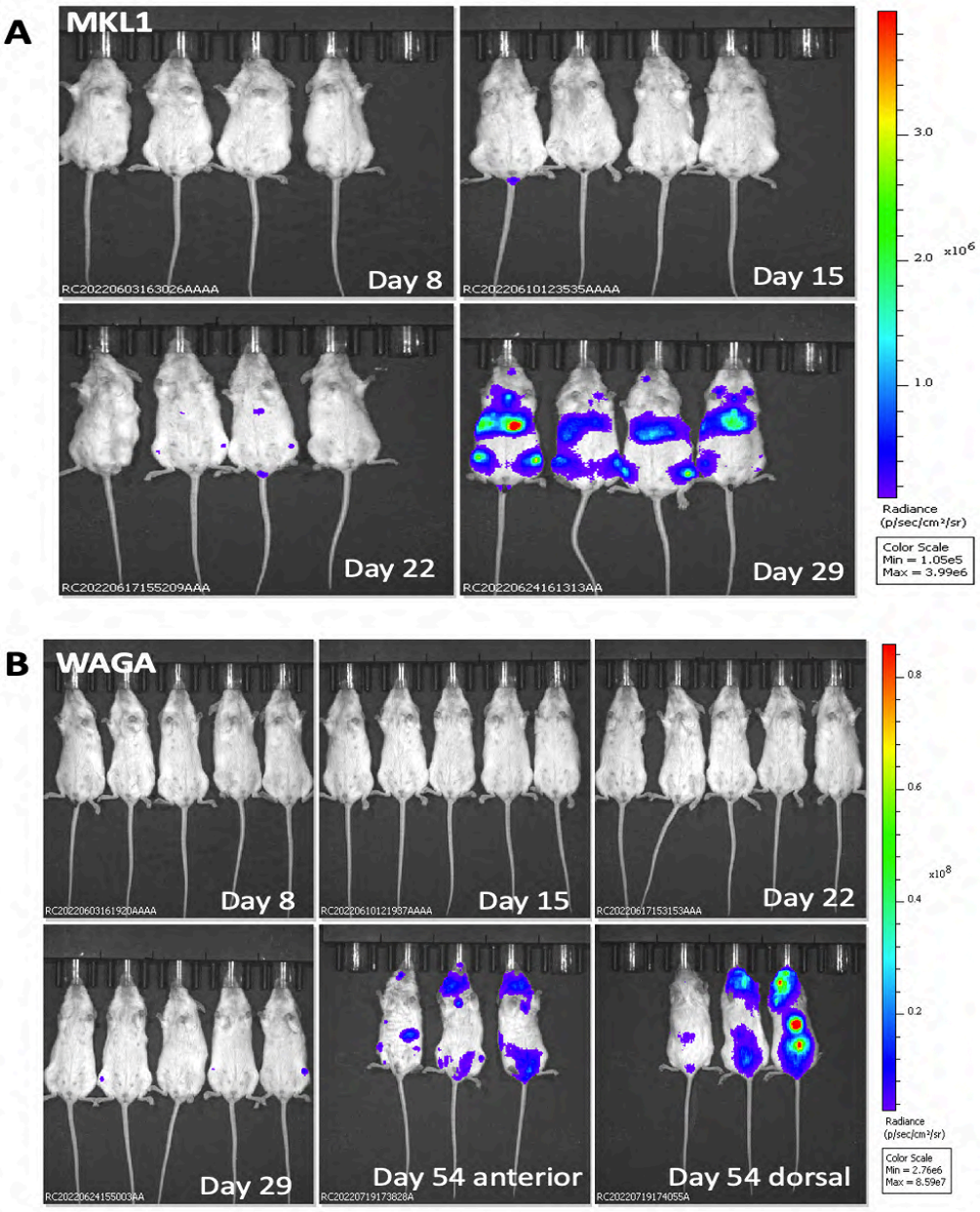

Figure 12. *Representative images of tumor growth monitoring (day 8, 15, 22 and 29 from inoculation for MKL1 as well as day 54 for WAGA) of Ffluc-transduced MKL1 (panel A) and WAGA (panel B) cell lines, i.v. into NOD/SCID/IL2Rγ−/− (NSG) mice, as detected by bioluminescence imaging using IVIS Spectrum in vivo imaging system (PerkinElmer).*

Three out of four MKL1-inoculated mice died on day 46, and the remaining mouse was euthanized. Tumor masses was detected at the level of liver and both ovaries (all mice), while one mouse demonstrated spleen tumor also.

Regarding WAGA-inoculated mice, one died on the day 46, showing only a small ovary mass. Second mouse died on the day 54, however necropsy was not performed.
The remaining 3 mice died on the day 59 demonstrating tumor enlargement of the ovaries in all of them, and several liver mases in two mice.

DISCUSSION

Merkel cell carcinoma is a rare and aggressive skin cancer with a neuroendocrine phenotype.
Infection with MCPyV, ultraviolet radiation exposure and immunosuppression are the main factors associated with the pathogenesis of this disease. Surgery is the first-line treatment for localized MCC, followed by adjuvant radiation and/or chemotherapy (692).

Insights into the critical role of the immune system in tumorigenesis paved the way for development of several immunotherapeutics, such as checkpoint inhibitors, cancer vaccines and adoptive T cell therapy. To date, in the advanced form of MCC, chemotherapy is still considered to be the standard treatment. However, the therapeutic landscape for metastatic MCC is evolving rapidly (393) and recent advances in the development of well-tolerated immunotherapy agents (693) have the potential to provide effective treatment options for these patients (613).

Molecular alterations leading to heightened ALK activation have been implicated in several cancers including non-Hodgkin's lymphoma, rhabdomyosarcomas, renal cell carcinoma, thyroid cancer, neuroblastoma, and NSCLC (694). *ALK*-targeted therapies are currently used in clinical practice and are endorsed in multiple clinical oncology guidelines.
In our study, positive ALK immunohistochemical reaction was observed in 87.1% of human MCCs tissue samples. A significant correlation between ALK expression and viral status was detected, with MCPyV positive MCCs being significantly more likely to show positive and higher ALK expression compared to MCPyV negative cases (p=0.0001). This relatively high ALK expression and positive correlation with MCPyV status was reported in various papers (676,682).
In line with literature data (682), we didn't observe ALK phosphorylation in MCC cell lines, as assessed by western blot analyses, nor the effect of ALK inhibitors, lorlatinib and ceritinib. Our results suggest that ALK is expressed but likely not active in MCC cell lines.
On the other hand, literature data report presence of phospho-ALK by IHC in approximately 50% of human tissue sample of MCC. The authors hypothesized that the *in vivo* MCC tumor microenvironment could promote activation of ALK via an unknown mechanism. However, the cell line models lack the tumor microenvironment that consist of different cell types surrounding the cancer cells such as epithelial cells, fibroblasts, lymphocytes, lymphovascular network and extracellular matrix, as well as all the immanent cytokines, growth factors and other molecules (682).

CARs are recombinant receptors for cell surface antigen redirected the specificity and activity of T lymphocytes and other types of the immune cells (695).
To the best of our knowledge, this is the first study that explored the efficacy of ALK- and GD2.CAR-Ts in MCC cell lines.

Of note, diminished HLA class-I expression on cancer cells is one of the major immune escape mechanisms both spontaneously and in response to immunotherapy (696,697). In fact,

we demonstrated low/absent surface expression of HLA class-I in MCPyV-positive cell lines, namely, WAGA and MKL1, respectively. In contrast to MCC26 cell line (MCPyV-negative cell line) that showed high expression of HLA class-I, as detected by HLA-A, -B and -C antibody. These results are in line with so far reported in the literature (669). In a recent study by Gavvovidis et al (670), the authors described the isolation and characterization of four HLA-A2-restricted T cell receptors (TCRs) specific to two epitopes derived from Merkel cell polyomavirus-encoded T-antigens (MCV Tags). Genetically modified T cells expressing these TCRs consistently recognized peptide-pulsed T2 cells and HLA-A2-positive target cells transduced with cDNA encoding MCV Tags. They also showed reactivity of one of the TCRs against HLA-$A2^{+}$ MCPyV positive tumor cell lines in vitro and confirmed its potential to destroy large established tumors in vivo, suggesting a potential therapeutic approach.

This reasoning led to the development of chimeric antigen receptor-modified T (CAR T)-cells to overcome the HLA restriction, the effective presentation of target epitopes, and the lack of a broad TCR gene repertoire (698). MCC cell lines were co-cultured at different T cell to tumor cell ratios (1:1, 1:5, 1:10) with control UT, CD19.CAR-Ts (negative control), GD2.CAR-Ts, and ALK.CAR-Ts, alone and in combination with lorlatinib.
ALK.CAR-Ts efficiently eliminated most of the MKL1 and WAGA cells at the T cell to tumor cell ratio of 1:1, with or without the combination with lorlatinib. On the other hand, at higher T cell to tumor cell ratios, namely 1:5 and 1:10, variable killing effect was observed. ALK.CAR-Ts were still efficient against WAGA at the ratio 1:5 with or without lorlatinib, however killing effect was considerably low at 1:10 ratio, and only combination with lorlatinib gave significant effect. In case of MKL1, at 1:5 ratio only ALK.CAR-Ts combined with lorlatinib gave significant killing effect. No significant effect was seen in other modalities. As expected, no ALK.CAR-T killing effect was observed in MCC26, that was considered as negative control.

The GD2 expression in MCC was not reported so far in the literature. However, it's expression in other neuroendocrine tumor models, such as neuroblastomas, small cell lung carcinomas and variety of embryonal cancers including brain tumors, retinoblastoma, Ewing's sarcoma, rhabdomyosarcoma, osteosarcoma has been described (699–701).
In normal tissues, GD2 expression on is largely limited to neurons, skin melanocytes, and peripheral pain fibers (702), making it well suited for targeted antitumor therapy. GD2 remains the most frequently targeted antigen for neuroblastoma immunotherapy (703).
In line with relatively low GD2 expression levels reported in our study, as determined by flow cytometry, there was a modest killing activity observed in case of GD2.CAR.Ts across cell lines at ratio 1:1, with or without combination with lorlatinib. However, this effect was not sustained at higher ratios.

Of note, successful development of metastatic MCC mice model, determining the anatomical layout of tumor growth and identifying the possible treatment period based on tumor visualization by IVIS imaging system will elucidate the effectiveness and mechanisms of CAR.T treatment in the future experiments.

CONCLUSIONS

In conclusion, to the best of our knowledge, this is the first study to explore the potential therapeutic use of ALK- and GD2.CAR-Ts in MCC cell lines. Overall, our study has revealed several insights into the molecular background of MCCs, identifying specific alterations of immunity and tumor microenvironment that favor tumor escape, and that might be useful when developing novel treatment options for these patients.

Bibliography

1. Idoate MA, Vazquez JJ, Soto J, de Castro P. Diagnosis of Lafora's disease in apocrine sweat glands of the axilla. Am J Dermatopathol. 1991 Aug;13(4):410–3.

2. Montuenga LM, Guembe L, Burrell MA, Bodegas ME, Calvo A, Sola JJ, et al. The diffuse endocrine system: from embryogenesis to carcinogenesis. Prog Histochem Cytochem. 2003;38(2):155–272.

3. Linnoila RI. Functional facets of the pulmonary neuroendocrine system. Lab Investig J Tech Methods Pathol. 2006 May;86(5):425–44.

4. Grigore AD, Ben-Jacob E, Farach-Carson MC. Prostate cancer and neuroendocrine differentiation: more neuronal, less endocrine? Front Oncol. 2015;5:37.

5. Pearse AG. The APUD concept and hormone production. Clin Endocrinol Metab. 1980 Jul;9(2):211–22.

6. Gunawardene AR, Corfe BM, Staton CA. Classification and functions of enteroendocrine cells of the lower gastrointestinal tract. Int J Exp Pathol. 2011 Aug;92(4):219–31.

7. Bernick PE, Klimstra DS, Shia J, Minsky B, Saltz L, Shi W, et al. Neuroendocrine carcinomas of the colon and rectum. Dis Colon Rectum. 2004 Feb;47(2):163–9.

8. Shinji S, Naito Z, Ishiwata T, Tanaka N, Furukawa K, Suzuki H, et al. Neuroendocrine cell differentiation of poorly differentiated colorectal adenocarcinoma correlates with liver metastasis. Int J Oncol. 2006 Aug;29(2):357–64.

9. Zeng YJ, Lai W, Liu L, Wu H, Luo XX, Wang J, et al. Prognostic significance of neuroendocrine differentiation in colorectal adenocarcinoma after radical operation: a meta-analysis. J Gastrointest Surg Off J Soc Surg Aliment Tract. 2014 May;18(5):968–76.

10. Inamura K. Update on Immunohistochemistry for the Diagnosis of Lung Cancer. Cancers. 2018 Mar 14;10(3):E72.

11. Annaratone L, Medico E, Rangel N, Castellano I, Marchiò C, Sapino A, et al. Search for neuro-endocrine markers (chromogranin A, synaptophysin and VGF) in breast cancers. An integrated approach using immunohistochemistry and gene expression profiling. Endocr Pathol. 2014 Sep;25(3):219–28.

12. Brehm Hoej L, Parkner T, Soendersoe Knudsen C, Grønbaek H. A comparison of three chromogranin A assays in patients with neuroendocrine tumours. J Gastrointest Liver Dis JGLD. 2014 Dec;23(4):419–24.

13. Mjønes P, Sagatun L, Nordrum IS, Waldum HL. Neuron-Specific Enolase as an Immunohistochemical Marker Is Better Than Its Reputation. J Histochem Cytochem Off J Histochem Soc. 2017 Dec;65(12):687–703.

14. Sohda M, Saeki H, Kuwano H, Miyazaki T, Yokobori T, Sano A, et al. Diagnostic Immunostaining and Tumor Markers Predict the Prognosis of Esophageal Neuroendocrine Cell Carcinoma Patients. Ann Surg Oncol. 2021 Nov;28(12):7983–9.

15. Blaschko H, Comline RS, Schneider FH, Silver M, Smith AD. Secretion of a chromaffin granule protein, chromogranin, from the adrenal gland after splanchnic stimulation. Nature. 1967 Jul 1;215(5096):58–9.

16. Winkler H, Westhead E. The molecular organization of adrenal chromaffin granules. Neuroscience. 1980;5(11):1803–23.

17. Kriegsmann K, Zgorzelski C, Muley T, Christopoulos P, Thomas M, Winter H, et al. Role of Synaptophysin, Chromogranin and CD56 in adenocarcinoma and squamous cell carcinoma of the lung lacking morphological features of neuroendocrine differentiation: a retrospective large-scale study on 1170 tissue samples. BMC Cancer. 2021 May 1;21(1):486.

18. Schmechel D, Marangos PJ, Brightman M. Neurone-specific enolase is a molecular marker for peripheral and central neuroendocrine cells. Nature. 1978 Dec 21;276(5690):834–6.

19. Seshi B, True L, Carter D, Rosai J. Immunohistochemical characterization of a set of monoclonal antibodies to human neuron-specific enolase. Am J Pathol. 1988 May;131(2):258–69.

20. Organisation mondiale de la santé, Centre international de recherche sur le cancer, editors. Thoracic tumours. 5th ed. Lyon: International agency for research on cancer; 2021. (World health organization classification of tumours).

21. Rindi G, Mete O, Uccella S, Basturk O, La Rosa S, Brosens LAA, et al. Overview of the 2022 WHO Classification of Neuroendocrine Neoplasms. Endocr Pathol. 2022 Mar;33(1):115–54.

22. Rindi G, Klimstra DS, Abedi-Ardekani B, Asa SL, Bosman FT, Brambilla E, et al. A common classification framework for neuroendocrine neoplasms: an International Agency for Research on Cancer (IARC) and World Health Organization (WHO) expert consensus proposal. Mod Pathol Off J U S Can Acad Pathol Inc. 2018 Dec;31(12):1770–86.

23. Milione M, Maisonneuve P, Pellegrinelli A, Grillo F, Albarello L, Spaggiari P, et al. Ki67 proliferative index of the neuroendocrine component drives MANEC prognosis. Endocr Relat Cancer. 2018 May;25(5):583–93.

24. La Rosa S, Uccella S. Classification of neuroendocrine neoplasms: lights and shadows. Rev Endocr Metab Disord. 2021 Sep;22(3):527–38.

25. Lakhani SR, Ellis IO, Schnitt SJ, Tan PH. WHO Classification of Tumours of the Breast. :242.

26. Rakha E, Tan PH. Head to head: do neuroendocrine tumours in the breast truly exist? Histopathology. 2022 Feb 8;

27. Organisation mondiale de la santé, editor. Breast tumours. 5th ed. Geneva: OMS; (World health organization classification of tumours).

28. Uccella S. The classification of neuroendocrine neoplasms of the breast and its clinical relevance. Virchows Arch Int J Pathol. 2021 Oct 26;

29. Pelosi G, Sonzogni A, Harari S, Albini A, Bresaola E, Marchiò C, et al. Classification of pulmonary neuroendocrine tumors: new insights. Transl Lung Cancer Res. 2017 Oct;6(5):513–29.

30. Travis WD. Advances in neuroendocrine lung tumors. Ann Oncol Off J Eur Soc Med Oncol. 2010 Oct;21 Suppl 7:vii65-71.

31. Organisation mondiale de la santé, Centre international de recherche sur le cancer, editors. WHO classification of tumours of the lung, pleura, thymus and heart. Lyon: International agency for research on cancer; 2015. (World Health Organization classification of tumours).

32. Travis WD, World Health Organization, International Agency for Research on Cancer, International Association for the Study of Lung Cancer, International Academy of Pathology, editors. Pathology and genetics of tumours of the lung, pleura, thymus and heart. Lyon : Oxford: IARC Press, Oxford University Press (distributor); 2004. 344 p. (World Health Organization classification of tumours).

33. Metovic J, Barella M, Harari S, Pattini L, Albini A, Sonzogni A, et al. Clinical implications of lung neuroendocrine neoplasm classification. Expert Rev Anticancer Ther. 2021 Apr;21(4):377–87.

34. Wang Y, Qian F, Chen Y, Yang Z, Hu M, Lu J, et al. Comparative Study of Pulmonary Combined Large-Cell Neuroendocrine Carcinoma and Combined Small-Cell Carcinoma in Surgically Resected High-Grade Neuroendocrine Tumors of the Lung. Front Oncol. 2021;11:714549.

35. Travis WD, Brambilla E, Nicholson AG, Yatabe Y, Austin JHM, Beasley MB, et al. The 2015 World Health Organization Classification of Lung Tumors: Impact of Genetic, Clinical and Radiologic Advances Since the 2004 Classification. J Thorac Oncol Off Publ Int Assoc Study Lung Cancer. 2015 Sep;10(9):1243–60.

36. Pelosi G, Rindi G, Travis WD, Papotti M. Ki-67 antigen in lung neuroendocrine tumors: unraveling a role in clinical practice. J Thorac Oncol Off Publ Int Assoc Study Lung Cancer. 2014 Mar;9(3):273–84.

37. Fabbri A, Cossa M, Sonzogni A, Papotti M, Righi L, Gatti G, et al. Ki-67 labeling index of neuroendocrine tumors of the lung has a high level of correspondence between biopsy samples and surgical specimens when strict counting guidelines are applied. Virchows Arch Int J Pathol. 2017 Feb;470(2):153–64.

38. Metovic J, Barella M, Pelosi G. Neuroendocrine neoplasms of the lung: a pathology update. Memo - Mag Eur Med Oncol. 2021 Dec;14(4):381–5.

39. Simbolo M, Barbi S, Fassan M, Mafficini A, Ali G, Vicentini C, et al. Gene Expression Profiling of Lung Atypical Carcinoids and Large Cell Neuroendocrine Carcinomas Identifies Three Transcriptomic Subtypes with Specific Genomic Alterations. J Thorac Oncol Off Publ Int Assoc Study Lung Cancer. 2019 Sep;14(9):1651–61.

40. Simbolo M, Mafficini A, Sikora KO, Fassan M, Barbi S, Corbo V, et al. Lung neuroendocrine tumours: deep sequencing of the four World Health Organization histotypes reveals chromatin-remodelling genes as major players and a prognostic role for TERT, RB1, MEN1 and KMT2D. J Pathol. 2017 Mar;241(4):488–500.

41. Laddha SV, da Silva EM, Robzyk K, Untch BR, Ke H, Rekhtman N, et al. Integrative Genomic Characterization Identifies Molecular Subtypes of Lung Carcinoids. Cancer Res. 2019 Sep 1;79(17):4339–47.

42. Fernandez-Cuesta L, Peifer M, Lu X, Sun R, Ozretić L, Seidel D, et al. Frequent mutations in chromatin-remodelling genes in pulmonary carcinoids. Nat Commun. 2014 May;5(1):3518.

43. Rekhtman N, Pietanza MC, Hellmann MD, Naidoo J, Arora A, Won H, et al. Next-Generation Sequencing of Pulmonary Large Cell Neuroendocrine Carcinoma Reveals Small Cell Carcinoma-like and Non-Small Cell Carcinoma-like Subsets. Clin Cancer Res Off J Am Assoc Cancer Res. 2016 Jul 15;22(14):3618–29.

44. George J, Lim JS, Jang SJ, Cun Y, Ozretić L, Kong G, et al. Comprehensive genomic profiles of small cell lung cancer. Nature. 2015 Aug 6;524(7563):47–53.

45. Metovic J, Bianchi F, Rossi G, Barella M, Sonzogni A, Harari S, et al. Recent advances and current controversies in lung neuroendocrine neoplasms☆. Semin Diagn Pathol. 2021 Sep;38(5):90–7.

46. Lou G, Yu X, Song Z. Molecular Profiling and Survival of Completely Resected Primary Pulmonary Neuroendocrine Carcinoma. Clin Lung Cancer. 2017 May;18(3):e197–201.

47. Vollbrecht C, Werner R, Walter RFH, Christoph DC, Heukamp LC, Peifer M, et al. Mutational analysis of pulmonary tumours with neuroendocrine features using targeted massive parallel sequencing: a comparison of a neglected tumour group. Br J Cancer. 2015 Dec 22;113(12):1704–11.

48. Travis WD. Pathology and diagnosis of neuroendocrine tumors: lung neuroendocrine. Thorac Surg Clin. 2014 Aug;24(3):257–66.

49. Prelaj A, Rebuzzi SE, Del Bene G, Giròn Berrìos JR, Emiliani A, De Filippis L, et al. Evaluation of the efficacy of cisplatin-etoposide and the role of thoracic radiotherapy and prophylactic cranial irradiation in LCNEC. ERJ Open Res. 2017 Jan;3(1):00128–2016.

50. Caplin ME, Baudin E, Ferolla P, Filosso P, Garcia-Yuste M, Lim E, et al. Pulmonary neuroendocrine (carcinoid) tumors: European Neuroendocrine Tumor Society expert consensus and recommendations for best practice for typical and atypical pulmonary carcinoids. Ann Oncol Off J Eur Soc Med Oncol. 2015 Aug;26(8):1604–20.

51. Travis WD. Update on small cell carcinoma and its differentiation from squamous cell carcinoma and other non-small cell carcinomas. Mod Pathol. 2012 Jan;25(S1):S18–30.

52. Travis WD, Linnoila RI, Tsokos MG, Hitchcock CL, Cutler GB, Nieman L, et al. Neuroendocrine tumors of the lung with proposed criteria for large-cell neuroendocrine carcinoma. An ultrastructural, immunohistochemical, and flow cytometric study of 35 cases.

Am J Surg Pathol. 1991 Jun;15(6):529–53.

53. Yao JC, Hassan M, Phan A, Dagohoy C, Leary C, Mares JE, et al. One hundred years after "carcinoid": epidemiology of and prognostic factors for neuroendocrine tumors in 35,825 cases in the United States. J Clin Oncol Off J Am Soc Clin Oncol. 2008 Jun 20;26(18):3063–72.

54. Melosky B. Advanced typical and atypical carcinoid tumours of the lung: management recommendations. Curr Oncol Tor Ont. 2018 Jun;25(Suppl 1):S86–93.

55. George J, Walter V, Peifer M, Alexandrov LB, Seidel D, Leenders F, et al. Integrative genomic profiling of large-cell neuroendocrine carcinomas reveals distinct subtypes of high-grade neuroendocrine lung tumors. Nat Commun. 2018 Dec;9(1):1048.

56. Simbolo M, Barbi S, Fassan M, Mafficini A, Ali G, Vicentini C, et al. Gene Expression Profiling of Lung Atypical Carcinoids and Large Cell Neuroendocrine Carcinomas Identifies Three Transcriptomic Subtypes with Specific Genomic Alterations. J Thorac Oncol Off Publ Int Assoc Study Lung Cancer. 2019 Sep;14(9):1651–61.

57. Alcala N, Leblay N, Gabriel AAG, Mangiante L, Hervas D, Giffon T, et al. Integrative and comparative genomic analyses identify clinically relevant pulmonary carcinoid groups and unveil the supra-carcinoids. Nat Commun. 2019 Dec;10(1):3407.

58. Rekhtman N, Desmeules P, Litvak AM, Pietanza MC, Santos-Zabala ML, Ni A, et al. Stage IV lung carcinoids: spectrum and evolution of proliferation rate, focusing on variants with elevated proliferation indices. Mod Pathol Off J U S Can Acad Pathol Inc. 2019 Jul;32(8):1106–22.

59. Metovic J, Barella M, Bianchi F, Hofman P, Hofman V, Remmelink M, et al. Morphologic and molecular classification of lung neuroendocrine neoplasms. Virchows Arch Int J Pathol. 2021 Jan;478(1):5–19.

60. Pelosi G, Bianchi F, Hofman P, Pattini L, Ströbel P, Calabrese F, et al. Recent advances in the molecular landscape of lung neuroendocrine tumors. Expert Rev Mol Diagn. 2019 Apr;19(4):281–97.

61. Peifer M, Fernández-Cuesta L, Sos ML, George J, Seidel D, Kasper LH, et al. Integrative genome analyses identify key somatic driver mutations of small-cell lung cancer. Nat Genet. 2012 Oct;44(10):1104–10.

62. Miyoshi T, Umemura S, Matsumura Y, Mimaki S, Tada S, Makinoshima H, et al. Genomic Profiling of Large-Cell Neuroendocrine Carcinoma of the Lung. Clin Cancer Res Off J Am Assoc Cancer Res. 2017 Feb 1;23(3):757–65.

63. Derks JL, Leblay N, Lantuejoul S, Dingemans AMC, Speel EJM, Fernandez-Cuesta L. New Insights into the Molecular Characteristics of Pulmonary Carcinoids and Large Cell Neuroendocrine Carcinomas, and the Impact on Their Clinical Management. J Thorac Oncol Off Publ Int Assoc Study Lung Cancer. 2018 Jun;13(6):752–66.

64. Rekhtman N, Pietanza CM, Sabari J, Montecalvo J, Wang H, Habeeb O, et al. Pulmonary large cell neuroendocrine carcinoma with adenocarcinoma-like features: napsin A expression and genomic alterations. Mod Pathol Off J U S Can Acad Pathol Inc. 2018 Jan;31(1):111–21.

65. Zhuo M, Guan Y, Yang X, Hong L, Wang Y, Li Z, et al. The Prognostic and Therapeutic Role of Genomic Subtyping by Sequencing Tumor or Cell-Free DNA in Pulmonary Large-Cell Neuroendocrine Carcinoma. Clin Cancer Res Off J Am Assoc Cancer Res. 2020 Feb 15;26(4):892–901.

66. Derks JL, Leblay N, Thunnissen E, van Suylen RJ, den Bakker M, Groen HJM, et al. Molecular Subtypes of Pulmonary Large-cell Neuroendocrine Carcinoma Predict Chemotherapy Treatment Outcome. Clin Cancer Res Off J Am Assoc Cancer Res. 2018 Jan 1;24(1):33–42.

67. Uccella S, La Rosa S, Metovic J, Marchiori D, Scoazec JY, Volante M, et al. Genomics of High-Grade Neuroendocrine Neoplasms: Well-Differentiated Neuroendocrine Tumor with High-Grade Features (G3 NET) and Neuroendocrine Carcinomas (NEC) of Various Anatomic Sites. Endocr Pathol. 2021 Mar;32(1):192–210.

68. Kalemkerian GP, Akerley W, Bogner P, Borghaei H, Chow LQ, Downey RJ, et al. Small Cell Lung Cancer. J Natl Compr Canc Netw. 2013 Jan;11(1):78–98.

69. Torre LA, Siegel RL, Jemal A. Lung Cancer Statistics. In: Ahmad A, Gadgeel S, editors. Lung Cancer and Personalized Medicine [Internet]. Cham: Springer International Publishing; 2016 [cited 2022 May 6]. p. 1–19. (Advances in Experimental Medicine and Biology; vol. 893). Available from: http://link.springer.com/10.1007/978-3-319-24223-1_1

70. Yang S, Zhang Z, Wang Q. Emerging therapies for small cell lung cancer. J Hematol OncolJ Hematol Oncol. 2019 Dec;12(1):47.

71. Rudin CM, Durinck S, Stawiski EW, Poirier JT, Modrusan Z, Shames DS, et al. Comprehensive genomic analysis identifies SOX2 as a frequently amplified gene in small-cell lung cancer. Nat Genet. 2012 Oct;44(10):1111–6.

72. Lee JK, Lee J, Kim S, Kim S, Youk J, Park S, et al. Clonal History and Genetic Predictors of Transformation Into Small-Cell Carcinomas From Lung Adenocarcinomas. J Clin Oncol Off J Am Soc Clin Oncol. 2017 Sep 10;35(26):3065–74.

73. Poirier JT, Dobromilskaya I, Moriarty WF, Peacock CD, Hann CL, Rudin CM. Selective tropism of Seneca Valley virus for variant subtype small cell lung cancer. J Natl Cancer Inst. 2013 Jul 17;105(14):1059–65.

74. Ito T, Udaka N, Yazawa T, Okudela K, Hayashi H, Sudo T, et al. Basic helix-loop-helix transcription factors regulate the neuroendocrine differentiation of fetal mouse pulmonary epithelium. Dev Camb Engl. 2000 Sep;127(18):3913–21.

75. Horie M, Miyashita N, Mattsson JSM, Mikami Y, Sandelin M, Brunnström H, et al. An integrative transcriptome analysis reveals a functional role for thyroid transcription factor-1 in small cell lung cancer. J Pathol. 2018 Oct;246(2):154–65.

76. Sakaeda M, Sato H, Ishii J, Miyata C, Kamma H, Shishido-Hara Y, et al. Neural lineage-specific homeoprotein BRN2 is directly involved in TTF1 expression in small-cell lung cancer. Lab Investig J Tech Methods Pathol. 2013 Apr;93(4):408–21.

77. Borromeo MD, Savage TK, Kollipara RK, He M, Augustyn A, Osborne JK, et al. ASCL1 and

NEUROD1 Reveal Heterogeneity in Pulmonary Neuroendocrine Tumors and Regulate Distinct Genetic Programs. Cell Rep. 2016 Aug 2;16(5):1259–72.

78. Mollaoglu G, Guthrie MR, Böhm S, Brägelmann J, Can I, Ballieu PM, et al. MYC Drives Progression of Small Cell Lung Cancer to a Variant Neuroendocrine Subtype with Vulnerability to Aurora Kinase Inhibition. Cancer Cell. 2017 Feb 13;31(2):270–85.

79. Lantuejoul S, Fernandez-Cuesta L, Damiola F, Girard N, McLeer A. New molecular classification of large cell neuroendocrine carcinoma and small cell lung carcinoma with potential therapeutic impacts. Transl Lung Cancer Res. 2020 Oct;9(5):2233–44.

80. Borges M, Linnoila RI, van de Velde HJ, Chen H, Nelkin BD, Mabry M, et al. An achaete-scute homologue essential for neuroendocrine differentiation in the lung. Nature. 1997 Apr 24;386(6627):852–5.

81. Augustyn A, Borromeo M, Wang T, Fujimoto J, Shao C, Dospoy PD, et al. ASCL1 is a lineage oncogene providing therapeutic targets for high-grade neuroendocrine lung cancers. Proc Natl Acad Sci U S A. 2014 Oct 14;111(41):14788–93.

82. Rudin CM, Poirier JT, Byers LA, Dive C, Dowlati A, George J, et al. Molecular subtypes of small cell lung cancer: a synthesis of human and mouse model data. Nat Rev Cancer. 2019 May;19(5):289–97.

83. Zhang W, Girard L, Zhang YA, Haruki T, Papari-Zareei M, Stastny V, et al. Small cell lung cancer tumors and preclinical models display heterogeneity of neuroendocrine phenotypes. Transl Lung Cancer Res. 2018 Feb;7(1):32–49.

84. La Rosa S, Marando A, Gatti G, Rapa I, Volante M, Papotti M, et al. Achaete-scute homolog 1 as a marker of poorly differentiated neuroendocrine carcinomas of different sites: a validation study using immunohistochemistry and quantitative real-time polymerase chain reaction on 335 cases. Hum Pathol. 2013 Jul;44(7):1391–9.

85. Osada H, Tatematsu Y, Yatabe Y, Horio Y, Takahashi T. ASH1 gene is a specific therapeutic target for lung cancers with neuroendocrine features. Cancer Res. 2005 Dec 1;65(23):10680–5.

86. Kudoh S, Tenjin Y, Kameyama H, Ichimura T, Yamada T, Matsuo A, et al. Significance of achaete-scute complex homologue 1 (ASCL1) in pulmonary neuroendocrine carcinomas; RNA sequence analyses using small cell lung cancer cells and Ascl1-induced pulmonary neuroendocrine carcinoma cells. Histochem Cell Biol. 2020 Jun;153(6):443–56.

87. Altree-Tacha D, Tyrrell J, Li F. mASH1 is Highly Specific for Neuroendocrine Carcinomas: An Immunohistochemical Evaluation on Normal and Various Neoplastic Tissues. Arch Pathol Lab Med. 2017 Feb;141(2):288–92.

88. Ye B, Cappel J, Findeis-Hosey J, McMahon L, Yang Q, Xiao GQ, et al. hASH1 is a specific immunohistochemical marker for lung neuroendocrine tumors. Hum Pathol. 2016 Feb;48:142–7.

89. Gazdar AF, Minna JD. Small cell lung cancers made from scratch. J Exp Med. 2019 Mar 4;216(3):476–8.

90. Tsuruoka K, Horinouchi H, Goto Y, Kanda S, Fujiwara Y, Nokihara H, et al. PD-L1 expression in neuroendocrine tumors of the lung. Lung Cancer Amst Neth. 2017 Jun;108:115–20.

91. Vesterinen T, Kuopio T, Ahtiainen M, Knuuttila A, Mustonen H, Salmenkivi K, et al. PD-1 and PD-L1 expression in pulmonary carcinoid tumors and their association to tumor spread. Endocr Connect. 2019 Aug 1;8(8):1168–75.

92. Schultheis AM, Scheel AH, Ozretić L, George J, Thomas RK, Hagemann T, et al. PD-L1 expression in small cell neuroendocrine carcinomas. Eur J Cancer Oxf Engl 1990. 2015 Feb;51(3):421–6.

93. Organisation mondiale de la santé, Centre international de recherche sur le cancer, editors. Digestive system tumours. 5th ed. Lyon: International agency for research on cancer; 2019. (World health organization classification of tumours).

94. Dasari A, Mehta K, Byers LA, Sorbye H, Yao JC. Comparative study of lung and extrapulmonary poorly differentiated neuroendocrine carcinomas: A SEER database analysis of 162,983 cases. Cancer. 2018 Feb 15;124(4):807–15.

95. Sorbye H, Strosberg J, Baudin E, Klimstra DS, Yao JC. Gastroenteropancreatic high-grade neuroendocrine carcinoma: Neuroendocrine Carcinoma. Cancer. 2014 Sep 15;120(18):2814–23.

96. Volante M, Birocco N, Gatti G, Duregon E, Lorizzo K, Fazio N, et al. Extrapulmonary neuroendocrine small and large cell carcinomas: a review of controversial diagnostic and therapeutic issues. Hum Pathol. 2014 Apr;45(4):665–73.

97. Conte B, George B, Overman M, Estrella J, Jiang ZQ, Mehrvarz Sarshekeh A, et al. High-Grade Neuroendocrine Colorectal Carcinomas: A Retrospective Study of 100 Patients. Clin Colorectal Cancer. 2016 Jun;15(2):e1-7.

98. Cicin I, Karagol H, Uzunoglu S, Uygun K, Usta U, Kocak Z, et al. Extrapulmonary small-cell carcinoma compared with small-cell lung carcinoma: a retrospective single-center study. Cancer. 2007 Sep 1;110(5):1068–76.

99. Stelwagen J, de Vries EGE, Walenkamp AME. Current Treatment Strategies and Future Directions for Extrapulmonary Neuroendocrine Carcinomas: A Review. JAMA Oncol. 2021 May 1;7(5):759.

100. Garcia-Carbonero R, Sorbye H, Baudin E, Raymond E, Wiedenmann B, Niederle B, et al. ENETS Consensus Guidelines for High-Grade Gastroenteropancreatic Neuroendocrine Tumors and Neuroendocrine Carcinomas. Neuroendocrinology. 2016;103(2):186–94.

101. McCluggage WG, Kennedy K, Busam KJ. An immunohistochemical study of cervical neuroendocrine carcinomas: Neoplasms that are commonly TTF1 positive and which may express CK20 and P63. Am J Surg Pathol. 2010 Apr;34(4):525–32.

102. Ordóñez NG. Value of thyroid transcription factor-1 immunostaining in distinguishing small cell lung carcinomas from other small cell carcinomas. Am J Surg Pathol. 2000 Sep;24(9):1217–23.

103. Jiang SX, Mikami T, Umezawa A, Saegusa M, Kameya T, Okayasu I. Gastric large cell neuroendocrine carcinomas: a distinct clinicopathologic entity. Am J Surg Pathol. 2006 Aug;30(8):945–53.

104. Wang W, Epstein JI. Small cell carcinoma of the prostate. A morphologic and immunohistochemical study of 95 cases. Am J Surg Pathol. 2008 Jan;32(1):65–71.

105. Thompson S, Cioffi-Lavina M, Chapman-Fredricks J, Gomez-Fernandez C, Fernandez-Castro G, Jorda M. Distinction of high-grade neuroendocrine carcinoma/small cell carcinoma from conventional urothelial carcinoma of urinary bladder: an immunohistochemical approach. Appl Immunohistochem Mol Morphol AIMM. 2011 Oct;19(5):395–9.

106. Horn LC, Hentschel B, Bilek K, Richter CE, Einenkel J, Leo C. Mixed small cell carcinomas of the uterine cervix: prognostic impact of focal neuroendocrine differentiation but not of Ki-67 labeling index. Ann Diagn Pathol. 2006 Jun;10(3):140–3.

107. Becker JC, Stang A, DeCaprio JA, Cerroni L, Lebbé C, Veness M, et al. Merkel cell carcinoma. Nat Rev Dis Primer. 2017 Oct 26;3:17077.

108. Pelosi G, Rodriguez J, Viale G, Rosai J. Typical and atypical pulmonary carcinoid tumor overdiagnosed as small-cell carcinoma on biopsy specimens: a major pitfall in the management of lung cancer patients. Am J Surg Pathol. 2005 Feb;29(2):179–87.

109. Basturk O, Yang Z, Tang LH, Hruban RH, Adsay V, McCall CM, et al. The high-grade (WHO G3) pancreatic neuroendocrine tumor category is morphologically and biologically heterogenous and includes both well differentiated and poorly differentiated neoplasms. Am J Surg Pathol. 2015 May;39(5):683–90.

110. Heetfeld M, Chougnet CN, Olsen IH, Rinke A, Borbath I, Crespo G, et al. Characteristics and treatment of patients with G3 gastroenteropancreatic neuroendocrine neoplasms. Endocr Relat Cancer. 2015 Aug;22(4):657–64.

111. Milione M, Maisonneuve P, Spada F, Pellegrinelli A, Spaggiari P, Albarello L, et al. The Clinicopathologic Heterogeneity of Grade 3 Gastroenteropancreatic Neuroendocrine Neoplasms: Morphological Differentiation and Proliferation Identify Different Prognostic Categories. Neuroendocrinology. 2017;104(1):85–93.

112. Tang LH, Basturk O, Sue JJ, Klimstra DS. A Practical Approach to the Classification of WHO Grade 3 (G3) Well-differentiated Neuroendocrine Tumor (WD-NET) and Poorly Differentiated Neuroendocrine Carcinoma (PD-NEC) of the Pancreas. Am J Surg Pathol. 2016 Sep;40(9):1192–202.

113. Sorbye H, Welin S, Langer SW, Vestermark LW, Holt N, Osterlund P, et al. Predictive and prognostic factors for treatment and survival in 305 patients with advanced gastrointestinal neuroendocrine carcinoma (WHO G3): The NORDIC NEC study. Ann Oncol. 2013 Jan;24(1):152–60.

114. Brodeur GM. Molecular pathology of human neuroblastomas. Semin Diagn Pathol. 1994 May;11(2):118–25.

115. Brodeur GM. Neuroblastoma: biological insights into a clinical enigma. Nat Rev Cancer. 2003 Mar;3(3):203–16.

116. Sung KW, Yoo KH, Koo HH, Kim JY, Cho EJ, Seo YL, et al. Neuroblastoma originating from extra-abdominal sites: association with favorable clinical and biological features. J Korean Med Sci. 2009 Jun;24(3):461–7.

117. Morris JA, Shcochat SJ, Smith EI, Look AT, Brodeur GM, Cantor AB, et al. Biological variables in thoracic neuroblastoma: a Pediatric Oncology Group study. J Pediatr Surg. 1995 Feb;30(2):296–302; discussion 302-303.

118. Suita S, Tajiri T, Sera Y, Takamatsu H, Mizote H, Ohgami H, et al. The characteristics of mediastinal neuroblastoma. Eur J Pediatr Surg Off J Austrian Assoc Pediatr Surg Al Z Kinderchir. 2000 Dec;10(6):353–9.

119. Adams GA, Shochat SJ, Smith EI, Shuster JJ, Joshi VV, Altshuler G, et al. Thoracic neuroblastoma: a Pediatric Oncology Group study. J Pediatr Surg. 1993 Mar;28(3):372–7; discussion 377-378.

120. London WB, Castleberry RP, Matthay KK, Look AT, Seeger RC, Shimada H, et al. Evidence for an age cutoff greater than 365 days for neuroblastoma risk group stratification in the Children's Oncology Group. J Clin Oncol Off J Am Soc Clin Oncol. 2005 Sep 20;23(27):6459–65.

121. Maris JM. Recent advances in neuroblastoma. N Engl J Med. 2010 Jun 10;362(23):2202–11.

122. Brodeur GM, Pritchard J, Berthold F, Carlsen NL, Castel V, Castelberry RP, et al. Revisions of the international criteria for neuroblastoma diagnosis, staging, and response to treatment. J Clin Oncol Off J Am Soc Clin Oncol. 1993 Aug;11(8):1466–77.

123. Brodeur GM, Seeger RC, Barrett A, Berthold F, Castleberry RP, D'Angio G, et al. International criteria for diagnosis, staging, and response to treatment in patients with neuroblastoma. J Clin Oncol Off J Am Soc Clin Oncol. 1988 Dec;6(12):1874–81.

124. Seeger RC, Brodeur GM, Sather H, Dalton A, Siegel SE, Wong KY, et al. Association of multiple copies of the N-myc oncogene with rapid progression of neuroblastomas. N Engl J Med. 1985 Oct 31;313(18):1111–6.

125. Bown N, Cotterill S, Lastowska M, O'Neill S, Pearson AD, Plantaz D, et al. Gain of chromosome arm 17q and adverse outcome in patients with neuroblastoma. N Engl J Med. 1999 Jun 24;340(25):1954–61.

126. Caron H, van Sluis P, de Kraker J, Bökkerink J, Egeler M, Laureys G, et al. Allelic loss of chromosome 1p as a predictor of unfavorable outcome in patients with neuroblastoma. N Engl J Med. 1996 Jan 25;334(4):225–30.

127. Maris JM, Weiss MJ, Guo C, Gerbing RB, Stram DO, White PS, et al. Loss of heterozygosity at 1p36 independently predicts for disease progression but not decreased overall survival probability in neuroblastoma patients: a Children's Cancer Group study. J Clin Oncol Off J Am Soc Clin Oncol. 2000 May;18(9):1888–99.

128. Attiyeh EF, London WB, Mossé YP, Wang Q, Winter C, Khazi D, et al. Chromosome 1p and 11q deletions and outcome in neuroblastoma. N Engl J Med. 2005 Nov 24;353(21):2243–53.

129. Monclair T, Brodeur GM, Ambros PF, Brisse HJ, Cecchetto G, Holmes K, et al. The International Neuroblastoma Risk Group (INRG) staging system: an INRG Task Force report. J Clin Oncol Off J Am Soc Clin Oncol. 2009 Jan 10;27(2):298–303.

130. Shimada H, Ambros IM, Dehner LP, Hata J, Joshi VV, Roald B, et al. The International Neuroblastoma Pathology Classification (the Shimada system). Cancer. 1999 Jul 15;86(2):364–72.

131. Maris JM, Hogarty MD, Bagatell R, Cohn SL. Neuroblastoma. Lancet Lond Engl. 2007 Jun 23;369(9579):2106–20.

132. Weiss WA, Aldape K, Mohapatra G, Feuerstein BG, Bishop JM. Targeted expression of MYCN causes neuroblastoma in transgenic mice. EMBO J. 1997 Jun 2;16(11):2985–95.

133. Hackett CS, Hodgson JG, Law ME, Fridlyand J, Osoegawa K, de Jong PJ, et al. Genome-wide array CGH analysis of murine neuroblastoma reveals distinct genomic aberrations which parallel those in human tumors. Cancer Res. 2003 Sep 1;63(17):5266–73.

134. Burkhart CA, Cheng AJ, Madafiglio J, Kavallaris M, Mili M, Marshall GM, et al. Effects of MYCN antisense oligonucleotide administration on tumorigenesis in a murine model of neuroblastoma. J Natl Cancer Inst. 2003 Sep 17;95(18):1394–403.

135. Lutz W, Stöhr M, Schürmann J, Wenzel A, Löhr A, Schwab M. Conditional expression of N-myc in human neuroblastoma cells increases expression of alpha-prothymosin and ornithine decarboxylase and accelerates progression into S-phase early after mitogenic stimulation of quiescent cells. Oncogene. 1996 Aug 15;13(4):803–12.

136. Schulte JH, Horn S, Otto T, Samans B, Heukamp LC, Eilers UC, et al. MYCN regulates oncogenic MicroRNAs in neuroblastoma. Int J Cancer. 2008 Feb 1;122(3):699–704.

137. Nuchtern JG, London WB, Barnewolt CE, Naranjo A, McGrady PW, Geiger JD, et al. A prospective study of expectant observation as primary therapy for neuroblastoma in young infants: a Children's Oncology Group study. Ann Surg. 2012 Oct;256(4):573–80.

138. Park JR, Bagatell R, London WB, Maris JM, Cohn SL, Mattay KK, et al. Children's Oncology Group's 2013 blueprint for research: neuroblastoma. Pediatr Blood Cancer. 2013 Jun;60(6):985–93.

139. Louis CU, Shohet JM. Neuroblastoma: molecular pathogenesis and therapy. Annu Rev Med. 2015;66:49–63.

140. Yu AL, Gilman AL, Ozkaynak MF, London WB, Kreissman SG, Chen HX, et al. Anti-GD2 antibody with GM-CSF, interleukin-2, and isotretinoin for neuroblastoma. N Engl J Med. 2010 Sep 30;363(14):1324–34.

141. Wang XD, Hu R, Ding Q, Savage TK, Huffman KE, Williams N, et al. Subtype-specific secretomic characterization of pulmonary neuroendocrine tumor cells. Nat Commun. 2019 Jul

19;10(1):3201.

142. Lamarca A, Frizziero M, Barriuso J, McNamara MG, Hubner RA, Valle JW. Urgent need for consensus: international survey of clinical practice exploring use of platinum-etoposide chemotherapy for advanced extra-pulmonary high grade neuroendocrine carcinoma (EP-G3-NEC). Clin Transl Oncol Off Publ Fed Span Oncol Soc Natl Cancer Inst Mex. 2019 Jul;21(7):950–3.

143. González I, Lu HC, Sninsky J, Yang C, Bishnupuri K, Dieckgraefe B, et al. Insulinoma-associated protein 1 expression in primary and metastatic neuroendocrine neoplasms of the gastrointestinal and pancreaticobiliary tracts. Histopathology. 2019 Oct;75(4):568–77.

144. Roy M, Buehler DG, Zhang R, Schwalbe ML, Baus RM, Salamat MS, et al. Expression of Insulinoma-Associated Protein 1 (INSM1) and Orthopedia Homeobox (OTP) in Tumors with Neuroendocrine Differentiation at Rare Sites. Endocr Pathol. 2019 Mar;30(1):35–42.

145. Kim IE, Amin A, Wang LJ, Cheng L, Perrino CM. Insulinoma-associated Protein 1 (INSM1) Expression in Small Cell Neuroendocrine Carcinoma of the Urinary Tract. Appl Immunohistochem Mol Morphol AIMM. 2020 Oct;28(9):687–93.

146. Sinha N, Gaston D, Manders D, Goudie M, Matsuoka M, Xie T, et al. Characterization of genome-wide copy number aberrations in colonic mixed adenoneuroendocrine carcinoma and neuroendocrine carcinoma reveals recurrent amplification of PTGER4 and MYC genes. Hum Pathol. 2018 Mar;73:16–25.

147. Jesinghaus M, Konukiewitz B, Keller G, Kloor M, Steiger K, Reiche M, et al. Colorectal mixed adenoneuroendocrine carcinomas and neuroendocrine carcinomas are genetically closely related to colorectal adenocarcinomas. Mod Pathol Off J U S Can Acad Pathol Inc. 2017 Apr;30(4):610–9.

148. Organisation mondiale de la santé, Centre international de recherche sur le cancer, editors. Female genital tumours. 5th ed. Lyon: International agency for research on cancer; 2020. (World health organization classification of tumours).

149. Organisation mondiale de la santé, Centre international de recherche sur le cancer, editors. WHO classification of tumours of the urinary system and male genital organs. Lyon: International agency for research on cancer; 2016. (World health organization classification of tumours).

150. Pelosi G, Bianchi F, Dama E, Simbolo M, Mafficini A, Sonzogni A, et al. Most high-grade neuroendocrine tumours of the lung are likely to secondarily develop from pre-existing carcinoids: innovative findings skipping the current pathogenesis paradigm. Virchows Arch Int J Pathol. 2018 Apr;472(4):567–77.

151. Miyashita N, Horie M, Suzuki HI, Yoshihara M, Djureinovic D, Persson J, et al. An Integrative Analysis of Transcriptome and Epigenome Features of ASCL1-Positive Lung Adenocarcinomas. J Thorac Oncol Off Publ Int Assoc Study Lung Cancer. 2018 Nov;13(11):1676–91.

152. Rudin CM, Pietanza MC, Bauer TM, Ready N, Morgensztern D, Glisson BS, et al.

Rovalpituzumab tesirine, a DLL3-targeted antibody-drug conjugate, in recurrent small-cell lung cancer: a first-in-human, first-in-class, open-label, phase 1 study. Lancet Oncol. 2017 Jan;18(1):42–51.

153. Hermans BCM, Derks JL, Thunnissen E, van Suylen RJ, den Bakker MA, Groen HJM, et al. DLL3 expression in large cell neuroendocrine carcinoma (LCNEC) and association with molecular subtypes and neuroendocrine profile. Lung Cancer Amst Neth. 2019 Dec;138:102–8.

154. Koshkin VS, Garcia JA, Reynolds J, Elson P, Magi-Galluzzi C, McKenney JK, et al. Transcriptomic and Protein Analysis of Small-cell Bladder Cancer (SCBC) Identifies Prognostic Biomarkers and DLL3 as a Relevant Therapeutic Target. Clin Cancer Res Off J Am Assoc Cancer Res. 2019 Jan 1;25(1):210–21.

155. Wael H, Yoshida R, Kudoh S, Hasegawa K, Niimori-Kita K, Ito T. Notch1 signaling controls cell proliferation, apoptosis and differentiation in lung carcinoma. Lung Cancer Amst Neth. 2014 Aug;85(2):131–40.

156. Sakakibara R, Kobayashi M, Takahashi N, Inamura K, Ninomiya H, Wakejima R, et al. Insulinoma-associated Protein 1 (INSM1) Is a Better Marker for the Diagnosis and Prognosis Estimation of Small Cell Lung Carcinoma Than Neuroendocrine Phenotype Markers Such as Chromogranin A, Synaptophysin, and CD56. Am J Surg Pathol. 2020 Jun;44(6):757–64.

157. Chen C, Breslin MB, Lan MS. Sonic hedgehog signaling pathway promotes INSM1 transcription factor in neuroendocrine lung cancer. Cell Signal. 2018 Jun;46:83–91.

158. McColl K, Wildey G, Sakre N, Lipka MB, Behtaj M, Kresak A, et al. Reciprocal expression of INSM1 and YAP1 defines subgroups in small cell lung cancer. Oncotarget. 2017 Sep 26;8(43):73745–56.

159. Jung M, Russell AJ, Liu B, George J, Liu PY, Liu T, et al. A Myc Activity Signature Predicts Poor Clinical Outcomes in Myc-Associated Cancers. Cancer Res. 2017 Feb 15;77(4):971–81.

160. Zafar A, Wang W, Liu G, Wang X, Xian W, McKeon F, et al. Molecular targeting therapies for neuroblastoma: Progress and challenges. Med Res Rev. 2021 Mar;41(2):961–1021.

161. Matthay KK, Maris JM, Schleiermacher G, Nakagawara A, Mackall CL, Diller L, et al. Neuroblastoma. Nat Rev Dis Primer. 2016 Nov 10;2:16078.

162. Liang WH, Federico SM, London WB, Naranjo A, Irwin MS, Volchenboum SL, et al. Tailoring Therapy for Children With Neuroblastoma on the Basis of Risk Group Classification: Past, Present, and Future. JCO Clin Cancer Inform. 2020 Oct;4:895–905.

163. Crabtree JS, Singleton CS, Miele L. Notch Signaling in Neuroendocrine Tumors. Front Oncol. 2016;6:94.

164. Baine MK, Hsieh MS, Lai WV, Egger JV, Jungbluth AA, Daneshbod Y, et al. SCLC Subtypes Defined by ASCL1, NEUROD1, POU2F3, and YAP1: A Comprehensive Immunohistochemical and Histopathologic Characterization. J Thorac Oncol Off Publ Int Assoc Study Lung Cancer. 2020 Dec;15(12):1823–35.

165. Gay CM, Stewart CA, Park EM, Diao L, Groves SM, Heeke S, et al. Patterns of transcription factor programs and immune pathway activation define four major subtypes of SCLC with distinct therapeutic vulnerabilities. Cancer Cell. 2021 Mar 8;39(3):346-360.e7.

166. Derks JL, Dingemans AMC, van Suylen RJ, den Bakker MA, Damhuis RAM, van den Broek EC, et al. Is the sum of positive neuroendocrine immunohistochemical stains useful for diagnosis of large cell neuroendocrine carcinoma (LCNEC) on biopsy specimens? Histopathology. 2019 Mar;74(4):555–66.

167. Shida T, Furuya M, Kishimoto T, Nikaido T, Tanizawa T, Koda K, et al. The expression of NeuroD and mASH1 in the gastroenteropancreatic neuroendocrine tumors. Mod Pathol Off J U S Can Acad Pathol Inc. 2008 Nov;21(11):1363–70.

168. Juhlin CC. Second-Generation Neuroendocrine Immunohistochemical Markers: Reflections from Clinical Implementation. Biology. 2021 Sep 5;10(9):874.

169. Rostomily RC, Bermingham-McDonogh O, Berger MS, Tapscott SJ, Reh TA, Olson JM. Expression of neurogenic basic helix-loop-helix genes in primitive neuroectodermal tumors. Cancer Res. 1997 Aug 15;57(16):3526–31.

170. Kitazono I, Hamada T, Yoshimura T, Kirishima M, Yokoyama S, Akahane T, et al. PCP4/PEP19 downregulates neurite outgrowth via transcriptional regulation of Ascl1 and NeuroD1 expression in human neuroblastoma M17 cells. Lab Investig J Tech Methods Pathol. 2020 Dec;100(12):1551–63.

171. Lee TY, Cho IS, Bashyal N, Naya FJ, Tsai MJ, Yoon JS, et al. ERK Regulates NeuroD1-mediated Neurite Outgrowth via Proteasomal Degradation. Exp Neurobiol. 2020 Jun 30;29(3):189–206.

172. Lu F, Kishida S, Mu P, Huang P, Cao D, Tsubota S, et al. NeuroD1 promotes neuroblastoma cell growth by inducing the expression of ALK. Cancer Sci. 2015 Apr;106(4):390–6.

173. Li J, Neumann I, Volkmer I, Staege MS. Down-regulation of achaete-scute complex homolog 1 (ASCL1) in neuroblastoma cells induces up-regulation of insulin-like growth factor 2 (IGF2). Mol Biol Rep. 2011 Mar;38(3):1515–21.

174. Kasim M, Heß V, Scholz H, Persson PB, Fähling M. Achaete-Scute Homolog 1 Expression Controls Cellular Differentiation of Neuroblastoma. Front Mol Neurosci. 2016;9:156.

175. Chen C, Lan MS. A promoter-driven assay for INSM1-associated signaling pathway in neuroblastoma. Cell Signal. 2020 Dec;76:109785.

176. Chen C, Breslin MB, Guidry JJ, Lan MS. 5'-Iodotubercidin represses insulinoma-associated-1 expression, decreases cAMP levels, and suppresses human neuroblastoma cell growth. J Biol Chem. 2019 Apr 5;294(14):5456–65.

177. Chen C, Breslin MB, Lan MS. INSM1 increases N-myc stability and oncogenesis via a positive-feedback loop in neuroblastoma. Oncotarget. 2015 Nov 3;6(34):36700–12.

178. Wang H, Krishnan C, Charville GW. INSM1 Expression in Peripheral Neuroblastic Tumors and

Other Embryonal Neoplasms. Pediatr Dev Pathol Off J Soc Pediatr Pathol Paediatr Pathol Soc. 2019 Oct;22(5):440–8.

179. Organisation mondiale de la santé, Centre international de recherche sur le cancer, editors. WHO classification of tumours of endocrine organs. 4th ed. Lyon: International agency for research on cancer; 2017. (World health organization classification of tumours).

180. Chang HH, Lee H, Hu MK, Tsao PN, Juan HF, Huang MC, et al. Notch1 expression predicts an unfavorable prognosis and serves as a therapeutic target of patients with neuroblastoma. Clin Cancer Res Off J Am Assoc Cancer Res. 2010 Sep 1;16(17):4411–20.

181. Dorneburg C, Goß AV, Fischer M, Roels F, Barth TFE, Berthold F, et al. γ-Secretase inhibitor I inhibits neuroblastoma cells, with NOTCH and the proteasome among its targets. Oncotarget. 2016 Sep 27;7(39):62799–813.

182. Shiraishi T, Sakaitani M, Otsuguro S, Maenaka K, Suzuki T, Nakaya T. Novel Notch signaling inhibitor NSI-1 suppresses nuclear translocation of the Notch intracellular domain. Int J Mol Med [Internet]. 2019 Jul 19 [cited 2022 Apr 26]; Available from: http://www.spandidos-publications.com/10.3892/ijmm.2019.4280

183. Ross RA, Walton JD, Han D, Guo HF, Cheung NKV. A distinct gene expression signature characterizes human neuroblastoma cancer stem cells. Stem Cell Res. 2015 Sep;15(2):419–26.

184. Minami K, Jimbo N, Tanaka Y, Ogawa H, Hokka D, Nishio W, et al. Insulinoma-associated protein 1 is a prognostic biomarker in pulmonary high-grade neuroendocrine carcinoma. J Surg Oncol. 2020 Aug;122(2):243–53.

185. Huang P, Kishida S, Cao D, Murakami-Tonami Y, Mu P, Nakaguro M, et al. The neuronal differentiation factor NeuroD1 downregulates the neuronal repellent factor Slit2 expression and promotes cell motility and tumor formation of neuroblastoma. Cancer Res. 2011 Apr 15;71(8):2938–48.

186. Shen X, Xu X, Xie C, Liu H, Yang D, Zhang J, et al. YAP promotes the proliferation of neuroblastoma cells through decreasing the nuclear location of p27Kip1 mediated by Akt. Cell Prolif. 2020 Feb;53(2):e12734.

187. Yang C, Tan J, Zhu J, Wang S, Wei G. YAP promotes tumorigenesis and cisplatin resistance in neuroblastoma. Oncotarget. 2017 Jun 6;8(23):37154–63.

188. Coggins GE, Farrel A, Rathi KS, Hayes CM, Scolaro L, Rokita JL, et al. YAP1 Mediates Resistance to MEK1/2 Inhibition in Neuroblastomas with Hyperactivated RAS Signaling. Cancer Res. 2019 Dec 15;79(24):6204–14.

189. Liu M, Inoue K, Leng T, Zhou A, Guo S, Xiong ZG. ASIC1 promotes differentiation of neuroblastoma by negatively regulating Notch signaling pathway. Oncotarget. 2017 Jan 31;8(5):8283–93.

190. Curado MP, International Agency for Research on Cancer, editors. Cancer incidence in five continents. Vol. 9 / ed. by M. P. Curado. Lyon: International Agency for Research on Cancer; 2008. 837 p. (IARC scientific publications; vol. 9).

191. Parkin DM, Bray F, Ferlay J, Pisani P. Global cancer statistics, 2002. CA Cancer J Clin. 2005 Apr;55(2):74–108.

192. Davies L, Welch HG. Increasing incidence of thyroid cancer in the United States, 1973-2002. JAMA. 2006 May 10;295(18):2164–7.

193. Leenhardt L, Bernier MO, Boin-Pineau MH, Conte Devolx B, Maréchaud R, Niccoli-Sire P, et al. Advances in diagnostic practices affect thyroid cancer incidence in France. Eur J Endocrinol. 2004 Feb;150(2):133–9.

194. Yu GP, Li JCL, Branovan D, McCormick S, Schantz SP. Thyroid cancer incidence and survival in the national cancer institute surveillance, epidemiology, and end results race/ethnicity groups. Thyroid Off J Am Thyroid Assoc. 2010 May;20(5):465–73.

195. Noone AM, Cronin KA, Altekruse SF, Howlader N, Lewis DR, Petkov VI, et al. Cancer Incidence and Survival Trends by Subtype Using Data from the Surveillance Epidemiology and End Results Program, 1992-2013. Cancer Epidemiol Biomark Prev Publ Am Assoc Cancer Res Cosponsored Am Soc Prev Oncol. 2017 Apr;26(4):632–41.

196. Smallridge RC, Ain KB, Asa SL, Bible KC, Brierley JD, Burman KD, et al. American Thyroid Association guidelines for management of patients with anaplastic thyroid cancer. Thyroid Off J Am Thyroid Assoc. 2012 Nov;22(11):1104–39.

197. Ron E, Lubin JH, Shore RE, Mabuchi K, Modan B, Pottern LM, et al. Thyroid cancer after exposure to external radiation: a pooled analysis of seven studies. Radiat Res. 1995 Mar;141(3):259–77.

198. Williams D. Radiation carcinogenesis: lessons from Chernobyl. Oncogene. 2008 Dec;27 Suppl 2:S9-18.

199. Dal Maso L, Lise M, Zambon P, Falcini F, Crocetti E, Serraino D, et al. Incidence of thyroid cancer in Italy, 1991-2005: time trends and age-period-cohort effects. Ann Oncol Off J Eur Soc Med Oncol. 2011 Apr;22(4):957–63.

200. Cardis E, Kesminiene A, Ivanov V, Malakhova I, Shibata Y, Khrouch V, et al. Risk of thyroid cancer after exposure to 131I in childhood. J Natl Cancer Inst. 2005 May 18;97(10):724–32.

201. Fiore E, Rago T, Provenzale MA, Scutari M, Ugolini C, Basolo F, et al. L-thyroxine-treated patients with nodular goiter have lower serum TSH and lower frequency of papillary thyroid cancer: results of a cross-sectional study on 27 914 patients. Endocr Relat Cancer. 2010 Mar;17(1):231–9.

202. Fiore E, Rago T, Provenzale MA, Scutari M, Ugolini C, Basolo F, et al. Lower levels of TSH are associated with a lower risk of papillary thyroid cancer in patients with thyroid nodular disease: thyroid autonomy may play a protective role. Endocr Relat Cancer. 2009 Dec;16(4):1251–60.

203. Haymart MR, Repplinger DJ, Leverson GE, Elson DF, Sippel RS, Jaume JC, et al. Higher serum thyroid stimulating hormone level in thyroid nodule patients is associated with greater risks of differentiated thyroid cancer and advanced tumor stage. J Clin Endocrinol Metab. 2008

Mar;93(3):809–14.

204. Fiore E, Latrofa F, Vitti P. Iodine, thyroid autoimmunity and cancer. Eur Thyroid J. 2015 Mar;4(1):26–35.

205. D'Avanzo B, La Vecchia C, Franceschi S, Negri E, Talamini R. History of thyroid diseases and subsequent thyroid cancer risk. Cancer Epidemiol Biomark Prev Publ Am Assoc Cancer Res Cosponsored Am Soc Prev Oncol. 1995 May;4(3):193–9.

206. Franceschi S, Preston-Martin S, Dal Maso L, Negri E, La Vecchia C, Mack WJ, et al. A pooled analysis of case-control studies of thyroid cancer. IV. Benign thyroid diseases. Cancer Causes Control CCC. 1999 Dec;10(6):583–95.

207. Hemminki K, Eng C, Chen B. Familial risks for nonmedullary thyroid cancer. J Clin Endocrinol Metab. 2005 Oct;90(10):5747–53.

208. Giannelli SM, McPhaul L, Nakamoto J, Gianoukakis AG. Familial adenomatous polyposis-associated, cribriform morular variant of papillary thyroid carcinoma harboring a K-RAS mutation: case presentation and review of molecular mechanisms. Thyroid Off J Am Thyroid Assoc. 2014 Jul;24(7):1184–9.

209. Pilarski R, Burt R, Kohlman W, Pho L, Shannon KM, Swisher E. Cowden syndrome and the PTEN hamartoma tumor syndrome: systematic review and revised diagnostic criteria. J Natl Cancer Inst. 2013 Nov 6;105(21):1607–16.

210. Wells SA, Pacini F, Robinson BG, Santoro M. Multiple endocrine neoplasia type 2 and familial medullary thyroid carcinoma: an update. J Clin Endocrinol Metab. 2013 Aug;98(8):3149–64.

211. Hay ID. Papillary thyroid carcinoma. Endocrinol Metab Clin North Am. 1990 Sep;19(3):545–76.

212. Tscholl-Ducommun J, Hedinger ChrE. Papillary thyroid carcinomas: Morphology and prognosis. Virchows Arch A Pathol Anat Histol. 1982 Jun;396(1):19–39.

213. Frauenhoffer CM, Patchefsky AS, Cobanoglu A. Thyroid carcinoma: a clinical and pathologic study of 125 cases. Cancer. 1979 Jun;43(6):2414–21.

214. LiVolsi VA. Papillary neoplasms of the thyroid. Pathologic and prognostic features. Am J Clin Pathol. 1992 Mar;97(3):426–34.

215. Nikiforov YE, Seethala RR, Tallini G, Baloch ZW, Basolo F, Thompson LDR, et al. Nomenclature Revision for Encapsulated Follicular Variant of Papillary Thyroid Carcinoma: A Paradigm Shift to Reduce Overtreatment of Indolent Tumors. JAMA Oncol. 2016 Aug 1;2(8):1023–9.

216. Fischer AH, Bond JA, Taysavang P, Battles OE, Wynford-Thomas D. Papillary thyroid carcinoma oncogene (RET/PTC) alters the nuclear envelope and chromatin structure. Am J Pathol. 1998 Nov;153(5):1443–50.

217. Scopa CD, Melachrinou M, Saradopoulou C, Merino MJ. The significance of the grooved

nucleus in thyroid lesions. Mod Pathol Off J U S Can Acad Pathol Inc. 1993 Nov;6(6):691–4.

218. Baloch ZW, LiVolsi VA. Etiology and significance of the optically clear nucleus. Endocr Pathol. 2002;13(4):289–99.

219. Chan JK, Saw D. The grooved nucleus. A useful diagnostic criterion of papillary carcinoma of the thyroid. Am J Surg Pathol. 1986 Oct;10(10):672–9.

220. Johannessen JV, Sobrinho-Simões M. The origin and significance of thyroid psammoma bodies. Lab Investig J Tech Methods Pathol. 1980 Sep;43(3):287–96.

221. Tunio GM, Hirota S, Nomura S, Kitamura Y. Possible relation of osteopontin to development of psammoma bodies in human papillary thyroid cancer. Arch Pathol Lab Med. 1998 Dec;122(12):1087–90.

222. Franssila KO. Is the differentiation between papillary and follicular thyroid carcinoma valid? Cancer. 1973 Oct;32(4):853–64.

223. Carcangiu ML, Zampi G, Pupi A, Castagnoli A, Rosai J. Papillary carcinoma of the thyroid. A clinicopathologic study of 241 cases treated at the University of Florence, Italy. Cancer. 1985 Feb 15;55(4):805–28.

224. Koperek O, Asari R, Niederle B, Kaserer K. Desmoplastic stromal reaction in papillary thyroid microcarcinoma. Histopathology. 2011 May;58(6):919–24.

225. Chan JK, Carcangiu ML, Rosai J. Papillary carcinoma of thyroid with exuberant nodular fasciitis-like stroma. Report of three cases. Am J Clin Pathol. 1991 Mar;95(3):309–14.

226. Guiter GE, DeLellis RA. Multinucleate giant cells in papillary thyroid carcinoma. A morphologic and immunohistochemical study. Am J Clin Pathol. 1996 Dec;106(6):765–8.

227. Bejarano PA, Nikiforov YE, Swenson ES, Biddinger PW. Thyroid transcription factor-1, thyroglobulin, cytokeratin 7, and cytokeratin 20 in thyroid neoplasms. Appl Immunohistochem Mol Morphol AIMM. 2000 Sep;8(3):189–94.

228. Henzen-Logmans SC, Mullink H, Ramaekers FC, Tadema T, Meijer CJ. Expression of cytokeratins and vimentin in epithelial cells of normal and pathologic thyroid tissue. Virchows Arch A Pathol Anat Histopathol. 1987;410(4):347–54.

229. Stanta G, Carcangiu ML, Rosai J. The biochemical and immunohistochemical profile of thyroid neoplasia. Pathol Annu. 1988;23 Pt 1:129–57.

230. Permanetter W, Nathrath WB, Löhrs U. Immunohistochemical analysis of thyroglobulin and keratin in benign and malignant thyroid tumours. Virchows Arch A Pathol Anat Histopathol. 1982;398(2):221–8.

231. Buley ID, Gatter KC, Heryet A, Mason DY. Expression of intermediate filament proteins in normal and diseased thyroid glands. J Clin Pathol. 1987 Feb;40(2):136–42.

232. Damiani S, Fratamico F, Lapertosa G, Dina R, Eusebi V. Alcian blue and epithelial membrane

antigen are useful markers in differentiating benign from malignant papillae in thyroid lesions. Virchows Arch A Pathol Anat Histopathol. 1991;419(2):131–5.

233. Chan JK, Tse CC. Mucin production in metastatic papillary carcinoma of the thyroid. Hum Pathol. 1988 Feb;19(2):195–200.

234. Torregrossa L, Faviana P, Camacci T, Materazzi G, Berti P, Minuto M, et al. Galectin-3 is highly expressed in nonencapsulated papillary thyroid carcinoma but weakly expressed in encapsulated type; comparison with Hector Battifora mesothelial cell 1 immunoreactivity. Hum Pathol. 2007 Oct;38(10):1482–8.

235. Casey MB, Lohse CM, Lloyd RV. Distinction between papillary thyroid hyperplasia and papillary thyroid carcinoma by immunohistochemical staining for cytokeratin 19, galectin-3, and HBME-1. Endocr Pathol. 2003;14(1):55–60.

236. Bartolazzi A, Gasbarri A, Papotti M, Bussolati G, Lucante T, Khan A, et al. Application of an immunodiagnostic method for improving preoperative diagnosis of nodular thyroid lesions. Lancet Lond Engl. 2001 May 26;357(9269):1644–50.

237. Nakamura N, Erickson LA, Jin L, Kajita S, Zhang H, Qian X, et al. Immunohistochemical separation of follicular variant of papillary thyroid carcinoma from follicular adenoma. Endocr Pathol. 2006;17(3):213–23.

238. Scognamiglio T, Hyjek E, Kao J, Chen YT. Diagnostic usefulness of HBME1, galectin-3, CK19, and CITED1 and evaluation of their expression in encapsulated lesions with questionable features of papillary thyroid carcinoma. Am J Clin Pathol. 2006 Nov;126(5):700–8.

239. Nechifor-Boilă A, Cătană R, Loghin A, Radu TG, Borda A. Diagnostic value of HBME-1, CD56, Galectin-3 and Cytokeratin-19 in papillary thyroid carcinomas and thyroid tumors of uncertain malignant potential. Romanian J Morphol Embryol Rev Roum Morphol Embryol. 2014;55(1):49–56.

240. Sahoo S, Hoda SA, Rosai J, DeLellis RA. Cytokeratin 19 immunoreactivity in the diagnosis of papillary thyroid carcinoma: a note of caution. Am J Clin Pathol. 2001 Nov;116(5):696–702.

241. Lang W, Borrusch H, Bauer L. Occult Carcinomas of the Thyroid: Evaluation of 1,020 Sequential Autopsies. Am J Clin Pathol. 1988 Jul 1;90(1):72–6.

242. Poli F, Trezzi R, Rosai J. Images in pathology. Single thyroid follicle involved by papillary carcinoma: partially classic and partially oncocytic. Int J Surg Pathol. 2009 Jun;17(3):272–3.

243. Yamamoto Y, Maeda T, Izumi K, Otsuka H. Occult papillary carcinoma of the thyroid. A study of 408 autopsy cases. Cancer. 1990 Mar 1;65(5):1173–9.

244. Carcangiu ML, Zampi G, Rosai J. Papillary thyroid carcinoma: a study of its many morphologic expressions and clinical correlates. Pathol Annu. 1985;20 Pt 1:1–44.

245. Rosai J, LiVolsi VA, Sobrinho-Simoes M, Williams ED. Renaming papillary microcarcinoma of the thyroid gland: the Porto proposal. Int J Surg Pathol. 2003 Oct;11(4):249–51.

246. Gikas PW, Labow SS, DiGiulio W, Finger JE. Occult metastasis from occult papillary carcinoma of the thyroid. Cancer. 1967 Dec;20(12):2100–4.

247. Mercante G, Frasoldati A, Pedroni C, Formisano D, Renna L, Piana S, et al. Prognostic factors affecting neck lymph node recurrence and distant metastasis in papillary microcarcinoma of the thyroid: results of a study in 445 patients. Thyroid Off J Am Thyroid Assoc. 2009 Jul;19(7):707–16.

248. Bernstein J, Virk RK, Hui P, Prasad A, Westra WH, Tallini G, et al. Tall cell variant of papillary thyroid microcarcinoma: clinicopathologic features with BRAF(V600E) mutational analysis. Thyroid Off J Am Thyroid Assoc. 2013 Dec;23(12):1525–31.

249. Evans HL. Encapsulated papillary neoplasms of the thyroid. A study of 14 cases followed for a minimum of 10 years. Am J Surg Pathol. 1987 Aug;11(8):592–7.

250. Schröder S, Böcker W, Dralle H, Kortmann KB, Stern C. The encapsulated papillary carcinoma of the thyroid a morphologic subtype of the papillary thyroid carcinoma. Cancer. 1984 Jul 1;54(1):90–3.

251. Eloy C, Santos J, Soares P, Sobrinho-Simões M. Intratumoural lymph vessel density is related to presence of lymph node metastases and separates encapsulated from infiltrative papillary thyroid carcinoma. Virchows Arch Int J Pathol. 2011 Dec;459(6):595–605.

252. Rosaí J, Zampi G, Carcangiu ML. Papillary carcinoma of the thyroid. A discussion of its several morphologic expressions, with particular emphasis on the follicular variant. Am J Surg Pathol. 1983 Dec;7(8):809–17.

253. Gupta S, Ajise O, Dultz L, Wang B, Nonaka D, Ogilvie J, et al. Follicular variant of papillary thyroid cancer: encapsulated, nonencapsulated, and diffuse: distinct biologic and clinical entities. Arch Otolaryngol Head Neck Surg. 2012 Mar;138(3):227–33.

254. Nakamura T, Moriyama S, Nariya S, Sano K, Shirota H, Kato R. Macrofollicular variant of papillary thyroid carcinoma. Pathol Int. 1998 Jun;48(6):467–70.

255. Lugli A, Terracciano LM, Oberholzer M, Bubendorf L, Tornillo L. Macrofollicular variant of papillary carcinoma of the thyroid: a histologic, cytologic, and immunohistochemical study of 3 cases and review of the literature. Arch Pathol Lab Med. 2004 Jan;128(1):54–8.

256. Albores-Saavedra J, Gould E, Vardaman C, Vuitch F. The macrofollicular variant of papillary thyroid carcinoma: a study of 17 cases. Hum Pathol. 1991 Dec;22(12):1195–205.

257. Vanzati A, Mercalli F, Rosai J. The “sprinkling” sign in the follicular variant of papillary thyroid carcinoma: a clue to the recognition of this entity. Arch Pathol Lab Med. 2013 Dec;137(12):1707–9.

258. Ivanova R, Soares P, Castro P, Sobrinho-Simões M. Diffuse (or multinodular) follicular variant of papillary thyroid carcinoma: a clinicopathologic and immunohistochemical analysis of ten cases of an aggressive form of differentiated thyroid carcinoma. Virchows Arch Int J Pathol. 2002 Apr;440(4):418–24.

259. Mizukami Y, Nonomura A, Michigishi T, Ohmura K, Noguchi M, Ishizaki T. Diffuse follicular variant of papillary carcinoma of the thyroid. Histopathology. 1995 Dec;27(6):575–7.

260. Carcangiu ML, Bianchi S. Diffuse sclerosing variant of papillary thyroid carcinoma. Clinicopathologic study of 15 cases. Am J Surg Pathol. 1989 Dec;13(12):1041–9.

261. Fujimoto Y, Obara T, Ito Y, Kodama T, Aiba M, Yamaguchi K. Diffuse sclerosing variant of papillary carcinoma of the thyroid. Clinical importance, surgical treatment, and follow-up study. Cancer. 1990 Dec 1;66(11):2306–12.

262. Chan JK, Tsui MS, Tse CH. Diffuse sclerosing variant of papillary carcinoma of the thyroid: a histological and immunohistochemical study of three cases. Histopathology. 1987 Feb;11(2):191–201.

263. Walsh J, Griffin TP, Ryan CB, Fitzgibbon J, Sheahan P, Murphy MS. A Case Report Demonstrating How the Clinical Presentation of the Diffuse Sclerosing Variant of Papillary Thyroid Carcinoma Can Mimic Benign Riedel's Thyroiditis. Case Rep Endocrinol. 2015;2015:686085.

264. Thompson LDR, Wieneke JA, Heffess CS. Diffuse sclerosing variant of papillary thyroid carcinoma: a clinicopathologic and immunophenotypic analysis of 22 cases. Endocr Pathol. 2005;16(4):331–48.

265. Koo JS, Shin E, Hong SW. Immunohistochemical characteristics of diffuse sclerosing variant of papillary carcinoma: comparison with conventional papillary carcinoma. APMIS Acta Pathol Microbiol Immunol Scand. 2010 Oct;118(10):744–52.

266. Adeniran AJ, Zhu Z, Gandhi M, Steward DL, Fidler JP, Giordano TJ, et al. Correlation between genetic alterations and microscopic features, clinical manifestations, and prognostic characteristics of thyroid papillary carcinomas. Am J Surg Pathol. 2006 Feb;30(2):216–22.

267. Joung JY, Kim TH, Jeong DJ, Park SM, Cho YY, Jang HW, et al. Diffuse sclerosing variant of papillary thyroid carcinoma: major genetic alterations and prognostic implications. Histopathology. 2016 Jul;69(1):45–53.

268. Sheu SY, Schwertheim S, Worm K, Grabellus F, Schmid KW. Diffuse sclerosing variant of papillary thyroid carcinoma: lack of BRAF mutation but occurrence of RET/PTC rearrangements. Mod Pathol Off J U S Can Acad Pathol Inc. 2007 Jul;20(7):779–87.

269. Regalbuto C, Malandrino P, Tumminia A, Le Moli R, Vigneri R, Pezzino V. A diffuse sclerosing variant of papillary thyroid carcinoma: clinical and pathologic features and outcomes of 34 consecutive cases. Thyroid Off J Am Thyroid Assoc. 2011 Apr;21(4):383–9.

270. Koo JS, Hong S, Park CS. Diffuse sclerosing variant is a major subtype of papillary thyroid carcinoma in the young. Thyroid Off J Am Thyroid Assoc. 2009 Nov;19(11):1225–31.

271. Fukushima M, Ito Y, Hirokawa M, Akasu H, Shimizu K, Miyauchi A. Clinicopathologic characteristics and prognosis of diffuse sclerosing variant of papillary thyroid carcinoma in Japan: an 18-year experience at a single institution. World J Surg. 2009 May;33(5):958–62.

272. Chow SM, Chan JKC, Law SCK, Tang DLC, Ho CM, Cheung WY, et al. Diffuse sclerosing variant of papillary thyroid carcinoma--clinical features and outcome. Eur J Surg Oncol J Eur Soc Surg Oncol Br Assoc Surg Oncol. 2003 Jun;29(5):446–9.

273. Akaishi J, Sugino K, Kameyama K, Masaki C, Matsuzu K, Suzuki A, et al. Clinicopathologic features and outcomes in patients with diffuse sclerosing variant of papillary thyroid carcinoma. World J Surg. 2015 Jul;39(7):1728–35.

274. Ganly I, Ibrahimpasic T, Rivera M, Nixon I, Palmer F, Patel SG, et al. Prognostic implications of papillary thyroid carcinoma with tall-cell features. Thyroid Off J Am Thyroid Assoc. 2014 Apr;24(4):662–70.

275. Ghossein R, Livolsi VA. Papillary thyroid carcinoma tall cell variant. Thyroid Off J Am Thyroid Assoc. 2008 Nov;18(11):1179–81.

276. Morris LGT, Shaha AR, Tuttle RM, Sikora AG, Ganly I. Tall-cell variant of papillary thyroid carcinoma: a matched-pair analysis of survival. Thyroid Off J Am Thyroid Assoc. 2010 Feb;20(2):153–8.

277. Ghossein RA, Leboeuf R, Patel KN, Rivera M, Katabi N, Carlson DL, et al. Tall cell variant of papillary thyroid carcinoma without extrathyroid extension: biologic behavior and clinical implications. Thyroid Off J Am Thyroid Assoc. 2007 Jul;17(7):655–61.

278. Rivera M, Ghossein RA, Schoder H, Gomez D, Larson SM, Tuttle RM. Histopathologic characterization of radioactive iodine-refractory fluorodeoxyglucose-positron emission tomography-positive thyroid carcinoma. Cancer. 2008 Jul 1;113(1):48–56.

279. Liu X, Bishop J, Shan Y, Pai S, Liu D, Murugan AK, et al. Highly prevalent TERT promoter mutations in aggressive thyroid cancers. Endocr Relat Cancer. 2013 Aug;20(4):603–10.

280. Amacher AM, Goyal B, Lewis JS, El-Mofty SK, Chernock RD. Prevalence of a hobnail pattern in papillary, poorly differentiated, and anaplastic thyroid carcinoma: a possible manifestation of high-grade transformation. Am J Surg Pathol. 2015 Feb;39(2):260–5.

281. Asioli S, Erickson LA, Righi A, Lloyd RV. Papillary thyroid carcinoma with hobnail features: histopathologic criteria to predict aggressive behavior. Hum Pathol. 2013 Mar;44(3):320–8.

282. Kakudo K, Bai Y, Liu Z, Li Y, Ito Y, Ozaki T. Classification of thyroid follicular cell tumors: with special reference to borderline lesions. Endocr J. 2012;59(1):1–12.

283. Motosugi U, Murata SI, Nagata K, Yasuda M, Shimizu M. Thyroid papillary carcinoma with micropapillary and hobnail growth pattern: a histological variant with intermediate malignancy? Thyroid Off J Am Thyroid Assoc. 2009 May;19(5):535–7.

284. Lino-Silva LS, Domínguez-Malagón HR, Caro-Sánchez CH, Salcedo-Hernández RA. Thyroid gland papillary carcinomas with “micropapillary pattern,” a recently recognized poor prognostic finding: clinicopathologic and survival analysis of 7 cases. Hum Pathol. 2012 Oct;43(10):1596–600.

285. Asioli S, Erickson LA, Sebo TJ, Zhang J, Jin L, Thompson GB, et al. Papillary thyroid

carcinoma with prominent hobnail features: a new aggressive variant of moderately differentiated papillary carcinoma. A clinicopathologic, immunohistochemical, and molecular study of eight cases. Am J Surg Pathol. 2010 Jan;34(1):44–52.

286. Asioli S, Maletta F, Pagni F, Pacchioni D, Vanzati A, Mariani S, et al. Cytomorphologic and molecular features of hobnail variant of papillary thyroid carcinoma: case series and literature review. Diagn Cytopathol. 2014 Jan;42(1):78–84.

287. Bellevicine C, Cozzolino I, Malapelle U, Zeppa P, Troncone G. Cytological and molecular features of papillary thyroid carcinoma with prominent hobnail features: a case report. Acta Cytol. 2012;56(5):560–4.

288. Lubitz CC, Economopoulos KP, Pawlak AC, Lynch K, Dias-Santagata D, Faquin WC, et al. Hobnail variant of papillary thyroid carcinoma: an institutional case series and molecular profile. Thyroid Off J Am Thyroid Assoc. 2014 Jun;24(6):958–65.

289. Lam AKY, Lo CY, Lam KSL. Papillary carcinoma of thyroid: A 30-yr clinicopathological review of the histological variants. Endocr Pathol. 2005;16(4):323–30.

290. Nikiforov YE, Erickson LA, Nikiforova MN, Caudill CM, Lloyd RV. Solid variant of papillary thyroid carcinoma: incidence, clinical-pathologic characteristics, molecular analysis, and biologic behavior. Am J Surg Pathol. 2001 Dec;25(12):1478–84.

291. Nikiforov Y, Gnepp DR. Pediatric thyroid cancer after the Chernobyl disaster. Pathomorphologic study of 84 cases (1991-1992) from the Republic of Belarus. Cancer. 1994 Jul 15;74(2):748–66.

292. Tronko MD, Bogdanova TI, Komissarenko IV, Epstein OV, Oliynyk V, Kovalenko A, et al. Thyroid carcinoma in children and adolescents in Ukraine after the Chernobyl nuclear accident: statistical data and clinicomorphologic characteristics. Cancer. 1999 Jul 1;86(1):149–56.

293. Mizukami Y, Noguchi M, Michigishi T, Nonomura A, Hashimoto T, Otakes S, et al. Papillary thyroid carcinoma in Kanazawa, Japan: prognostic significance of histological subtypes. Histopathology. 1992 Mar;20(3):243–50.

294. Nikiforov YE, Rowland JM, Bove KE, Monforte-Munoz H, Fagin JA. Distinct pattern of ret oncogene rearrangements in morphological variants of radiation-induced and sporadic thyroid papillary carcinomas in children. Cancer Res. 1997 May 1;57(9):1690–4.

295. Berho M, Suster S. The oncocytic variant of papillary carcinoma of the thyroid: a clinicopathologic study of 15 cases. Hum Pathol. 1997 Jan;28(1):47–53.

296. Dickersin GR, Vickery AL, Smith SB. Papillary carcinoma of the thyroid, oxyphil cell type, “clear cell” variant: a light- and electron-microscopic study. Am J Surg Pathol. 1980 Oct;4(5):501–9.

297. Montone KT, Baloch ZW, LiVolsi VA. The thyroid Hürthle (oncocytic) cell and its associated pathologic conditions: a surgical pathology and cytopathology review. Arch Pathol Lab Med. 2008 Aug;132(8):1241–50.

298. Mai KT, Thomas J, Yazdi HM, Commons AS, Lamba M, Stinson AW. Pathologic study and clinical significance of Hürthle cell papillary thyroid carcinoma. Appl Immunohistochem Mol Morphol AIMM. 2004 Dec;12(4):329–37.

299. Lloyd RV, Buehler D, Khanafshar E. Papillary thyroid carcinoma variants. Head Neck Pathol. 2011 Mar;5(1):51–6.

300. Cohen Y, Xing M, Mambo E, Guo Z, Wu G, Trink B, et al. BRAF mutation in papillary thyroid carcinoma. J Natl Cancer Inst. 2003 Apr 16;95(8):625–7.

301. Kimura ET, Nikiforova MN, Zhu Z, Knauf JA, Nikiforov YE, Fagin JA. High prevalence of BRAF mutations in thyroid cancer: genetic evidence for constitutive activation of the RET/PTC-RAS-BRAF signaling pathway in papillary thyroid carcinoma. Cancer Res. 2003 Apr 1;63(7):1454–7.

302. Soares P, Trovisco V, Rocha AS, Lima J, Castro P, Preto A, et al. BRAF mutations and RET/PTC rearrangements are alternative events in the etiopathogenesis of PTC. Oncogene. 2003 Jul 17;22(29):4578–80.

303. Basolo F, Torregrossa L, Giannini R, Miccoli M, Lupi C, Sensi E, et al. Correlation between the BRAF V600E mutation and tumor invasiveness in papillary thyroid carcinomas smaller than 20 millimeters: analysis of 1060 cases. J Clin Endocrinol Metab. 2010 Sep;95(9):4197–205.

304. Trovisco V, Vieira de Castro I, Soares P, Máximo V, Silva P, Magalhães J, et al. BRAF mutations are associated with some histological types of papillary thyroid carcinoma. J Pathol. 2004 Feb;202(2):247–51.

305. Cancer Genome Atlas Research Network. Integrated genomic characterization of papillary thyroid carcinoma. Cell. 2014 Oct 23;159(3):676–90.

306. Ciampi R, Knauf JA, Kerler R, Gandhi M, Zhu Z, Nikiforova MN, et al. Oncogenic AKAP9-BRAF fusion is a novel mechanism of MAPK pathway activation in thyroid cancer. J Clin Invest. 2005 Jan;115(1):94–101.

307. Zhu Z, Gandhi M, Nikiforova MN, Fischer AH, Nikiforov YE. Molecular profile and clinical-pathologic features of the follicular variant of papillary thyroid carcinoma. An unusually high prevalence of ras mutations. Am J Clin Pathol. 2003 Jul;120(1):71–7.

308. Xing M, Liu R, Liu X, Murugan AK, Zhu G, Zeiger MA, et al. BRAF V600E and TERT promoter mutations cooperatively identify the most aggressive papillary thyroid cancer with highest recurrence. J Clin Oncol Off J Am Soc Clin Oncol. 2014 Sep 1;32(25):2718–26.

309. Bullock M, Ren Y, O'Neill C, Gill A, Aniss A, Sywak M, et al. TERT promoter mutations are a major indicator of recurrence and death due to papillary thyroid carcinomas. Clin Endocrinol (Oxf). 2016 Aug;85(2):283–90.

310. Melo M, da Rocha AG, Vinagre J, Batista R, Peixoto J, Tavares C, et al. TERT promoter mutations are a major indicator of poor outcome in differentiated thyroid carcinomas. J Clin Endocrinol Metab. 2014 May;99(5):E754-765.

311. Collini P, Sampietro G, Rosai J, Pilotti S. Minimally invasive (encapsulated) follicular carcinoma of the thyroid gland is the low-risk counterpart of widely invasive follicular carcinoma but not of insular carcinoma. Virchows Arch Int J Pathol. 2003 Jan;442(1):71–6.

312. Baloch ZW, LiVolsi VA. Follicular-patterned afflictions of the thyroid gland: reappraisal of the most discussed entity in endocrine pathology. Endocr Pathol. 2014 Mar;25(1):12–20.

313. Thompson LD, Wieneke JA, Paal E, Frommelt RA, Adair CF, Heffess CS. A clinicopathologic study of minimally invasive follicular carcinoma of the thyroid gland with a review of the English literature. Cancer. 2001 Feb 1;91(3):505–24.

314. Sobrinho-Simões M, Eloy C, Magalhães J, Lobo C, Amaro T. Follicular thyroid carcinoma. Mod Pathol Off J U S Can Acad Pathol Inc. 2011 Apr;24 Suppl 2:S10-18.

315. Ito Y, Hirokawa M, Masuoka H, Yabuta T, Kihara M, Higashiyama T, et al. Prognostic factors of minimally invasive follicular thyroid carcinoma: extensive vascular invasion significantly affects patient prognosis. Endocr J. 2013;60(5):637–42.

316. De Crea C, Raffaelli M, Sessa L, Ronti S, Fadda G, Bellantone C, et al. Actual incidence and clinical behaviour of follicular thyroid carcinoma: an institutional experience. ScientificWorldJournal. 2014;2014:952095.

317. Prasad ML, Pellegata NS, Huang Y, Nagaraja HN, de la Chapelle A, Kloos RT. Galectin-3, fibronectin-1, CITED-1, HBME1 and cytokeratin-19 immunohistochemistry is useful for the differential diagnosis of thyroid tumors. Mod Pathol Off J U S Can Acad Pathol Inc. 2005 Jan;18(1):48–57.

318. Roque L, Rodrigues R, Pinto A, Moura-Nunes V, Soares J. Chromosome imbalances in thyroid follicular neoplasms: a comparison between follicular adenomas and carcinomas. Genes Chromosomes Cancer. 2003 Mar;36(3):292–302.

319. Roque L, Clode A, Belge G, Pinto A, Bartnitzke S, Santos JR, et al. Follicular thyroid carcinoma: chromosome analysis of 19 cases. Genes Chromosomes Cancer. 1998 Mar;21(3):250–5.

320. Vuong HG, Kondo T, Oishi N, Nakazawa T, Mochizuki K, Inoue T, et al. Genetic alterations of differentiated thyroid carcinoma in iodine-rich and iodine-deficient countries. Cancer Med. 2016 Aug;5(8):1883–9.

321. Nikiforova MN, Lynch RA, Biddinger PW, Alexander EK, Dorn GW, Tallini G, et al. RAS point mutations and PAX8-PPAR gamma rearrangement in thyroid tumors: evidence for distinct molecular pathways in thyroid follicular carcinoma. J Clin Endocrinol Metab. 2003 May;88(5):2318–26.

322. Kroll TG, Sarraf P, Pecciarini L, Chen CJ, Mueller E, Spiegelman BM, et al. PAX8-PPARgamma1 fusion oncogene in human thyroid carcinoma [corrected]. Science. 2000 Aug 25;289(5483):1357–60.

323. Lui WO, Zeng L, Rehrmann V, Deshpande S, Tretiakova M, Kaplan EL, et al. CREB3L2-PPARgamma fusion mutation identifies a thyroid signaling pathway regulated by

intramembrane proteolysis. Cancer Res. 2008 Sep 1;68(17):7156–64.

324. Wang Y, Hou P, Yu H, Wang W, Ji M, Zhao S, et al. High prevalence and mutual exclusivity of genetic alterations in the phosphatidylinositol-3-kinase/akt pathway in thyroid tumors. J Clin Endocrinol Metab. 2007 Jun;92(6):2387–90.

325. Hou P, Liu D, Shan Y, Hu S, Studeman K, Condouris S, et al. Genetic alterations and their relationship in the phosphatidylinositol 3-kinase/Akt pathway in thyroid cancer. Clin Cancer Res Off J Am Assoc Cancer Res. 2007 Feb 15;13(4):1161–70.

326. Nikiforova MN, Wald AI, Roy S, Durso MB, Nikiforov YE. Targeted next-generation sequencing panel (ThyroSeq) for detection of mutations in thyroid cancer. J Clin Endocrinol Metab. 2013 Nov;98(11):E1852-1860.

327. Liu R, Xing M. TERT promoter mutations in thyroid cancer. Endocr Relat Cancer. 2016 Mar;23(3):R143-155.

328. Chen KT. Fine-needle aspiration cytology of papillary Hürthle-cell tumors of thyroid: a report of three cases. Diagn Cytopathol. 1991;7(1):53–6.

329. Máximo V, Sobrinho-Simões M. Hürthle cell tumours of the thyroid. A review with emphasis on mitochondrial abnormalities with clinical relevance. Virchows Arch Int J Pathol. 2000 Aug;437(2):107–15.

330. Sobrinho-Simões M, Máximo V, Castro IV de, Fonseca E, Soares P, Garcia-Rostan G, et al. Hürthle (oncocytic) cell tumors of thyroid: etiopathogenesis, diagnosis and clinical significance. Int J Surg Pathol. 2005 Jan;13(1):29–35.

331. Kini SR. Post-fine-needle biopsy infarction of thyroid neoplasms: a review of 28 cases. Diagn Cytopathol. 1996 Sep;15(3):211–20.

332. Bishop JA, Wu G, Tufano RP, Westra WH. Histological patterns of locoregional recurrence in Hürthle cell carcinoma of the thyroid gland. Thyroid Off J Am Thyroid Assoc. 2012 Jul;22(7):690–4.

333. Haq M, Harmer C. Differentiated thyroid carcinoma with distant metastases at presentation: prognostic factors and outcome. Clin Endocrinol (Oxf). 2005 Jul;63(1):87–93.

334. Bai S, Baloch ZW, Samulski TD, Montone KT, LiVolsi VA. Poorly differentiated oncocytic (hürthle cell) follicular carcinoma: an institutional experience. Endocr Pathol. 2015 May;26(2):164–9.

335. Máximo V, Soares P, Lima J, Cameselle-Teijeiro J, Sobrinho-Simões M. Mitochondrial DNA somatic mutations (point mutations and large deletions) and mitochondrial DNA variants in human thyroid pathology: a study with emphasis on Hürthle cell tumors. Am J Pathol. 2002 May;160(5):1857–65.

336. Gasparre G, Porcelli AM, Bonora E, Pennisi LF, Toller M, Iommarini L, et al. Disruptive mitochondrial DNA mutations in complex I subunits are markers of oncocytic phenotype in thyroid tumors. Proc Natl Acad Sci U S A. 2007 May 22;104(21):9001–6.

337. Máximo V, Sobrinho-Simões M. Mitochondrial DNA “common” deletion in Hürthle cell lesions of the thyroid. J Pathol. 2000 Dec;192(4):561–2.

338. Máximo V, Lima J, Prazeres H, Soares P, Sobrinho-Simões M. The biology and the genetics of Hurthle cell tumors of the thyroid. Endocr Relat Cancer. 2012 Aug;19(4):R131-147.

339. Gasparre G, Bonora E, Tallini G, Romeo G. Molecular features of thyroid oncocytic tumors. Mol Cell Endocrinol. 2010 May 28;321(1):67–76.

340. Mayr JA, Meierhofer D, Zimmermann F, Feichtinger R, Kögler C, Ratschek M, et al. Loss of complex I due to mitochondrial DNA mutations in renal oncocytoma. Clin Cancer Res Off J Am Assoc Cancer Res. 2008 Apr 15;14(8):2270–5.

341. Máximo V, Botelho T, Capela J, Soares P, Lima J, Taveira A, et al. Somatic and germline mutation in GRIM-19, a dual function gene involved in mitochondrial metabolism and cell death, is linked to mitochondrion-rich (Hurthle cell) tumours of the thyroid. Br J Cancer. 2005 May 23;92(10):1892–8.

342. Ganly I, Ricarte Filho J, Eng S, Ghossein R, Morris LGT, Liang Y, et al. Genomic dissection of Hurthle cell carcinoma reveals a unique class of thyroid malignancy. J Clin Endocrinol Metab. 2013 May;98(5):E962-972.

343. Sahin M, Allard BL, Yates M, Powell JG, Wang XL, Hay ID, et al. PPARgamma staining as a surrogate for PAX8/PPARgamma fusion oncogene expression in follicular neoplasms: clinicopathological correlation and histopathological diagnostic value. J Clin Endocrinol Metab. 2005 Jan;90(1):463–8.

344. Evangelisti C, de Biase D, Kurelac I, Ceccarelli C, Prokisch H, Meitinger T, et al. A mutation screening of oncogenes, tumor suppressor gene TP53 and nuclear encoded mitochondrial complex I genes in oncocytic thyroid tumors. BMC Cancer. 2015 Dec;15(1):157.

345. Wei S, LiVolsi VA, Montone KT, Morrissette JJD, Baloch ZW. PTEN and TP53 Mutations in Oncocytic Follicular Carcinoma. Endocr Pathol. 2015 Dec;26(4):365–9.

346. Rainwater LM, Farrow GM, Hay ID, Lieber MM. Oncocytic tumours of the salivary gland, kidney, and thyroid: nuclear DNA patterns studied by flow cytometry. Br J Cancer. 1986 Jun;53(6):799–804.

347. Carcangiu ML, Zampi G, Rosai J. Poorly differentiated (“insular”) thyroid carcinoma. A reinterpretation of Langhans’ “wuchernde Struma.” Am J Surg Pathol. 1984 Sep;8(9):655–68.

348. Ito Y, Hirokawa M, Fukushima M, Inoue H, Yabuta T, Uruno T, et al. Prevalence and Prognostic Significance of Poor Differentiation and Tall Cell Variant in Papillary Carcinoma in Japan. World J Surg. 2008 Jul;32(7):1535–43.

349. Asioli S, Erickson LA, Righi A, Jin L, Volante M, Jenkins S, et al. Poorly differentiated carcinoma of the thyroid: validation of the Turin proposal and analysis of IMP3 expression. Mod Pathol Off J U S Can Acad Pathol Inc. 2010 Sep;23(9):1269–78.

350. Dettmer MS, Schmitt A, Komminoth P, Perren A. Poorly differentiated thyroid carcinoma : An

underdiagnosed entity. Pathol. 2020 Jun;41(Suppl 1):1–8.

351. Volante M, Rapa I, Gandhi M, Bussolati G, Giachino D, Papotti M, et al. RAS mutations are the predominant molecular alteration in poorly differentiated thyroid carcinomas and bear prognostic impact. J Clin Endocrinol Metab. 2009 Dec;94(12):4735–41.

352. Papotti M, Torchio B, Grassi L, Favero A, Bussolati G. Poorly differentiated oxyphilic (Hurthle cell) carcinomas of the thyroid. Am J Surg Pathol. 1996 Jun;20(6):686–94.

353. Kondo T, Kato K, Nakazawa T, Miyata K, Murata SI, Katoh R. Mucinous carcinoma (poorly differentiated carcinoma with extensive extracellular mucin deposition) of the thyroid: a case report with immunohistochemical studies. Hum Pathol. 2005 Jun;36(6):698–701.

354. Fellegara G, Rosai J. Signet Ring Cells in a Poorly Differentiated Hurthle Cell Carcinoma of the Thyroid Combined With Two Papillary Microcarcinomas. Int J Surg Pathol. 2007 Oct;15(4):388–90.

355. Volante M, Landolfi S, Chiusa L, Palestini N, Motta M, Codegone A, et al. Poorly differentiated carcinomas of the thyroid with trabecular, insular, and solid patterns: a clinicopathologic study of 183 patients. Cancer. 2004 Mar 1;100(5):950–7.

356. Decaussin M, Bernard MH, Adeleine P, Treilleux I, Peix JL, Pugeat M, et al. Thyroid carcinomas with distant metastases: a review of 111 cases with emphasis on the prognostic significance of an insular component. Am J Surg Pathol. 2002 Aug;26(8):1007–15.

357. Volante M, Collini P, Nikiforov YE, Sakamoto A, Kakudo K, Katoh R, et al. Poorly differentiated thyroid carcinoma: the Turin proposal for the use of uniform diagnostic criteria and an algorithmic diagnostic approach. Am J Surg Pathol. 2007 Aug;31(8):1256–64.

358. Collini P, Massimino M, Leite SF, Mattavelli F, Seregni E, Zucchini N, et al. Papillary thyroid carcinoma of childhood and adolescence: a 30-year experience at the Istituto Nazionale Tumori in Milan. Pediatr Blood Cancer. 2006 Mar;46(3):300–6.

359. Sanders EM, LiVolsi VA, Brierley J, Shin J, Randolph GW. An evidence-based review of poorly differentiated thyroid cancer. World J Surg. 2007 May;31(5):934–45.

360. Flynn SD, Forman BH, Stewart AF, Kinder BK. Poorly differentiated ("insular") carcinoma of the thyroid gland: an aggressive subset of differentiated thyroid neoplasms. Surgery. 1988 Dec;104(6):963–70.

361. Bongiovanni M, Bloom L, Krane JF, Baloch ZW, Powers CN, Hintermann S, et al. Cytomorphologic features of poorly differentiated thyroid carcinoma: a multi-institutional analysis of 40 cases. Cancer. 2009 Jun 25;117(3):185–94.

362. Dettmer M, Schmitt A, Steinert H, Moch H, Komminoth P, Perren A. Poorly differentiated oncocytic thyroid carcinoma--diagnostic implications and outcome. Histopathology. 2012 Jun;60(7):1045–51.

363. Asioli S, Righi A, Volante M, Chiusa L, Lloyd RV, Bussolati G. Cell size as a prognostic factor in oncocytic poorly differentiated carcinomas of the thyroid. Hum Pathol. 2014 Jul;45(7):1489–

95.

364. Dupain C, Ali HM, Mouhoub TA, Urbinati G, Massaad-Massade L. Induction of TTF-1 or PAX-8 expression on proliferation and tumorigenicity in thyroid carcinomas. Int J Oncol. 2016 Sep;49(3):1248–58.

365. Rosai J, editor. Tumors ot the thyroid and parathyroid glands. Silver Spring, Md: American Registry of Pathology; 2014. 606 p. (AFIP atlas of tumor pathology).

366. Soares P, Cameselle-Teijeiro J, Sobrinho-Simões M. Immunohistochemical detection of p53 in differentiated, poorly differentiated and undifferentiated carcinomas of the thyroid. Histopathology. 1994 Mar;24(3):205–10.

367. Xu B, Ghossein R. Genomic Landscape of poorly Differentiated and Anaplastic Thyroid Carcinoma. Endocr Pathol. 2016 Sep;27(3):205–12.

368. Soares P, Lima J, Preto A, Castro P, Vinagre J, Celestino R, et al. Genetic Alterations in Poorly Differentiated and Undifferentiated Thyroid Carcinomas. Curr Genomics. 2011 Dec 1;12(8):609–17.

369. Landa I, Ibrahimpasic T, Boucai L, Sinha R, Knauf JA, Shah RH, et al. Genomic and transcriptomic hallmarks of poorly differentiated and anaplastic thyroid cancers. J Clin Invest. 2016 Mar 1;126(3):1052–66.

370. Haugen BR, Alexander EK, Bible KC, Doherty GM, Mandel SJ, Nikiforov YE, et al. 2015 American Thyroid Association Management Guidelines for Adult Patients with Thyroid Nodules and Differentiated Thyroid Cancer: The American Thyroid Association Guidelines Task Force on Thyroid Nodules and Differentiated Thyroid Cancer. Thyroid Off J Am Thyroid Assoc. 2016 Jan;26(1):1–133.

371. Ibrahimpasic T, Ghossein R, Carlson DL, Nixon I, Palmer FL, Shaha AR, et al. Outcomes in patients with poorly differentiated thyroid carcinoma. J Clin Endocrinol Metab. 2014 Apr;99(4):1245–52.

372. Ibrahimpasic T, Ghossein R, Shah JP, Ganly I. Poorly Differentiated Carcinoma of the Thyroid Gland: Current Status and Future Prospects. Thyroid Off J Am Thyroid Assoc. 2019 Mar;29(3):311–21.

373. Viola D, Materazzi G, Valerio L, Molinaro E, Agate L, Faviana P, et al. Prophylactic central compartment lymph node dissection in papillary thyroid carcinoma: clinical implications derived from the first prospective randomized controlled single institution study. J Clin Endocrinol Metab. 2015 Apr;100(4):1316–24.

374. Wang LY, Palmer FL, Nixon IJ, Thomas D, Shah JP, Patel SG, et al. Central lymph node characteristics predictive of outcome in patients with differentiated thyroid cancer. Thyroid Off J Am Thyroid Assoc. 2014 Dec;24(12):1790–5.

375. Hiltzik D, Carlson DL, Tuttle RM, Chuai S, Ishill N, Shaha A, et al. Poorly differentiated thyroid carcinomas defined on the basis of mitosis and necrosis: a clinicopathologic study of 58 patients. Cancer. 2006 Mar 15;106(6):1286–95.

376. Vassilopoulou-Sellin R, Schultz PN, Haynie TP. Clinical outcome of patients with papillary thyroid carcinoma who have recurrence after initial radioactive iodine therapy. Cancer. 1996 Aug 1;78(3):493–501.

377. Nishida T, Katayama S, Tsujimoto M, Nakamura J, Matsuda H. Clinicopathological significance of poorly differentiated thyroid carcinoma. Am J Surg Pathol. 1999 Feb;23(2):205–11.

378. Brierley J, Tsang R, Panzarella T, Bana N. Prognostic factors and the effect of treatment with radioactive iodine and external beam radiation on patients with differentiated thyroid cancer seen at a single institution over 40 years. Clin Endocrinol (Oxf). 2005 Oct;63(4):418–27.

379. Walczyk A, Kowalska A, Sygut J. The clinical course of poorly differentiated thyroid carcinoma (insular carcinoma) - own observations. Endokrynol Pol. 2010 Oct;61(5):467–73.

380. Sackett DL. Rules of evidence and clinical recommendations on the use of antithrombotic agents. Chest. 1989 Feb;95(2 Suppl):2S-4S.

381. Auersperg M, Us-Krasovec M, Petric G, Pogacnik A, Besic N. Results of combined modality treatment in poorly differentiated and anaplastic thyroid carcinoma. Wien Klin Wochenschr. 1990 Apr 27;102(9):267–70.

382. Silberstein EB. Radioiodine: the classic theranostic agent. Semin Nucl Med. 2012 May;42(3):164–70.

383. Pacini F, Castagna MG, Brilli L, Pentheroudakis G, ESMO Guidelines Working Group. Thyroid cancer: ESMO Clinical Practice Guidelines for diagnosis, treatment and follow-up. Ann Oncol Off J Eur Soc Med Oncol. 2012 Oct;23 Suppl 7:vii110-119.

384. Luster M, Clarke SE, Dietlein M, Lassmann M, Lind P, Oyen WJG, et al. Guidelines for radioiodine therapy of differentiated thyroid cancer. Eur J Nucl Med Mol Imaging. 2008 Oct;35(10):1941–59.

385. Perros P, Boelaert K, Colley S, Evans C, Evans RM, Gerrard Ba G, et al. Guidelines for the management of thyroid cancer. Clin Endocrinol (Oxf). 2014 Jul;81 Suppl 1:1–122.

386. Grani G, Ramundo V, Verrienti A, Sponziello M, Durante C. Thyroid hormone therapy in differentiated thyroid cancer. Endocrine. 2019 Oct;66(1):43–50.

387. Na KJ, Choi H. Immune landscape of papillary thyroid cancer and immunotherapeutic implications. Endocr Relat Cancer. 2018 May;25(5):523–31.

388. Giannini R, Moretti S, Ugolini C, Macerola E, Menicali E, Nucci N, et al. Immune Profiling of Thyroid Carcinomas Suggests the Existence of Two Major Phenotypes: An ATC-Like and a PDTC-Like. J Clin Endocrinol Metab. 2019 Aug 1;104(8):3557–75.

389. Prendergast GC. Immune escape as a fundamental trait of cancer: focus on IDO. Oncogene. 2008 Jun 26;27(28):3889–900.

390. Mehnert JM, Varga A, Brose MS, Aggarwal RR, Lin CC, Prawira A, et al. Safety and antitumor

activity of the anti–PD-1 antibody pembrolizumab in patients with advanced, PD-L1–positive papillary or follicular thyroid cancer. BMC Cancer. 2019 Dec;19(1):196.

391. Moretti S, Menicali E, Nucci N, Guzzetti M, Morelli S, Puxeddu E. THERAPY OF ENDOCRINE DISEASE Immunotherapy of advanced thyroid cancer: from bench to bedside. Eur J Endocrinol. 2020 Aug;183(2):R41–55.

392. Brauner E, Gunda V, Vanden Borre P, Zurakowski D, Kim YS, Dennett KV, et al. Combining BRAF inhibitor and anti PD-L1 antibody dramatically improves tumor regression and anti tumor immunity in an immunocompetent murine model of anaplastic thyroid cancer. Oncotarget. 2016 Mar 29;7(13):17194–211.

393. Pardoll DM. The blockade of immune checkpoints in cancer immunotherapy. Nat Rev Cancer. 2012 Apr;12(4):252–64.

394. Bardhan K, Anagnostou T, Boussiotis VA. The PD1:PD-L1/2 Pathway from Discovery to Clinical Implementation. Front Immunol. 2016;7:550.

395. Devji T, Levine O, Neupane B, Beyene J, Xie F. Systemic Therapy for Previously Untreated Advanced *BRAF* -Mutated Melanoma: A Systematic Review and Network Meta-Analysis of Randomized Clinical Trials. JAMA Oncol. 2017 Mar 1;3(3):366.

396. Ellis PM, Vella ET, Ung YC. Immune Checkpoint Inhibitors for Patients With Advanced Non-Small-Cell Lung Cancer: A Systematic Review. Clin Lung Cancer. 2017 Sep;18(5):444-459.e1.

397. Mirghani H, Amen F, Blanchard P, Moreau F, Guigay J, Hartl DM, et al. Treatment de-escalation in HPV-positive oropharyngeal carcinoma: ongoing trials, critical issues and perspectives. Int J Cancer. 2015 Apr 1;136(7):1494–503.

398. Kaufman HL, Russell J, Hamid O, Bhatia S, Terheyden P, D'Angelo SP, et al. Avelumab in patients with chemotherapy-refractory metastatic Merkel cell carcinoma: a multicentre, single-group, open-label, phase 2 trial. Lancet Oncol. 2016 Oct;17(10):1374–85.

399. Bergamo RR, Cominelli F, Kopple JD, Zipser RD. Comparative acute effects of aspirin, diflunisal, ibuprofen and indomethacin on renal function in healthy man. Am J Nephrol. 1989;9(6):460–3.

400. Chen DS, Irving BA, Hodi FS. Molecular pathways: next-generation immunotherapy--inhibiting programmed death-ligand 1 and programmed death-1. Clin Cancer Res Off J Am Assoc Cancer Res. 2012 Dec 15;18(24):6580–7.

401. Cunha LL, Marcello MA, Morari EC, Nonogaki S, Conte FF, Gerhard R, et al. Differentiated thyroid carcinomas may elude the immune system by B7H1 upregulation. Endocr Relat Cancer. 2013 Feb;20(1):103–10.

402. Kollipara R, Schneider B, Radovich M, Babu S, Kiel PJ. Exceptional Response with Immunotherapy in a Patient with Anaplastic Thyroid Cancer. The Oncologist. 2017 Oct;22(10):1149–51.

403. Rosenbaum MW, Gigliotti BJ, Pai SI, Parangi S, Wachtel H, Mino-Kenudson M, et al. PD-L1

and IDO1 Are Expressed in Poorly Differentiated Thyroid Carcinoma. Endocr Pathol. 2018 Mar;29(1):59–67.

404. Asa SL. The Current Histologic Classification of Thyroid Cancer. Endocrinol Metab Clin North Am. 2019 Mar;48(1):1–22.

405. Volante M, Bussolati G, Papotti M. The story of poorly differentiated thyroid carcinoma: From Langhans' description to the Turin proposal via Juan Rosai. Semin Diagn Pathol. 2016 Sep;33(5):277–83.

406. Asa SL. My approach to oncocytic tumours of the thyroid. J Clin Pathol. 2004 Mar;57(3):225–32.

407. Savagner F, Chevrollier A, Loiseau D, Morgan C, Reynier P, Clark O, et al. Mitochondrial activity in XTC.UC1 cells derived from thyroid oncocytoma. Thyroid Off J Am Thyroid Assoc. 2001 Apr;11(4):327–33.

408. Jacques C, Baris O, Prunier-Mirebeau D, Savagner F, Rodien P, Rohmer V, et al. Two-step differential expression analysis reveals a new set of genes involved in thyroid oncocytic tumors. J Clin Endocrinol Metab. 2005 Apr;90(4):2314–20.

409. Bonora E, Porcelli AM, Gasparre G, Biondi A, Ghelli A, Carelli V, et al. Defective oxidative phosphorylation in thyroid oncocytic carcinoma is associated with pathogenic mitochondrial DNA mutations affecting complexes I and III. Cancer Res. 2006 Jun 15;66(12):6087–96.

410. Gopal RK, Kübler K, Calvo SE, Polak P, Livitz D, Rosebrock D, et al. Widespread Chromosomal Losses and Mitochondrial DNA Alterations as Genetic Drivers in Hürthle Cell Carcinoma. Cancer Cell. 2018 Aug 13;34(2):242-255.e5.

411. Dettmer MS, Perren A, Moch H, Komminoth P, Nikiforov YE, Nikiforova MN. MicroRNA profile of poorly differentiated thyroid carcinomas: new diagnostic and prognostic insights. J Mol Endocrinol. 2014 Apr;52(2):181–9.

412. de la Fouchardière C, Decaussin-Petrucci M, Berthiller J, Descotes F, Lopez J, Lifante JC, et al. Predictive factors of outcome in poorly differentiated thyroid carcinomas. Eur J Cancer. 2018 Mar;92:40–7.

413. Danaher P, Warren S, Dennis L, D'Amico L, White A, Disis ML, et al. Gene expression markers of Tumor Infiltrating Leukocytes. J Immunother Cancer. 2017;5:18.

414. Varricchi G, Loffredo S, Marone G, Modestino L, Fallahi P, Ferrari SM, et al. The Immune Landscape of Thyroid Cancer in the Context of Immune Checkpoint Inhibition. Int J Mol Sci. 2019 Aug 13;20(16):E3934.

415. Chowdhury S, Veyhl J, Jessa F, Polyakova O, Alenzi A, MacMillan C, et al. Programmed death-ligand 1 overexpression is a prognostic marker for aggressive papillary thyroid cancer and its variants. Oncotarget. 2016 May 31;7(22):32318–28.

416. Bai Y, Niu D, Huang X, Jia L, Kang Q, Dou F, et al. PD-L1 and PD-1 expression are correlated with distinctive clinicopathological features in papillary thyroid carcinoma. Diagn Pathol. 2017

Oct 3;12(1):72.

417. Cantara S, Bertelli E, Occhini R, Regoli M, Brilli L, Pacini F, et al. Blockade of the programmed death ligand 1 (PD-L1) as potential therapy for anaplastic thyroid cancer. Endocrine. 2019 Apr;64(1):122–9.

418. Zhuravel OV, Gerashchenko OL, Khetsuriani MR, Soldatkina MA, Pogrebnoy PV. Expression of human beta-defensins-1-4 in thyroid cancer cells and new insight on biologic activity of hBD-2 in vitro. Exp Oncol. 2014 Sep;36(3):174–8.

419. Pignatti E, Vighi E, Magnani E, Kara E, Roncati L, Maiorana A, et al. Expression and clinicopathological role of miR146a in thyroid follicular carcinoma. Endocrine. 2019 Jun;64(3):575–83.

420. Cheng BY, Lau EY, Leung HW, Leung CON, Ho NP, Gurung S, et al. IRAK1 Augments Cancer Stemness and Drug Resistance via the AP-1/AKR1B10 Signaling Cascade in Hepatocellular Carcinoma. Cancer Res. 2018 May 1;78(9):2332–42.

421. Liu PH, Shah RB, Li Y, Arora A, Ung PMU, Raman R, et al. An IRAK1-PIN1 signalling axis drives intrinsic tumour resistance to radiation therapy. Nat Cell Biol. 2019 Feb;21(2):203–13.

422. Singer JW, Fleischman A, Al-Fayoumi S, Mascarenhas JO, Yu Q, Agarwal A. Inhibition of interleukin-1 receptor-associated kinase 1 (IRAK1) as a therapeutic strategy. Oncotarget. 2018 Sep 7;9(70):33416–39.

423. Celestino R, Nome T, Pestana A, Hoff AM, Gonçalves AP, Pereira L, et al. CRABP1, C1QL1 and LCN2 are biomarkers of differentiated thyroid carcinoma, and predict extrathyroidal extension. BMC Cancer. 2018 Jan 10;18(1):68.

424. Iannetti A, Pacifico F, Acquaviva R, Lavorgna A, Crescenzi E, Vascotto C, et al. The neutrophil gelatinase-associated lipocalin (NGAL), a NF-kappaB-regulated gene, is a survival factor for thyroid neoplastic cells. Proc Natl Acad Sci U S A. 2008 Sep 16;105(37):14058–63.

425. Dunn GP, Koebel CM, Schreiber RD. Interferons, immunity and cancer immunoediting. Nat Rev Immunol. 2006 Nov;6(11):836–48.

426. Chen DS, Mellman I. Oncology meets immunology: the cancer-immunity cycle. Immunity. 2013 Jul 25;39(1):1–10.

427. Máximo V, Rios E, Sobrinho-Simões M. Oncocytic lesions of the thyroid, kidney, salivary glands, adrenal cortex, and parathyroid glands. Int J Surg Pathol. 2014 Feb;22(1):33–6.

428. da Silva Correia J, Miranda Y, Austin-Brown N, Hsu J, Mathison J, Xiang R, et al. Nod1-dependent control of tumor growth. Proc Natl Acad Sci U S A. 2006 Feb 7;103(6):1840–5.

429. Mey L, Jung M, Roos F, Blaheta R, Hegele A, Kinscherf R, et al. NOD1 and NOD2 of the innate immune system is differently expressed in human clear cell renal cell carcinoma, corresponding healthy renal tissue, its vasculature and primary isolated renal tubular epithelial cells. J Cancer Res Clin Oncol. 2019 Jun;145(6):1405–16.

430. Wang H, Hu WM, Xia ZJ, Liang Y, Lu Y, Lin SX, et al. High numbers of CD163+ tumor-associated macrophages correlate with poor prognosis in multiple myeloma patients receiving bortezomib-based regimens. J Cancer. 2019;10(14):3239–45.

431. Kumar AT, Knops A, Swendseid B, Martinez-Outschoom U, Harshyne L, Philp N, et al. Prognostic Significance of Tumor-Associated Macrophage Content in Head and Neck Squamous Cell Carcinoma: A Meta-Analysis. Front Oncol. 2019;9:656.

432. Chen Y, Song Y, Du W, Gong L, Chang H, Zou Z. Tumor-associated macrophages: an accomplice in solid tumor progression. J Biomed Sci. 2019 Dec;26(1):78.

433. Mazzoni M, Mauro G, Erreni M, Romeo P, Minna E, Vizioli MG, et al. Senescent thyrocytes and thyroid tumor cells induce M2-like macrophage polarization of human monocytes via a PGE2-dependent mechanism. J Exp Clin Cancer Res CR. 2019 May 21;38(1):208.

434. Ni YH, Ding L, Huang XF, Dong Y chun, Hu QG, Hou YY. Microlocalization of CD68+ tumor-associated macrophages in tumor stroma correlated with poor clinical outcomes in oral squamous cell carcinoma patients. Tumour Biol J Int Soc Oncodevelopmental Biol Med. 2015 Jul;36(7):5291–8.

435. Hu JM, Liu K, Liu JH, Jiang XL, Wang XL, Chen YZ, et al. CD163 as a marker of M2 macrophage, contribute to predicte aggressiveness and prognosis of Kazakh esophageal squamous cell carcinoma. Oncotarget. 2017 Mar 28;8(13):21526–38.

436. Genere N, El Kawkgi OM, Giblon RE, Vaccarella S, Morris JC, Hay ID, et al. Incidence of Clinically Relevant Thyroid Cancers Remains Stable for Almost a Century: A Population-Based Study. Mayo Clin Proc. 2021 Nov;96(11):2823–30.

437. Li M, Delafosse P, Meheus F, Borson-Chazot F, Lifante JC, Simon R, et al. Temporal and geographical variations of thyroid cancer incidence and mortality in France during 1986-2015: The impact of overdiagnosis. Cancer Epidemiol. 2021 Dec;75:102051.

438. Roman BR, Morris LG, Davies L. The thyroid cancer epidemic, 2017 perspective. Curr Opin Endocrinol Diabetes Obes. 2017 Oct;24(5):332–6.

439. Nath MC, Erickson LA. Aggressive Variants of Papillary Thyroid Carcinoma: Hobnail, Tall Cell, Columnar, and Solid. Adv Anat Pathol. 2018 May;25(3):172–9.

440. Papp S, Asa SL. When thyroid carcinoma goes bad: a morphological and molecular analysis. Head Neck Pathol. 2015 Mar;9(1):16–23.

441. Shaha AR, Shah JP, Loree TR. Risk group stratification and prognostic factors in papillary carcinoma of thyroid. Ann Surg Oncol. 1996 Nov;3(6):534–8.

442. Voutilainen PE, Multanen MM, Leppäniemi AK, Haglund CH, Haapiainen RK, Franssila KO. Prognosis after lymph node recurrence in papillary thyroid carcinoma depends on age. Thyroid Off J Am Thyroid Assoc. 2001 Oct;11(10):953–7.

443. Galuppini F, Censi S, Merante Boschin I, Fassan M, Sbaraglia M, Valeri N, et al. Papillary Thyroid Carcinoma: Molecular Distinction by MicroRNA Profiling. Front Endocrinol.

2022;13:834075.

444. Chitikova Z, Pusztaszeri M, Makhlouf AM, Berczy M, Delucinge-Vivier C, Triponez F, et al. Identification of new biomarkers for human papillary thyroid carcinoma employing NanoString analysis. Oncotarget. 2015 May 10;6(13):10978–93.

445. Armanious H, Adam B, Meunier D, Formenti K, Izevbaye I. Digital gene expression analysis might aid in the diagnosis of thyroid cancer. Curr Oncol Tor Ont. 2020 Apr;27(2):e93–9.

446. Yip L, Nikiforova MN, Carty SE, Yim JH, Stang MT, Tublin MJ, et al. Optimizing surgical treatment of papillary thyroid carcinoma associated with BRAF mutation. Surgery. 2009 Dec;146(6):1215–23.

447. Xing M, Haugen BR, Schlumberger M. Progress in molecular-based management of differentiated thyroid cancer. Lancet Lond Engl. 2013 Mar 23;381(9871):1058–69.

448. Ricarte-Filho JC, Ryder M, Chitale DA, Rivera M, Heguy A, Ladanyi M, et al. Mutational profile of advanced primary and metastatic radioactive iodine-refractory thyroid cancers reveals distinct pathogenetic roles for BRAF, PIK3CA, and AKT1. Cancer Res. 2009 Jun 1;69(11):4885–93.

449. Gandolfi G, Ragazzi M, Frasoldati A, Piana S, Ciarrocchi A, Sancisi V. TERT promoter mutations are associated with distant metastases in papillary thyroid carcinoma. Eur J Endocrinol. 2015 Apr;172(4):403–13.

450. Ilie MI, Lassalle S, Long-Mira E, Hofman V, Zangari J, Bénaim G, et al. In papillary thyroid carcinoma, TIMP-1 expression correlates with BRAF (V600E) mutation status and together with hypoxia-related proteins predicts aggressive behavior. Virchows Arch Int J Pathol. 2013 Sep;463(3):437–44.

451. Tomei S, Mazzanti C, Marchetti I, Rossi L, Zavaglia K, Lessi F, et al. c-KIT receptor expression is strictly associated with the biological behaviour of thyroid nodules. J Transl Med. 2012 Jan 10;10:7.

452. Sierra JR, Tsao MS. c-MET as a potential therapeutic target and biomarker in cancer. Ther Adv Med Oncol. 2011 Nov;3(1 Suppl):S21-35.

453. Romei C, Ciampi R, Faviana P, Agate L, Molinaro E, Bottici V, et al. BRAFV600E mutation, but not RET/PTC rearrangements, is correlated with a lower expression of both thyroperoxidase and sodium iodide symporter genes in papillary thyroid cancer. Endocr Relat Cancer. 2008 Jun;15(2):511–20.

454. Nikiforov YE. RET/PTC rearrangement in thyroid tumors. Endocr Pathol. 2002;13(1):3–16.

455. Romei C, Elisei R. RET/PTC Translocations and Clinico-Pathological Features in Human Papillary Thyroid Carcinoma. Front Endocrinol. 2012;3:54.

456. Nikiforov YE. Thyroid carcinoma: molecular pathways and therapeutic targets. Mod Pathol Off J U S Can Acad Pathol Inc. 2008 May;21 Suppl 2:S37-43.

457. Knauf JA, Kuroda H, Basu S, Fagin JA. RET/PTC-induced dedifferentiation of thyroid cells is mediated through Y1062 signaling through SHC-RAS-MAP kinase. Oncogene. 2003 Jul 10;22(28):4406–12.

458. Mitsutake N, Knauf JA, Mitsutake S, Mesa C, Zhang L, Fagin JA. Conditional BRAFV600E expression induces DNA synthesis, apoptosis, dedifferentiation, and chromosomal instability in thyroid PCCL3 cells. Cancer Res. 2005 Mar 15;65(6):2465–73.

459. American Thyroid Association (ATA) Guidelines Taskforce on Thyroid Nodules and Differentiated Thyroid Cancer, Cooper DS, Doherty GM, Haugen BR, Hauger BR, Kloos RT, et al. Revised American Thyroid Association management guidelines for patients with thyroid nodules and differentiated thyroid cancer. Thyroid Off J Am Thyroid Assoc. 2009 Nov;19(11):1167–214.

460. Terezakis SA, Lee KS, Ghossein RA, Rivera M, Tuttle RM, Wolden SL, et al. Role of external beam radiotherapy in patients with advanced or recurrent nonanaplastic thyroid cancer: Memorial Sloan-kettering Cancer Center experience. Int J Radiat Oncol Biol Phys. 2009 Mar 1;73(3):795–801.

461. Urken ML, Milas M, Randolph GW, Tufano R, Bergman D, Bernet V, et al. Management of recurrent and persistent metastatic lymph nodes in well-differentiated thyroid cancer: a multifactorial decision-making guide for the Thyroid Cancer Care Collaborative. Head Neck. 2015 Apr;37(4):605–14.

462. Romesser PB, Sherman EJ, Shaha AR, Lian M, Wong RJ, Sabra M, et al. External beam radiotherapy with or without concurrent chemotherapy in advanced or recurrent non-anaplastic non-medullary thyroid cancer. J Surg Oncol. 2014 Sep;110(4):375–82.

463. Vuong HG, Duong UNP, Pham TQ, Tran HM, Oishi N, Mochizuki K, et al. Clinicopathological Risk Factors for Distant Metastasis in Differentiated Thyroid Carcinoma: A Meta-analysis. World J Surg. 2018 Apr;42(4):1005–17.

464. Bastman JJ, Serracino HS, Zhu Y, Koenig MR, Mateescu V, Sams SB, et al. Tumor-Infiltrating T Cells and the PD-1 Checkpoint Pathway in Advanced Differentiated and Anaplastic Thyroid Cancer. J Clin Endocrinol Metab. 2016 Jul;101(7):2863–73.

465. French JD, Weber ZJ, Fretwell DL, Said S, Klopper JP, Haugen BR. Tumor-associated lymphocytes and increased FoxP3+ regulatory T cell frequency correlate with more aggressive papillary thyroid cancer. J Clin Endocrinol Metab. 2010 May;95(5):2325–33.

466. Cox TR, Erler JT. Remodeling and homeostasis of the extracellular matrix: implications for fibrotic diseases and cancer. Dis Model Mech. 2011 Mar;4(2):165–78.

467. Takeda M, Mikami T, Numata Y, Okamoto M, Okayasu I. Papillary thyroid carcinoma with heterotopic ossification is a special subtype with extensive progression. Am J Clin Pathol. 2013 May;139(5):587–98.

468. Cabanillas ME, McFadden DG, Durante C. Thyroid cancer. Lancet Lond Engl. 2016 Dec 3;388(10061):2783–95.

469. Sui X, Geng J, Li YH, Zhu G, Wang WH. Calcium channel α2δ1 subunit (CACNA2D1) enhances radioresistance in cancer stem-like cells in non-small cell lung cancer cell lines. Cancer Manag Res. 2018 Oct;Volume 10:5009–18.

470. Yu D, Holm R, Goscinski MA, Trope CG, Nesland JM, Suo Z. Prognostic and clinicopathological significance of Cacna2d1 expression in epithelial ovarian cancers: a retrospective study. Am J Cancer Res. 2016;6(9):2088–97.

471. Vogt PK. Fortuitous convergences: the beginnings of JUN. Nat Rev Cancer. 2002 Jun;2(6):465–9.

472. Chen W, Liu Q, Lv Y, Xu D, Chen W, Yu J. Special role of JUN in papillary thyroid carcinoma based on bioinformatics analysis. World J Surg Oncol. 2017 Jul 3;15(1):119.

473. Eferl R, Ricci R, Kenner L, Zenz R, David JP, Rath M, et al. Liver tumor development. c-Jun antagonizes the proapoptotic activity of p53. Cell. 2003 Jan 24;112(2):181–92.

474. Song YS, Lim JA, Choi H, Won JK, Moon JH, Cho SW, et al. Prognostic effects of TERT promoter mutations are enhanced by coexistence with BRAF or RAS mutations and strengthen the risk prediction by the ATA or TNM staging system in differentiated thyroid cancer patients. Cancer. 2016 May 1;122(9):1370–9.

475. Bottrell A, Meng YH, Najy AJ, Hurst N, Kim S, Kim CJ, et al. An oncogenic activity of PDGF-C and its splice variant in human breast cancer. Growth Factors Chur Switz. 2019 Aug;37(3–4):131–45.

476. Yoon H, Tang CM, Banerjee S, Yebra M, Noh S, Burgoyne AM, et al. Cancer-associated fibroblast secretion of PDGFC promotes gastrointestinal stromal tumor growth and metastasis. Oncogene. 2021 Mar 18;40(11):1957–73.

477. Liu Y, Cheng G, Song Z, Xu T, Ruan H, Cao Q, et al. RAC2 acts as a prognostic biomarker and promotes the progression of clear cell renal cell carcinoma. Int J Oncol. 2019 Sep;55(3):645–56.

478. Lim MBH, Kuiper JWP, Katchky A, Goldberg H, Glogauer M. Rac2 is required for the formation of neutrophil extracellular traps. J Leukoc Biol. 2011 Oct;90(4):771–6.

479. Joshi S, Singh AR, Zulcic M, Bao L, Messer K, Ideker T, et al. Rac2 controls tumor growth, metastasis and M1-M2 macrophage differentiation in vivo. PloS One. 2014;9(4):e95893.

480. Thomas DC. The phagocyte respiratory burst: Historical perspectives and recent advances. Immunol Lett. 2017 Dec;192:88–96.

481. Alhmoud JF, Woolley JF, Al Moustafa AE, Malki MI. DNA Damage/Repair Management in Cancers. Cancers. 2020 Apr 23;12(4):E1050.

482. Harrison JC, Haber JE. Surviving the breakup: the DNA damage checkpoint. Annu Rev Genet. 2006;40:209–35.

483. McGowan CH, Russell P. The DNA damage response: sensing and signaling. Curr Opin Cell Biol. 2004 Dec;16(6):629–33.

484. Kiwerska K, Szyfter K. DNA repair in cancer initiation, progression, and therapy-a double-edged sword. J Appl Genet. 2019 Nov;60(3–4):329–34.

485. Silva Nogueira GA, Dias Costa EF, Lopes-Aguiar L, Penna Lima TR, Visacri MB, Pincinato EC, et al. Polymorphisms in DNA mismatch repair pathway genes predict toxicity and response to cisplatin chemoradiation in head and neck squamous cell carcinoma patients. Oncotarget. 2018 Jul 3;9(51):29538–47.

486. Vladimirova U, Rumiantsev P, Zolotovskaia M, Albert E, Abrosimov A, Slashchuk K, et al. DNA repair pathway activation features in follicular and papillary thyroid tumors, interrogated using 95 experimental RNA sequencing profiles. Heliyon. 2021 Mar;7(3):e06408.

487. Ricaud L, Proux C, Renou JP, Pichon O, Fochesato S, Ortet P, et al. ATM-Mediated Transcriptional and Developmental Responses to γ-rays in Arabidopsis. Kepinski S, editor. PLoS ONE. 2007 May 9;2(5):e430.

488. Savitsky K, Bar-Shira A, Gilad S, Rotman G, Ziv Y, Vanagaite L, et al. A Single Ataxia Telangiectasia Gene with a Product Similar to PI-3 Kinase. Science. 1995 Jun 23;268(5218):1749–53.

489. Lavin MF, Scott S, Gueven N, Kozlov S, Peng C, Chen P. Functional consequences of sequence alterations in the ATM gene. DNA Repair. 2004 Aug;3(8–9):1197–205.

490. Bakkenist CJ, Kastan MB. DNA damage activates ATM through intermolecular autophosphorylation and dimer dissociation. Nature. 2003 Jan;421(6922):499–506.

491. Flanagan JM, Munoz-Alegre M, Henderson S, Tang T, Sun P, Johnson N, et al. Gene-body hypermethylation of ATM in peripheral blood DNA of bilateral breast cancer patients. Hum Mol Genet. 2009 Apr 1;18(7):1332–42.

492. Kim JH, Kim H, Lee KY, Choe KH, Ryu JS, Yoon HI, et al. Genetic polymorphisms of ataxia telangiectasia mutated affect lung cancer risk. Hum Mol Genet. 2006 Apr 1;15(7):1181–6.

493. Akulevich NM, Saenko VA, Rogounovitch TI, Drozd VM, Lushnikov EF, Ivanov VK, et al. Polymorphisms of DNA damage response genes in radiation-related and sporadic papillary thyroid carcinoma. Endocr Relat Cancer. 2009 Jun;16(2):491–503.

494. Meyer A, Wilhelm B, Dörk T, Bremer M, Baumann R, Karstens JH, et al. ATM missense variant P1054R predisposes to prostate cancer. Radiother Oncol. 2007 Jun;83(3):283–8.

495. Rudd MF, Sellick GS, Webb EL, Catovsky D, Houlston RS. Variants in the ATM-BRCA2-CHEK2 axis predispose to chronic lymphocytic leukemia. Blood. 2006 Jul 15;108(2):638–44.

496. He Y, Chen Q, Li B. ATM in oral carcinogenesis: association with clinicopathological features. J Cancer Res Clin Oncol. 2008 Sep;134(9):1013–20.

497. Kang B, Guo RF, Tan XH, Zhao M, Tang ZB, Lu YY. Expression status of ataxia-telangiectasia-mutated gene correlated with prognosis in advanced gastric cancer. Mutat Res Mol Mech Mutagen. 2008 Feb;638(1–2):17–25.

498. Sun M, Guo X, Qian X, Wang H, Yang C, Brinkman KL, et al. Activation of the ATM-Snail pathway promotes breast cancer metastasis. J Mol Cell Biol. 2012 Oct;4(5):304–15.

499. Lee J, Sung CO, Lee EJ, Do IG, Kim HC, Yoon SH, et al. Metastasis of Neuroendocrine Tumors Are Characterized by Increased Cell Proliferation and Reduced Expression of the ATM Gene. Agoulnik I, editor. PLoS ONE. 2012 Apr 2;7(4):e34456.

500. Bassing CH, Chua KF, Sekiguchi J, Suh H, Whitlow SR, Fleming JC, et al. Increased ionizing radiation sensitivity and genomic instability in the absence of histone H2AX. Proc Natl Acad Sci U S A. 2002 Jun 11;99(12):8173–8.

501. Bassing CH, Suh H, Ferguson DO, Chua KF, Manis J, Eckersdorff M, et al. Histone H2AX: a dosage-dependent suppressor of oncogenic translocations and tumors. Cell. 2003 Aug 8;114(3):359–70.

502. Parikh RA, White JS, Huang X, Schoppy DW, Baysal BE, Baskaran R, et al. Loss of distal 11q is associated with DNA repair deficiency and reduced sensitivity to ionizing radiation in head and neck squamous cell carcinoma. Genes Chromosomes Cancer. 2007 Aug;46(8):761–75.

503. Srivastava N, Gochhait S, Gupta P, Bamezai RNK. Copy number alterations of the H2AFX gene in sporadic breast cancer patients. Cancer Genet Cytogenet. 2008 Jan 15;180(2):121–8.

504. Novik KL, Spinelli JJ, Macarthur AC, Shumansky K, Sipahimalani P, Leach S, et al. Genetic variation in H2AFX contributes to risk of non-Hodgkin lymphoma. Cancer Epidemiol Biomark Prev Publ Am Assoc Cancer Res Cosponsored Am Soc Prev Oncol. 2007 Jun;16(6):1098–106.

505. Liu Y, Tseng M, Perdreau SA, Rossi F, Antonescu C, Besmer P, et al. Histone H2AX is a mediator of gastrointestinal stromal tumor cell apoptosis following treatment with imatinib mesylate. Cancer Res. 2007 Mar 15;67(6):2685–92.

506. Murakumo Y, Ogura Y, Ishii H, Numata S, Ichihara M, Croce CM, et al. Interactions in the error-prone postreplication repair proteins hREV1, hREV3, and hREV7. J Biol Chem. 2001 Sep 21;276(38):35644–51.

507. Chen J, Fang G. MAD2B is an inhibitor of the anaphase-promoting complex. Genes Dev. 2001 Jul 15;15(14):1765–70.

508. Zhang L, Yang SH, Sharrocks AD. Rev7/MAD2B links c-Jun N-terminal protein kinase pathway signaling to activation of the transcription factor Elk-1. Mol Cell Biol. 2007 Apr;27(8):2861–9.

509. Watanabe N, Mii S, Asai N, Asai M, Niimi K, Ushida K, et al. The REV7 subunit of DNA polymerase ζ is essential for primordial germ cell maintenance in the mouse. J Biol Chem. 2013 Apr 12;288(15):10459–71.

510. Pirouz M, Rahjouei A, Shamsi F, Eckermann KN, Salinas-Riester G, Pommerenke C, et al. Destabilization of pluripotency in the absence of Mad2l2. Cell Cycle Georget Tex. 2015;14(10):1596–610.

511. Rahjouei A, Pirouz M, Di Virgilio M, Kamin D, Kessel M. MAD2L2 Promotes Open

Chromatin in Embryonic Stem Cells and Derepresses the Dppa3 Locus. Stem Cell Rep. 2017 Apr 11;8(4):813–21.

512. Feng L, Wei W, Heng Z, Yantao H, Chunbo W. Knockdown of REV7 Inhibits Breast Cancer Cell Migration and Invasion. Oncol Res. 2016;24(5):315–25.

513. Niimi K, Murakumo Y, Watanabe N, Kato T, Mii S, Enomoto A, et al. Suppression of REV7 enhances cisplatin sensitivity in ovarian clear cell carcinoma cells. Cancer Sci. 2014 May;105(5):545–52.

514. Zhao J, Liu S, Wang H, Zhang X, Kang T, Li Z, et al. Mitotic arrest deficient protein MAD2B is overexpressed in human glioma, with depletion enhancing sensitivity to ionizing radiation. J Clin Neurosci Off J Neurosurg Soc Australas. 2011 Jun;18(6):827–33.

515. Cheung HW, Chun ACS, Wang Q, Deng W, Hu L, Guan XY, et al. Inactivation of human MAD2B in nasopharyngeal carcinoma cells leads to chemosensitization to DNA-damaging agents. Cancer Res. 2006 Apr 15;66(8):4357–67.

516. Li Y, Li L, Chen M, Yu X, Gu Z, Qiu H, et al. MAD2L2 inhibits colorectal cancer growth by promoting NCOA3 ubiquitination and degradation. Mol Oncol. 2018 Mar;12(3):391–405.

517. Schadendorf D, Lebbé C, Zur Hausen A, Avril MF, Hariharan S, Bharmal M, et al. Merkel cell carcinoma: Epidemiology, prognosis, therapy and unmet medical needs. Eur J Cancer Oxf Engl 1990. 2017 Jan;71:53–69.

518. Paulson KG, Park SY, Vandeven NA, Lachance K, Thomas H, Chapuis AG, et al. Merkel cell carcinoma: Current US incidence and projected increases based on changing demographics. J Am Acad Dermatol. 2018 Mar;78(3):457-463.e2.

519. Köksal Y, Toy H, Talim B, Unal E, Akçören Z, Cengiz M. Merkel cell carcinoma in a child. J Pediatr Hematol Oncol. 2009 May;31(5):359–61.

520. Kaae J, Hansen AV, Biggar RJ, Boyd HA, Moore PS, Wohlfahrt J, et al. Merkel cell carcinoma: incidence, mortality, and risk of other cancers. J Natl Cancer Inst. 2010 Jun 2;102(11):793–801.

521. Harms KL, Healy MA, Nghiem P, Sober AJ, Johnson TM, Bichakjian CK, et al. Analysis of Prognostic Factors from 9387 Merkel Cell Carcinoma Cases Forms the Basis for the New 8th Edition AJCC Staging System. Ann Surg Oncol. 2016 Oct;23(11):3564–71.

522. Heath M, Jaimes N, Lemos B, Mostaghimi A, Wang LC, Peñas PF, et al. Clinical characteristics of Merkel cell carcinoma at diagnosis in 195 patients: the AEIOU features. J Am Acad Dermatol. 2008 Mar;58(3):375–81.

523. Ma JE, Brewer JD. Merkel cell carcinoma in immunosuppressed patients. Cancers. 2014 Jun 27;6(3):1328–50.

524. Paulson KG, Iyer JG, Blom A, Warton EM, Sokil M, Yelistratova L, et al. Systemic immune suppression predicts diminished Merkel cell carcinoma-specific survival independent of stage. J Invest Dermatol. 2013 Mar;133(3):642–6.

525. Husseiny MI, Anastasi B, Singer J, Lacey SF. A comparative study of Merkel cell, BK and JC polyomavirus infections in renal transplant recipients and healthy subjects. J Clin Virol Off Publ Pan Am Soc Clin Virol. 2010 Oct;49(2):137–40.

526. Engels EA, Frisch M, Goedert JJ, Biggar RJ, Miller RW. Merkel cell carcinoma and HIV infection. Lancet Lond Engl. 2002 Feb 9;359(9305):497–8.

527. Lemasson G, Coquart N, Lebonvallet N, Boulais N, Galibert MD, Marcorelles P, et al. Presence of putative stem cells in Merkel cell carcinomas. J Eur Acad Dermatol Venereol JEADV. 2012 Jun;26(6):789–95.

528. Visscher D, Cooper PH, Zarbo RJ, Crissman JD. Cutaneous neuroendocrine (Merkel cell) carcinoma: an immunophenotypic, clinicopathologic, and flow cytometric study. Mod Pathol Off J U S Can Acad Pathol Inc. 1989 Jul;2(4):331–8.

529. Sauer CM, Haugg AM, Chteinberg E, Rennspiess D, Winnepenninckx V, Speel EJ, et al. Reviewing the current evidence supporting early B-cells as the cellular origin of Merkel cell carcinoma. Crit Rev Oncol Hematol. 2017 Aug;116:99–105.

530. Sunshine JC, Jahchan NS, Sage J, Choi J. Are there multiple cells of origin of Merkel cell carcinoma? Oncogene. 2018 Mar;37(11):1409–16.

531. Maricich SM, Wellnitz SA, Nelson AM, Lesniak DR, Gerling GJ, Lumpkin EA, et al. Merkel Cells Are Essential for Light-Touch Responses. Science. 2009 Jun 19;324(5934):1580–2.

532. Moll I, Roessler M, Brandner JM, Eispert AC, Houdek P, Moll R. Human Merkel cells – aspects of cell biology, distribution and functions. Eur J Cell Biol. 2005 Mar;84(2–3):259–71.

533. Tilling T, Moll I. Which Are the Cells of Origin in Merkel Cell Carcinoma? J Skin Cancer. 2012;2012:1–6.

534. Walsh NMG. Primary neuroendocrine (Merkel cell) carcinoma of the skin: Morphologic diversity and implications thereof. Hum Pathol. 2001 Jul;32(7):680–9.

535. Zur Hausen A, Rennspiess D, Winnepenninckx V, Speel EJ, Kurz AK. Early B-cell differentiation in Merkel cell carcinomas: clues to cellular ancestry. Cancer Res. 2013 Aug 15;73(16):4982–7.

536. Calder KB, Smoller BR. New Insights Into Merkel Cell Carcinoma. Adv Anat Pathol. 2010 May;17(3):155–61.

537. Shiver MB, Mahmoud F, Gao L. Response to Idelalisib in a Patient with Stage IV Merkel-Cell Carcinoma. N Engl J Med. 2015 Oct 15;373(16):1580–2.

538. Kervarrec T, Aljundi M, Appenzeller S, Samimi M, Maubec E, Cribier B, et al. Polyomavirus-Positive Merkel Cell Carcinoma Derived from a Trichoblastoma Suggests an Epithelial Origin of this Merkel Cell Carcinoma. J Invest Dermatol. 2020 May;140(5):976–85.

539. Liu W, Yang R, Payne AS, Schowalter RM, Spurgeon ME, Lambert PF, et al. Identifying the Target Cells and Mechanisms of Merkel Cell Polyomavirus Infection. Cell Host Microbe. 2016

Jun 8;19(6):775–87.

540. Dancey AL, Rayatt SS, Soon C, Ilchshyn A, Brown I, Srivastava S. Merkel cell carcinoma: a report of 34 cases and literature review. J Plast Reconstr Aesthet Surg. 2006 Dec;59(12):1294–9.

541. Goessling W, McKee PH, Mayer RJ. Merkel cell carcinoma. J Clin Oncol Off J Am Soc Clin Oncol. 2002 Jan 15;20(2):588–98.

542. Walsh NM. Complete spontaneous regression of Merkel cell carcinoma (1986-2016): a 30 year perspective. J Cutan Pathol. 2016 Dec;43(12):1150–4.

543. Messina JL, Reintgen DS, Cruse CW, Rappaport DP, Berman C, Fenske NA, et al. Selective lymphadenectomy in patients with Merkel cell (cutaneous neuroendocrine) carcinoma. Ann Surg Oncol. 1997 Jul;4(5):389–95.

544. Amin MB, American Joint Committee on Cancer, American Cancer Society, editors. AJCC cancer staging manual. Eight edition / editor-in-chief, Mahul B. Amin, MD, FCAP ; editors, Stephen B. Edge, MD, FACS [and 16 others] ; Donna M. Gress, RHIT, CTR-Technical editor ; Laura R. Meyer, CAPM-Managing editor. Chicago IL: American Joint Committee on Cancer, Springer; 2017. 1024 p.

545. Gupta SG, Wang LC, Peñas PF, Gellenthin M, Lee SJ, Nghiem P. Sentinel Lymph Node Biopsy for Evaluation and Treatment of Patients With Merkel Cell Carcinoma: The Dana-Farber Experience and Meta-analysis of the Literature. Arch Dermatol [Internet]. 2006 Jun 1 [cited 2022 May 10];142(6). Available from: http://archderm.jamanetwork.com/article.aspx?doi=10.1001/archderm.142.6.685

546. Pan D, Narayan D, Ariyan S. Merkel Cell Carcinoma: Five Case Reports Using Sentinel Lymph Node Biopsy and a Review of 110 New Cases: Plast Reconstr Surg. 2002 Oct;110(5):1259–65.

547. Ortin-Perez J, van Rijk MC, Valdes-Olmos RA, Vidal-Sicart S, Nieweg OE, Vilalta A, et al. Lymphatic mapping and sentinel node biopsy in Merkel's cell carcinoma. Eur J Surg Oncol EJSO. 2007 Feb;33(1):119–22.

548. Fields RC, Busam KJ, Chou JF, Panageas KS, Pulitzer MP, Kraus DH, et al. Recurrence and Survival in Patients Undergoing Sentinel Lymph Node Biopsy for Merkel Cell Carcinoma: Analysis of 153 Patients from a Single Institution. Ann Surg Oncol. 2011 Sep;18(9):2529–37.

549. Schmalbach CE, Lowe L, Teknos TN, Johnson TM, Bradford CR. Reliability of Sentinel Lymph Node Biopsy for Regional Staging of Head and Neck Merkel Cell Carcinoma. Arch Otolaryngol Neck Surg. 2005 Jul 1;131(7):610.

550. Walsh NM, Cerroni L. Merkel cell carcinoma: A review. J Cutan Pathol. 2021 Mar;48(3):411–21.

551. Organisation mondiale de la santé, Centre international de recherche sur le cancer, editors. WHO classification of skin tumours. 4th ed. Lyon: International agency for research on cancer; 2018. (World health organization classification of tumours).

552. Miettinen M. Keratin 20: immunohistochemical marker for gastrointestinal, urothelial, and Merkel cell carcinomas. Mod Pathol Off J U S Can Acad Pathol Inc. 1995 May;8(4):384–8.

553. Jensen K, Kohler S, Rouse RV. Cytokeratin staining in Merkel cell carcinoma: an immunohistochemical study of cytokeratins 5/6, 7, 17, and 20. Appl Immunohistochem Mol Morphol AIMM. 2000 Dec;8(4):310–5.

554. Cheuk W, Kwan MY, Suster S, Chan JK. Immunostaining for thyroid transcription factor 1 and cytokeratin 20 aids the distinction of small cell carcinoma from Merkel cell carcinoma, but not pulmonary from extrapulmonary small cell carcinomas. Arch Pathol Lab Med. 2001 Feb;125(2):228–31.

555. Su LD, Lowe L, Bradford CR, Yahanda AI, Johnson TM, Sondak VK. Immunostaining for cytokeratin 20 improves detection of micrometastatic Merkel cell carcinoma in sentinel lymph nodes. J Am Acad Dermatol. 2002 May;46(5):661–6.

556. Su LD, Fullen DR, Lowe L, Uherova P, Schnitzer B, Valdez R. CD117 (KIT receptor) expression in Merkel cell carcinoma. Am J Dermatopathol. 2002 Aug;24(4):289–93.

557. Nicholson SA, McDermott MB, Swanson PE, Wick MR. CD99 and cytokeratin-20 in small-cell and basaloid tumors of the skin. Appl Immunohistochem Mol Morphol AIMM. 2000 Mar;8(1):37–41.

558. Ames HM, Bichakjian CK, Liu GY, Oravecz-Wilson KI, Fullen DR, Verhaegen ME, et al. Huntingtin-interacting protein 1: a Merkel cell carcinoma marker that interacts with c-Kit. J Invest Dermatol. 2011 Oct;131(10):2113–20.

559. Stetsenko GY, Malekirad J, Paulson KG, Iyer JG, Thibodeau RM, Nagase K, et al. p63 expression in Merkel cell carcinoma predicts poorer survival yet may have limited clinical utility. Am J Clin Pathol. 2013 Dec;140(6):838–44.

560. Rush PS, Rosenbaum JN, Roy M, Baus RM, Bennett DD, Lloyd RV. Insulinoma-associated 1: A novel nuclear marker in Merkel cell carcinoma (cutaneous neuroendocrine carcinoma). J Cutan Pathol. 2018 Feb;45(2):129–35.

561. Polyomaviridae Study Group of the International Committee on Taxonomy of Viruses, Calvignac-Spencer S, Feltkamp MCW, Daugherty MD, Moens U, Ramqvist T, et al. A taxonomy update for the family Polyomaviridae. Arch Virol. 2016 Jun;161(6):1739–50.

562. Gjoerup O, Chang Y. Update on human polyomaviruses and cancer. Adv Cancer Res. 2010;106:1–51.

563. Carter JJ, Daugherty MD, Qi X, Bheda-Malge A, Wipf GC, Robinson K, et al. Identification of an overprinting gene in Merkel cell polyomavirus provides evolutionary insight into the birth of viral genes. Proc Natl Acad Sci U S A. 2013 Jul 30;110(31):12744–9.

564. Coursaget P, Samimi M, Nicol JTJ, Gardair C, Touzé A. Human Merkel cell polyomavirus: virological background and clinical implications. APMIS Acta Pathol Microbiol Immunol Scand. 2013 Aug;121(8):755–69.

565. Feng H, Shuda M, Chang Y, Moore PS. Clonal integration of a polyomavirus in human Merkel cell carcinoma. Science. 2008 Feb 22;319(5866):1096–100.

566. Grundhoff A, Fischer N. Merkel cell polyomavirus, a highly prevalent virus with tumorigenic potential. Curr Opin Virol. 2015 Oct;14:129–37.

567. Liu W, MacDonald M, You J. Merkel cell polyomavirus infection and Merkel cell carcinoma. Curr Opin Virol. 2016 Oct;20:20–7.

568. Van Ghelue M, Khan MTH, Ehlers B, Moens U. Genome analysis of the new human polyomaviruses. Rev Med Virol. 2012 Nov;22(6):354–77.

569. Shuda M, Feng H, Kwun HJ, Rosen ST, Gjoerup O, Moore PS, et al. T antigen mutations are a human tumor-specific signature for Merkel cell polyomavirus. Proc Natl Acad Sci U S A. 2008 Oct 21;105(42):16272–7.

570. Kwun HJ, Guastafierro A, Shuda M, Meinke G, Bohm A, Moore PS, et al. The minimum replication origin of merkel cell polyomavirus has a unique large T-antigen loading architecture and requires small T-antigen expression for optimal replication. J Virol. 2009 Dec;83(23):12118–28.

571. Chang Y, Moore PS. Merkel cell carcinoma: a virus-induced human cancer. Annu Rev Pathol. 2012;7:123–44.

572. Cheng J, Rozenblatt-Rosen O, Paulson KG, Nghiem P, DeCaprio JA. Merkel cell polyomavirus large T antigen has growth-promoting and inhibitory activities. J Virol. 2013 Jun;87(11):6118–26.

573. Moens U, Krumbholz A, Ehlers B, Zell R, Johne R, Calvignac-Spencer S, et al. Biology, evolution, and medical importance of polyomaviruses: An update. Infect Genet Evol J Mol Epidemiol Evol Genet Infect Dis. 2017 Oct;54:18–38.

574. Temblador A, Topalis D, Andrei G, Snoeck R. CRISPR/Cas9 Editing of the Polyomavirus Tumor Antigens Inhibits Merkel Cell Carcinoma Growth In Vitro. Cancers. 2019 Aug 28;11(9):E1260.

575. Pietropaolo V, Prezioso C, Moens U. Merkel Cell Polyomavirus and Merkel Cell Carcinoma. Cancers. 2020 Jul 3;12(7):E1774.

576. Shuda M, Kwun HJ, Feng H, Chang Y, Moore PS. Human Merkel cell polyomavirus small T antigen is an oncoprotein targeting the 4E-BP1 translation regulator. J Clin Invest. 2011 Sep;121(9):3623–34.

577. Hesbacher S, Pfitzer L, Wiedorfer K, Angermeyer S, Borst A, Haferkamp S, et al. RB1 is the crucial target of the Merkel cell polyomavirus Large T antigen in Merkel cell carcinoma cells. Oncotarget. 2016 May 31;7(22):32956–68.

578. Houben R, Angermeyer S, Haferkamp S, Aue A, Goebeler M, Schrama D, et al. Characterization of functional domains in the Merkel cell polyoma virus Large T antigen. Int J Cancer. 2015 Mar 1;136(5):E290-300.

579. Li J, Wang X, Diaz J, Tsang SH, Buck CB, You J. Merkel cell polyomavirus large T antigen disrupts host genomic integrity and inhibits cellular proliferation. J Virol. 2013 Aug;87(16):9173–88.

580. Li J, Diaz J, Wang X, Tsang SH, You J. Phosphorylation of Merkel cell polyomavirus large tumor antigen at serine 816 by ATM kinase induces apoptosis in host cells. J Biol Chem. 2015 Jan 16;290(3):1874–84.

581. Moens U, Macdonald A. Effect of the Large and Small T-Antigens of Human Polyomaviruses on Signaling Pathways. Int J Mol Sci. 2019 Aug 12;20(16):E3914.

582. Santos-Juanes J, Fernández-Vega I, Fuentes N, Galache C, Coto-Segura P, Vivanco B, et al. Merkel cell carcinoma and Merkel cell polyomavirus: a systematic review and meta-analysis. Br J Dermatol. 2015 Jul;173(1):42–9.

583. Garneski KM, Warcola AH, Feng Q, Kiviat NB, Leonard JH, Nghiem P. Merkel cell polyomavirus is more frequently present in North American than Australian Merkel cell carcinoma tumors. J Invest Dermatol. 2009 Jan;129(1):246–8.

584. Rodig SJ, Cheng J, Wardzala J, DoRosario A, Scanlon JJ, Laga AC, et al. Improved detection suggests all Merkel cell carcinomas harbor Merkel polyomavirus. J Clin Invest. 2012 Dec;122(12):4645–53.

585. Andres C, Belloni B, Puchta U, Sander CA, Flaig MJ. Prevalence of MCPyV in Merkel cell carcinoma and non-MCC tumors. J Cutan Pathol. 2010 Jan;37(1):28–34.

586. Foulongne V, Kluger N, Dereure O, Brieu N, Guillot B, Segondy M. Merkel cell polyomavirus and Merkel cell carcinoma, France. Emerg Infect Dis. 2008 Sep;14(9):1491–3.

587. Harms PW, Patel RM, Verhaegen ME, Giordano TJ, Nash KT, Johnson CN, et al. Distinct gene expression profiles of viral- and nonviral-associated merkel cell carcinoma revealed by transcriptome analysis. J Invest Dermatol. 2013 Apr;133(4):936–45.

588. Kassem A, Schöpflin A, Diaz C, Weyers W, Stickeler E, Werner M, et al. Frequent detection of Merkel cell polyomavirus in human Merkel cell carcinomas and identification of a unique deletion in the VP1 gene. Cancer Res. 2008 Jul 1;68(13):5009–13.

589. Katano H, Ito H, Suzuki Y, Nakamura T, Sato Y, Tsuji T, et al. Detection of Merkel cell polyomavirus in Merkel cell carcinoma and Kaposi's sarcoma. J Med Virol. 2009 Nov;81(11):1951–8.

590. Leroux-Kozal V, Lévêque N, Brodard V, Lesage C, Dudez O, Makeieff M, et al. Merkel cell carcinoma: histopathologic and prognostic features according to the immunohistochemical expression of Merkel cell polyomavirus large T antigen correlated with viral load. Hum Pathol. 2015 Mar;46(3):443–53.

591. Nardi V, Song Y, Santamaria-Barria JA, Cosper AK, Lam Q, Faber AC, et al. Activation of PI3K signaling in Merkel cell carcinoma. Clin Cancer Res Off J Am Assoc Cancer Res. 2012 Mar 1;18(5):1227–36.

592. Sihto H, Kukko H, Koljonen V, Sankila R, Böhling T, Joensuu H. Clinical factors associated with Merkel cell polyomavirus infection in Merkel cell carcinoma. J Natl Cancer Inst. 2009 Jul 1;101(13):938–45.

593. Schrama D, Peitsch WK, Zapatka M, Kneitz H, Houben R, Eib S, et al. Merkel cell polyomavirus status is not associated with clinical course of Merkel cell carcinoma. J Invest Dermatol. 2011 Aug;131(8):1631–8.

594. Moshiri AS, Doumani R, Yelistratova L, Blom A, Lachance K, Shinohara MM, et al. Polyomavirus-Negative Merkel Cell Carcinoma: A More Aggressive Subtype Based on Analysis of 282 Cases Using Multimodal Tumor Virus Detection. J Invest Dermatol. 2017 Apr;137(4):819–27.

595. Shuda M, Arora R, Kwun HJ, Feng H, Sarid R, Fernández-Figueras MT, et al. Human Merkel cell polyomavirus infection I. MCV T antigen expression in Merkel cell carcinoma, lymphoid tissues and lymphoid tumors. Int J Cancer. 2009 Sep 15;125(6):1243–9.

596. Wong SQ, Waldeck K, Vergara IA, Schröder J, Madore J, Wilmott JS, et al. UV-Associated Mutations Underlie the Etiology of MCV-Negative Merkel Cell Carcinomas. Cancer Res. 2015 Dec 15;75(24):5228–34.

597. Busam KJ, Jungbluth AA, Rekthman N, Coit D, Pulitzer M, Bini J, et al. Merkel cell polyomavirus expression in merkel cell carcinomas and its absence in combined tumors and pulmonary neuroendocrine carcinomas. Am J Surg Pathol. 2009 Sep;33(9):1378–85.

598. Kuwamoto S, Higaki H, Kanai K, Iwasaki T, Sano H, Nagata K, et al. Association of Merkel cell polyomavirus infection with morphologic differences in Merkel cell carcinoma. Hum Pathol. 2011 May;42(5):632–40.

599. Starrett GJ, Thakuria M, Chen T, Marcelus C, Cheng J, Nomburg J, et al. Clinical and molecular characterization of virus-positive and virus-negative Merkel cell carcinoma. Genome Med. 2020 Dec;12(1):30.

600. Mogha A, Fautrel A, Mouchet N, Guo N, Corre S, Adamski H, et al. Merkel cell polyomavirus small T antigen mRNA level is increased following in vivo UV-radiation. PloS One. 2010 Jul 2;5(7):e11423.

601. Dowlatshahi M, Huang V, Gehad AE, Jiang Y, Calarese A, Teague JE, et al. Tumor-specific T cells in human Merkel cell carcinomas: a possible role for Tregs and T-cell exhaustion in reducing T-cell responses. J Invest Dermatol. 2013 Jul;133(7):1879–89.

602. Harms PW, Vats P, Verhaegen ME, Robinson DR, Wu YM, Dhanasekaran SM, et al. The Distinctive Mutational Spectra of Polyomavirus-Negative Merkel Cell Carcinoma. Cancer Res. 2015 Sep 15;75(18):3720–7.

603. Goh G, Walradt T, Markarov V, Blom A, Riaz N, Doumani R, et al. Mutational landscape of MCPyV-positive and MCPyV-negative Merkel cell carcinomas with implications for immunotherapy. Oncotarget. 2016 Jan 19;7(3):3403–15.

604. González-Vela MDC, Curiel-Olmo S, Derdak S, Beltran S, Santibañez M, Martínez N, et al.

Shared Oncogenic Pathways Implicated in Both Virus-Positive and UV-Induced Merkel Cell Carcinomas. J Invest Dermatol. 2017 Jan;137(1):197–206.

605. Hafner C, Houben R, Baeurle A, Ritter C, Schrama D, Landthaler M, et al. Activation of the PI3K/AKT pathway in Merkel cell carcinoma. PloS One. 2012;7(2):e31255.

606. Pickering CR, Zhou JH, Lee JJ, Drummond JA, Peng SA, Saade RE, et al. Mutational landscape of aggressive cutaneous squamous cell carcinoma. Clin Cancer Res Off J Am Assoc Cancer Res. 2014 Dec 15;20(24):6582–92.

607. Wang NJ, Sanborn Z, Arnett KL, Bayston LJ, Liao W, Proby CM, et al. Loss-of-function mutations in Notch receptors in cutaneous and lung squamous cell carcinoma. Proc Natl Acad Sci U S A. 2011 Oct 25;108(43):17761–6.

608. Chitsazzadeh V, Coarfa C, Drummond JA, Nguyen T, Joseph A, Chilukuri S, et al. Cross-species identification of genomic drivers of squamous cell carcinoma development across preneoplastic intermediates. Nat Commun. 2016 Aug 30;7:12601.

609. Al-Rohil RN, Tarasen AJ, Carlson JA, Wang K, Johnson A, Yelensky R, et al. Evaluation of 122 advanced-stage cutaneous squamous cell carcinomas by comprehensive genomic profiling opens the door for new routes to targeted therapies. Cancer. 2016 Jan 15;122(2):249–57.

610. Knepper TC, Montesion M, Russell JS, Sokol ES, Frampton GM, Miller VA, et al. The Genomic Landscape of Merkel Cell Carcinoma and Clinicogenomic Biomarkers of Response to Immune Checkpoint Inhibitor Therapy. Clin Cancer Res Off J Am Assoc Cancer Res. 2019 Oct 1;25(19):5961–71.

611. Harring TR, Nguyen NTN, Goss JA, O'Mahony CA. Treatment of liver metastases in patients with neuroendocrine tumors: a comprehensive review. Int J Hepatol. 2011;2011:154541.

612. DeCaprio JA. Molecular Pathogenesis of Merkel Cell Carcinoma. Annu Rev Pathol. 2021 Jan 24;16:69–91.

613. Villani A, Fabbrocini G, Costa C, Carmela Annunziata M, Scalvenzi M. Merkel Cell Carcinoma: Therapeutic Update and Emerging Therapies. Dermatol Ther. 2019 Jun;9(2):209–22.

614. Frohm ML, Griffith KA, Harms KL, Hayman JA, Fullen DR, Nelson CC, et al. Recurrence and Survival in Patients With Merkel Cell Carcinoma Undergoing Surgery Without Adjuvant Radiation Therapy to the Primary Site. JAMA Dermatol. 2016 Sep 1;152(9):1001–7.

615. Chan IS, Bhatia S, Kaufman HL, Lipson EJ. Immunotherapy for Merkel cell carcinoma: a turning point in patient care. J Immunother Cancer. 2018 Mar 23;6(1):23.

616. Gollard R, Weber R, Kosty MP, Greenway HT, Massullo V, Humberson C. Merkel cell carcinoma: review of 22 cases with surgical, pathologic, and therapeutic considerations. Cancer. 2000 Apr 15;88(8):1842–51.

617. O'Connor WJ, Brodland DG. Merkel cell carcinoma. Dermatol Surg Off Publ Am Soc Dermatol Surg Al. 1996 Mar;22(3):262–7.

618. Yiengpruksawan A, Coit DG, Thaler HT, Urmacher C, Knapper WK. Merkel cell carcinoma. Prognosis and management. Arch Surg Chic Ill 1960. 1991 Dec;126(12):1514–9.

619. Allen PJ, Bowne WB, Jaques DP, Brennan MF, Busam K, Coit DG. Merkel cell carcinoma: prognosis and treatment of patients from a single institution. J Clin Oncol Off J Am Soc Clin Oncol. 2005 Apr 1;23(10):2300–9.

620. Tarabadkar ES, Fu T, Lachance K, Hippe DS, Pulliam T, Thomas H, et al. Narrow excision margins are appropriate for Merkel cell carcinoma when combined with adjuvant radiation: Analysis of 188 cases of localized disease and proposed management algorithm. J Am Acad Dermatol. 2021 Feb;84(2):340–7.

621. Pape E, Rezvoy N, Penel N, Salleron J, Martinot V, Guerreschi P, et al. Radiotherapy alone for Merkel cell carcinoma: a comparative and retrospective study of 25 patients. J Am Acad Dermatol. 2011 Nov;65(5):983–90.

622. Veness M, Foote M, Gebski V, Poulsen M. The role of radiotherapy alone in patients with merkel cell carcinoma: reporting the Australian experience of 43 patients. Int J Radiat Oncol Biol Phys. 2010 Nov 1;78(3):703–9.

623. Leonard JH, Ramsay JR, Kearsley JH, Birrell GW. Radiation sensitivity of Merkel cell carcinoma cell lines. Int J Radiat Oncol Biol Phys. 1995 Jul 30;32(5):1401–7.

624. Harrington C, Kwan W. Outcomes of Merkel cell carcinoma treated with radiotherapy without radical surgical excision. Ann Surg Oncol. 2014 Oct;21(11):3401–5.

625. Fang LC, Lemos B, Douglas J, Iyer J, Nghiem P. Radiation monotherapy as regional treatment for lymph node-positive Merkel cell carcinoma. Cancer. 2010 Apr 1;116(7):1783–90.

626. Bichakjian CK, Olencki T, Aasi SZ, Alam M, Andersen JS, Blitzblau R, et al. Merkel Cell Carcinoma, Version 1.2018, NCCN Clinical Practice Guidelines in Oncology. J Natl Compr Cancer Netw JNCCN. 2018 Jun;16(6):742–74.

627. Tai PT, Yu E, Winquist E, Hammond A, Stitt L, Tonita J, et al. Chemotherapy in neuroendocrine/Merkel cell carcinoma of the skin: case series and review of 204 cases. J Clin Oncol Off J Am Soc Clin Oncol. 2000 Jun;18(12):2493–9.

628. Voog E, Biron P, Martin JP, Blay JY. Chemotherapy for patients with locally advanced or metastatic Merkel cell carcinoma. Cancer. 1999 Jun 15;85(12):2589–95.

629. Iyer JG, Blom A, Doumani R, Lewis C, Tarabadkar ES, Anderson A, et al. Response rates and durability of chemotherapy among 62 patients with metastatic Merkel cell carcinoma. Cancer Med. 2016 Sep;5(9):2294–301.

630. Crown J, Lipzstein R, Cohen S, Goldsmith M, Wisch N, Paciucci PA, et al. Chemotherapy of metastatic Merkel cell cancer. Cancer Invest. 1991;9(2):129–32.

631. Bhatia S, Storer BE, Iyer JG, Moshiri A, Parvathaneni U, Byrd D, et al. Adjuvant Radiation Therapy and Chemotherapy in Merkel Cell Carcinoma: Survival Analyses of 6908 Cases From the National Cancer Data Base. J Natl Cancer Inst. 2016 Sep;108(9):djw042.

632. Houben R, Shuda M, Weinkam R, Schrama D, Feng H, Chang Y, et al. Merkel cell polyomavirus-infected Merkel cell carcinoma cells require expression of viral T antigens. J Virol. 2010 Jul;84(14):7064–72.

633. Wooff JC, Trites JR, Walsh NMG, Bullock MJ. Complete spontaneous regression of metastatic merkel cell carcinoma: a case report and review of the literature. Am J Dermatopathol. 2010 Aug;32(6):614–7.

634. Pang C, Sharma D, Sankar T. Spontaneous regression of Merkel cell carcinoma: A case report and review of the literature. Int J Surg Case Rep. 2015;7C:104–8.

635. Sihto H, Böhling T, Kavola H, Koljonen V, Salmi M, Jalkanen S, et al. Tumor infiltrating immune cells and outcome of Merkel cell carcinoma: a population-based study. Clin Cancer Res Off J Am Assoc Cancer Res. 2012 May 15;18(10):2872–81.

636. Paulson KG, Iyer JG, Tegeder AR, Thibodeau R, Schelter J, Koba S, et al. Transcriptome-wide studies of merkel cell carcinoma and validation of intratumoral CD8+ lymphocyte invasion as an independent predictor of survival. J Clin Oncol Off J Am Soc Clin Oncol. 2011 Apr 20;29(12):1539–46.

637. Paulson KG, Lewis CW, Redman MW, Simonson WT, Lisberg A, Ritter D, et al. Viral oncoprotein antibodies as a marker for recurrence of Merkel cell carcinoma: A prospective validation study. Cancer. 2017 Apr 15;123(8):1464–74.

638. Paulson KG, Tegeder A, Willmes C, Iyer JG, Afanasiev OK, Schrama D, et al. Downregulation of MHC-I expression is prevalent but reversible in Merkel cell carcinoma. Cancer Immunol Res. 2014 Nov;2(11):1071–9.

639. Vinay DS, Ryan EP, Pawelec G, Talib WH, Stagg J, Elkord E, et al. Immune evasion in cancer: Mechanistic basis and therapeutic strategies. Semin Cancer Biol. 2015 Dec;35 Suppl:S185–98.

640. Ugel S, De Sanctis F, Mandruzzato S, Bronte V. Tumor-induced myeloid deviation: when myeloid-derived suppressor cells meet tumor-associated macrophages. J Clin Invest. 2015 Sep;125(9):3365–76.

641. Afanasiev OK, Yelistratova L, Miller N, Nagase K, Paulson K, Iyer JG, et al. Merkel polyomavirus-specific T cells fluctuate with merkel cell carcinoma burden and express therapeutically targetable PD-1 and Tim-3 exhaustion markers. Clin Cancer Res Off J Am Assoc Cancer Res. 2013 Oct 1;19(19):5351–60.

642. Stachyra K, Dudzisz-Śledź M, Bylina E, Szumera-Ciećkiewicz A, Spałek MJ, Bartnik E, et al. Merkel Cell Carcinoma from Molecular Pathology to Novel Therapies. Int J Mol Sci. 2021 Jun 11;22(12):6305.

643. Lipson EJ, Vincent JG, Loyo M, Kagohara LT, Luber BS, Wang H, et al. PD-L1 expression in the Merkel cell carcinoma microenvironment: association with inflammation, Merkel cell polyomavirus and overall survival. Cancer Immunol Res. 2013 Jul;1(1):54–63.

644. Nghiem PT, Bhatia S, Lipson EJ, Kudchadkar RR, Miller NJ, Annamalai L, et al. PD-1 Blockade with Pembrolizumab in Advanced Merkel-Cell Carcinoma. N Engl J Med. 2016 Jun

30;374(26):2542–52.

645. Garon EB, Rizvi NA, Hui R, Leighl N, Balmanoukian AS, Eder JP, et al. Pembrolizumab for the treatment of non-small-cell lung cancer. N Engl J Med. 2015 May 21;372(21):2018–28.

646. Nghiem P, Bhatia S, Lipson EJ, Sharfman WH, Kudchadkar RR, Brohl AS, et al. Three-year survival, correlates and salvage therapies in patients receiving first-line pembrolizumab for advanced Merkel cell carcinoma. J Immunother Cancer. 2021 Apr;9(4):e002478.

647. Tanda ET, d'Amato AL, Rossi G, Croce E, Boutros A, Cecchi F, et al. Merkel Cell Carcinoma: An Immunotherapy Fairy-Tale? Front Oncol. 2021 Sep 23;11:739006.

648. Rabinowits G, Lezcano C, Catalano PJ, McHugh P, Becker H, Reilly MM, et al. Cabozantinib in Patients with Advanced Merkel Cell Carcinoma. The Oncologist. 2018 Jul;23(7):814–21.

649. Leccia MT, Mouret S, Dalle S, Dequatrebarbes J, Dreno B, Dupuy A, et al. Traitement des carcinomes de Merkel inopérables et/ou métastatiques par analogue de la somatostatine. Étude nationale multicentrique mono-bras de phase II. Ann Dermatol Vénéréologie. 2018 Dec;145(12):S126.

650. Dummer R, Michielin O, Nägeli MC, Goldinger SM, Campigotto F, Kriemler-Krahn U, et al. Phase I, open-label study of pasireotide in patients with BRAF-wild type and NRAS-wild type, unresectable and/or metastatic melanoma. ESMO Open. 2018;3(5):e000388.

651. Akaike T, Qazi J, Anderson A, Behnia FS, Shinohara MM, Akaike G, et al. High somatostatin receptor expression and efficacy of somatostatin analogues in patients with metastatic Merkel cell carcinoma. Br J Dermatol. 2021 Feb;184(2):319–27.

652. Queirolo P, Boutros A, Tanda E, Spagnolo F, Quaglino P. Immune-checkpoint inhibitors for the treatment of metastatic melanoma: a model of cancer immunotherapy. Semin Cancer Biol. 2019 Dec;59:290–7.

653. Tanda ET, Vanni I, Boutros A, Andreotti V, Bruno W, Ghiorzo P, et al. Current State of Target Treatment in BRAF Mutated Melanoma. Front Mol Biosci. 2020;7:154.

654. Hassel JC, Berking C, Eigentler T, Gutzmer R, Ascierto PA, Schilling B, et al. Phase Ib/II study (SENSITIZE) assessing safety, pharmacokinetics (PK), pharmacodynamics (PD), and clinical outcome of domatinostat in combination with pembrolizumab in patients with advanced melanoma refractory/non-responding to prior checkpoint inhibitor therapy. Ann Oncol. 2019 Oct;30:v559.

655. Hodgson NC. Merkel cell carcinoma: changing incidence trends. J Surg Oncol. 2005 Jan 1;89(1):1–4.

656. Cornejo C, Miller CJ. Merkel Cell Carcinoma: Updates on Staging and Management. Dermatol Clin. 2019 Jul;37(3):269–77.

657. Nghiem P, Kaufman HL, Bharmal M, Mahnke L, Phatak H, Becker JC. Systematic literature review of efficacy, safety and tolerability outcomes of chemotherapy regimens in patients with metastatic Merkel cell carcinoma. Future Oncol Lond Engl. 2017 Jun;13(14):1263–79.

658. Harms KL, Zhao L, Johnson B, Wang X, Carskadon S, Palanisamy N, et al. Virus-positive Merkel Cell Carcinoma Is an Independent Prognostic Group with Distinct Predictive Biomarkers. Clin Cancer Res Off J Am Assoc Cancer Res. 2021 May 1;27(9):2494–504.

659. Garza-Davila VF, Valdespino-Valdes J, Barrera FJ, Ocampo-Candiani J, Garza-Rodríguez V. Clinical impact of immunotherapy in Merkel cell carcinoma patients: A systematic review and meta-analysis. J Am Acad Dermatol. 2021 Apr 19;S0190-9622(21)00824-0.

660. Spassova I, Ugurel S, Terheyden P, Sucker A, Hassel JC, Ritter C, et al. Predominance of Central Memory T Cells with High T-Cell Receptor Repertoire Diversity is Associated with Response to PD-1/PD-L1 Inhibition in Merkel Cell Carcinoma. Clin Cancer Res Off J Am Assoc Cancer Res. 2020 May 1;26(9):2257–67.

661. Gehrcken L, Sauerer T, Schaft N, Dörrie J. T-Cell Responses in Merkel Cell Carcinoma: Implications for Improved Immune Checkpoint Blockade and Other Therapeutic Options. Int J Mol Sci. 2021 Aug 12;22(16):8679.

662. Walsh NM, Fleming KE, Hanly JG, Dakin Hache K, Doucette S, Ferrara G, et al. A morphological and immunophenotypic map of the immune response in Merkel cell carcinoma. Hum Pathol. 2016 Jun;52:190–6.

663. Bukur J, Jasinski S, Seliger B. The role of classical and non-classical HLA class I antigens in human tumors. Semin Cancer Biol. 2012 Aug;22(4):350–8.

664. Garrido F, Aptsiauri N. Cancer immune escape: MHC expression in primary tumours versus metastases. Immunology. 2019 Dec;158(4):255–66.

665. Cornel AM, Mimpen IL, Nierkens S. MHC Class I Downregulation in Cancer: Underlying Mechanisms and Potential Targets for Cancer Immunotherapy. Cancers. 2020 Jul 2;12(7):E1760.

666. Anderson P, Aptsiauri N, Ruiz-Cabello F, Garrido F. HLA class I loss in colorectal cancer: implications for immune escape and immunotherapy. Cell Mol Immunol. 2021 Mar;18(3):556–65.

667. Haque M, Ueda K, Nakano K, Hirata Y, Parravicini C, Corbellino M, et al. Major histocompatibility complex class I molecules are down-regulated at the cell surface by the K5 protein encoded by Kaposi's sarcoma-associated herpesvirus/human herpesvirus-8. J Gen Virol. 2001 May;82(Pt 5):1175–80.

668. Koopman LA, van Der Slik AR, Giphart MJ, Fleuren GJ. Human leukocyte antigen class I gene mutations in cervical cancer. J Natl Cancer Inst. 1999 Oct 6;91(19):1669–77.

669. Ritter C, Fan K, Paschen A, Reker Hardrup S, Ferrone S, Nghiem P, et al. Epigenetic priming restores the HLA class-I antigen processing machinery expression in Merkel cell carcinoma. Sci Rep. 2017 May 23;7(1):2290.

670. Gavvovidis I, Leisegang M, Willimsky G, Miller N, Nghiem P, Blankenstein T. Targeting Merkel Cell Carcinoma by Engineered T Cells Specific to T-Antigens of Merkel Cell Polyomavirus. Clin Cancer Res Off J Am Assoc Cancer Res. 2018 Aug 1;24(15):3644–55.

671. Morris SW, Kirstein MN, Valentine MB, Dittmer KG, Shapiro DN, Saltman DL, et al. Fusion of a kinase gene, ALK, to a nucleolar protein gene, NPM, in non-Hodgkin's lymphoma. Science. 1994 Mar 4;263(5151):1281–4.

672. Golding B, Luu A, Jones R, Viloria-Petit AM. The function and therapeutic targeting of anaplastic lymphoma kinase (ALK) in non-small cell lung cancer (NSCLC). Mol Cancer. 2018 Dec;17(1):52.

673. Palmer RH, Vernersson E, Grabbe C, Hallberg B. Anaplastic lymphoma kinase: signalling in development and disease. Biochem J. 2009 Jun 15;420(3):345–61.

674. Mano H. Non-solid oncogenes in solid tumors: *EML4-ALK* fusion genes in lung cancer. Cancer Sci. 2008 Dec;99(12):2349–55.

675. Veija T, Koljonen V, Bohling T, Kero M, Knuutila S, Sarhadi VK. Aberrant expression of ALK and EZH2 in Merkel cell carcinoma. BMC Cancer. 2017 Dec;17(1):236.

676. Veija T, Kero M, Koljonen V, Böhling T. ALK and EGFR expression by immunohistochemistry are associated with Merkel cell polyomavirus status in Merkel cell carcinoma. Histopathology. 2019 May;74(6):829–35.

677. Filtenborg-Barnkob BE, Bzorek M. Expression of anaplastic lymphoma kinase in Merkel cell carcinomas. Hum Pathol. 2013 Aug;44(8):1656–64.

678. Liu J, Jin H, Tian H, Lian G, Chen S, Li J, et al. Anaplastic lymphoma kinase protein expression predicts micrometastases and prognosis for patients with hepatocellular carcinoma. Oncol Lett. 2016 Jan;11(1):213–23.

679. Kim MH, Lee S, Koo JS, Jung KH, Park IH, Jeong J, et al. Anaplastic lymphoma kinase gene copy number gain in inflammatory breast cancer (IBC): prevalence, clinicopathologic features and prognostic implication. PloS One. 2015;10(3):e0120320.

680. Bresler SC, Weiser DA, Huwe PJ, Park JH, Krytska K, Ryles H, et al. ALK mutations confer differential oncogenic activation and sensitivity to ALK inhibition therapy in neuroblastoma. Cancer Cell. 2014 Nov 10;26(5):682–94.

681. Yu Z, Zhao R. Inhibition of anaplastic lymphoma kinase promotes apoptosis and suppresses proliferation in human hepatocellular carcinoma. Anticancer Drugs. 2018 Jul;29(6):513–9.

682. Jaatinen J, Veija T, Salmikangas M, Böhling T, Sihto H, Koljonen V. ALK is frequently phosphorylated in Merkel cell carcinoma and associates with longer survival. PloS One. 2021;16(5):e0252099.

683. Horn L, Whisenant JG, Wakelee H, Reckamp KL, Qiao H, Leal TA, et al. Monitoring Therapeutic Response and Resistance: Analysis of Circulating Tumor DNA in Patients With ALK+ Lung Cancer. J Thorac Oncol. 2019 Nov;14(11):1901–11.

684. Gainor JF, Dardaei L, Yoda S, Friboulet L, Leshchiner I, Katayama R, et al. Molecular Mechanisms of Resistance to First- and Second-Generation ALK Inhibitors in *ALK* -Rearranged Lung Cancer. Cancer Discov. 2016 Oct;6(10):1118–33.

685. Zou HY, Friboulet L, Kodack DP, Engstrom LD, Li Q, West M, et al. PF-06463922, an ALK/ROS1 Inhibitor, Overcomes Resistance to First and Second Generation ALK Inhibitors in Preclinical Models. Cancer Cell. 2015 Jul;28(1):70–81.

686. Shaw AT, Felip E, Bauer TM, Besse B, Navarro A, Postel-Vinay S, et al. Lorlatinib in non-small-cell lung cancer with ALK or ROS1 rearrangement: an international, multicentre, open-label, single-arm first-in-man phase 1 trial. Lancet Oncol. 2017 Dec;18(12):1590–9.

687. Johnson TW, Richardson PF, Bailey S, Brooun A, Burke BJ, Collins MR, et al. Discovery of (10 *R*)-7-Amino-12-fluoro-2,10,16-trimethyl-15-oxo-10,15,16,17-tetrahydro- *2H* -8,4-(metheno)pyrazolo[4,3- *h*][2,5,11]-benzoxadiazacyclotetradecine-3-carbonitrile (PF-06463922), a Macrocyclic Inhibitor of Anaplastic Lymphoma Kinase (ALK) and c-ros Oncogene 1 (ROS1) with Preclinical Brain Exposure and Broad-Spectrum Potency against ALK-Resistant Mutations. J Med Chem. 2014 Jun 12;57(11):4720–44.

688. Solomon BJ, Besse B, Bauer TM, Felip E, Soo RA, Camidge DR, et al. Lorlatinib in patients with ALK-positive non-small-cell lung cancer: results from a global phase 2 study. Lancet Oncol. 2018 Dec;19(12):1654–67.

689. Sano R, Krytska K, Larmour CE, Raman P, Martinez D, Ligon GF, et al. An antibody-drug conjugate directed to the ALK receptor demonstrates efficacy in preclinical models of neuroblastoma. Sci Transl Med. 2019 Mar 13;11(483):eaau9732.

690. Diaconu I, Ballard B, Zhang M, Chen Y, West J, Dotti G, et al. Inducible Caspase-9 Selectively Modulates the Toxicities of CD19-Specific Chimeric Antigen Receptor-Modified T Cells. Mol Ther J Am Soc Gene Ther. 2017 Mar 1;25(3):580–92.

691. Chen Y, Sun C, Landoni E, Metelitsa L, Dotti G, Savoldo B. Eradication of Neuroblastoma by T Cells Redirected with an Optimized GD2-Specific Chimeric Antigen Receptor and Interleukin-15. Clin Cancer Res Off J Am Assoc Cancer Res. 2019 May 1;25(9):2915–24.

692. Pulitzer M. Merkel Cell Carcinoma. Surg Pathol Clin. 2017 Jun;10(2):399–408.

693. Harms PW, Harms KL, Moore PS, DeCaprio JA, Nghiem P, Wong MKK, et al. The biology and treatment of Merkel cell carcinoma: current understanding and research priorities. Nat Rev Clin Oncol. 2018 Dec;15(12):763–76.

694. Atherly AJ, Camidge DR. The cost-effectiveness of screening lung cancer patients for targeted drug sensitivity markers. Br J Cancer. 2012 Mar 13;106(6):1100–6.

695. Curran KJ, Pegram HJ, Brentjens RJ. Chimeric antigen receptors for T cell immunotherapy: current understanding and future directions. J Gene Med. 2012 Jun;14(6):405–15.

696. Zaretsky JM, Garcia-Diaz A, Shin DS, Escuin-Ordinas H, Hugo W, Hu-Lieskovan S, et al. Mutations Associated with Acquired Resistance to PD-1 Blockade in Melanoma. N Engl J Med. 2016 Sep 1;375(9):819–29.

697. Garcia-Lora A, Martinez M, Algarra I, Gaforio JJ, Garrido F. MHC class I-deficient metastatic tumor variants immunoselected by T lymphocytes originate from the coordinated downregulation of APM components. Int J Cancer. 2003 Sep 10;106(4):521–7.

698. Grupp SA, Kalos M, Barrett D, Aplenc R, Porter DL, Rheingold SR, et al. Chimeric antigen receptor-modified T cells for acute lymphoid leukemia. N Engl J Med. 2013 Apr 18;368(16):1509–18.

699. Dobrenkov K, Ostrovnaya I, Gu J, Cheung IY, Cheung NKV. Oncotargets GD2 and GD3 are highly expressed in sarcomas of children, adolescents, and young adults. Pediatr Blood Cancer. 2016 Oct;63(10):1780–5.

700. Terzic T, Cordeau M, Herblot S, Teira P, Cournoyer S, Beaunoyer M, et al. Expression of Disialoganglioside (GD2) in Neuroblastic Tumors: A Prognostic Value for Patients Treated With Anti-GD2 Immunotherapy. Pediatr Dev Pathol Off J Soc Pediatr Pathol Paediatr Pathol Soc. 2018 Aug;21(4):355–62.

701. Cheresh DA, Rosenberg J, Mujoo K, Hirschowitz L, Reisfeld RA. Biosynthesis and expression of the disialoganglioside GD2, a relevant target antigen on small cell lung carcinoma for monoclonal antibody-mediated cytolysis. Cancer Res. 1986 Oct;46(10):5112–8.

702. Svennerholm L, Boström K, Fredman P, Jungbjer B, Lekman A, Månsson JE, et al. Gangliosides and allied glycosphingolipids in human peripheral nerve and spinal cord. Biochim Biophys Acta. 1994 Sep 15;1214(2):115–23.

703. Suzuki M, Cheung NKV. Disialoganglioside GD2 as a therapeutic target for human diseases. Expert Opin Ther Targets. 2015 Mar;19(3):349–62.

ACKNOWLEDGMENTS

First and foremost, I would like to thank my mentor, Prof. Mauro Papotti for his invaluable supervision, guidance, and support during the course of my PhD degree, and for challenging me to grow as a scientist.

I would also like to express my gratitude to Prof. Marco Volante, for his constructive advices and overall insights which were really influential in shaping my experiment methods and critical thinking.

I could not have undertaken this journey without Prof. Isabella Castellano, I was fortunate to make my first steps into the research world with her. She taught me to ask clinically relevant research questions and answer them with scientific rigor.

I am indebted to Prof. Roberto Chiarle for giving me opportunity to be part of his team widening my research from various perspectives.

Special thanks to Prof. Paola Cassoni, for her unlimited support and encouragement, but also valuable discussions we had along the road.

I am grateful to everyone I've collaborated with: Prof. Giovanni Bussolati, Prof. Giuseppe Pelosi, Prof. Luisella Righi, Dr. Simona Osella-Abate, Dr. Luca Molinaro, Dr. Francesca Maletta, Dr. Luisa Delsedime, Dr. Giancarlo Abbona: your levels of knowledge and ingenuity is something I will always keep aspiring to.

I would like to thank all staff of Pathology Divisions of Città della Salute e della Scienza and San Luigi Hospitals, my friends, lab mates, colleagues, and research team; I can't thank you enough for your enthusiasm, teamwork, collective efforts, and dedication.

My appreciation also goes out to my husband, my family and friends for their encouragement and support all through my studies.

And to my parents, who set me off on the road to this PhD a long time ago.